THE UNIVERSITY OF HULL

LASER BASED CUTTING TOOL CONDITION MONITORING

being a Thesis submitted for the Degree of PhD

in the University of Hull

by

David Robert Aitchison BEng, MEng

April 1995

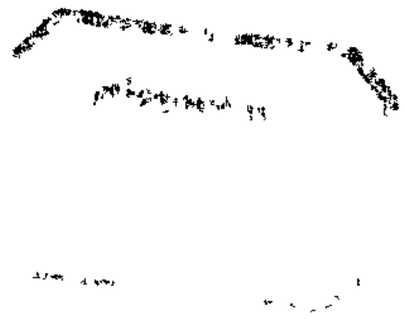

Abstract

The laser back-scatter technique has already been successfully applied to a wide range of scanning/imaging applications and is supported by a number of theories and hypotheses. However, many of the optimum, fundamental operating parameters for specific applications are not formally documented. They are more often established by trial and error or through familiarisation with the nature of the particular scanning system. As a concequence, the research work undertaken attempts to determine optimum conditions for the laser back-scatter technique applied specifically to cutting tool condition monitoring.

Due to the complex and interrelated nature of the prime characteristics which contributed significantly to the overall performance of the laser scanning system, it was recognised at an early stage that parameters would have to be isolated and their effects observed independently. The research work was structured around this condition and a series of tests were undertaken with all but one parameter fixed in each case. A response signal was recorded for each of the tests. Families of results were subsequently compared so that optimum system response parameters could be identified. Furthermore, relationships between the parameters were also sought.

As a precursor to the experimental work, the extent of acceptable cutting tool wear and range of damage most frequently found was investigated. A representative collection of cutting tools was then established. This collection reflected not only the defects to be encountered and screened but also the scope of geometries to be handled by the laser inspection system.

The testing spanned a wide range of subject specimens in an attempt to make the resultant conclusions appropriate and transferable to other applications. Plane (flat) specimens were used to overcome the need for complex movements in three or more axes, which were

necessary to scan the vast majority of milling cutters. Thus the primary scanning work was undertaken on these control samples. The plane specimens were prepared with control defects present, the range of which represented those most likely to occur during routine metal cutting operations. Samples with pre-defined surface textures were gathered together, again control defects were introduced. Through this arrangement, defect response signals with and without background contouring (surface roughness) were assessed independently. The subsequent assessment and screening of the response signals was discussed in the context of the synthesised data.

To conclude the work, a scanner configured with the optimum operational parameters, identified in the earlier tests, was used to view the cutting edges of a restricted range of cutting tools. The response signals, which represented each of the tool's cutting edges, were in turn assessed.

The research commitment necessitated the design and development of a suitable device to manipulate a range of cutting tools in order to present them to the laser scanning head in the appropriate orientation. From a system management view-point this dictated the need for efficient and dedicated supervisory software also for the implementation of multi-axis control and interfacing techniques. Furthermore, developments in the area of machine tool control through macro programming were investigated, to offer high levels of interactivity, automation and advanced cutting tool management.

Conclusions were drawn based on the findings and outcomes of the developed system for inspection. Recommendations for enhanced system design and further research work are also made.

It is hoped that this research program and subsequent activities evolving from it make a significant contribution to resolving the problem of inadequate cutting tool management at

shop floor level. It has been identified that poor cutting tool management and screening, leading to the issue of unacceptable, worn or damaged cutting tools results in considerable amounts of rework and scrap. Furthermore, in the other extreme, the unnecessary refurbishment of cutting tools means the waste of not only an expensive commodity but also of manpower and capital equipment, in the form of dedicated grinding facilities. This problem, one so frequently encountered in European manufacturing industry, has gone unresolved for too long.

Acknowledgements

My thanks must go to Rob James for his role of mentor. His help and guidance was freely given and greatly received on many occasions during production of this thesis.

I owe a great deal of gratitude and thanks to my wife Lynda due to her patience, support and encouragement throughout the period dedicated to this line of study.

I would also like to thank Kenny, Bob and Dave for their support, hard work and friendship without which a conclusion to this work would have been considerably delayed. Also my thanks must go to Isabel for her clerical support.

To my Father, Bob Aitchison.

Table of Contents

Chapter 3.0

Chapter 4.0

List of figures

Chapter 5.0

List of tables

Chapter 6.0

No tables

Chapter 1.0

Introduction

1.0 Introduction

The demands of modern society is placing an ever increasing pressure on industry and manufacturing facilities. The pressure is to respond more quickly to trends and to produce a wider range of products at a lower cost in less time. This is one of the reasons why industry quickly adopted the concept of Computer Numerical Control (CNC) of machines and machine tools. CNC was one of the first major steps towards the development of an automated production environment which was perceived, and remains so today, as the solution to satisfying the material demands of modern society.

Indirectly such demands determine development of the country's manufacturing resource. The driving forces are not seen directly at the production level as solely monetary reward, there is an intermediate platform of demands which are more subtle and wide ranging. These production demands would typically include:-

Efficient Production	Equated to lower levels of scrap and re-work
Work Standards	Relating to closer tolerancing and tighter surface finish control
Productivity Optimisation	Realised by increased levels of automation by the introduction of tool, work-piece and machine handling & management by computers and logic controllers.

Leading machine-tool manufacturers (Mandelli Spa, Italy) suggest that the main thrust of development over the ensuing years will be dedicated to improving the quality, surface finish and dimensional accuracy of the machined component. This belief is endorsed in a report compiled by the Japanese Machine-Tool Builders' Association [1].

Since the introduction of Numerical Control (NC) machines, in the early 1950s, a wide range of support activities have been automated. To date, the successful and widely used developments can be placed into one of the following categories;

- cutting tool and work-piece transportation,
- work piece handling,
- tool change,
- tool and part program management.

Despite considerable effort one task which has not yet been successful on a wide scale is the automation of tool inspection/tool condition monitoring.

Cutting tool inspection and integration of this facility into the over-all tool management strategy is a practice which is implemented at extremely low levels in a broad range of industrial manufacturing companies world-wide. The need for the correct tool in serviceable condition at the time requested is essential for optimum productivity. However, this scenario is seldom achieved due not only to the lack of proper tooling but also its condition being unacceptable.

In a large manufacturing facility where thousands of tools are in circulation an efficient and effective management strategy should be employed. Unfortunately this is generally not the case. Typically, in a leading manufacturing company, thousands of tools are stored centrally and are issued as appropriate groups in response to production orders.
The tools are not always methodically inspected when issued or returned. As a result, defects or breakages may be detected by chance but many inevitably go unnoticed. In an attempt to monitor/estimate cutting tool condition, simple models of time expired life are widely used at present. This method of tool management is grossly inefficient and does not actually monitor the cutting tool's condition. Based on a service history model this technique simply sums up the total number of hours a tool has been used to remove material so as to determine when it has reached the end of its serviceable life. The tool is then

withdrawn and is passed to the re-grinding facility, in the case of solid monolithic tools, or has the individual inserts replaced (See Figure 1-1 below).

Figure 1-1 Typical monolithic and insert cutting tools

The result is a system which does not optimise fully the life of cutting tools and the deficiencies of this system are immediately apparent. Many tools may quickly lose their cutting edges but are continually used until the timed life decrees, by which time the damage has been done and the work piece quality is down graded. At the opposite end of the scale, some tools are recalled and refurbished ahead of the optimum life of the tool, resulting in wastage of an expensive commodity and of labour in the grinding or insert replacement operations. Investigation has shown that in one year, several million pounds are wasted by a single leading manufacturing company site alone, due to an over-simplified approach to tool management.

By introducing an effective and efficient cutting tool condition monitoring system a revised strategy could be implemented with dramatic effect on:-

- the supply of tooling in optimum condition
- reduced work piece re-work and scrap
- reduced levels of unnecessary refurbishment of tooling
- interception of premature failure/degradation of tooling
- optimisation of machine tool productivity and serviceability

These factors could contribute significantly to dramatic reductions in tooling consumption and thus costs, also reductions in labour commitment to tooling management and increased levels of production with less scrap and re-work. These savings would in turn produce higher profits or reduced product costs.

Alternative systems used to monitor cutting tool condition are available but are not used widely. This could be due to the fact that they often lack the ability to be integrated into a company-wide or even local tool management system. Systems which rely upon cutting force and acoustic emission attempt to assess the condition of the active tool, which leads to extremely complicated mathematical models and software management. Off-line methods using electromechanical systems (Touch-trigger probes) have had some degree of acceptance but tend to be used solely for offset measurement and breakage detection. Thus, a weak link remains in the automated production cycle of machined components. The solution is an automated, integrated and intelligent, tool condition monitoring system. The work reported in this thesis is intended to contribute to the development and realisation of such a system. Fundamental principles of a laser scattering technique form the basis of the research work. Additional concepts which are considered to be essential in the development of the integrated, automatic and intelligent facility are introduced as prototype models while their operation, relevance and unique technical contribution are discussed.

Chapter 2.0

Literature Review

2.0 Literature review

Since the useful life and condition of cutting tools to some extent dictate the economics of machining operations, it is vitally important that the condition or serviceability of tools held in the central or local machine-tool stores are known. Most important must be the awareness of when the cutting tool requires changing. This is normally a result of either gradual and progressive wear or premature edge failure due to chipping, burning or plastic deformation. A condition monitoring system must therefore be capable of detecting complete failure as well as degrees of gradual wear of the cutting edges. As a consequence the applied monitoring technique must command high levels of sensitivity, reliability and accuracy. Additionally, a union between the condition monitoring device and the machine tool could make full use of potential computer-based intelligence - Artificial Intelligence (AI). As a consequence the machine tool could be selective and as a result offer Adaptive Control (AC) by accepting or rejecting cutting tools based on a decision evolving from the gathered, tool specific, sensory information.

This type of Adaptive Control technique is being actively sought by manufacturing personnel, primarily for the following reasons [2]:-

- A definite need for employing higher material removal rates for a better utilisation of new generation computer-controlled machine tools
- A keen awareness of the tool and scrap costs due to excessive tool wear
- An increasing use of 'hard to machine' aerospace alloys requiring tighter control of tool wear rates
- The continuous introduction of new tool grades as well as work materials, leading to the absolute necessity of using automation in order to optimise machining conditions
- The necessity of tool changing before production parts are lost, due to excessive tool wear or catastrophic tool failure

This technological scenario is almost 3000 years away from the first documented evidence of machine tools (simple wood-working lathe) but only 300 years from the first recorded use of the metal working lathe complete with lead screws. During this latter period of time, tool condition monitoring was an activity performed by the operator or setter of a manually-operated machine. The smooth and efficient operation was due, almost entirely, to his skill and judgement. With the introduction of the automated NC and more recent CNC machine tools, the aim to increasingly limit operator intervention has been actively pursued. As a result machines are now expected to operate for lengthy periods with the minimum of intervention. Work-piece handling, swarf removal and tool change are just some of the resident automatic facilities which enable this mode of operation to be supported.

Tool changes resulting from an observed deterioration in cutting performance were initiated by the operator and were undertaken at the most convenient point in the machining cycle; immediately, at the end of cut or at the end of the job. Predominantly, CNC machine tools do not offer this range of flexibility when left to run with the minimum of supervision. Most frequently the tool change strategy is based on a time expired life or in the worst case, at the end of the cutting cycle for that tool.

Now, with an ever increasing use of Computer Integrated Manufacturing (CIM) and the general move towards minimally manned manufacture, the situation can only deteriorate unless action is taken. Through CIM, Flexible Manufacturing Systems (FMS) work to an overall plan which is frequently updated to meet system and order requirements. In this type of environment the operator can introduce inefficiencies, with unplanned tool changes disrupting the work schedule and thus the efficiency of the system. Therefore if automated machining operations are to be optimised and successful in producing high quality components efficiently then some form of integrated cutting tool condition sensing device is required [2].

The trend towards the use of unmanned production systems in manufacturing industry dictates a requirement for monitoring systems and sensors, which have an ability to survive

in hostile environments, and which can provide the overall control system with an accurate picture of machine and cutting tool status. Consequently new technologies and developments should be combined with good software engineering practice to produce 'intelligent' and self-correcting manufacturing systems. Developments in this domain offer benefits of reduced operating costs and improved product quality. Iwata's paper, *'Sensing technologies for improving the machine tool function*', [3], strongly supports this belief. The paper is based on a questionnaire circulated to all members of the Japanese Machine Tool Manufacturers Association during February 1988. The intention of the exercise was to gather information on the types of sensors used in machine tools manufactured in Japan. The findings were grouped and presented in the following subject areas; machine functions, tool functions, accessories, functions for work-pieces and machining performance. A notable point was made under the heading of tool functions, relating to condition monitoring. "Many manufacturers expressed a wish for sensors to be used in machining centres to detect tool breakage and tool wear". On the whole, this subject area showed "high interest is in-process monitoring/on-the-machine measurement of wear and breakage and in tool identification by data provided on the tool itself". In conclusion, Iwata introduced a phrase directed at the new generation of machine tools - "living machines". Machines with the five senses, a nervous system and an intellectual system, which may well become a reality.

Tool condition monitoring systems fall into one of two categories, active and passive, depending upon how and when the tool is monitored. Passive techniques tend to be direct and are generally involved with taking measurements associated with the volumetric losses of the cutting tool body. Hence this type of system tends to operate off-line, with the cutting tool in a passive state (out of cut). Active techniques utilise measurements of cutting parameters and are thus dependant upon the cutting tool being active in removing material.

A summary of the active and passive systems currently available for tool wear and breakage detection are introduced in the following sections. The work by Lister and Barrow [4],

who reported on the range of tool condition monitoring systems widely available in their paper entitled *'Tool condition monitoring systems'* is particularly relevant.

A summary of sensing techniques for tool wear and failure, under research or development, can be found in Appendix I.

2.1 Passive cutting tool condition monitoring techniques

Several passive inspection techniques are introduced below. The techniques are grouped into areas which pertain to the core technology used.

Advantages of such systems include:-

- Pre and post cutting tool utilisation inspection,
- Improved tool management at the machine-tool and factory wide,
- Reduced machining times due to tools being in serviceable condition when selected by the NC part program instructions.

The main disadvantages of such systems are:-

- premature cutting edge failure, whilst the tool is in cut, cannot be detected,
- they can be time consuming when considering the production rate, because material removal has to be interrupted to allow inspection of a specific tool.

Despite these shortcomings, a considerable number of cutting tool condition monitoring systems currently in use are essentially passive. Active techniques offer a different blend of advantages and disadvantages.

A prerequisite for the majority of passive condition monitoring methods is that the cutting tool must be clean with all swarf removed, before the inspection cycle begins. This is generally achieved by blasting the tool with compressed air and/or mechanical brushing.

2.1.1 Touch trigger probes

The most commonly used probe is the Renishaw patented touch trigger probe invented in 1974. The touch trigger probe is able to perform a variety of tasks; initial job set-up, checking datum faces and general dimensions, in-cycle gauging, measuring tool off-sets and so on. In short, the probe transforms the machine-tool into a simple co-ordinate measuring machine [5].

The touch trigger probe essentially consists of a body and a stylus. The body takes one of two forms, which is dictated by the mounting method; spindle mounting (in place of the cutting tool in the spindle) or machine tool bed mounting. The stylus acts as an elongated switch lever which interrupts an electrical circuit when deflected from its neutral position. The signal is transmitted from the probe to the machine tool controller where the appropriate action is taken.

A spindle-mounted probe can be used to assess cutting tool wear by probing recently machined surfaces. Small dimensional deviations from those programmed can be sensed. Adaptive control techniques can then be applied which compensate for these small errors by introducing an off-set in subsequent machining operations. In the case of a probed dimension being outside a pre-defined acceptable limit, automatic tool replacement would be initiated by the management software.

Milling cutter breakage detection can be achieved in the following way using a probe mounted on the machine tool bed. The cutter is brought into range of the probe so that one of the cutting edges is just being sensed by the stylus. The cutter must then rotate one full turn backwards. The cutting edges are counted as they pass over the probe. Subsequently the number of cutting edges can be compared with the recorded value for that specific cutter. A problem tool can be detected and replaced.

In summary, electro-magnetic touch trigger probes are capable of rudimentary cutting tool wear and breakage detection. However, applications requiring an efficient and effective system are somewhat limited.

2.1.2 Optical techniques

Optical tool wear sensing devices utilise the light reflected from the wear land of a worn cutting tool as an indicator of tool wear. These techniques generally rely upon the higher reflective nature of the wear land compared with the unworn surface. The opto-electronic system reported by Giusti et al. [6], positions an optical probe with viewing window in front of the single-point cutting tools in a seven station turret lathe. Illumination is delivered by the probe and the resulting image, viewed through the window, is enlarged by a series of lenses and relayed to a Cathode Ray Tube (CRT) via a video camera. Measurements of the land wear width are taken directly form the video signal by means of a dedicated signal processing circuit. Values for the magnitude of wear land were noted to closely match those recorded when viewed under a microscope (for 95% of the cases considered).

Pedersen [7], developed a system for the *'Wear measurement of cutting tools by computer vision'*. The prototype system was designed to measure flank wear in a range of simple, single point turning tools. Like most computer vision systems a bright lamp illuminated the cutting tool at an optimum angle thus enhancing the wear features. An image captured by solid state camera was digitised into a rectangular array of intensity values. This digitised image was then processed by applying thresholding techniques on an IBM Personal Computer (PC) and a value for the flank (land) wear gained. In tests undertaken with the system, the wear measured by the system conformed with the traditional three-stage wear pattern normally observed in cutting tools (initial, steady-state and terminal wear). Limitations in the system were attributed largely to the optical lenses (aberration limited resolution). Similar work has also been reported by Matsushima [53].

Similar work was undertaken by Litu [8], in the development of a *'Computer vision approach to drill wear measurement'*. Close observation resulted in a new criterion being proposed for tool wear measurement of specialised multifaceted drills used in the production of crankshafts. Optimum results were gained by measuring the wear in terms of the flank wear area, rather than the flank wear width. In the purpose-built inspection system, illumination was supplied by two intense lamps. Under the illumination the flank wear area was clearly distinguishable due to the high level of reflectivity, when compared to the unworn surface. The vision system used to capture the image was based on a solid state charged couple device (CCD) camera. Once digitised the image was passed to an IBM compatible personal computer for data processing and feature extraction, where a general thresholding technique was applied. This offered the sharp contrast required to gain a measure for the area of wear. In conclusion, once calibrated, the vision system could measure the worn area much more efficiently than by using a tool-makers microscope with discrepancies not exceeding 5%. Also, the system was used to measure the progression of flank wear and by using a minimum risk principle based on the probability density function of the normal distribution, a threshold value was established to distinguish between usable and worn tools. Thus a good indicator was provided for shop-floor quality control of the drill, for subsequent use in an automated inspection system.

2.1.3 Radio-active techniques

Usually radio-active techniques to monitor tool wear involve the irradiation of the cutting tool, either generally or by local implantation. Wear measurement is thus based on the volumetric loss of cutting tool material.

A preferred technique is reported by Cook and Subramanian [9] which uses an exceedingly small amount of radio-active substance implanted in the flank face of the cutting tool a known distance from the cutting edge. After each cutting operation the tool is checked for presence of the radio-activity. The tool life is considered expired when the radio-active material cannot be traced. Limitations are apparent in that no account is made of the shape

of the flank wear. Thus the radio-active particle may reside in a zone which is affected more or less than the true measure. Similarly the system is not capable of accurately monitoring tool breakage or chipping in areas outside that of the implant.

Total irradiation techniques have also been investigated Codling and Erwall [10]. Typically, the radio-active level of the cut metal chip underside is measured and is then correlated with the amount of irradiated cutting tool flank face material carried away with it. High levels of accuracy are claimed for this arrangement. Despite claims of the technique being more accurate than conventional methods, slow response times, safety and general unsuitability to industrial environments cause doubt to be cast over this technique as a viable method of condition monitoring.

From a radiation hazard viewpoint, the micro-isotope method is considerably safer than the total irradiation technique. Complications are stacked against this latter option when tool storage, cleaning and waste disposal are considered. Customer acceptance of these types of system for tool wear assessment is most likely to be the limiting factor.

2.1.4 Proximity sensors

Several types of proximity sensors have been developed for detecting cutting tool damage [2], [4]. The majority being based upon inductive transducers. They usually operate by presenting the cutting tool to the sensor, which is mounted on the machining table. As a consequence the techniques are passive.

In a typical commercially available gauging station, Stauffer [5] proximity sensors are used to detect tool breakage whereas a contact switch is adopted for the automatic measurement of offsets. As with most systems the tool is cleaned prior to inspection with a directed blast of high-pressure air.

Another form of sensing device uses the measured variations in air pressure developed by minute changes in the gap between an air delivery nozzle and surface of interest. An application of this method is presented by Jetly [11].

2.2 Active cutting tool condition monitoring techniques

Real-time sensing is becoming ever more important in the competitive world of manufacturing. Attempts to maximise productivity and efficiency have never been more concentrated. Thus, in-process monitoring techniques are seen as highly desirable by enabling the machine tool to operate undisturbed whilst cutting tool condition is being assessed. Some of the most frequently occurring methods of active cutting tool (on-line) monitoring are reviewed below.

2.2.1 Electrical resistance

A number of investigative studies have based their analysis on the fact that the increase in contact area due to cutting tool flank face wear results in a corresponding and measurable decrease in interface resistance. Electrical resistance of a conductive body is a function of its resistivity, length and cross-sectional area.

Wilkinson and McClean [12], developed a method based upon this observation. The method, developed for single point turning operations, required an alternating current of 15A to be passed through the interface of resistance approximating to 1mΩ. The resulting potential drop was monitored. Measures of interface resistance for a given amount of flank wear correlated well with those derived from the simple mathematical model used.

Electrical resistance methods are clearly more suited to continuous cutting operations, primarily turning. Lack of success with intermittent cutting operations is due largely to the presence of cyclic temperatures, and thus resistance, at the cutting tool/work-piece interface which is exaggerated in the presence of a coolant.

2.2.2 Tool post/work-piece displacement and work-piece dimensional change

Tool-post/work-piece displacement techniques attempt to monitor the retreating cutting edge resulting from the progression of cutting tool flank wear. This is achieved indirectly by sensing the displacement of the machined surface and noting minute relative movement towards the tool holder/post indicating the advance of wear. Work reported offers a wide range of approaches to this technique, which include systems based on electric micrometers, pneumatic gauges, ultrasonic and inductive proximity devices. On the whole such techniques have been confined to continuous turning operations, Micheletti et al [2].

A system comprising of a stylus and proximity device has been designed and tested by Suzuki and Weinmann [13], which is based on the tool-post to work-piece displacement measurement approach to tool wear monitoring. The work is reported in a paper entitled '*An on-line tool wear sensor for straight turning operations - design and evaluation*'. A tungsten carbide stylus fitted to a holder was free to move in a single direction against the action of a spring. Movement detected by a small eddy current proximity transducer converted deviations of the stylus and thus the work-piece into an electrical signal. Tests carried out on a heavy duty lathe, with cast iron as the work-piece material and a range of speeds and feeds applied, were successful. From the work undertaken it was concluded that:-

- The results were seen to correlate closely with those taken by direct measurement from the tool wear zone. Tool wear and failure were accurately monitored.
- The device, though limited to straight turning, was seen as an inexpensive method of cutting tool condition monitoring. However, it was further limited by not being suited to rough turning operations.

Systems based on this technique have been applied to active and passive situations. However from the reported work it is apparent that the majority of cases are associated with the former.

Many reports exist of systems designed around pneumatic gauges [5], [4]. Such systems tend to be used widely due to their non-contact approach. Fluid delivered through a nozzle placed at close proximity to the work-piece develops an increased delivery pressure due to restricted fluid flow. This back-pressure correlates well with the work-piece to nozzle clearance. Thus, small deviations in the work-piece dimensions can be sensed. Problems encountered due to the air viscosity increasing with increased temperature were overcome by the use of a water/oil emulsion, which in turn presented pressure control problems.

Many drawbacks are recorded for cutting tool condition monitoring by the tool-post to work-piece displacement techniques, Takeyama [14]. These include sensitivity variation due to changes in work-piece physical properties, step changes in work-piece geometry and undesirable effects due to the use of cutting fluids. Furthermore, additional errors may result from thermal expansion of the work-piece and misalignment of the spindle axis. It was also suggested by Takeyama, [14], that work-piece displacements are relatively small when compared with the increase in flank wear it represents, typically around 10%. Therefore, a small error in the work-piece displacement measurement can be significant when related to the cutting tool flank wear.

2.2.3 Cutting forces and associated parameters

Numerous investigators have attempted to relate the measurable changes in cutting force or spindle torque to the extent of tool wear, on the basis that an increase in cutting tool wear results in a corresponding increase in the forces required for metal cutting. By virtue of their nature, such methods are highly suitable for on-line tool condition monitoring systems and adaptive control techniques. Systems in this category are perhaps the most prevalent in manufacturing industry.

Cutting forces can be measured in a variety of ways:-

- Table sensors on milling and drilling machines and machining centres, [15]. Sandvik Coromant Tool Monitoring System, *Plate Sensor.*

- Feed force sensors, [16].

  Sandvik Coromant Tool Monitoring System, *Feed Force Sensors.*

- Evaluating the cutting forces from the spindle motor current, voltage and speed, [17]. Sandvik Coromant Tool Monitoring System, *Multi-channel Tool Monitor Unit.*

- Sensors built into the spindle bearings, [18].

  AMTRI, *Hydrostatic Force-Sensing for Spindles.*

Relationships have been developed which correlate cutting forces or the spindle/chuck torque (ultimately the electrical power consumption) with the tool wear. The force signals obtained can be processed in a number of different ways depending upon the application. It has been proposed that the curve showing the relationship between feed rate and feed force was sensitive to both crater and flank wear, Uehara [19]. Further investigations have been based on an inter-dependency between the main cutting force, the feed force and the cutting temperature, Colwell [20].

The use of measured spindle motor power to estimate wear and detect the end of useful effective life of cutting tools for vertical milling machines has been investigated, among others, by Constantinides and Bennett, [21]. Data gathered from tests using a High Speed Steel (HSS) cutting tool on a stainless steel work-piece was presented using a range of analytical models. The researchers concluded that only gross tool wear could be detected using the basic measure of mean spindle motor power consumption. However, changes in spectral energy in the fluctuating part of the spindle motor power consumption were linearly related to the wear rate of the cutting tool. Measures to detect the onset of tertiary (critical) wear were also offered. The analysis, though requiring involved computation, yielded promising results. It was implied that the range of tests undertaken was somewhat limited and full acceptance of the proposed models must be delayed until further work was undertaken. Other force monitoring techniques have also been investigated which include intelligent filtering methods for defect detection [52].

2.2.4 Acoustic emission

The analysis of acoustic emission signals (noise) generated during machining has been proposed as a technique by which fundamental aspects of the cutting conditions, cutting tool wear and damage can be monitored. This technique has been widely associated with turning though some success in milling has also been reported. Research suggests that there are two types of acoustic emission (AE):-

Continuous emission	Steady, low amplitude, high frequency emission. Due to plastic straining of the work-piece and rubbing between the work-piece and cutting tool.
Burst emission	Erratic, high amplitude, low frequency emission. Due to tool and work material fracture, collision and breakage of chips.

The frequency content of the acoustic emission signal produced by the cutting operation (typically in excess of 100kHz) is well beyond the range of frequencies usually associated with conventional machine tools. Therefore, acoustic emission methodologies could be machine tool independent, with the signal analysis relating to the cutting operation only. There have been several methods proposed for analysing the acoustic emission signals, with the aim of detecting tool wear/fracture.

Monitoring techniques have been based on:-

- A noticeable step increase in amplitude of the signal at the time of cutting tool fracture, Inasaki and Yonetsu [22].
- Measuring the burst type events which exceed a pre-defined threshold (count rate), Inasaki and Yonetsu [22]. The count rate being directly proportional to flank wear.
- The amplitude of the averaged signal which is proportional to flank wear, Kakino [23].

- An apparent relationship between cross-sectional area of the cutting tool fracture surface and the acoustic emission signal amplitude, Kakino [23]

Many other techniques also exist.

The development of a prototype piezo electric sensor for the real-time monitoring of tool condition has been reported by Robbins et al [24]. This technique relied upon monitoring the acoustic emission generated during the cutting process. A piezoelectric crystal film was attached to the reverse of a cutting insert. As a consequence of this arrangement, the dynamic behaviour of the insert induced stresses in the crystal which resulted in small but measurable voltages being developed across the device. Tests on the sensor suggested that it had a suitable bandwidth (from 10 Hz to 500 kHz) and, furthermore, the output voltage signal compared well with that taken from a proprietary acoustic emission transducer, [25].

Acoustic emission related to the cutting process is certainly an area of research being actively pursued (see Appendix I). Investigators have reported success in relating features of the signal to the cutting process, tool wear and tool fracture [63], [64]. Furthermore, sensor arrays (including acoustic emission) are now being integrated using neural networks to offer intelligent tool condition monitoring systems [66]. This technique may ultimately replace the hearing and judgement of the skilled machine tool operator.

2.2.5 Roughness of machined surface

As a cutting tool approaches the end of its serviceable life, a deterioration of the work-piece surface finish is usually apparent. A relationship between the cutting edge integrity and surface finish can be assumed to exist. As a consequence considerable research has been dedicated to this subject in recent years.

Methods developed for the on-line measurement of surface roughness are generally based on optical systems, though contact sensors have been reported [2], [4]. For system reliability and speed of response it is important that the monitored surface is that produced

by the previous revolution of the cutting tool/work-piece. This however presents a considerable problem to optically-based systems. To maintain accuracy and repeatability the machined surface must be kept free from dirt, swarf, coolant and oil. Though it has been quoted that in tests this can be satisfactorily achieved with the aid of an air jet, industrial unmanned applications to machining centres may present new problems.

Luk and Huynh [26], explored a technique for analysing the unique light scattering pattern produced by a machined surface, due to material properties and surface topography. Statistical parameters gained from the grey-level histogram frequency distribution of light intensities, of the digitised image, were used to classify the surfaces according to roughness and quality.

Surface roughness could be determined reliably by considering the histogram ratio of spread to height then by transforming this value through a calibration curve. Surface flaws in the form of scratches and indents caused the histogram to shift from uni-modal to bi-modal with a second peak occurring in the distribution. The form of the second peak was dictated largely by the size and severity of the flaws. In support of this, a measure of the histogram skewness indicated the presence of a flaw, with flaws converting the skewness sign from a positive to a negative value.

2.2.6 Crack sensors

It has been noted that in several cutting processes tools often fail due to fracture rather than excessive wear. To verify this, laboratory tests were undertaken on a modified ceramic cutting insert, Pekelharing [27]. The insert built up as a sandwich of ceramic and electrically conductive tungsten enabled small currents to be passed and the integrity of the insert monitored. Upon the development of a crack in the insert, the current sensing system signalled an alarm to the machine controller so that the metal cutting process could be arrested immediately. Though this system was not originally developed to actively monitor

cutting tool condition in an industrial environment, considerable scope exists for its further development and utilisation.

2.2.7 Cutting temperature

Considerable effort has been dedicated to developing and understanding the relationship between cutting temperature and cutting tool wear. The temperature attained whilst cutting has been noted to increase with cutting speed and furthermore controls the mode and rate of tool wear.

This observation has been used to good effect in the development of a system for maintaining a constant cutting temperature, Billett [28]. Work reported suggests that an increase in cutting tool life, of up to 50%, can be attained by the system, along with increased metal removal rates by maintaining constant cutting temperature. The ability of the system to maintain the cutting temperature effectively meant that the wear rate was also being kept constant, for greater metal removal rates with a given tool, after coolant was added to the cutting zone.

The most popular approach to these techniques rely upon the tool/work-piece thermocouple effect [29]. Disadvantages of this method stem from the stray EMF's generated in the moving parts of the machine and the difficult calibration process for the tool/work-piece thermocouple.

In summary, temperature measurement based techniques are obviously better suited to continuous cutting operations such as turning, where steady state temperatures are attained. Thus, milling-tool condition monitoring by temperature measurement does not appear to be practicable approach.

It is apparent from the aforementioned techniques and the results presented in Appendix I that considerable effort has and continues to be spent on cutting tool condition monitoring. Many avenues are actively being pursued in an attempt to find the optimum system in terms

of sensitivity and reliability. With this aim in mind the following chapters are dedicated towards the development of an optically based, passive cutting tool condition monitoring system. More immediately, the following subsections provide an introduction to the background and terminology upon which this work is based.

2.3 Laser scanning technology applied to cutting tool condition monitoring

Laser-based inspection techniques have been used widely in industry to solve a range of quality control problems. During the 1970's Brook, [30], among others reported on work undertaken on behalf of the Aluminium Federation and British Non-Ferrous Metals Federation. The principal objective of the work was to detect and classify surface defects in metal sheets and strip moving at speeds of up to 3 000 m/min. Subsequent contributions to this subject area have been regularly documented [31],[32],[33]. Further reported applications of laser-based inspection techniques have been comprehensive, ranging from (West and Stocker, [34]) '*The automatic inspection of cylinder bores*' through (Dewhurst and Swift, [35]) '*Recent advances in laser tooling for flexible handling systems*', which deals with minute plastic switch components, to, Glass [36]) '*Detecting defects in glass sheet*'. Further to these developments, and perhaps more relevant to the reported work, various systems have been proposed which monitor or intermittently inspect the wear of single point cutting tools associated with NC turning centres. The list below presents a limited selection of those more recently published;

Micheletti et al, [2], '*In Process Tool Wear Sensors for Cutting Operations*',

Giusti et al, [6], '*A Flexible Tool Wear Sensor for N.C. Lathes*',

Giusti et al, [37], '*On-Line Sensing of Flank and Crater Wear of Cutting Tools*',

Pedersen , [7], '*Wear Measurement of Cutting Tools by Computer Vision*',

Suzuki et al, [13], '*An On-line Tool Wear Sensor for Straight Turning Operations - Design and Evaluation*'.

Thus the ability of the laser inspection device to detect minute flaws has been well proven and widely applied, but not yet successfully to the inspection of multi-point cutting tools as typified by milling cutters.

The ultimate aim of having an active (on-line) monitoring system is being pursued with some vigour by Sandvik (See Sub-section 2.2.3). With the Sandvik system, the tools are monitored in-cycle for relatively major defects, including edge failure and gross wear. By adding a passive inspection device which screens cutting tools for small scale defects and otherwise hard to detect wear and thermal cracking, machined component quality and machine tool efficiency could be improved. It is proposed that the cutting tools be monitored, continuously, in-cycle and then inspected out of cycle once they have been returned to the local tool storage centre (carousel, chain conveyor or paternoster). Having been thoroughly inspected, the tool would be flagged as either suitable or not for re-use. With this arrangement, cutting tools could be guaranteed to be in optimum condition when automatically selected by a machining centre and thus help produce high quality components with superior surface finish which are right first time. These production criteria are vitally important to many manufacturing industries, particularly the aircraft industry with whom this research was pursued.

2.4 Cutting-tool formats

As a necessary precursor to the research work, a representative collection of cutting tools was gathered together. This aspect of the work was undertaken primarily at a leading British military aircraft manufacturing facility. The close collaboration and support of the company throughout the work resulted in a representative range of monolithic cutting tools being the focus of attention. This was due primarily to the company's commitment to monolithic form tools as opposed to insert tooling.

Despite long-term cost advantages of insert cutting tools, the complex forms and relatively small diameters demanded by the aerospace industry precluded their use on all but the

simplest of operations. Furthermore, and as a direct result of this, examples were far more difficult to obtain. Hence insert tooling was not the focus of attention in the reported work.

Two fundamental tasks took place at the aircraft manufacturing site during the early stages of the research. Firstly, the aim was to collect an assortment of monolithic cutting tools with a representative range of wear patterns and defects present. The range of defects addressed are introduced and discussed in some detail in the following subsections. Secondly, an inventory of the cutting tools stocked and used by the manufacturing facility was considered necessary to ensure that the tools being addressed were a genuine and representative sample. A report based on the stock levels and frequency of tool use was compiled and is presented in Appendix II.

2.5 Cutting-tool geometries and terminology

Amongst many other operational parameters the profile of the cutting edge is fundamental to the quality of the surface finish and dimensional accuracy of the work-piece it produces. The form of a typical cutting tool edge profile is illustrated below in Figure 2-1. Both the rake and flank (clearance) faces are seen to present themselves at angles (rake and clearance angle respectively) to the work-piece surface. Suitable angles are prescribed based upon cutting conditions, tool and work-piece material.

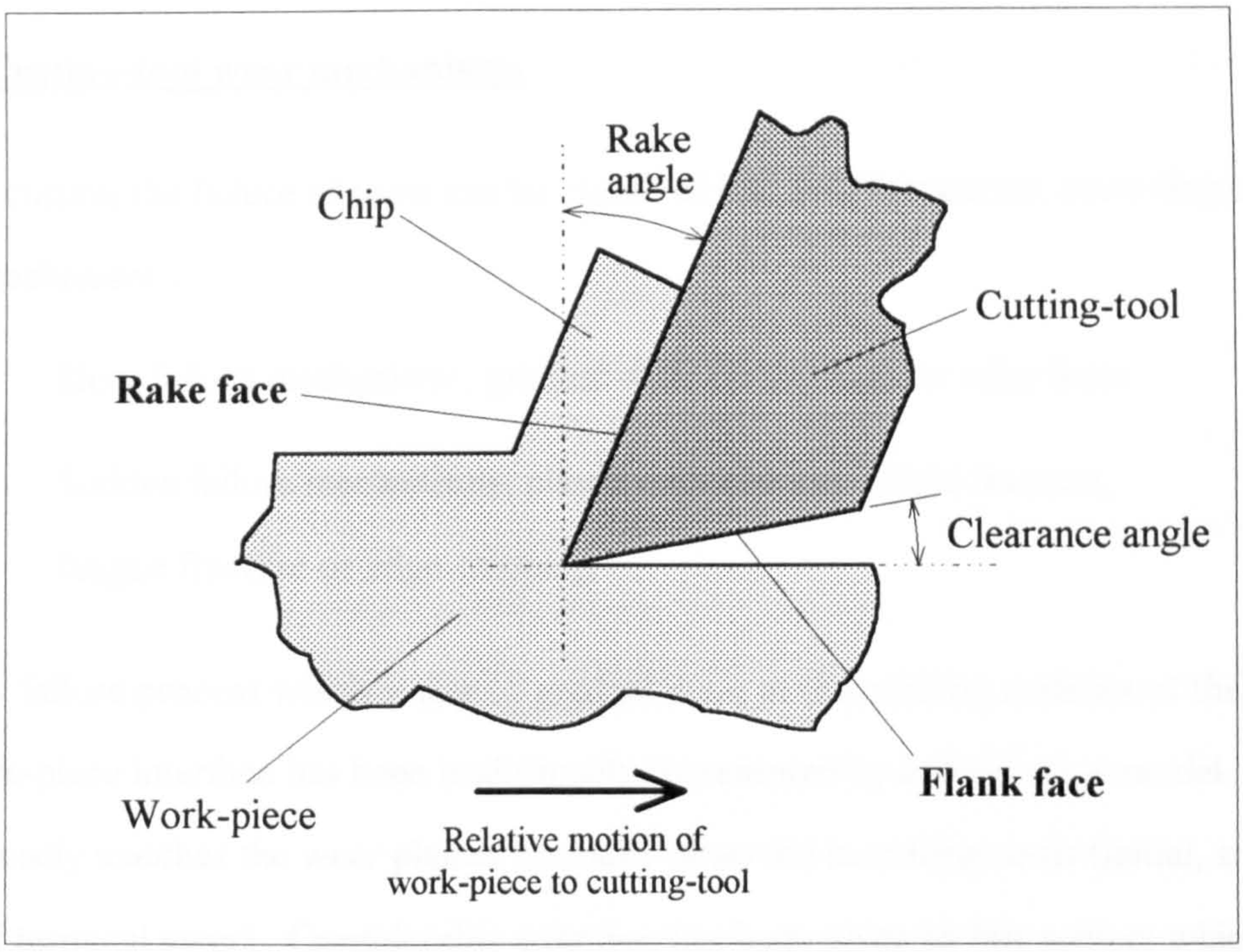

Figure 2-1 A typical cutting tool edge profile

The main geometrical features of a typical milling cutter are shown in figure 2-2 below.

The key features that have been referenced are; Shank, flute, chisel edge angle, helix angle, cutter diameter and shank diameter.

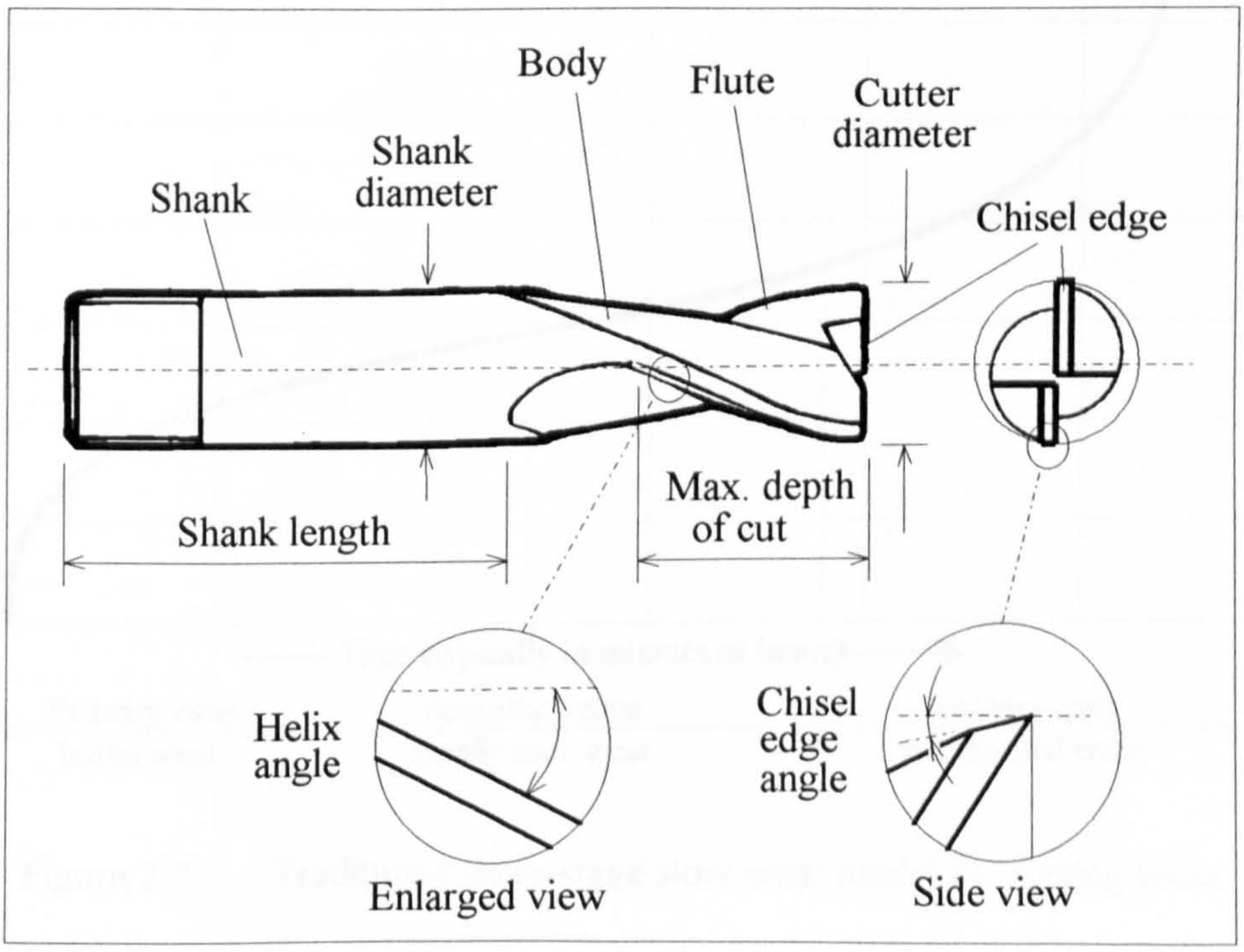

Figure 2-2 Main geometrical descriptive features for a typical milling cutter

2.6 Cutting-tool wear mechanisms

In metal cutting the failure of tools can be classified into two categories, according to the failure mechanism:-

- Slow failure mechanisms; gradual wear on the flank or rake faces
- Sudden failure mechanisms; plastic deformation, brittle fracture, fatigue fracture or edge chipping

The slow failure process which is due to gradual wear at the rubbing surfaces of the cutting tool/work-piece interface has been traditionally represented by a three stage model. The model closely matches the wear phases normally observed in cutting tools (initial, steady-state and terminal wear). Considerable attention has been given to this subject which has resulted in several life expectancy algorithms being proposed. However, it has been quoted by DeGarmo et al, [38], that "tool life should be treated as a random variable or probabilistically and not as a deterministic quantity".

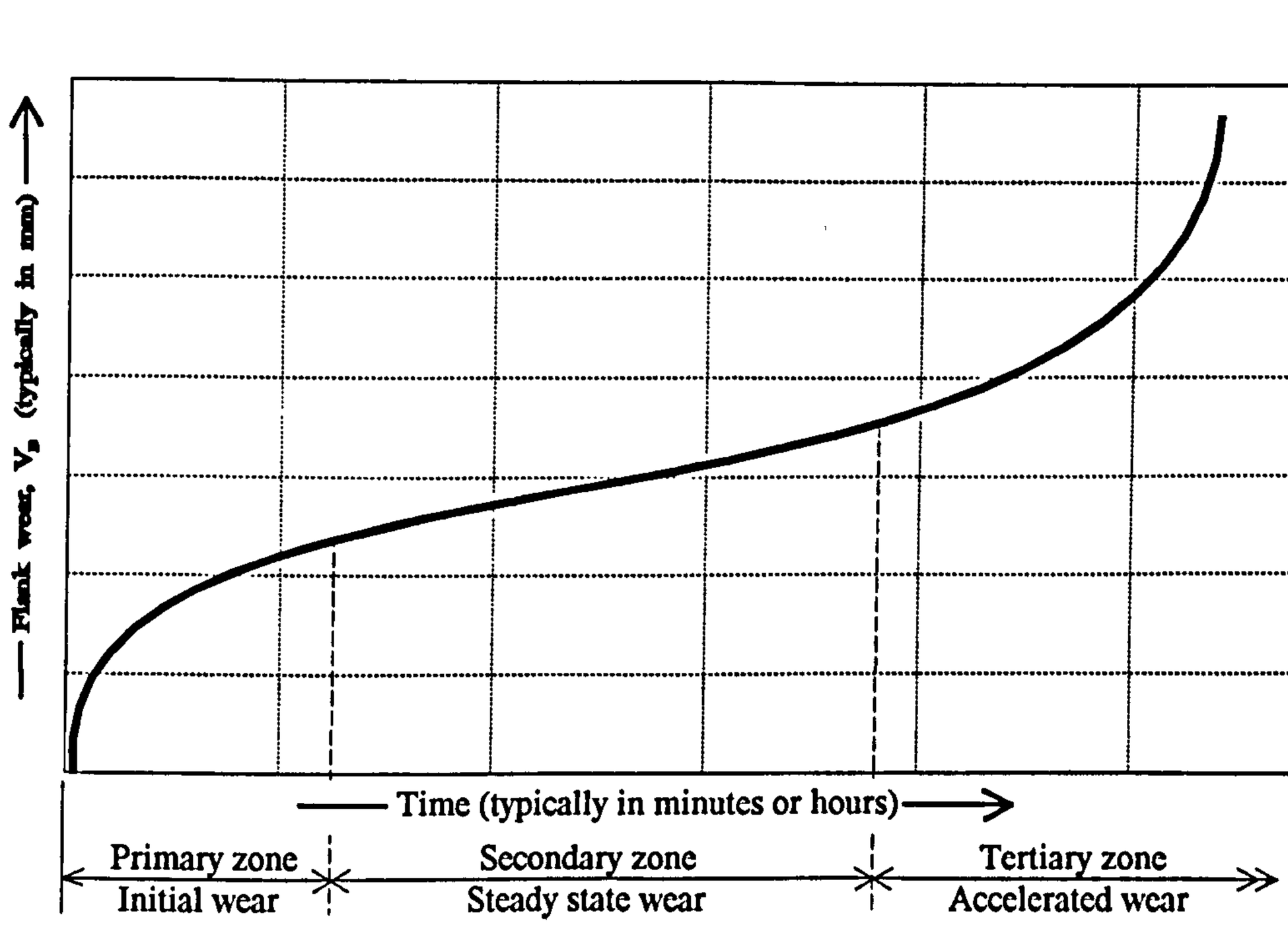

Figure 2-3 Traditional three-stage slow wear model for cutting tools

The most commonly encountered mechanisms associated with cutting tool wear and failure are introduced below:

Flank wear — Intense rubbing of the cutting tool flank (clearance) face against the newly formed work-piece surface causes the formation of flank wear (wear land, V_B). This is usually promoted by both abrasive and adhesive wear mechanisms. Clearly, despite being a normal wear mode it is undesirable due to its adverse effects on;

- work-piece dimensional control,
- work-piece surface finish,
- heat generation.

The recommended maximum allowable wear land, V_B, for various conditions is given in the table below. However, for improved dimensional accuracy and surface finish the values should be much reduced [62].

Allowable Average Wear Land (V_B) for Cutting-Tools in Various Operations		
Operation	High-Speed Steels (mm)	Carbides (mm)
Turning	1.5	0.4
Face milling	1.5	0.4
End milling	0.3	0.3
Drilling	0.4	0.4
Reaming	0.15	0.15

Table 2-1 Allowable wear land

Crater wear	Elevated temperatures in the cutting zone combine with high shear stresses to produce a crater, on the rake face, some distance away from the tool cutting edge. Wear of this type is usually quantified by measuring the depth of the resultant crater, K_T, or the cross-section area of the crater perpendicular to the cutting edge. Crater wear in itself is not damaging but in severe cases it can contribute to the promotion of catastrophic edge failure. However, when combined with a built-up-edge, crater wear can enhance cutting tool performance by effectively increasing the rake angle.
Edge rounding	The cutting edge may become rounded (dull) due to abrasion. This has an adverse effect on the cutting tool performance from the view-point of rake angle. As the edge becomes increasingly rounded the cutting action may cease with all energy being lost as elastic and plastic deformation of the work-piece and/or ultimately the cutting tool.
Edge chipping	In the extremes can be referred to as micro-chipping (small scale) and catastrophic failure (large scale). Micro-chipping most frequently results from the periodic break-off of the built-up-edge or when brittle tools are used in interrupted cuts. This may conclude in sudden, catastrophic failure of the tool. Work-piece surface finish obviously suffers as a consequence of edge chipping. Tools made from brittle materials (typically ceramics and carbides) are most prone to sudden, catastrophic (gross chipping or fracture) failure. Interrupted cutting processes such as milling promote failure of this type. Crater wear, edge chipping/cracking may contribute significantly to catastrophic failure.
Edge cracking	Thermal fatigue may cause hair-line cracks to form parallel or perpendicular to the cutting edge of brittle tools, resulting in sudden, catastrophic failure.

Chapter 3.0

Laser Based Imaging Techniques

3.0 Laser Based Imaging Techniques

In the introductory chapters it was noted that optical methods form a powerful, non-contact means for transferring physical information from an object or practical situation to the computer. Once inside the computer the digitised images can be processed to enhance visual features. Subsequent quantitative analysis may then be performed. It is this laser based inspection technique which is to be investigated in detail in the work that follows.

In the development of an imaging system for cutting tool inspection, technical information spanning several subject areas was investigated. The following chapters draw together some of the most pertinent points gathered together during the period of research. The information has been grouped to form three sections relating to; lighting and viewing techniques, solid-state image sensors and data capture/analysis.

3.1 Lighting and viewing techniques

In any visual inspection system the quality of the light source is paramount. Key features may be lost due to glare or a lack in intensity or uniformity. Specially modified light may have to be utilised, polarised for example, to achieve desired goals. Light is normally unpolarised and the effects of varying the lighting by polarisation and other ways can be quite dramatic.

The main characteristics of a lighting source are listed below:

- Spectral distribution
- Colour
- Power output
- Physical size
- Radiation pattern (point, line, hemisphere)
- Light distribution within radiation pattern (homogeneous or amorphous)

All of these characteristics were taken into consideration during the development of the cutting tool inspection device.

3.1.1 Methods for manipulating light

There are four main ways in which light is directed or modulated to carry information. These are: reflection, refraction, diffraction, scattering. The first three are controllable.

Reflection - Reflection is the redirection of light by the surface of a component. The light is reflected in accordance with the surface profile (concave, convex, plane). Surfaces which reflect light are often referred to as specular. Little information can be gained optically from a specular surface.

Refraction - The effect of deflecting light as it passes from one optical medium to another of different density. An optical lens depends upon refraction to direct light to a focus. The optical medium must, of course, be transparent.

Diffraction - Diffraction effects are both wavelength and phase dependent. An optical grid placed in the path of coherent light produces diffraction patterns, light and dark bands of constructive and destructive interference. Diffraction techniques are most readily applied to laser light as a result of its well-defined wavelength and phase.

Scattering - Light scattering is the most common optical process in nature and is the process by which light is returned from the surfaces of objects, enabling us to see and inspect them. The scattered light contains a vast amount of information about the shape and nature of the surface scattering it.

In the development of an inspection device it is optimisation of the optical system configuration, leading to enhanced information extraction (from the laser scattered light) which forms the basis of the research work undertaken.

3.1.2 Coherent Optical Techniques

In the mid-sixties the first systems based on laser (coherent light) scanning technology were introduced in to industry. By the end of the nineteen-eighties it was estimated that there were more than one thousand scanning systems operational world-wide Schmalfuss [39]. This is thought to be a conservative figure and obviously does not include non-industrial applications such as Compact Disk (CD) players.

System configurations for subject illumination and response sensing are usually dictated by the subject. In this context, most applications of laser scanning technology to surface analysis through light scattering are achieved with the basic V-scanner arrangement of Figure 3-1. Efforts have been made, within this field, to formulate a basic understanding of the fundamental, V scanner operational characteristics [54].

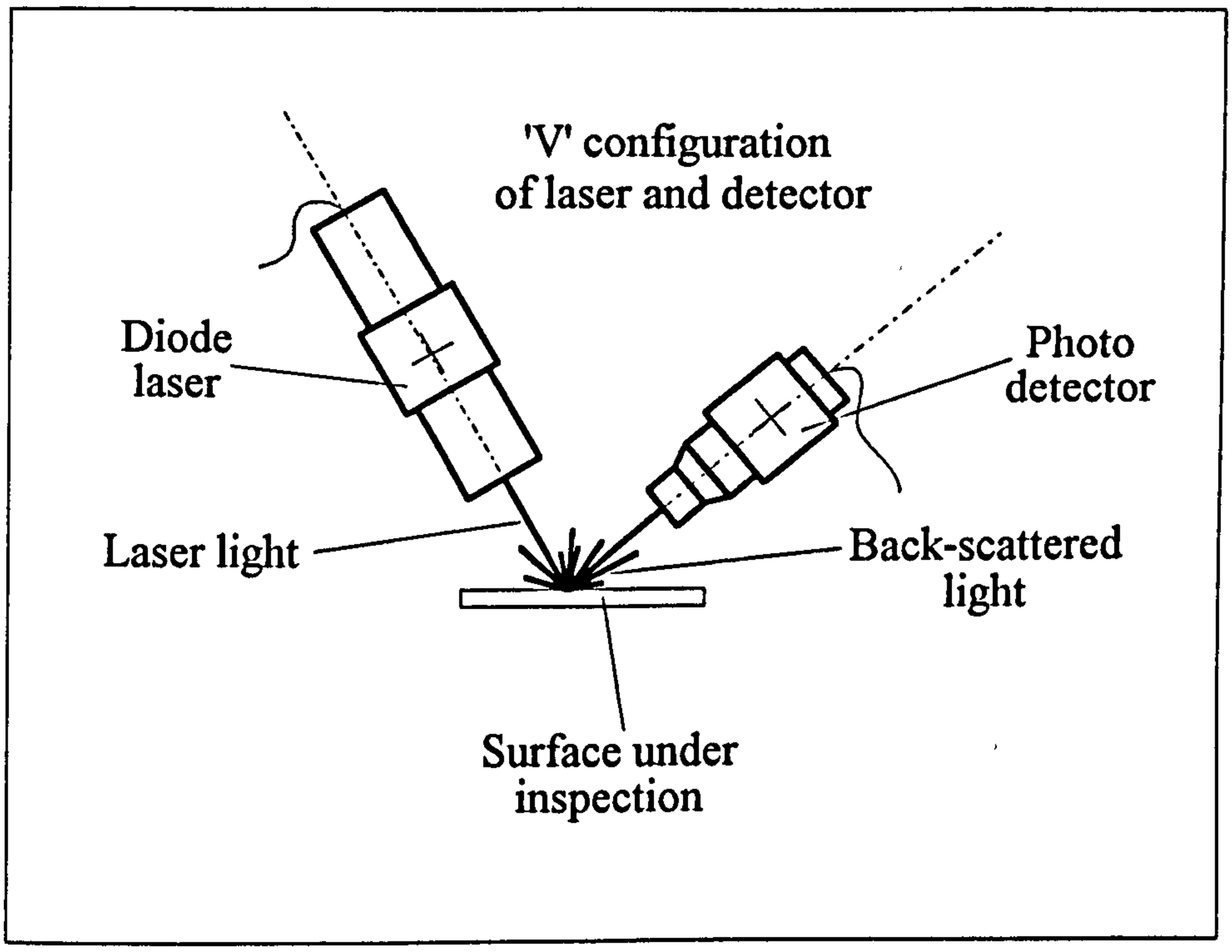

Figure 3-1 The basic laser-base V-scanner for surface interrogation

Coherent optical techniques have been applied to a wide range of industrial inspection duties. The limitations and scope of such systems have thus been clearly defined, Schmalfuss [39], and are summarised below;

- Scan-surface length: up to *'endless'*,
- Scan-surface width: up to several meters,
- Scan-surface speed: several hundred metres per second,
- Defect/feature size: 1/4000 - 1/20 000 of scan width,
- Material: wide range of metals, wood, rubber, woven and non-woven fabrics, paper, foils (different types), coated foils (e.g. light sensitive film), ceramics.
- Surface structure: with or without texture, reflective or diffuse, transparent, translucent or opaque,
- Environmental conditions: water spray, oily, dusty, vibrations, electronic and magnetic influences, stray light.

Optical surface texture monitoring offers a fundamentally different approach to surface assessment from the traditional stylus methods. Optical methods average (integrate) an area of a surface which may include several textural features, whereas a stylus would measure spatial and height details of the hills and valleys along a line between two arbitrary points. From this view-point it could be said that the optical technique is more appropriate as it samples an area; the stylus method is corrected by averaging several passes. The major difficulty however is that of obtaining specific information on a single feature from the vast amount of combined data in the sampled scattered wave front.

Non-contact optical surface measurement is possible using equipment supplied by such companies as UBM Gmbh, Germany. It is debated in metrology circles which system offers the most accurate results. However the optical system (*Microfocus*) has distinct advantages when it comes to measuring sensitive or fragile surfaces and as a result the system has its own niche market. The *Microfocus* system operates on a simple optical principle. A beam

of convergent laser light is shone, normally, at the sample surface. The laser scattered light is sensed by an optical detector. Minute adjustments are made to the laser light source focusing system so as to maximise the strength of the signal at the detector (focal point coincident with the inspected surface). The linear displacement of the lens is achieved by means of energising an electrical coil. The lens displacement is thus proportional to the applied voltage. Similarly the inspected surface elevation at a specific point is also proportional to the voltage. By sampling at consecutive locations along a straight line path a picture of the surface profile can be constructed. This arrangement is an exact copy of the CD player laser focusing system [40].

In a parallel but independent activity, Teague [41] suggested that laser speckle pattern correlation methods would be the most suitable technique to apply in the development of surface interrogation and analysis system.

Research in this and related areas continues to thrive (see Appendix I). Basic work on the light-scattering mechanisms and necessary theoretical models need further development before being applicable for broader measurement purposes. It is this area, related to cutting tool condition monitoring, that the reported work attempts to address.

3.2 Solid-state image sensors

Several years ago, because of the complexity, fragility and geometric instability of electron beam tubes, such as TV camera tubes, the idea was conceived of using arrays of solid-state photo-diodes arranged in the form of a matrix. In the 1950s and 60s, systems incorporating arrays of large discrete photo-diodes began to be used in such applications as surface inspection and width measurement. The advent of silicon integrated circuit technology enabled the manufacturer to arrange a large numbers of tiny photo-sensing elements on a single silicon chip. Further advances resulted in the scanning control circuits being integrated onto the same chip, resulting in a compact and easily managed device. In the late 1960s the first commercial, self-scanned photo-diode array was produced. Development

has continued at a tremendous pace resulting in a wide range of competitively priced imagers being readily available. The most common format being the Charged Couple Device (CCD).

3.2.1 Properties of solid-state sensors and arrays

There are several characteristics and limitations associated with the various configurations of solid-state image sensors. The less sophisticated single-site examples are on the whole free from many of the limitations which are apparent in the more complex multi-site units. It is considered to be of foremost importance to understand these limitations and know what can be achieved with the various classes of technology immediately available. With this in mind the following paragraphs highlight some of the problems, and introduce basic terminology which will contribute to the reader's understanding in the subsequent development of the reported work. Campana, [42], reported on techniques suitable for the evaluation of charged couple imagers.

Integration

A solid-state array is an example of an integrating detector, in that each element accumulates signals generated by the light falling on it, between one readout cycle and the next. In a linear array this means that each element accumulates signals for virtually the whole of the line scan time, and in a two-dimensional array for virtually the whole of the frame scan time. This means that their sensitivity is proportional to both the light level and exposure time. As a result, if an array is scanned at a very fast rate then a very high light level will be needed to produce the same signal which could have been achieved by a lower light level at a slower rate. The implication of this in industrial inspection is that the light level requirements for the inspection system will increase as the productivity increases.

In contrast to this, a single site photo-diode simply takes a snap-shot reading of the light level at the instance when it is scanned.

Saturation

As each element has a finite capacity, saturation occurs after a certain amount of light has fallen on the photo-sensitive surface. Output signal linearity is good at low levels but falls away before saturation. Typically, if high levels of signal linearity are required then the sensor should not be operated above 70% of its saturation value.

Dark signal

The action of incident light is not the only mechanism which generates a signal within the sensor. Temperature has a signal producing effect, which is indistinguishable from the photo-current. Thermal leakage current produces a 'dark signal' which is dependent on temperature. In an array, the dark signal produces an element-to-element non-uniformity which can be a severe performance limitation in simple instrumentation, when calibration is not feasible. As with the light-induced signal, the dark signal accumulation is proportional to exposure time. This is not a problem when using fast scanning rates but increases to be such as the rate is reduced. Therefore, large two-dimensional arrays, which as a result have long integration times (scan times), are affected the most. The remedy of cooling introduces additional cost and complexity to the system.

Non-uniformity

The existence of non-uniformities in signal level causes major problems with solid-state arrays. Non-uniformities exist in the form of response of the elements to light and the amount of dark signal generated. For critical applications there is a need to calibrate the device, resulting in an increase in cost and complexity. Non-uniformity is very dependent on colour. It generally increases as the wavelength of the light increases, so red wavelengths produce greater levels of non-uniformity than blue wavelengths.

Cross-talk and surface structure

The elements in a solid-state array cannot be considered as completely separate photo-detectors. Due to the methods of construction commonly used, cross-talk occurs between adjacent and some times distant elements. This is made worse when light of longer wavelengths is used, such as red light, which penetrates far deeper into the silicon than does blue light. Cross-talk between elements is very dependent upon the colour of the incident light and increases as the wavelength increases. The cross-talk reduces the contrast in the fine detail of images reproduced by a sensor.

Spectral response

The basic spectral responses for two common detector materials are shown in Figure 3-2.

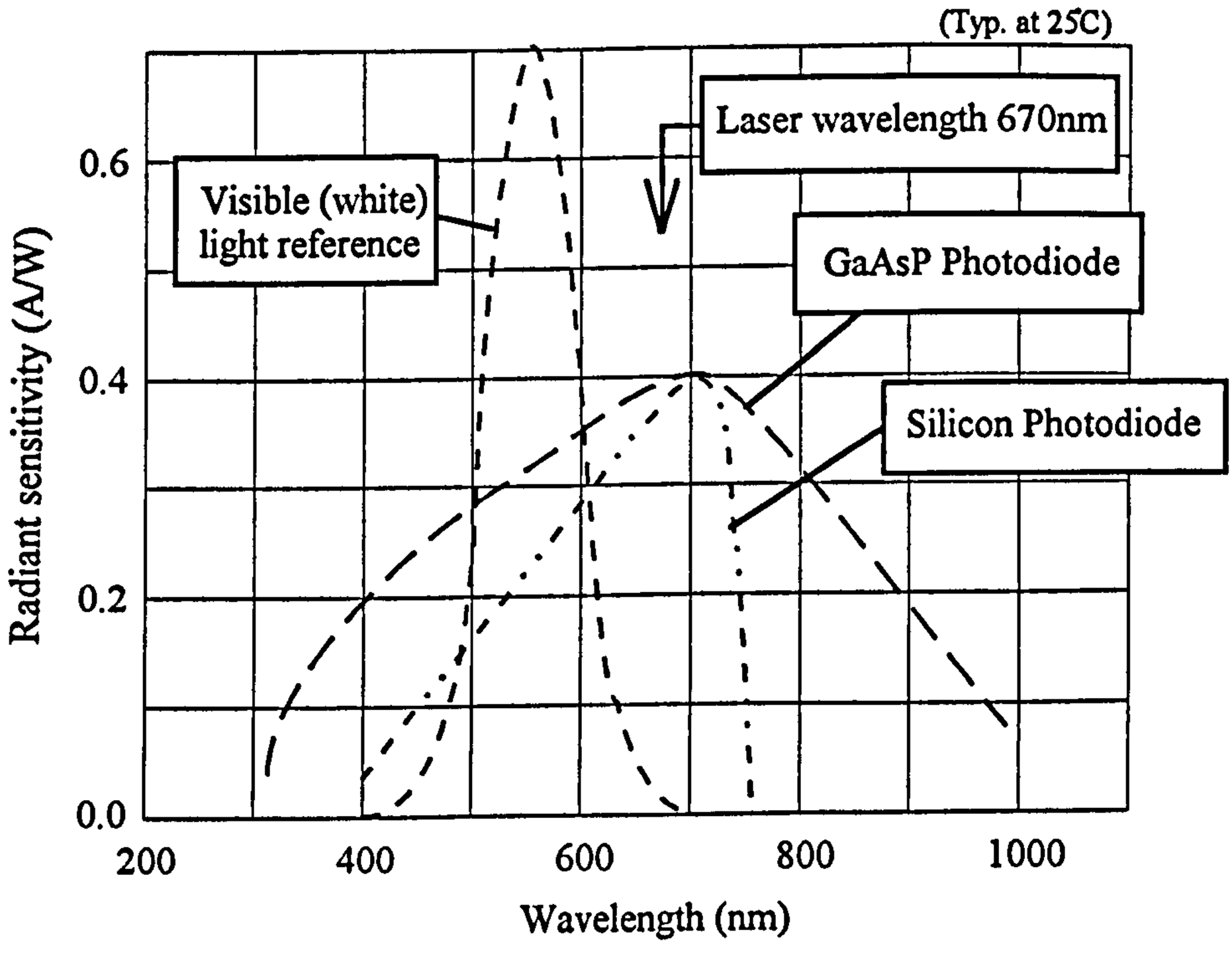

Figure 3-2 Sensor spectral response to light [55]

For the most common, silicon, the peak is usually in the near infrared, and the response is biased towards the infrared wavelengths. Using silicon sensors will produce a very red-sensitive system. Earlier it was stated that cross-talk between elements is very much worse

in the infrared wavelengths than in the visible. In high resolution applications it may be necessary to filter out the longer wavelengths by means of an infrared blocking filter. However, in some applications, this could reduce the signal strength by a factor of two or more.

3.2.2 The available forms of optical sensors

Several formats of opto-electronic sensor are currently available in the market place. Those which are most commonly used and considered appropriate to the envisaged application are introduced below.

Single site photo-detectors

Single site sensors are generally used where picture resolution exceeds approximately 1000 points per line or when high volumes of data are gathered and must be processed at speed. In high-speed applications, laser scanners must be used in conjunction with a single site photo-sensor. In this arrangement the light source is swept across the surface to be interrogated. The sensor, equipped with appropriate optics, is manipulated so as to capture the reflected light and thus produce an instantaneous response signal. The response signals are sampled at a predetermined rate (related to the scan rate and defect/feature size) so that subsequently an image can be formed. Work reported by West [32], entitled '*Laser Scanners for Automatic Inspection of Strip Products*' describes the use of a single site photo-detector as part of a laser scanning system.

Linear arrays

Many industrial inspection problems require only line scanning, since the part or product may be viewed as it moves along a transportation system, such that an image can be built-up line by line as it passes the imager. Photo-diodes arrays are often a better choice for linear scan applications, except where extremely high clock rates of 20 MHz and above are required, in which case only CCDs are fast enough. A typical application of a linear array to

image acquisition is described by Yanagi et al. [43], in '*A Practical Method of Optical Measurement for the Minute Surface Roughness of Cylindrical Machined Parts*'.

Virtual linear arrays

Like the conventional liner arrays the virtual linear array is suited to methods based on line scanning. The virtual array configuration, however, enables the imager to follow complex, even 3-D curved paths. This is achieved by the use of a single site photo-detector which is incrementally moved then sampled repeatedly between the two points at the start and end of the line of interest. In this way a line scan image is constructed. To support this technique a suitable electro-mechanical device is required to orientate the object and scanner also to make relative, incremental, moves during the scanning cycle. Due to the detector hugging the surface profile whilst scanning (contouring) this configuration is restricted to components supported by adequate information of surface geometry.

Two-dimensional arrays

Two-dimensional arrays are most commonly found in video cameras. Their application to a broad range of imaging techniques is widely reported [6], [44].

An illustrative example of the use of a two-dimensional array is presented by Pedersen [7], in his work '*Wear Measurement of Cutting Tools by Computer Vision*'.

The merits along side a wide range of applications of the two-dimensional CCD array are presented in the text *'Automated visual inspection'*, Batchelor et al [45].

3.2.3 Comparison of the CCD imager and line scanner

Solid-state imaging (CCD) cameras are compact, robust, long-lived, reliable and fundamentally advantageous when simultaneous dimensional measurement is required, but are unable to compete with laser scanners for resolution, sensitivity and through-put speed, Purll [44].

The main strengths and weaknesses of the CCD imager and line scanner are summarised and compared in the table below, Schmalfuss [39].

Characteristic	Laser Scanner	CCD imager
Spatial resolution	high*	medium
Scan frequency	high*	medium
Scan length	medium	high (multiple CCDs)
Colour detection	no	medium
Interface problems	yes	no
Energy density (J/m^2)	low	high
Illumination aperture	fixed	variable
Receiver aperture	variable	variable
Receiver sensitivity	high*	low
Mechanical complexity	high	low
Optical complexity	high	low
Maintenance	not applicable	medium

Table 3-1 Comparison of the laser scanner and CCD based imager

For the cutting tool condition-monitoring application the most suitable imaging configuration was identified as the V-scanner. This decision was based on several considerations;

- Inherent operational characteristics, most suited to the application (Resolution, sensitivity and suitable for complex surface scanning techniques - see starred (*) items in above table). Most notable was the sensitivity advantage offered by single site sensors over arrays. As the subject matter was usually low contrast and minute this was considered to be of paramount importance.
- Cost and availability of prototyping sub-systems
- Previous in-house work on V-scanners
- Inspection data rates (refer to sub-section 3.3.3)

3.3 Image acquisition and processing techniques

In the system under development surfaces are interrogated by illuminating them with visible laser light of wave length 670 nm. The surface interaction with the incident light causes a change in one or more of its characteristics. These changes are sensed and processed to yield the desired information about the surface. The following sub-sections address a range of methods by which response signal features can be detect, extracted and analysed.

3.3.1 Defect and feature detection in coherent illumination

Edge detection

Under coherent illumination the intensity profile of reflected light from across a well defined, sharp edged surface, is very different to that for incoherent light. Refer to Figure 3-3, below (Batchelor et al. [45]).

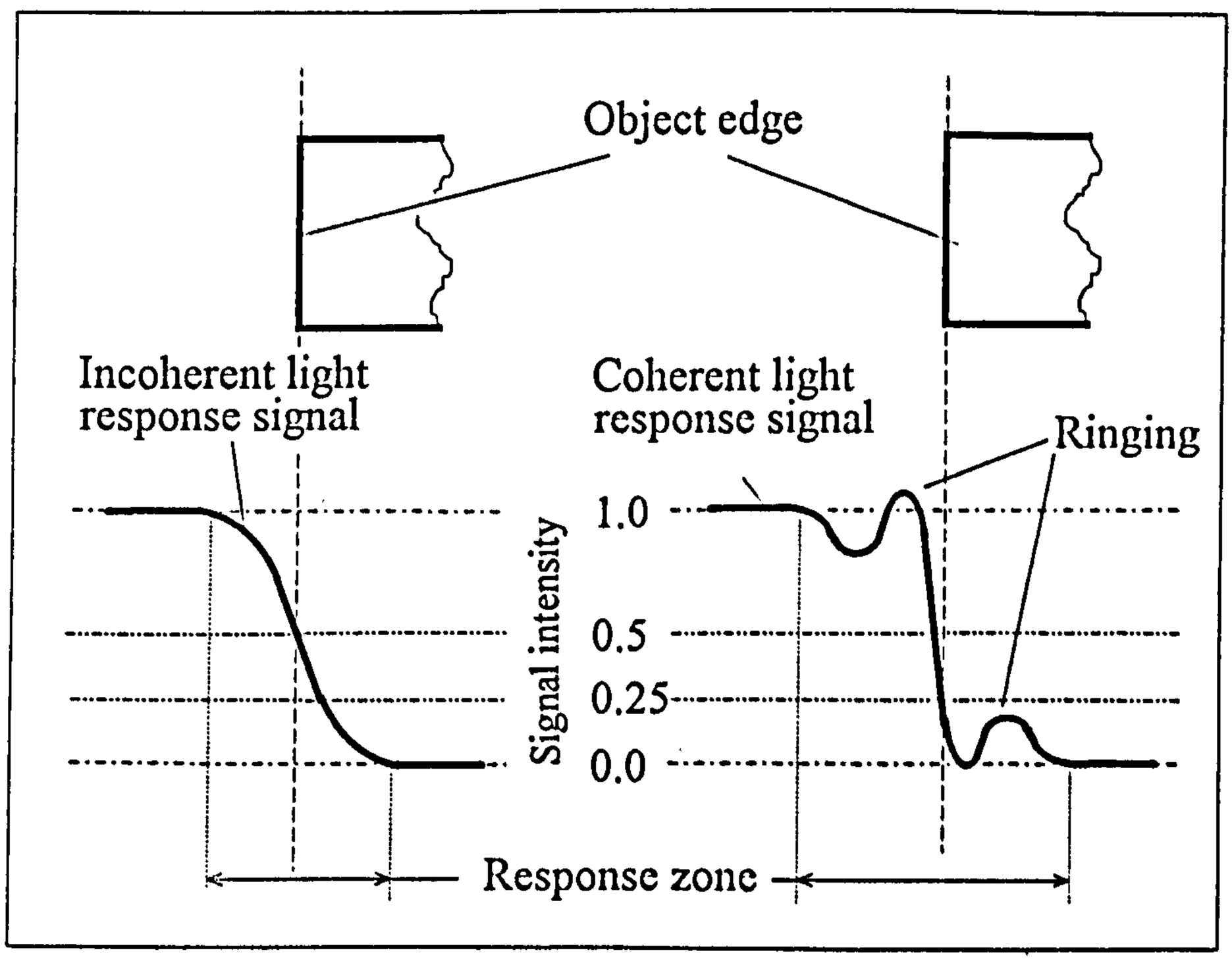

Figure 3-3 Edge detection using incoherent and coherent light sources

With coherent light the true edge is indicated by the 25% intensity point (threshold) whereas for incoherent light the value is 50% of full intensity [45]. The edge definition is about twice as sharp as for incoherent illumination, but is more prone to distortion when spurious reflections occur due to thick or rough edges. The undulations seen on the coherent signal (ringing) at top and bottom is a natural phenomena but can become a problem when viewing closely situated edges.

Errors are introduced into the true edge location by:

- Lens aberrations
- Electronic noise
- Finite resolution of the detector unit
- Non-square or otherwise imperfect edges

Defect Detection

Under certain conditions surface defects can give rise to absorption, scattering or deflection of the incident light and thus reduce or increase the amount specularly reflected. Such defects therefore manifest themselves in the response signal as pulses. By this reasoning, rapidly changing response signals (pulses) are the immediate key to locating and identifying the very defects they emanate from. Once a response signal has been captured, defect detection is initiated in the following way.

The signal is compared directly against a reference signal (see sub-section 4.1.3 Data capture, evaluation and display sub-systems). If the response signal crosses the reference signal, a defect is registered. This analytical approach is referred to as thresholding. The cross-over is easily detected through the use of a proprietary digital signal processing software package or by simple, dedicated software routines. A distinct advantage of the software based approach is that it supports simple attenuation (vary offset) of the reference signal, which can be changed to offer a range of sensitivity. Thus, as pulse amplitude is loosely related to defect severity, a measure of this severity may be obtained by utilising increased levels of reference signal attenuation. As indicated earlier, the laser scanners used

in the reported work do not respond directly to the surface profile, instead they portray the surface reflectivity which is not necessarily related to profile. Reduced reflectivity may be caused by absorbing defects such as localised variations in the degree of surface polish, or irregularities in the surface profile, such as chipping. Therefore, a system based entirely on the thresholding principle will be unable to distinguish between these types of defect and furthermore should not be seen to give a measure of the 'depth' of a defect.

Because of the attenuation, the crossing points between the response signal and the reference can never enclose the entire defect wave form. This is most apparent when the defect signal just crosses the reference.

In an attempt to overcome this deficiency the response signal can be compared directly with the unattenuated reference. Many crossings will be apparent but all may be disregarded except for the ones which bracket the attenuated reference crossings.

Phase and registration

Solid-state image sensors are sampling detectors. They divide an image into a number of discrete boxes corresponding to the photo-cell geometry and sampling interval. Detailed information contained within each box (site) is lost. Thus, the signal available from each site represents the integration of all the light falling on that site. This has serious implications when fine detail is to be extracted from an image, particularly if it consists of a regular pattern, a single edge or spot occurring within a very uniform background. During the development of an imaging system it is imperative that the internal mechanisms, limitations and potential solutions to such phenomena are clearly understood.

Subsequently, to ensure reliable and accurate system performance, the system design specification must accommodate such fundamental observations and associated rules. With this in mind, these and other interrelated aspects are introduced and discussed below.

Fundamental sampling theory suggests that a detector can only give useful detailed information about features/patterns which have a spatial frequency of half that of the

sampling interval or array structure, Meade and Dillon [46]. This can be reiterated as, 'the maximum frequency of an alternating black and white bar pattern, which can be reliably reproduced by a sensor, is one black and one white bar for every two sampling sites'. This spatial frequency is called the Nyquist limit.

With a sampling detector, the spatial phase between the image and the detector must also be considered. The reason for this is best represented by an illustration. Figure 3-4 (a) depicts a square wave bar pattern at the Nyquist limit of a linear array. When the pattern is in-phase with the array, it is reproduced in high contrast. When the pattern is in spatial anti-phase with the array elements at the Nyquist limit frequency, zero contrast is obtained, Figure 3-4 (b). This is due to each sampling site viewing half a white bar and half a black bar.

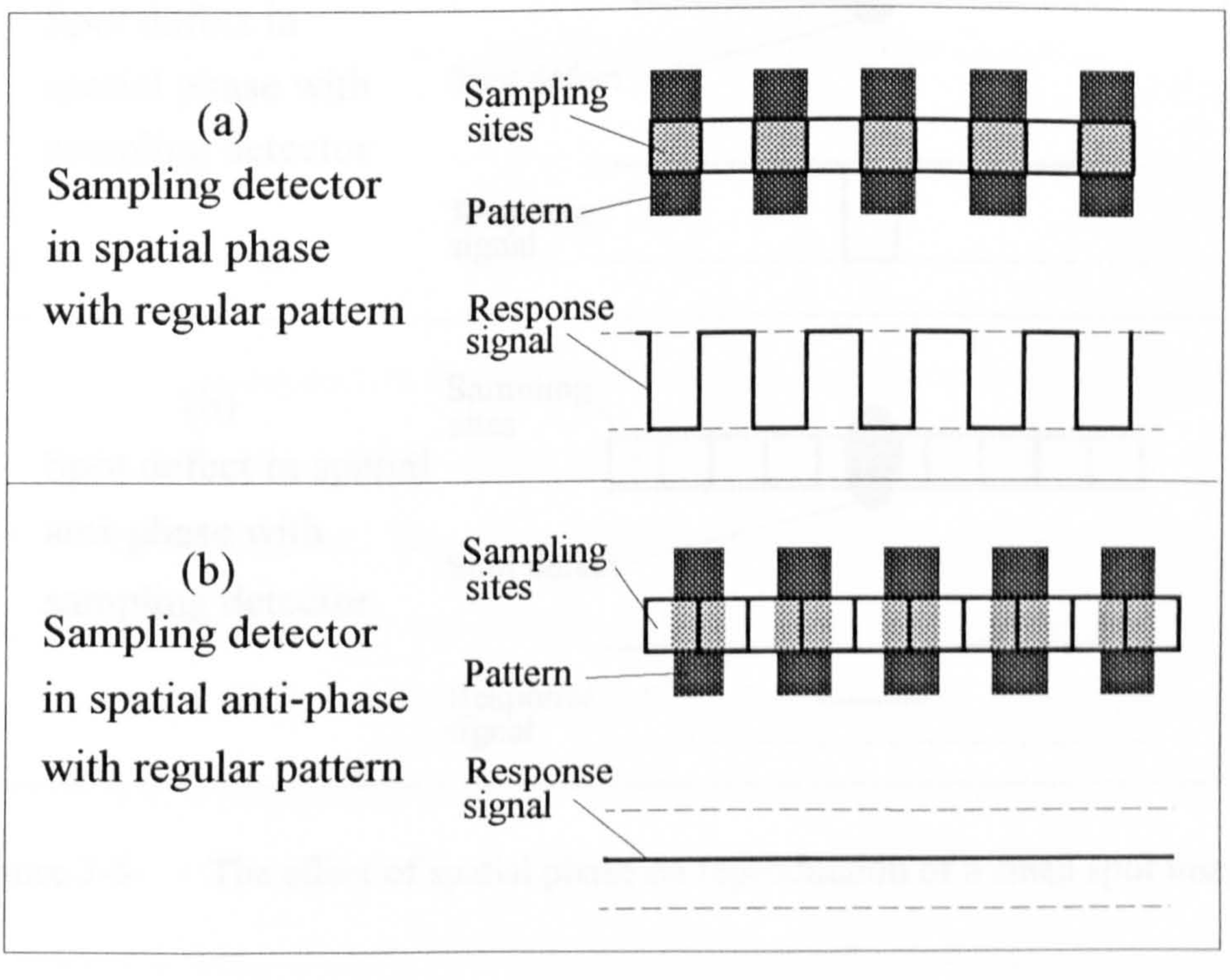

Figure 3-4 The effect of spatial phase on reproduction of a Nyquist limit pattern

For intermediate phase conditions the resulting contrast would be somewhere between the conditions described above. Below the Nyquist limit, except at sub-multiples of it, the

spatial phase relationship between the regular features/pattern and the sampling sites would vary. The contrast of the reproduced pattern would be seen to vary in sympathy.

The situation is quite different for an image that consists of a spot on a plain background. For a spot size equal to a single sampling site (half the Nyquist limit for the bar pattern) the situation is depicted in Figure 3-5. When the spot is in-phase with the element structure a single element is affected. This exhibits a strong contrast to the adjacent elements. The contrast is reduced and is distributed over two elements, suggesting an increased spot width, when the spot is in anti-phase with the sampling sites. Unlike the bar pattern the contrast never falls to zero.

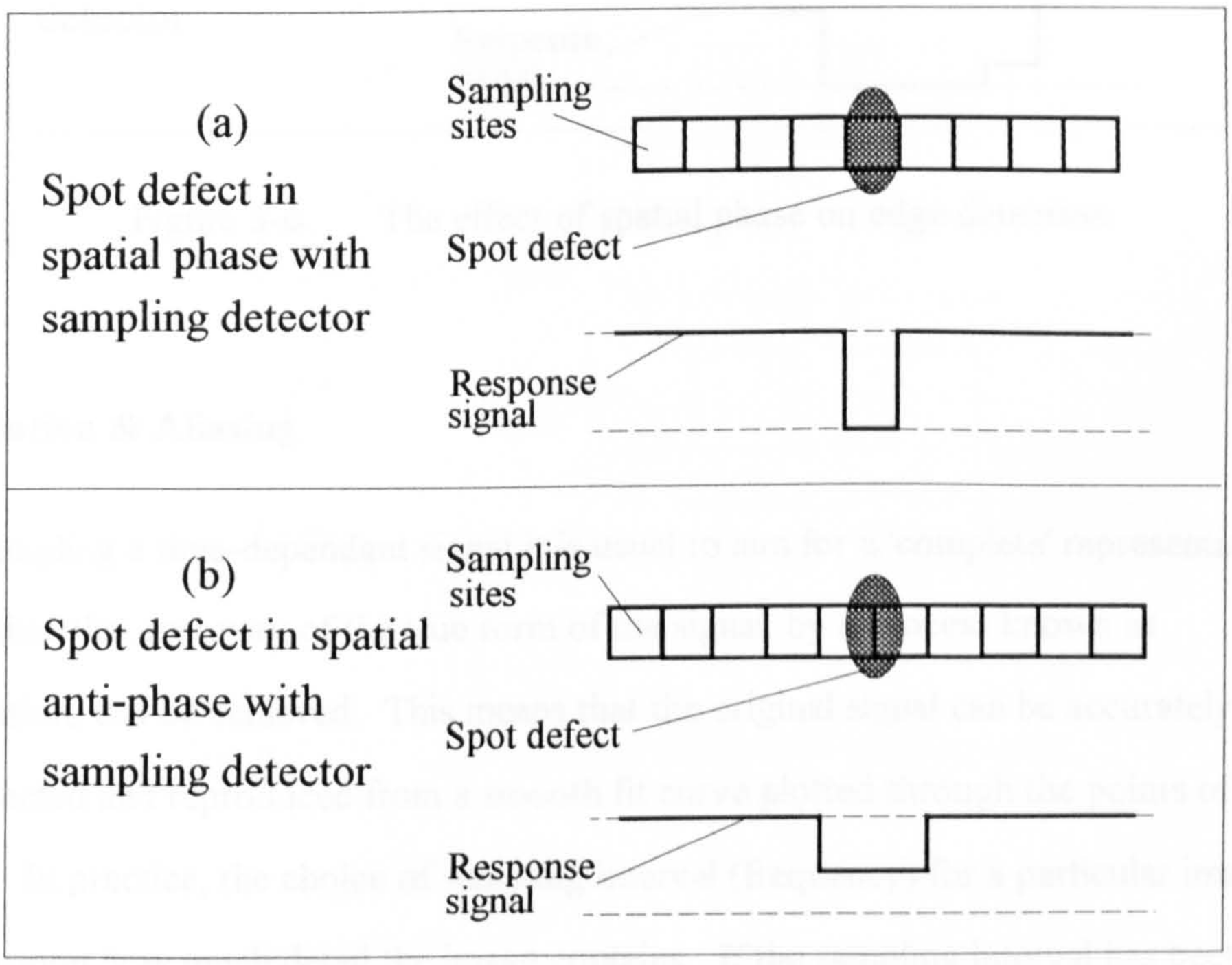

Figure 3-5 The effect of spatial phase on reproduction of a small spot image

The third case for feature analysis is edge detection. In all cases of spatial phase the edge can easily be located. However, the relative position of the edge and the sampling site structure can cause a one site uncertainty in the measurement of the edge position. Figure 3-6 illustrates this.

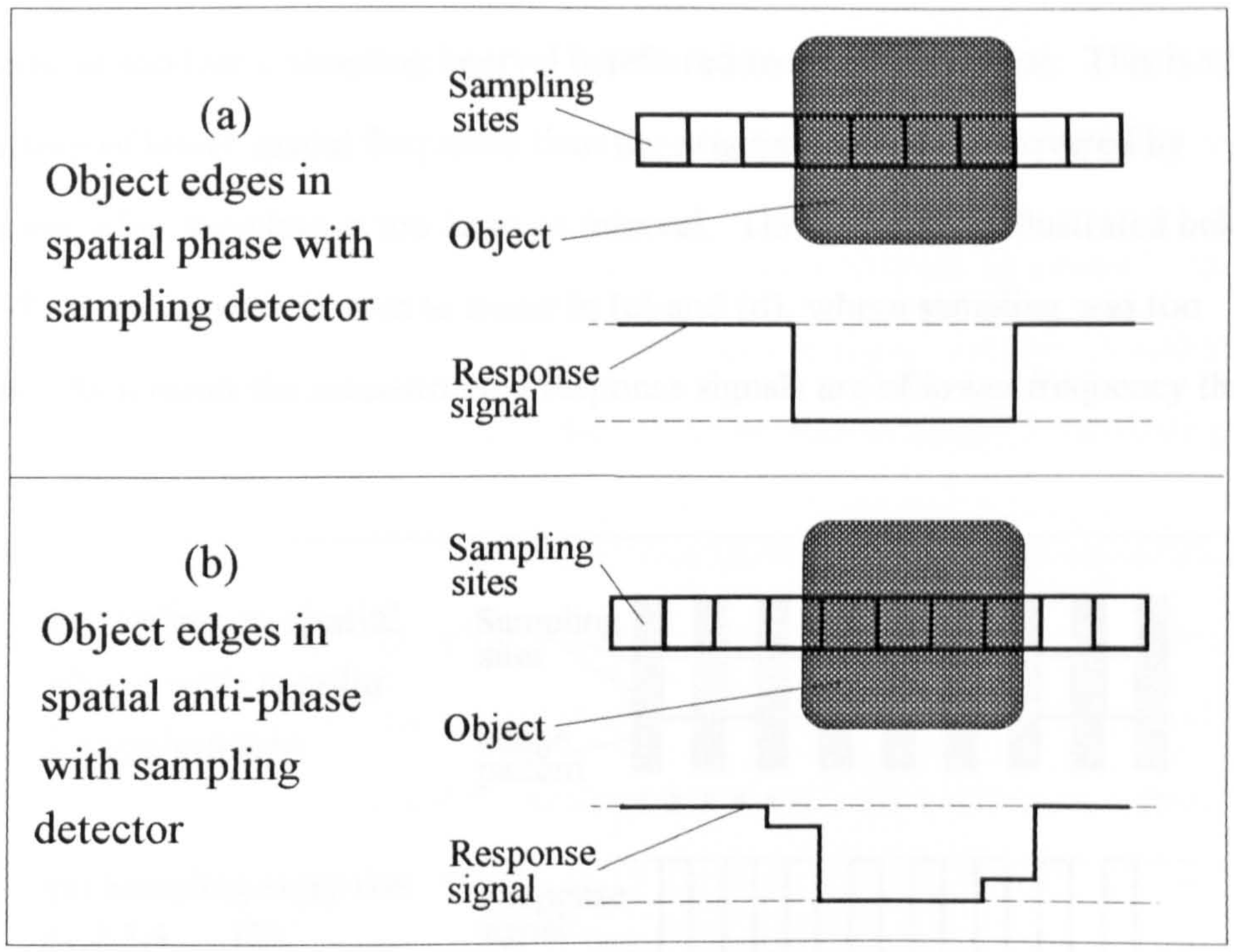

Figure 3-6 The effect of spatial phase on edge detection

Interpolation & Aliasing

When sampling a time-dependant signal it is usual to aim for a 'complete' representation. This implies that recovery of the true form of the signal, by a process known as interpolation, can be achieved. This means that the original signal can be accurately reconstructed and reproduced from a smooth fit curve plotted through the points of the samples. In practice, the choice of sampling interval (frequency) for a particular image depends upon how much detail the image contains. If the sampling interval has been chosen correctly, then recovery of the image detail can be achieved by interpolation. Otherwise, if too low a sampling rate is chosen, vital information about the fine details is lost and subsequent interpolation of the gathered data would simply suggest that the image has less detail content than the original.

Once information has been lost by inadequate sampling, recovery of the original image by interpolation or any other means is not possible. A further problem which may be

encountered at too low a sampling interval is referred to as aliasing error. This is when an image pattern of lower spatial frequency than the original pattern is recovered by interpolation, after sampling at too large an interval. This situation is illustrated below in Figure 3-7. Aliasing error is seen to occur in (c) and (d), where sampling was too infrequent. As a result the reconstructed response signals are of lower frequency than the original.

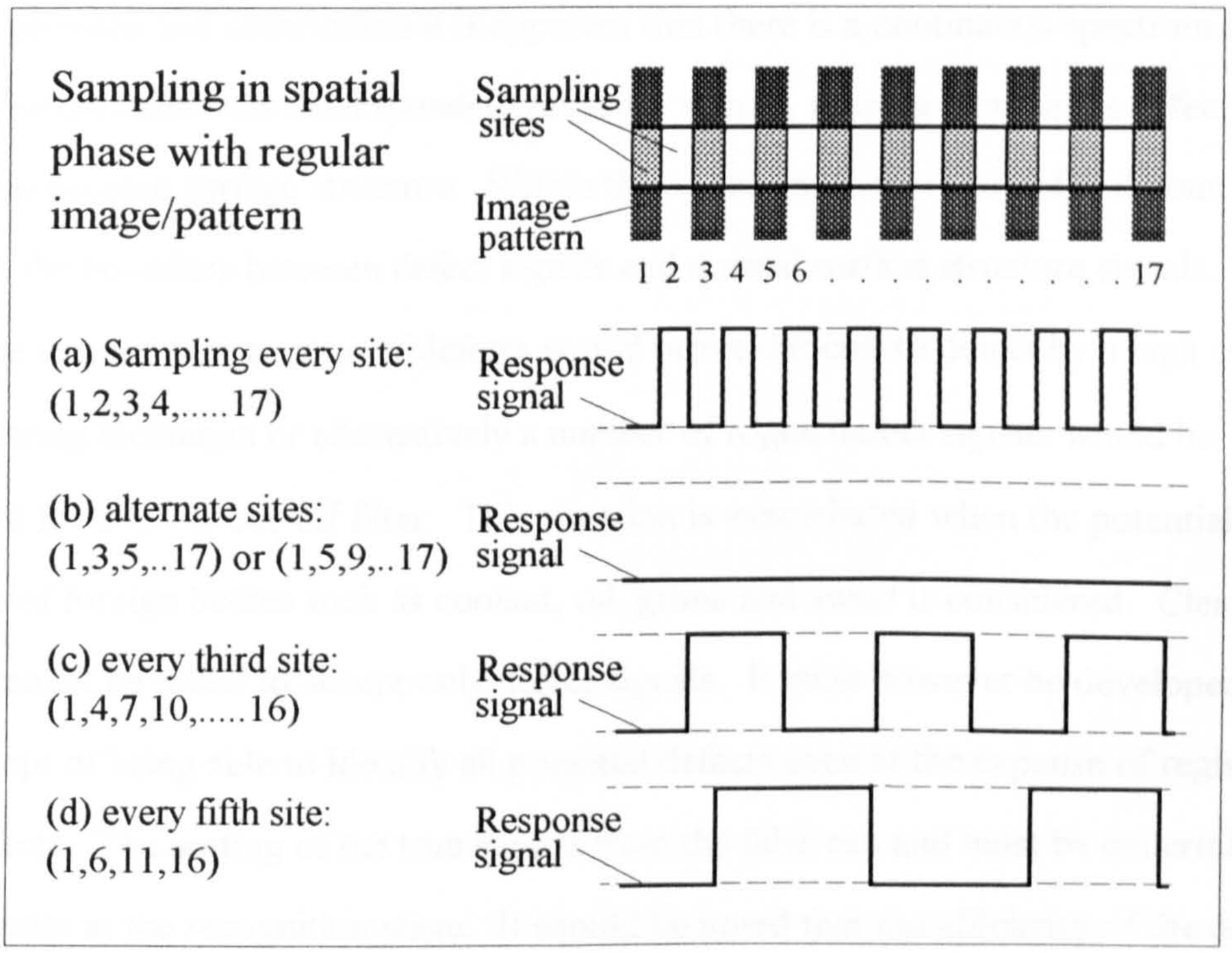

Figure 3-7 An illustrated example of aliasing error

3.3.2 Defect Recognition

Recognition need only act on those portions of the response signal which relate to the surface defect. This pre-supposes that a system exists which can detect and delineate those sections on each scan. In the optimum situation the recognition process would operate in the following way;

i. For each edge or flute of the cutting tool being inspected, detect and delineate defects from the response signal.

ii. Apply recognition processing to the full set of delineation signals arising from each cutting tool, taking into account the spatial relationship and the nature of any defects.

This analytical approach supports inspection at a microscopic level, by analysing the nature and detail of the defects through the shape of the response signal, section (i), and at a macroscopic level, by analysing the dispersion of the defects throughout the cutting tool (ii).

From experience and observation it is apparent that there is a continuous spectrum of surface features and thus corresponding response signals, ranging from gross defects down to the microscopic surface structure. Within this spectrum there is no defined point which indicates the boundary between defect signals and normal surface structure signals. Thus it cannot be ignored that a range of defects would prove difficult to detect by a high cut-off point filtering technique or alternatively a number of rogue defect signals would be registered for a lower cut-off filter. This situation is exacerbated when the potential presence of foreign bodies such as coolant, oil, grime and swarf is considered. Clearly a system cannot be tuned to accept only defect signals. It must however be developed around the concept of being able to identify all potential defects even at the expense of registering false defects. The sorting of the true signals from the false can and must be undertaken subsequently at the recognition stage. It should be noted that the efficiency of the defect detection process should not be assessed on the strength of it being able to exclusively locate defects of a pre-defined type and severity and at the same time screen out border-line cases.

Recognition processing should be in the region of seconds, with a data processing rate suited to representative cutting tool recall times. With this strategy no delay to the manufacturing operation would be imposed.

A number of signal processing techniques have been identified as being suitable for on-line inspection of surfaces. The true suitability of the analysis procedures can only be proven on real data collected from cutting tools taken from a representative manufacturing environment. The collecting and screening of the data to ensure it offers a true and typical

representation is in itself a mammoth task. This must be followed up in subsequent research activities.

3.3.3 Data reduction and processing rates

Data processing speeds still tend to set limits on the throughput and complexity of image analysis. An imaging system may typically acquire 1 to 10 million picture elements per second. At the higher rates a system based on processing the grey level (analogue), information for each element of the picture will be too slow or expensive for on-line inspection applications. To overcome these problems, intermediate data reduction is an essential operation. This can be achieved by dedicated electronic hardware or as a post-acquisition operation by computer software. On the whole, the hardware option tends to offer higher operating speeds but little flexibility whereas the software is highly flexible but with slower response times. Data reduction is implemented differently for linear and area array images:

Thresholding - The grey scale image is transformed to black and white by introducing a threshold. Picture element levels are then only recognised as being below or above this datum (black or white). This method is also applied to imaging techniques to enhance fine detail or contrast and this can be applied to both linear and area arrays.

Step changes - After the thresholding technique has been applied the volume of data can be dramatically reduced by recording the black to white transitions with the corresponding picture element number. In this way an image of several kilobytes can be reduced to perhaps only a few bytes. This technique is appropriately applied to linear arrays.

Averaging - By applying an averaging operator to adjacent picture elements the volume of data can be reduced/condensed.

For cutting tool condition monitoring the data processing rate is dependant upon the volume of data gathered. This in turn is dependant upon the following;

- The overall length of the cutting tool cutting edge to be inspected
- The sampling pitch (samples per mm)
- The sampling frequency of the hardware to be used dictated by the analogue to digital converter or the stepping motors whichever the slower.

The two important measures are the tool scan time and the volume of data resulting from the scan.

At this point it is important to first note the volumes of data associated with the two potential scanning techniques, cutting edge or complete tool scanning.

Scanning cutting edge only:

A typical cutting tool geometry is;

For a typical cutting tool of diameter, d = 20 mm, depth of cut, c = 60 mm, four flutes of helix angle, $\theta = 20°$.

The total length of the cutting edges is, $l = (c/\cos\theta) \times 4$

$= (60 / \cos 20°) \times 4$

$= 255$ mm

Thus for a suggested sampling pitch, p = 0.1 mm (and 1 byte per sample)

Total data collected for the tool, T_{edge} $= l/p$

$= 255/0.1$

$= 2550$ bytes ($\approx$ 2.5 Kilobytes)

Computer interfacing hardware with sampling facilities able to achieve 10 kHz as standard and upto 50 kHz with slight modification suggests no problems from the processing view-point.

Scanning whole of cutting tool:

The total surface area of the cutter is, A $= (\pi \times d) \times c$

$= (3.14 \times 20) \times 60$

$= 3770\ mm^2$

Again, for a suggested sampling pitch, p = 0.1 mm (and 1 byte per sample)

Total data collected for the tool, T_{area} $= A/p^2$

$= 3770/(0.1)^2$

$= 377000$ bytes ($\approx$ 368.2 Kilobytes)

Using the same computer interfacing hardware with sampling facilities able to achieve up to 50 kHz, data capture would not present any problems. However, an involved and problematic operation which would entail cutting edge data extraction would burden the processor and result in lengthy computation times. Furthermore this operation would be additional to the defect detection, extraction and analysis which would have to be subsequently performed. It must also be noted that in raw data form the ratio of cutter edge to whole of tool data is 1: 147.3 (T_{edge}:T_{area}). So, for the case cited above, 14 628 % (((368.2/2.5) × 100) - 100) more data has to be handled and stored for the whole of cutting tool scanning method as compared to scanning the cutting edges alone. This is a significant fact when several thousand cutting tools can exist on the shop-floor at any one time.

Chapter 4.0

Experimental Equipment

4.0 Experimental equipment

A range of experimental equipment evolved during the research program which adopted three discrete forms; the surface topography inspection device, the two axis inspection device and the four axis inspection system. Significant achievements and findings attained during the course of research are introduced and discussed below.

4.1 Enabling technologies

The enabling technologies had first to be identified and then manipulated in order to support the testing and development programme. At the lowest level these technologies, in the form of primary equipment, were initially introduced as discrete systems which were brought together during the later stages of development of the inspection devices. Each piece of primary equipment was essentially a stand-alone item but a sub-system of the final device. Compatibility was thus an important consideration when selecting each element. The most important of these sub-systems are introduced and discussed below.

4.1.1 Opto-electronic sub-systems

Laser diode technology was at that time becoming affordable and readily available for prototype applications. The benefits of such technology were many (Reduced; weight, size, cost), see Figure 4-1 which clearly illustrates the size advantage. Over the course of the research a range of laser diode modules was identified as suitable. Several were purchased and used extensively in the laboratory for a range of experimental work.

Figure 4-1 Comparison of a Diode laser (right) with conventional Helium-Neon laser (left)

A limited number of opto-electronic sensors were readily available but were without technical information pertaining to performance. Sensor suppliers were contacted and eventually suitable units were purchased. The devices were matched to the laser light sources and potential applications. In addition, a 128 photo-site CCD array was bought and used in simple image sampling operations. Due to the excessive amount of data collected when using the array, single-site devices were subsequently used in preference, throughout the work.

4.1.2 Motion and control sub-systems

Basic motion control

For the development of the component manipulation platforms two possible drive technologies were available; stepping or servo motor systems. Due to the perceived mode

of operation it was anticipated that the stepping motor drive system would offer superior performance. This decision was also based upon the relative ease of control and construction of the associated drive system.

In its simplest form the stepping motor movement control system consisted of a motor, control chip (SAA 1027) and power supply. This cheap and easy-to-construct development platform proved ideal in the early stages of research when high rates of movement were not required. Typically, the instrument motors available for this type of application came with a range of performance capabilities. The most important criteria were delivery torque and the number of steps for the motor shaft to complete one revolution (typically; 24, 48 and 200). Motor control was achieved through the setting and switching of the three control lines; step, direction and reset.

Step - For each pulse detected on the step input the motor would be incremented by a single step. Step rates of up to 350 steps/sec could be achieved with the above configuration. The performance curve in Figure 4-2 clearly illustrates the reason for the upper speed limit. A phenomenon which had to be accommodated was that of resonance in the motor at certain step rates, typically 100 steps/sec. This rate had to be avoided to ensure accountable performance, as steps were skipped and lost when driven at this speed.

Direction - The direction of rotation of the motor is dependant upon the state of the direction or 'mode' control line.

Reset - In a situation when the motor has stalled or during initial power-up the motor drive circuitry should be initialised by way of the reset facility. This simply zeros the control counters and establishes the default motor driver settings. The state of this control line must be maintained high throughout a move sequence.

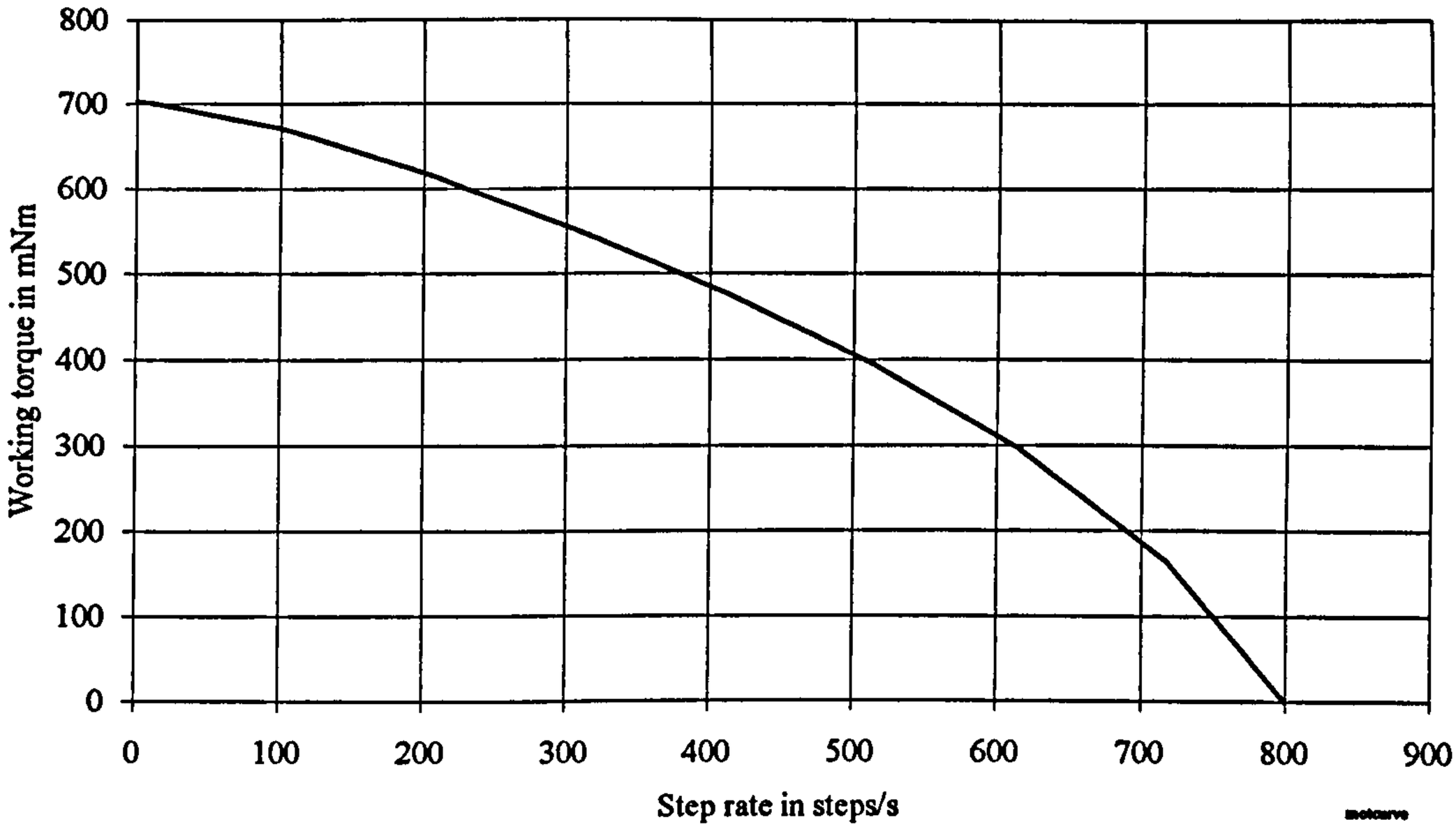

Figure 4-2 A typical stepper motor performance curve

From a control viewpoint the stepping motors are extremely easy to manage. Direct or buffered connection of the stepping motor driver to a computer digital input/output (I/O) interface offers the simplest, and most easily developed, movement control arrangement. Furthermore, software used to manage the I/O interface is easily integrated into a graphical display or analysis software suite. The flexibility of the software-driven, configurable, I/O gives it a distinct advantage over a pure hardware driven arrangement and a price advantage over a split hardware and software solution. However, performance is compromised, but this loss is outweighed by the merits of system flexibility. Therefore, in the fundamental development phase of the project this basic system configuration was used.

Enhanced drive and transmission systems

Enhanced control and performance options for stepping motor control which were adopted into the inspection application at some stage in the platform development are described below.

Hybrid Stepping motors - By powering the stepping motors with a higher than normally rated voltage and delivering it in a short pulse the speed and acceleration of the motors were dramatically increased.

Mechanical gearboxes - To increase the number of steps per revolution and thus the resolution of the motor a mechanical gearbox was incorporated into the drive system. At low speeds and steady feeds a conventional, low cost gearbox is adequate. For high speed and continuously varying rates an anti-backlash gearbox should be used. This is a considerably more expensive arrangement and no flexibility is attained by the inclusion of a mechanical gearbox.

Electronic gearbox - Primarily used to increase the number of steps required to complete one revolution of a stepping motor shaft, so that a smoother performance be obtained. Electronic gearboxes are usually switchable to produce a range of steps per revolution for a given motor. Typically the resolutions offered are:- 1:1, 1:2, 1:4, 1:5, 1:8, 1:10, 1:20 and 1:40. Due to the switchable ratios, electronic gearboxes offer increased flexibility over mechanical counterparts.

Advanced, high performance motion control

Low cost, prototyping multi-axis controllers suitable for the development of the inspection platform were not available at the outset of the project. However during the latter half of the work an ideal motion control option became available. This system, a Unimatic AT6400, the first to be sold in the UK, offered (Appendix III);

- Independent control of four axes
- Linear interpolated moves with four axes simultaneously
- Circular interpolation with two axes simultaneously and a third remaining perpendicular to the described surface.
- Auxiliary inputs and outputs
- High-performance stepper motor control

- Master clock signal output
- End of travel movement interlocking
- Programmable accelerations and velocities

This control system was managed by its own dedicated microprocessor and was designed to be located in a full-length expansion slot of an IBM compatible PC XT machine, thus giving it immediate access to the master computer data and address buses. Buffering enabled the master system to download a series of move commands yet maintain a high speed of response in the overall system control. Strings of commands sent to the control unit were processed sequentially. Maximum and minimum values of acceleration and velocity set by software in the first prototype systems were managed much more elegantly by hardware in this arrangement. Dedicated dynamic counters associated with each of the four axes could be monitored and read over the common data bus, resulting in high speeds of response and information transfer. Furthermore, a facility which enabled the master clock signal to be tapped and redirected out through an auxiliary I/O port enabled the use of data transfer from the external sensor to computer memory by Direct Memory Access (DMA). This method of data transfer dramatically reduced the burden on the central processor and thus resulted in a further improvement in overall system response.

4.1.3 Data analysis and evaluation sub-systems

Several methods for data analysis and evaluation were investigated during the research and development phases of the cutting-tool inspection system, ranging from *In Process Monitoring of Tool Breakage Based on Autoregressive Model* [56] through to the use of matched filter banks [57]. Three methods which were actively used in the research program are introduced and discussed below.

Thresholding

Initially a simple yet effective method of signal analysis/evaluation was utilised - Signal thresholding. Horizontal, confining lines plotted at perdetermined offsets, above and below the response signal, acted as action limits. When the response signal projected beyond the confining limits a defect/irregularity was registered (see Figure 4-3, laser based V-scanner response signal). Further analysis was required to determine the extent and nature of the sample surface defect/irregularity.

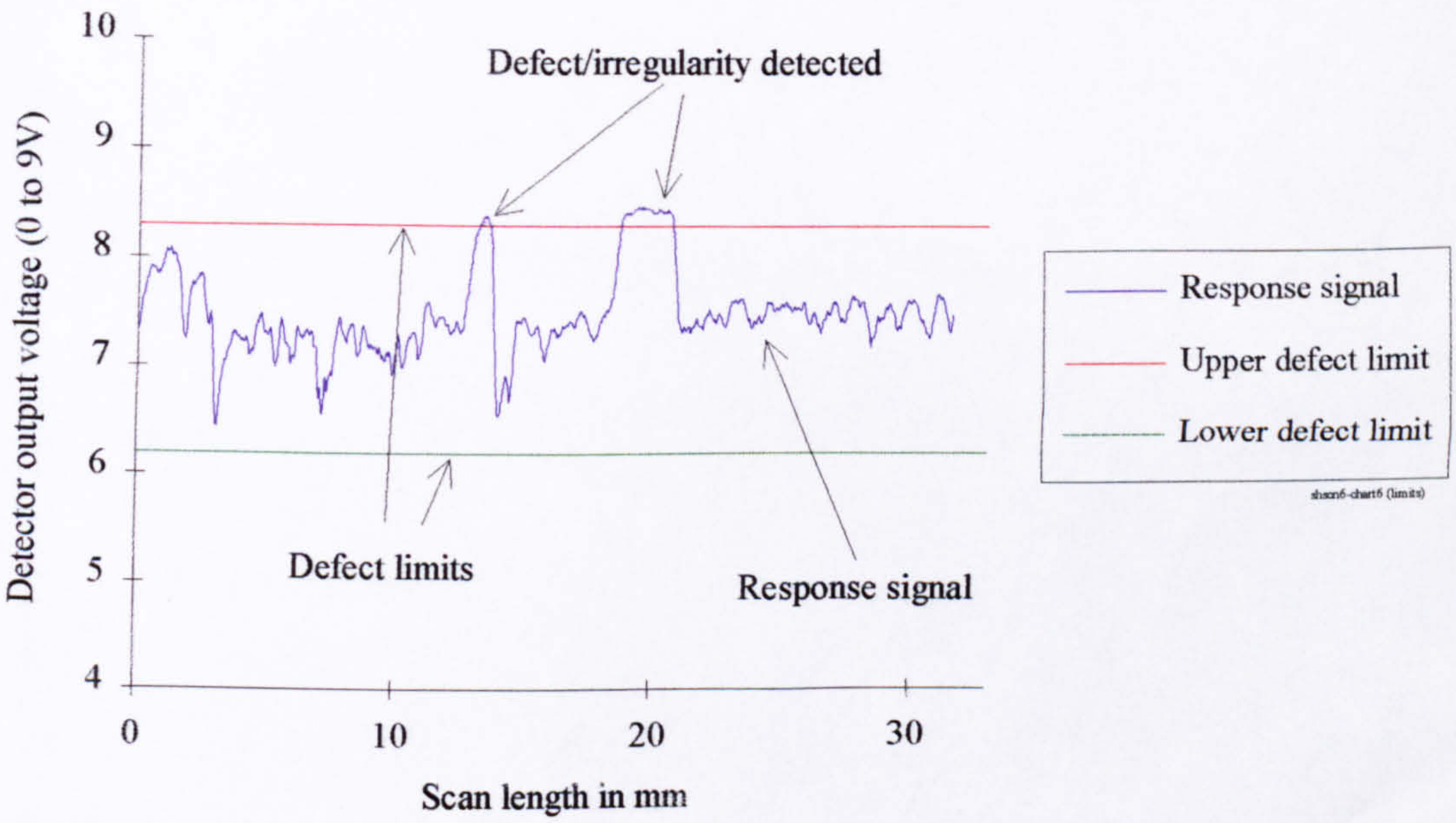

Figure 4-3 Signal thresholding for defect detection

Master signature comparison

A method which was originally thought to be most suited to the application of tool condition-monitoring was that of Master signature comparison. The fundamental principle of operation of the method, illustrated in Figure 4-4, was that a 'master image' (signature) would be recorded for each individual, unused cutting tool. This became the comparator datum for subsequent inspection cycles of the same tool.

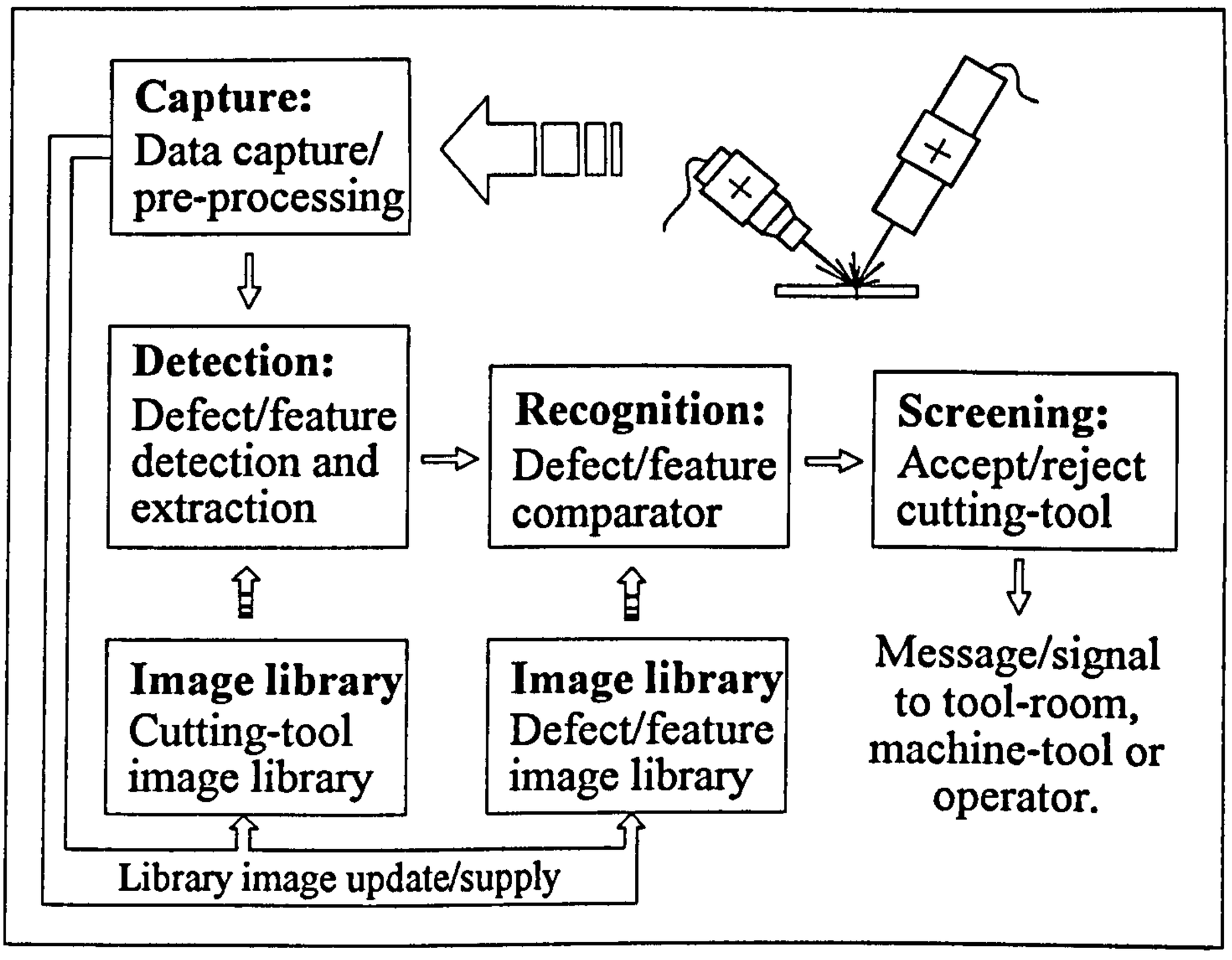

Figure 4-4 The fundamental principle of operation of the inspection system

Using this type of direct comparison philosophy the exact inspection scanning sequence for each tool had to be reproduced every time. Early work undertaken on the rotational inspection platform [47] suggested that the laser scatter signal would repeatedly offer the same characteristic pattern for a given scanned surface. This pattern would be reproduced in every detail if the surface were scanned again, under the same conditions. Further proof of this reliable nature was gained during early scanning tests on the surface topography inspection platform when signals were seen to overlay exactly when scanned in either the forward or reverse directions. At this stage in the investigation the minute detail captured in the signal did not however seem to accurately represent that of the surface under inspection. Further tests showed that surfaces identical to the naked eye would produced dramatically different laser scatter signatures. This immediately undermined an early thought that a common signature could be used for geometrically identical cutting tools. Thus, even geometrically identical cutting tools and cutting inserts had to have their own separate master images if they were to be inspected and screened successfully by this technique.

Intelligent filtering

As indicated above and by the results of earlier work [47], surfaces produce a unique signature despite being seemingly identical. To overcome this, the previous method storred a master signature and used it as a comparator for subsequent inspection cycles of the same surface. The main short-fall of this approach was a high volume of library data. The intelligent filtering method was proposed as an alternative means of defect detection in cutting-tool condition-monitoring. This method had been proven on a number of inspection applications and its use to detect defects in fast moving steel strip was documented in some detail by Hill [48] and more generally by Norton-Wayne [49]. This technique was based around the concept of curve regression, with the signal being converted to a curve. Attenuated curves were then superimposed above and below the original signal. By this means defect detection limits were set. This approach was similar to the threshold charts discussed above with the exception of the limits following the trend of the signal and thus producing a consistent offset (see Figure 4-5).

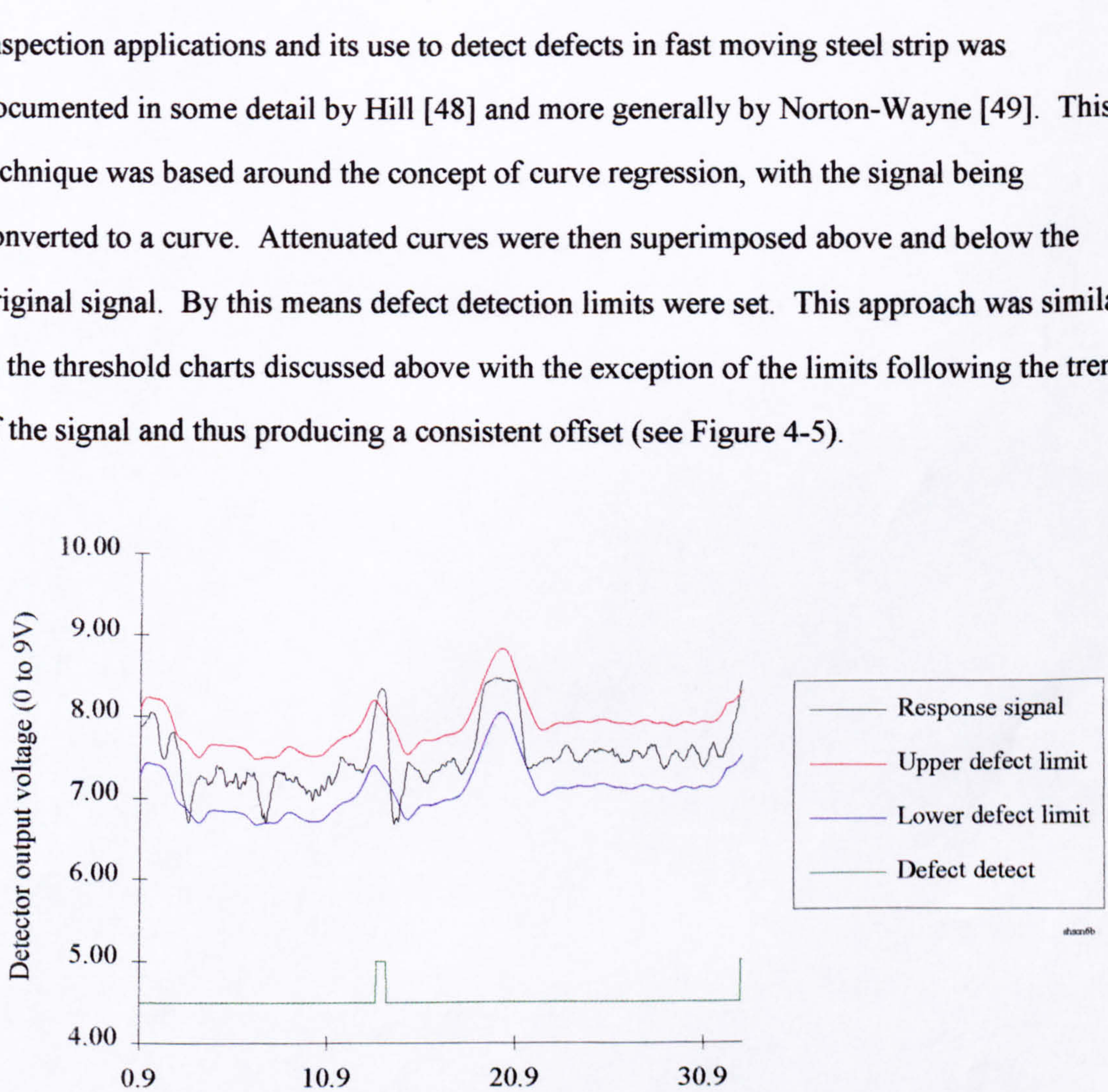

Figure 4-5 Intelligent filtering defect detection technique

4.2 Two-axis inspection device

During the early stages of research an inspection device was developed which could manipulate milling cutting tools and present the flank faces to a laser scanning head, see Figure 4-6. The system comprised of three main components; an inspection platform, control unit and management computer.

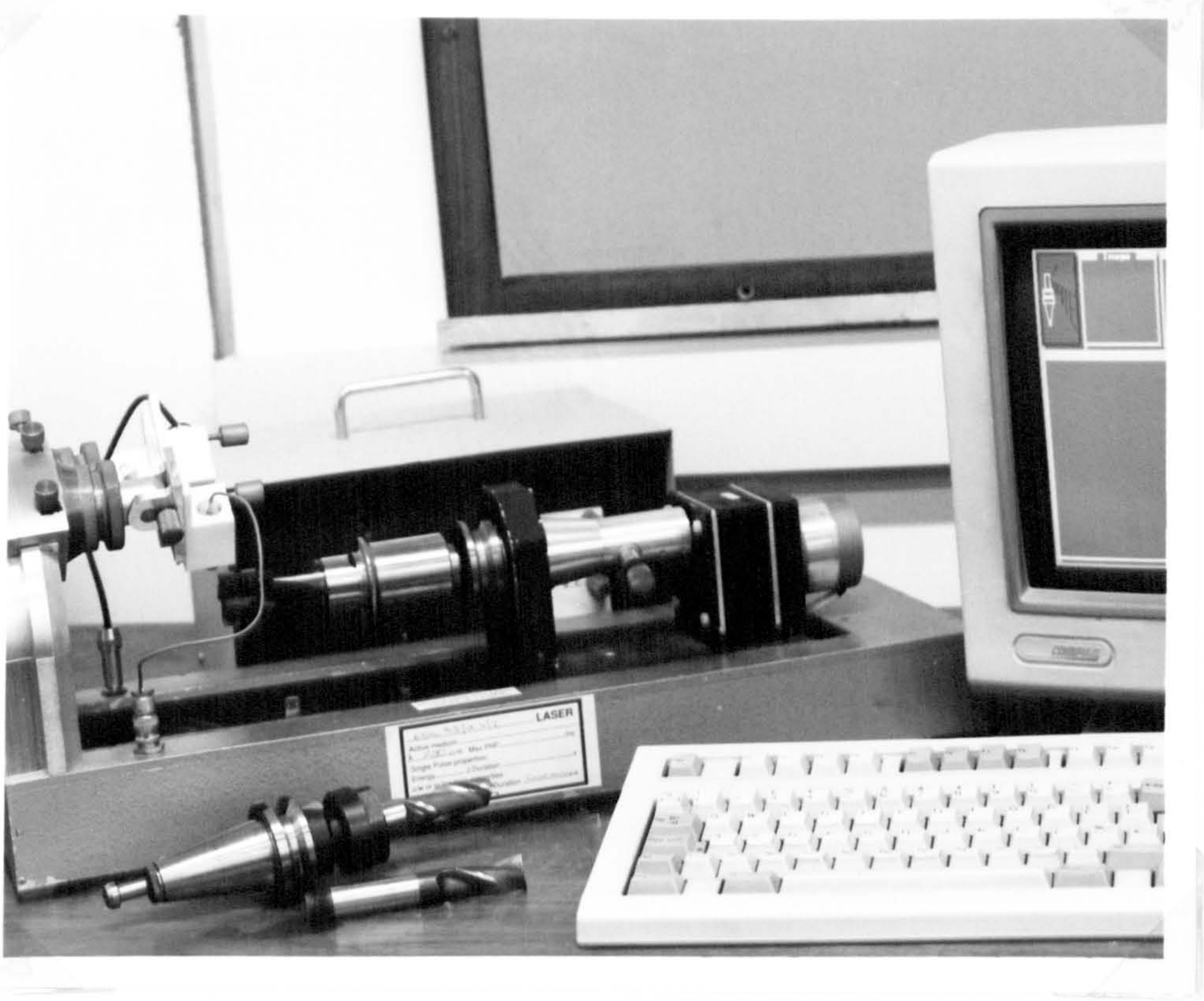

Figure 4-6 The two-axis inspection device

The inspection platform consisted of the mechanical sub-systems to provide relative movement of the tool and inspection head, all associated homing switches and the inspection head (laser and detector). A purpose-built control unit was constructed to house the drive circuitry, power supplies, open-circuit and power-up interlocks. The control unit acted as the interface, bridging between the system management computer (an IBM compatible 286 PC) and inspection platform. Assorted tools of various length, helix angle and number of flutes could be monitored by this device.

4.2.1 Significant system developments

The laser and detector were mounted independently on a semi-circular ring (Figure 4-7). Adjustments for tilt, angle and clearance were provided for both the laser and detector, as was the angular separation for both units.

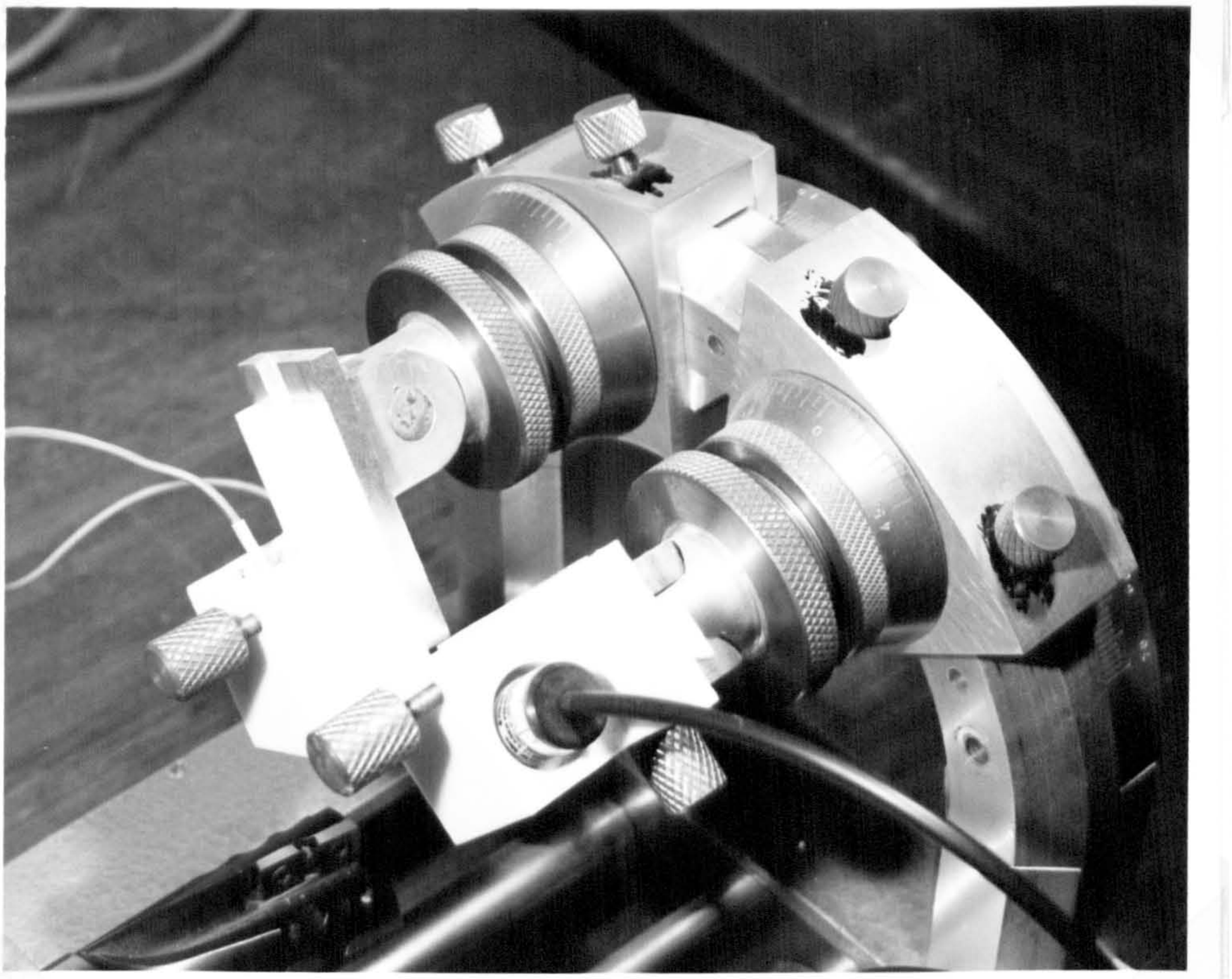

Figure 4-7 The laser and detector mounted on the annular ring

Fundamental laser scanning work, to find optimum angles and settings for the laser and detector inspection head, had not been undertaken prior to the development of this device. Thus, it was originally thought that the optimum settings would be evaluated during the cutting tool inspection trials. Despite having calibrated all the sliding and tilting clamps for the laser and detector units it proved almost impossible to conduct simple tests, primarily because of the complex forms of the cutting tool surfaces and the associated convoluted move sequences and furthermore due to the acute sensitivity of the laser/detector alignment. In response to these shortfalls a special, dedicated inspection device was developed entirely

for this purpose. The development and usage of this device is covered in some detail in Chapter 4.3. To simplify the ensuing transfer of experimental results the laser/detector arrangement used in the surface topography inspection device (see Figure 4-11) was grafted onto the two-axis platform and the redundant annular ring removed. This arrangement proved highly successful and very simple to implement.

Two independent axes, one rotational and the other linear translational, enabled the tools to be manipulated and presented to the inspection head. With the laser and detector inspection head fixed, the cutting tool which was held by a standard ISO taper (see Figure 4-8) in the tool manipulation carriage of the inspection device was either rotated or translated to present the cutting edges to the inspection head.

Figure 4-8 Standard ISO 35 tool holder/tapers

Helical movements were attained by a string of sequential commands driving the rotational and translational axes. To the naked eye the movement appeared helical but when analysed

in detail the move consisted of a series of perpendicular step-like moves, evolving from the movements made by alternating axes. Due to the resolution of the step-like movement the data capture routine was not affected, primarily so because the surface image was only sampled in the rest time between steps.

A series of move commands was developed to simplify programming and driving the stepper motors and data capture hardware. The commands enabled movements to be specified in steps, mm, degrees or radians as appropriate. Strings of move commands were compiled which, when accessed, would prescribe movements and allow a tool to be scanned by incrementing the axes through appropriate amounts and in the correct sequence. These command strings were collectively called 'move templates'. A move template was obviously specific to a cutting tool. Figure 4-9 illustrates this by mapping the move template sequences onto a conforming tool specimen.

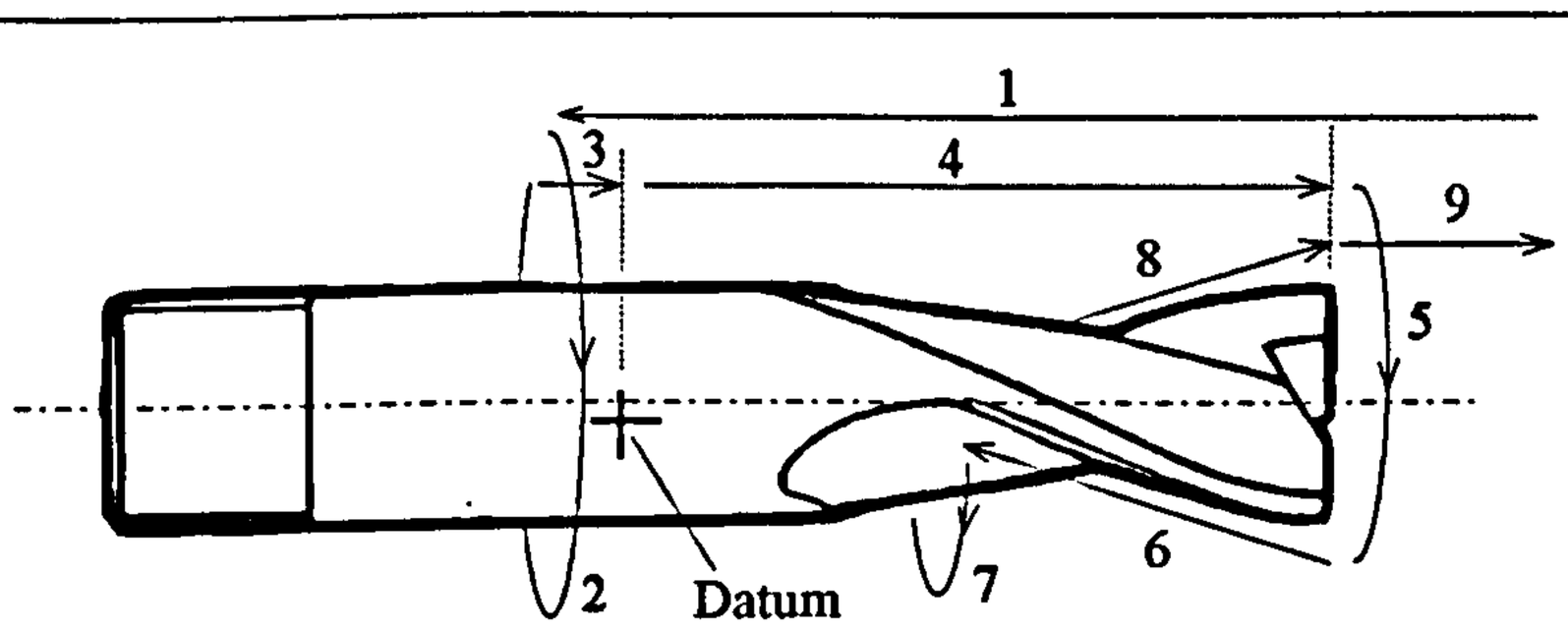

1	Linear	Present datuming zone to inspection head
2	Rotational	Rotate to find rotational datum marker
3	Linear	Translate to find linear datum marker
4	Linear	Move to extreme end of cutting-tool
5	Rotational	Position laser spot on tip of first cutting edge
6	Helical	Scan down first flute
7	Rotational	Position laser spot on tip of second flute
8	Helical	Scan up second flute
9	Linear	Home inspection station axes

Figure 4-9 A typical move template sequence with conforming cutting tool

Files of move templates in ASCII text format were accessible to the inspection system management computer. Move template files carried the same identification mark (file name)

as the cutting tool identification number and thus were restricted to eight alpha-numeric characters, in the prototype system. Subsequent developments in the cutting tool inspection system control led to the multi-axis system (Refer to Chapter 4.4) where a similar but considerably more sophisticated approach using move commands and templates was proposed.

A primary development essential to the on-going work of cutting tool condition monitoring by this manipulation technique was the ability of the system to locate a datum on the cutting tool body. Move commands based relative to this datum would ensure proper and accurate tracking of the tool cutting edges. Initial thoughts suggested that it would be possible to first locate the extreme end of the tool then identify the location of the cutting edges at an appropriate mid-point as they rotated past. The tool feature locations would then be calculated from the acquired information and mapped in the system co-ordinate reference frame. The weaknesses of this approach were two fold:-

- Slight wear on the cutting edges could result in the tool being wrongly placed in the co-ordinate reference frame. This small degree of misplacement could have a compound effect on the subsequent wear analysis for the tool and result in it being rendered unsuitable for use ahead of time. Thus, sensibly, the wearing faces cannot be used as a datum edge.

- The cutting edges could not be individually identified which would lead to problems when inspecting slot drills, due to the different lengths of the nose chisel edges. Figure 4-10 best illustrates this characteristic. Furthermore, multiple flute cutting tools demand each to be individually identifiable so that effective signal comparison can take place (See Chapter 4.1.3 - Data capture, evaluation and display).

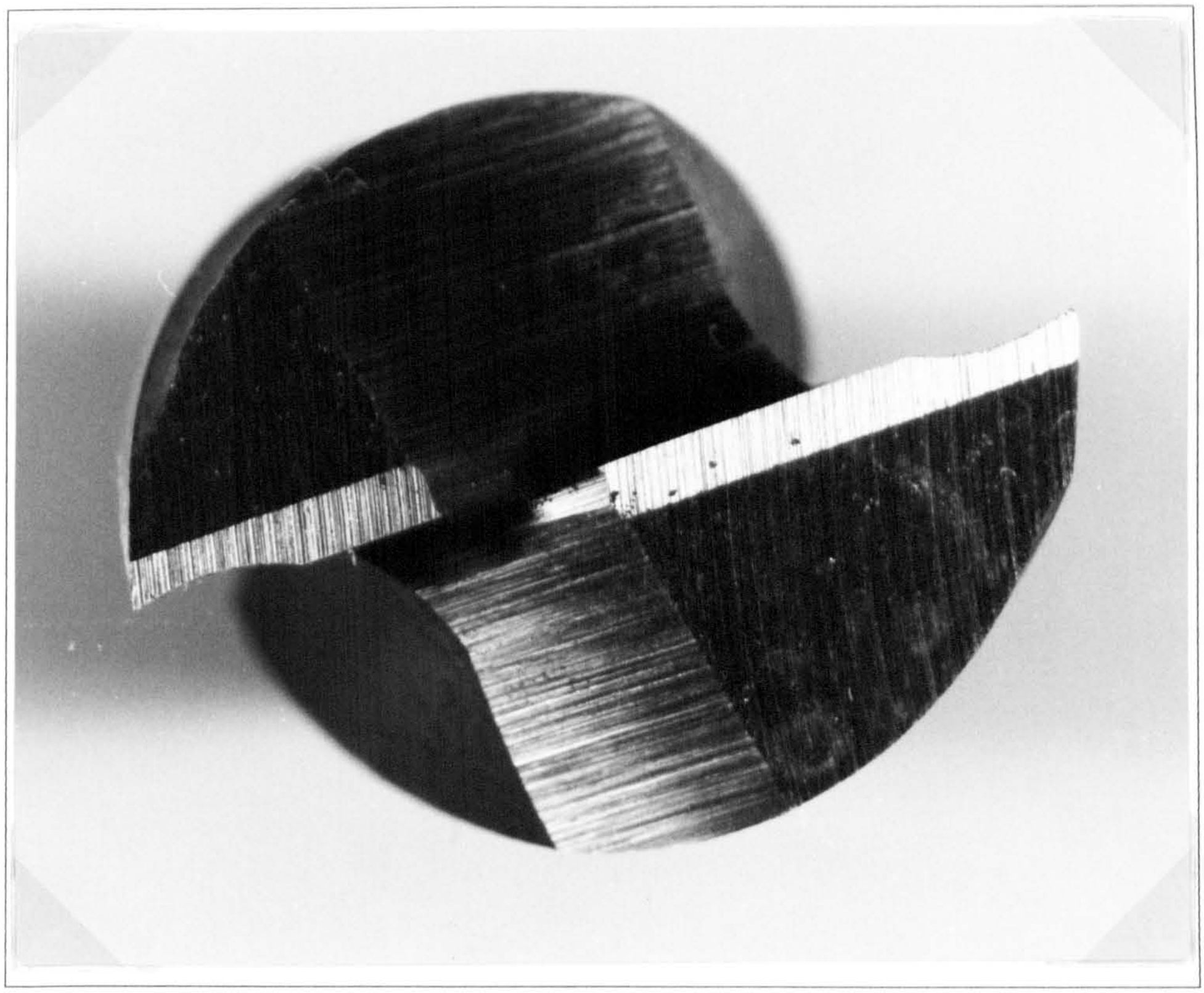

Figure 4-10 Asymmetrical cutting tool features

Lengthy reasoning and discussion resulted in a system for cutting tool datuming being proposed. Each cutting tool element would carry a datum mark, consisting of two engraved lines at right angles to each other, forming a cross. One datum mark (engraved axially along the element) would act as the rotational reference, while the other (a circumferential mark) would act as the linear datum. From the known location of these marks, the cutting tool would be placed in the system co-ordinate reference frame. The datum marks were placed on a plane section of the cutting tool shank or element body thus allowing a simple surface scan to take place without complicated moves having to take up irregularities in the surface geometry. Tools built up of several elements, typically an ISO taper, extension and cutting tool required a transformation vector to guide the inspection system from the datum of the base element, namely the ISO taper, to each element in turn until the cutting tool datum was located. Inspection moves based on the specific cutting

tool would then be implemented relative to the tool datum. The appropriate inspection cycle could commence without subsequent account of the taper and extension being taken.

The cutting tool datuming cycle was implemented in the following way. The inspection platform tool manipulation carriage would initially be homed in the linear translational axis. This was to allow the platform controller to zero associated move counters and set the system co-ordinate reference frame. The rotational axis was not homed or zeroed as the cutting tool could be subsequently placed in the carriage in any rotational attitude. At this stage the tool identification number would need entering into the system via the keyboard. An offset value extracted from the movement template, associated with the specified tool, would be retrieved. This value dictated the approximate distance of the datum zone along the linear axis, relative to the system co-ordinate reference frame . The controller then moved the tool in such a way so as to present this zone to the inspection head. A complete rotation of the tool would be made by means of the major rotational axis, while the surface was being scanned for the datum mark. Subsequent analysis of the data then revealed the exact location of the rotational datum marker. Simple software routines then manipulated this information to evaluate the minimum number of steps and direction of rotation to cause the scanning point to coincide with the marker. This move was then implemented with a small offset added so that the exact location of the linear datum mark could be found without interference by the rotational mark. A linear scan, with data capture, would then be implemented with the linear datum being found after processing.

The cutting tool co-ordinate reference frame was subsequently mapped, relative to the system co-ordinate reference frame. To offer visual and audible confirmation of the correct location of both the rotational and linear datum marks the system was programmed to move the laser spot (scanning zone) onto the datum, dwell, emit an audible tone and then move onto the first inspection command.

Though this system of locating the tool datum worked with a high degree of success it was envisaged that by using this simple, engraved datum mark problems would occur upon

introduction of the system into an industrial environment. It was however envisaged that a more dependable procedure could be achieved by utilising modified bar-code labels. Once bonded onto the shank the bar codes could contain embedded information such as the tool identification number and appropriate datum marks. The inspection head would be the ideal instrument to extract the information as it is essentially a bar-code reader. Furthermore, the nature of data storage on the bar-code would minimise data reading errors due to dirt or marking on the tool shank.

4.3 The surface topography inspection device

During the early stages of the work it was recognised that the fundamental laser scanning work had to be undertaken on samples with non-complex surface geometry. This was primarily for the following reasons:-

- To minimise the number of variables in a single scanning operation
- To remove the control and manipulation problem associated with milling cutters - a separate and somewhat involved issue.

4.3.1 Platform construction

The platform was designed with a degree of flexibility in mind and to a specification resulting from the perceived immediate and projected needs [58].

The main requirements of the inspection platform specification are listed below:-

- Independent and interpolated movements of the linear and rotational axes
- Independently adjustable distance from sample to detector/laser
- Independently adjustable angles for incident and detected laser light
- Variable step size (steps per mm of scan) by means of geared drives
- Adjustable scan distance
- Sample carrier capabilities;
  - (i) to hold a range of sizes, thicknesses and geometries.

(ii) to accept Scanning Electron Microscope (SEM) mounting stubs

(so that the scanned samples could subsequently be viewed in an SEM)

(iii) to enable similar samples to be positioned in a comparable orientation

- Detected signal displayed on control computer screen
- Detected signal stored on disk for future analysis
- Stored signal export facility, to support subsequent processing and display in appropriate software packages

The inspection device was constructed over a period of time with fine adjustment and refinements being made. The final design can be seen in Figure 4-11 below.

Figure 4-11 The surface topography inspection device - final design

The mechanical platform shown required motor drive electronics in addition to a computer to provide movement, control and a data capture facilities.

Overall system management was achieved through dedicated, purpose-written software. It was intended that the software should make the device easy to use, especially for those unfamiliar with details of the motor control technology. So, for the basic linear scan and data capture sequence a series of set-up phases were proposed to initialise the system. Upon initial power-up the table drove home by moving in a known direction until a limit switch was activated, at this point the table position counters were zeroed. A pre-defined off-set was then installed automatically by the computer. Prompted requests for linear movement (in mm) and a data storage file name would be made. A series of component scans could then be made by simply selecting the 'scan' option from the presented menu. The surface topography inspection system was subsequently put to the test by several undergraduate students during final-year research work on laser scanning techniques.

The rudimentary sequence of data capture is depicted in the flow chart below, (Figure 4-12). This technique was developed specifically for the scanning application and is used extensively in the work described in this thesis.

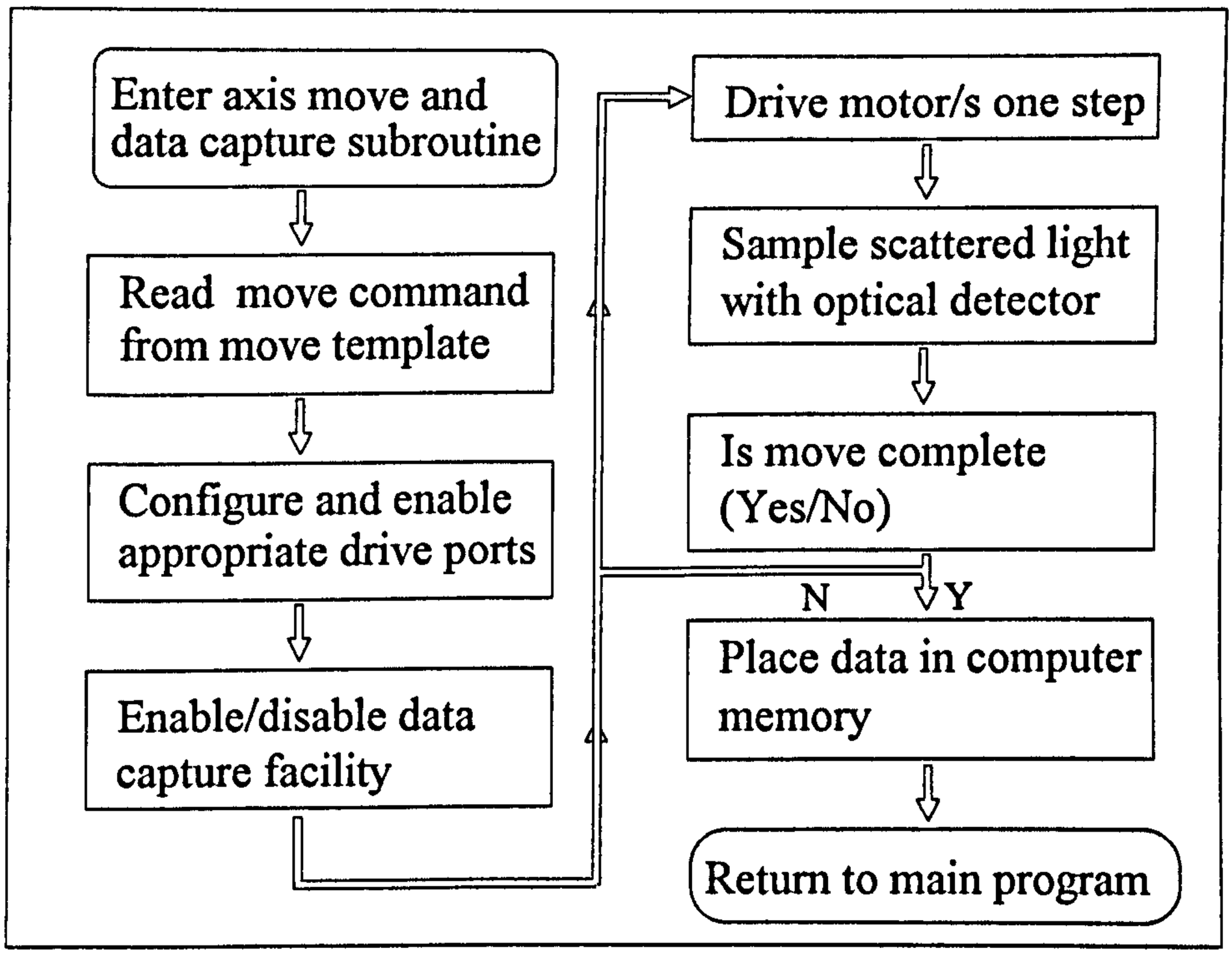

Figure 4-12 Data capture sequence flow chart

As can be seen, the data capture sequence follows a step-sample-step procedure. For this application the stepping motors were ideally suited. The data set, once gathered, was first printed to the computer screen and then saved to disk en-mass, thus keeping the actual scan-time to a minimum.

4.3.2 Fundamental laser scanning work

Due to the complexity of the laser light-scattering mechanism it was proposed that the tests would not be an attempt to measure and then create a mathematical model of the monitored situation. The aim was to limit the number of variables in each of the program tests and attempt to analyse the effect of a single variable on a range of scanned surface finishes and typical defects. By implementing this type of strategy it was recognised that the laser scatter process would not be quantified. However, the effect of the most significant process parameters and the optimum settings could be realistically attained.

The perceived most influential parameters of the laser scatter mechanism which were investigated by means of the surface topography inspection platform are listed below. Under a series of tests applied to a range of control surfaces, the optimum values for each were sought. The tests procedures are explained in some detail in the following subsections.

For a given surface topography, optimisation of the following values was sought:-

- Laser spot size
- Laser incidence angle
- Laser specular and diffuse reflectance angle
- Sampling interval (step size)

Control surface texture samples

For the fundamental scanning work it was proposed that standard surface samples should be utilised, offering a range of pre-defined surface textures. Furthermore, to comply with previously established recommendations, which were based on working experience, plane (flat) surfaces were also necessary. After some thought it was concluded that proprietary surface roughness samples, scratch samples, should be used. These were considered ideal for the test control samples throughout.

The acquired control samples were subsequently mounted on Scanning Electron Microscope (SEM) stubs, using a purpose built jig. This enabled the samples to be repeatedly set-up in the SEM or the laser scanning apparatus in a known, reproducible orientation. The samples each measured 20 by 12 mm and were produced by a range of manufacturing processes, offering a spread of surface finishes for each. The list below illustrates the selection of control samples used and the surface finishes associated with each.

Manufacturing Process	Surface roughness, Ra (in μm)
Ground	0.1
Ground	1.6
Ground	3.2
Polished	0.5
Shot blast	3.2
End milled	12.5

Table 4-1 Control samples used in the surface interrogation tests

Primarily, this range was chosen in an attempt to represent the surface textures/finishes typically encountered on cutting tools. The three ground finishes of varying degrees of

roughness best matched; the fine ground shank (0.1 μm), medium ground cutting edges (1.6 μm) and rough ground clearance edges (3.2 μm). The polished sample was included for two reasons; to represent coated tools/bar-code labels and act as a specular surface in the tests. Many tools have a general surface finish (between the flutes) which is relatively rough and irregular. It was thought that the shot blast sample best represented this form of surface and thus it was included in the sample range. Finally, the end milled sample was incorporate into the range to act as a visual reference. Early tests had shown a close correlation between the general surface form and the response signal. As a consequence it was considered that this would provide an ideal starting point in the experimental work.

Control surface defect samples

A range of cutting tools were available with defects present. These were considered unsuitable for the preliminary analysis due to the complex surface geometry. This problem was overcome by preparing a series of plain samples with control defects. The introduced defects were modelled on those typically found on cutting tools. The control defects utilised in the tests are discussed below:-

Built-up edge - SEM stub, conductive adhesive was used to represent a built-up edge. Small amounts of the adhesive were deposited on the sample then formed and allowed to dry. The electrically conductive adhesive was used in an attempt to model as accurately as possible the reflective nature of the aluminium - frequently the cause of built-up edges. Furthermore, the electrically conductive adhesive would enable the built-up edge sample to be viewed and photographed in the SEM.

Grooves and scratches - Simply attained by drawing a carbide tip across the sample.

Thermal cracking - Samples were immersed in liquid nitrogen and then fractured in an attempt to achieve a clean, brittle break. The samples however tended to fail with some degree of plasticity and thus resulted in an unclean break. The purpose of the exercise was to produce a fracture which could subsequently be reassembled and

then pass for a surface-resident thermal crack. At this stage there was a limited supply of the control samples and it was considered inappropriate to swap them for a substrate material more prone to brittle behaviour. Furthermore, the tests were being undertaken with the intention of fixing as many variables as possible so that the true impact of a single variable could be solely monitored. From this viewpoint it was justifiable that the substrate should remain the same for all samples and therefore the thermal cracking sample was disregarded.

4.3.3 V-Scanner performance parameter optimisation tests

Early, directed work undertaken by undergraduate students [50], comprised a series of grouped, similar tests. This was a conscious effort to isolate various critical operational parameters and analyse the system's response in terms of sensitivity and resolution over a wide range of operation.

The reported work of Chapter 5.0 takes the group testing many stages further. The most significant operational characteristics of the V-scanner are investigated with optimum settings determined. Each of the test series are introduced and discussed below. Throughout the tests a Class II, 670 nm Laser diode was used. The step size of the surface topography inspection device, traversing table, was restricted to 1.46×10^{-3} m and was consistent throughout. Other fixed parameters in the series of tests were:-

Laser spot size (diameter),	1.0 mm
Laser to surface clearance,	65 mm
Detector to surface clearance,	35 mm
Detection angle (variable),	20° to 50°

The effect of incidence angle on signal strength

A series of tests were initially undertaken to determine the optimum setting for the incidence angle of the laser light on the specimen surfaces. With the detector located at a

fixed angle, the laser incidence angle was varied in incremental steps of 10° through a range of +80° down to +20° (see Figure 4-13 below).

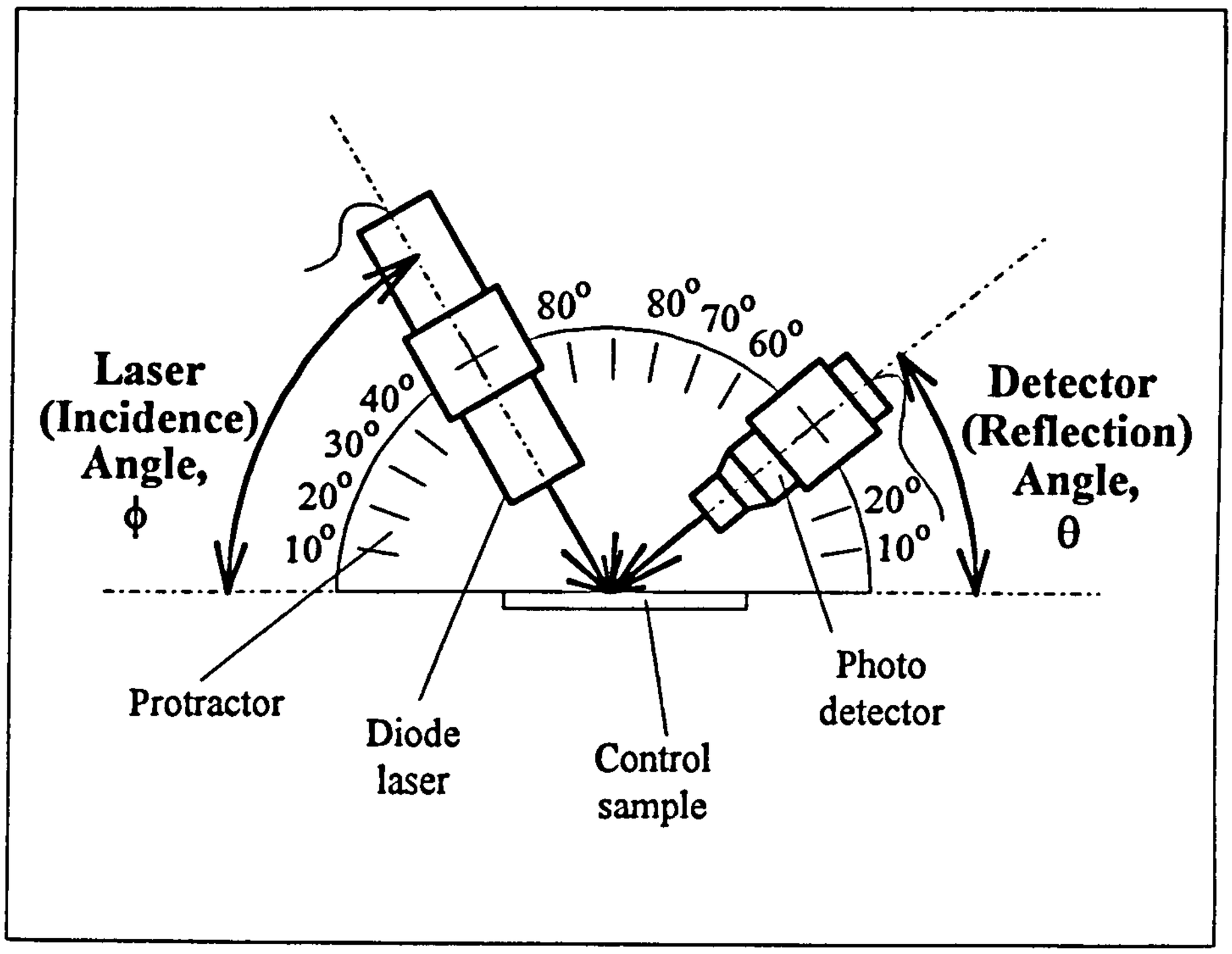

Figure 4-13 Relative angle measurements for the laser and detector units

Light intensity readings were taken at each laser position (incidence angle) in the series. This approach was applied to the plain control specimens and also to those with synthetic defects, in an attempt to establish differences in the optimum settings for each condition. A sample of the results are represented graphically below in figure 4-14. A compilation of pertinent test results can be found in Chapter 5.0.

The effect of detection angle on signal strength

The test described above ('The effect of incidence angle on signal strength') was repeated for a range of detector angular positions (detector angles). The detector was incremented in 10° intervals across the range of +50° down to +20°, again with scanning results being recorded. This test sequence was also applied to both the plain and synthetic defect control specimens. A compilation of the test results can be found in Chapter 5.0.

A Talysurf surface roughness measuring machine was used to accurately obtain the minute surface profile of each control specimen, in an attempt to establish a visual correlation between the specimen surface and the scanned image. The surface profile traces are presented along side the scanning results in Chapter 5.0.

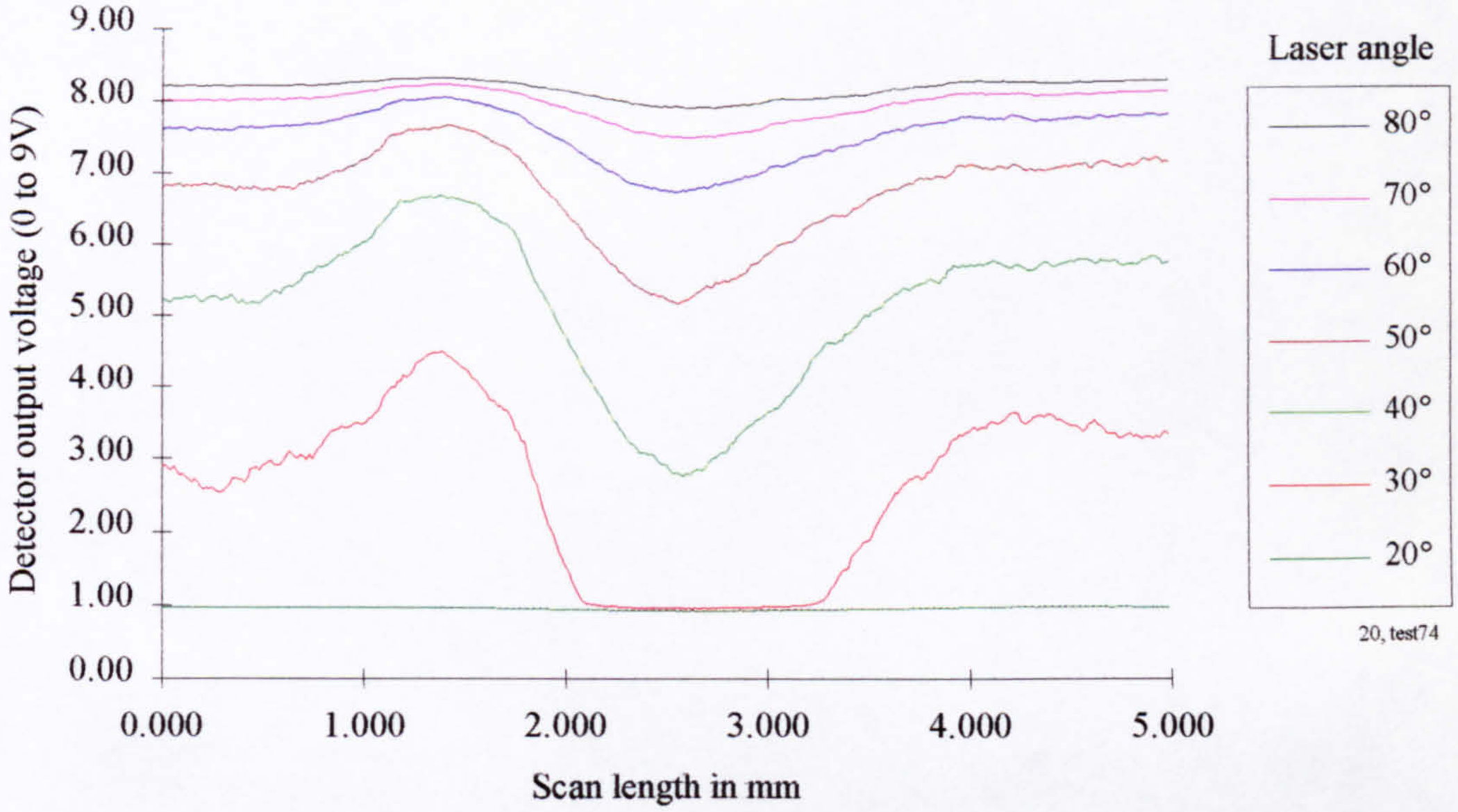

Figure 4-14 The effect of incidence angle on signal strength (detector angle 20°)

The effect of laser spot size on image resolution

The effect of laser spot size was known to be critical for the sensitivity and resolution of the inspection system. This basic knowledge was established in the early part of the research undertaking. As a consequence, a series of tests were directed at determining the optimum laser spot size for particular scanning operations. The results of the investigation are reported in Chapter 5.0.

Optimisation of laser spot size (diameter)

Optimum angles were subsequently applied to a range of samples and the effect of laser spot size (diameter) analysed by means of comparing response signals for each setting. The results of this test series are presented in Sub-section 5.1.4.

Optimised settings applied to cutting tool condition monitoring

Once the fundamental operating parameters had been optimised for a range of conditions it was then the intention to apply these to a restricted range of cutting tools with and without surface defects. The research programme concludes with the results obtained from this series of tests being presented and discussed (refer to Sub-section 5.2).

4.4 Four-axis inspection system

Earlier work and experience gained on the two-axis and surface topography inspection platforms was used to good effect by proposing a range of design rules and specific operational requirements for the specification of the advanced cutting tool inspection platform. The most critical aspects of the design specification of the multi-axis, advanced cutting tool inspection platform are listed below:-

- Due to the proposed scanning method it was mandatory that the cutting tools under inspection had to be orientated in a specific and precise manner.
- V-Scanner
- Single site photo detector
- Class II, visible laser diode
- Coincident observation point
- Range of moves
- Range of tool sizes accommodated
- Range of tool types accommodated
- Resolution (Step size)
- Speed

Further system requirements;

System cost should be commercially acceptable and perhaps fall in the range of an optional extra for a large-scale CNC machine tool. This requirement is however extremely difficult to quantify, for two reasons. Firstly, no knowledge of the perceived value of effectively screened cutting tools is at hand. However, raw material costs for a single, large-scale component are frequently in the region of £30 000, for the aerospace industry. Secondly, due to the high level of integration of state-of-the-art technology the prototype system costs are artificially high and no real indication of the projected price of such technologies is available for established, high volume markets.

The system should be adaptable and be suited to a range of related applications.

4.4.1 Development check-list for visual inspection systems

Further to the specific points mentioned above, a range of general points were considered. These are listed below, Batchelor et al [45]:-

- The output light level from the lighting source
- The temporal stability of this light level
- The spectrum of the radiation illuminating the object under examination
- The spectral responses of the various optical components.
- The reflectivity of the object being examined as a function of wavelength and the possibility of fluorescence.
- The spectral response of the image sensor
- The spatial distribution of the lighting i.e. uniform, shaded.
- The temporal distribution of the light i.e. steady, flashing
- The polarisation of the light
- The operating environment i.e. temperature , cleanliness
- The magnification of the optical system

- Whether image warping could enhance system performance
- Whether coherent or incoherent light should be used
- The physical size of the working volume available for the optical subsystem
- The resolution of the digital images which are to be used
- Whether an arc-scan or a line-scan imager is to be used
- How the object is to be moved past the camera
- Vibration
- Ambient light, especially sunlight and light from fluorescent lamps
- Whether a single view is adequate or whether two or more images obtained with different lighting arrangements should be used
- How often the optical system is likely to be disturbed and whether a skilled operator will be required to reset it
- Whether the optical system is to be fixed or adjustable to accommodate different classes of object for inspection
- Whether the lighting levels should be monitored automatically or checked manually

Two important rules were also followed when designing the inspection system :-

1. The optical subsystem must be designed in such a way as to reduce the demands on the image processor, by giving it the best possible image to analyse.

2. When designing the image processor, it was assumed that it would not be possible to obtain the same quality of image in a factory as those produced in the laboratory and robust algorithms were necessary.

4.4.2 Mechanical design and development

The design for the multi-axis, tool inspection platform evolved from the knowledge-base which had been established for the range of cutting tool geometries to be handled and the V-scanner operational requirements. Furthermore, considerations had to also account for the inspection device being used as a stand-alone facility as well as being dedicated to a CNC milling machine. Notably for the smooth interaction during tool transfer from the inspection device to the machine tool carousel or visa-versa.

To accommodate a range of cutting tools of different and/or varying diameter the need for an infinitely variable axis drive was also envisaged. To consistently comply with the defined inspection step size and consequent resolution, it was suggested that the major rotational axis had to include a programmable gear-ratio facility. By this means a change in step size could be used to produce a standard length peripheral arc movement at the tool surface. This in turn would enabled the system to inspect a range of tools of different/varying diameters. The non-availability of such a system resulted in a compromise solution being proposed. The device employed to achieve the constant ratio of number-of-steps to diameter was an electronic gearbox, capable of a range of ratios; 1:1, 1:2, 1:4, 1:5, 1:8, 1:10, 1:20 and 1:40. With this development cutting tools would be related to a diameter band and an appropriate gear ratio would be selected to provide the required step size. The step size was matched to the diameter band so as to offer the recommended scanning resolution.

From the earlier work concerned with the cutting tool inventory, it was noted that a considerable number of the tools were ball-nosed or had a radiused-nose. To ensure that the cutting tools were fully inspected it was essential that the tool condition monitoring device could inspect not only the flutes and leading chisel edge but also the nose radius, a part of the tool prone to wear and chipping. To attain this, the tool manipulation platform had to move the inspection head through a circular interpolation, relative to the cutting tool, and furthermore maintain a perpendicular attitude to the nose radius throughout. This

requirement in part contributed to the selection of the AT6400 four axis controller to be used as the axes driver. Standard facilities offered by the system enabled moves of this kind to be executed. Additional provision had to be made, in the mechanical design, to ensure the ability of the inspection head to scan the cutting edges efficiently and effectively. The minor rotational axis, which enabled the scanning head to rotate about a vertical axis, had to be coincident with the laser light source and the opto-electronic sensor's common view point. Figure 4-15 below best illustrates this concept. Provided the rotational axis of the scanning head is in-line with the surface being scanned, the common view point will remain on the surface despite any rotational movement - an essential part of the circular interpolation move discussed above. However if the common view point for the laser and detector is not coincident with the minor axis of rotation then it will essentially move below or above the surface plane being inspected as the axis rotates. This situation would require complex move command sequences and would inhibit active use of the resident circular interpolation function.

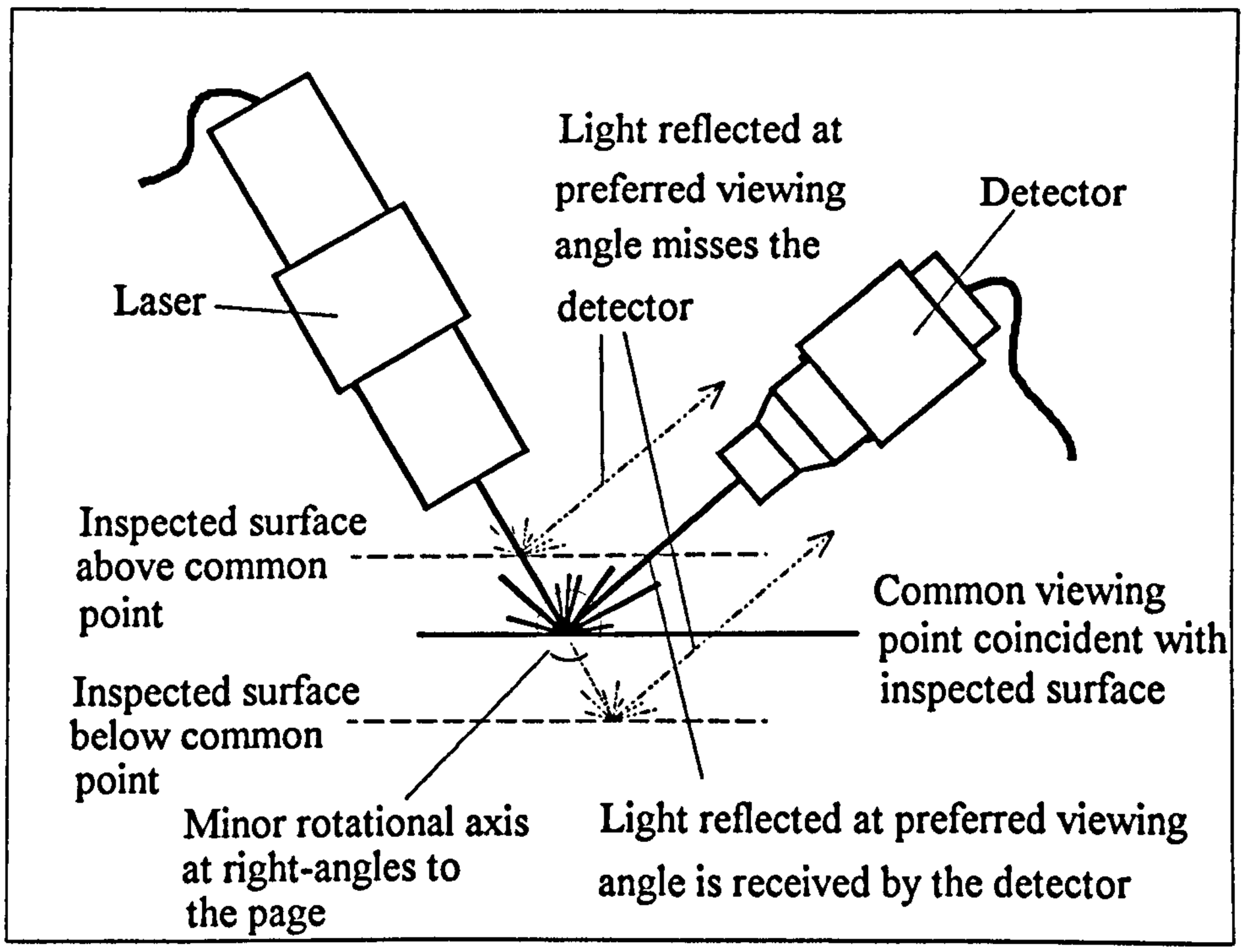

Figure 4-15 The effect of coincident viewing point on surface inspection

For ultimate protection of the somewhat delicate scanning head, it was suggested that provision was made for it to be parked in a shrouded location during tool transfer operations and generally when not in use. This was also to prevent excessive fouling of the optical systems with dust, grime or coolant. As further protection against accidental collision during tool transfer, the head was positioned on the platform at a location on the opposite side to the tool transfer access path. This would ultimately protect the fragile sensory head from a potential impact in the case of a stall or sudden power failure at the inspection station, during the tool transfer operation.

The head was designed to enable inter-changeability and thus subsequent developments in sensor, laser or optical systems could be accommodated. Ultimately the inclusion of additional sensors at pre-defined viewing angles was considered to be an area for continuing research. These aspects are dealt with in Chapter 6.0.

The results of the fundamental laser scanning work, discussed in Sub-section 4.3.2, are presented in the following Chapter. For each of the described tests, the results are discussed and presented graphically. Suitable scanning conditions identified by the program of testing are applied to a sample range of cutting tools in the closing Sub-section (5.2) of the Chapter.

System configuration for the Surface topography inspection device.

The surface topography device consisted of the following system elements;

- Inspection platform,
- Dedicated interface and break-out unit,
- IBM compatible computer with expansion interface card (supplied by Amplicon Liveline)
- Signal conditioning unit (proprietary unit designed and built at Hull University, originator K.G.Swift)

The figure below indicates how the system elements were interconnected for the series of laser and detector angle optimisation tests.

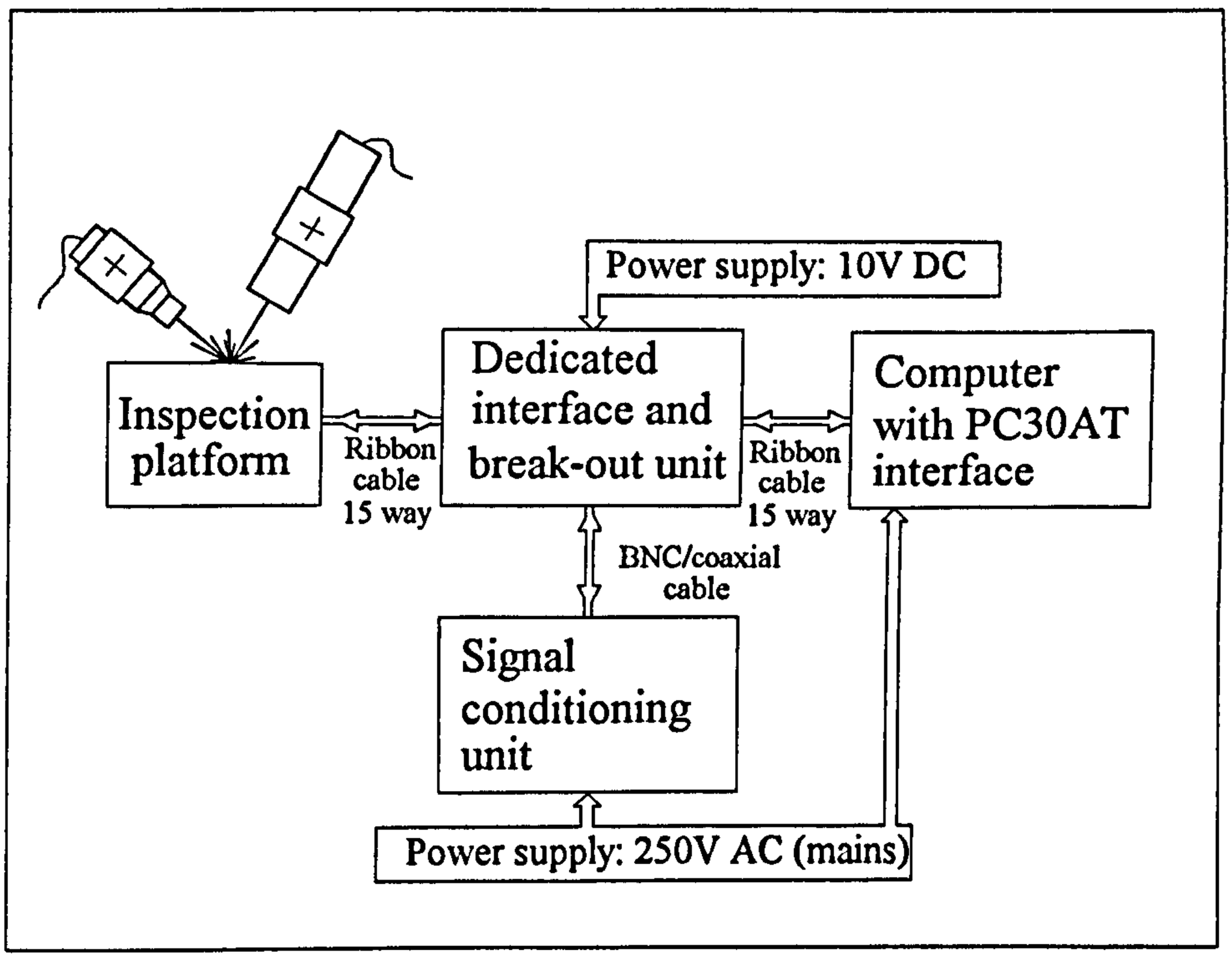

Figure 4-16 Surface topography device system structure

The control software run on the computer system was written in Turbo Pascal. The main program (*controlk.exe*) was designed to be user friendly. System variables such as destination file name (for captured data) could be specified by the user as could be the scan length (in mm). The automatically generated data files were written to a sub-directory

Lasertes resident immediately below the root directory of the host computer. During initial system auto-configuration the platform was designed to home onto a limit switch then moves to a software specified offset. This can be modified to suit different applications by altering the *LOffSet* variable (default value 1850 steps, with 0.7mm of travel for every 48 motor steps (1 revolution)) in the source code *controlk.pas*.

System configuration for the Two-axis inspection device.

The two-axis inspection device consisted of the following system elements;

- Inspection platform,
- Dedicated interface and power supply unit (purpose built),
- IBM compatible computer with expansion interface card (supplied by Amplicon Liveline)
- Signal conditioning unit (proprietary unit designed and built at Hull University, originator K.G.Swift)

The elements were configured in the following way for the Two-axis inspection device.

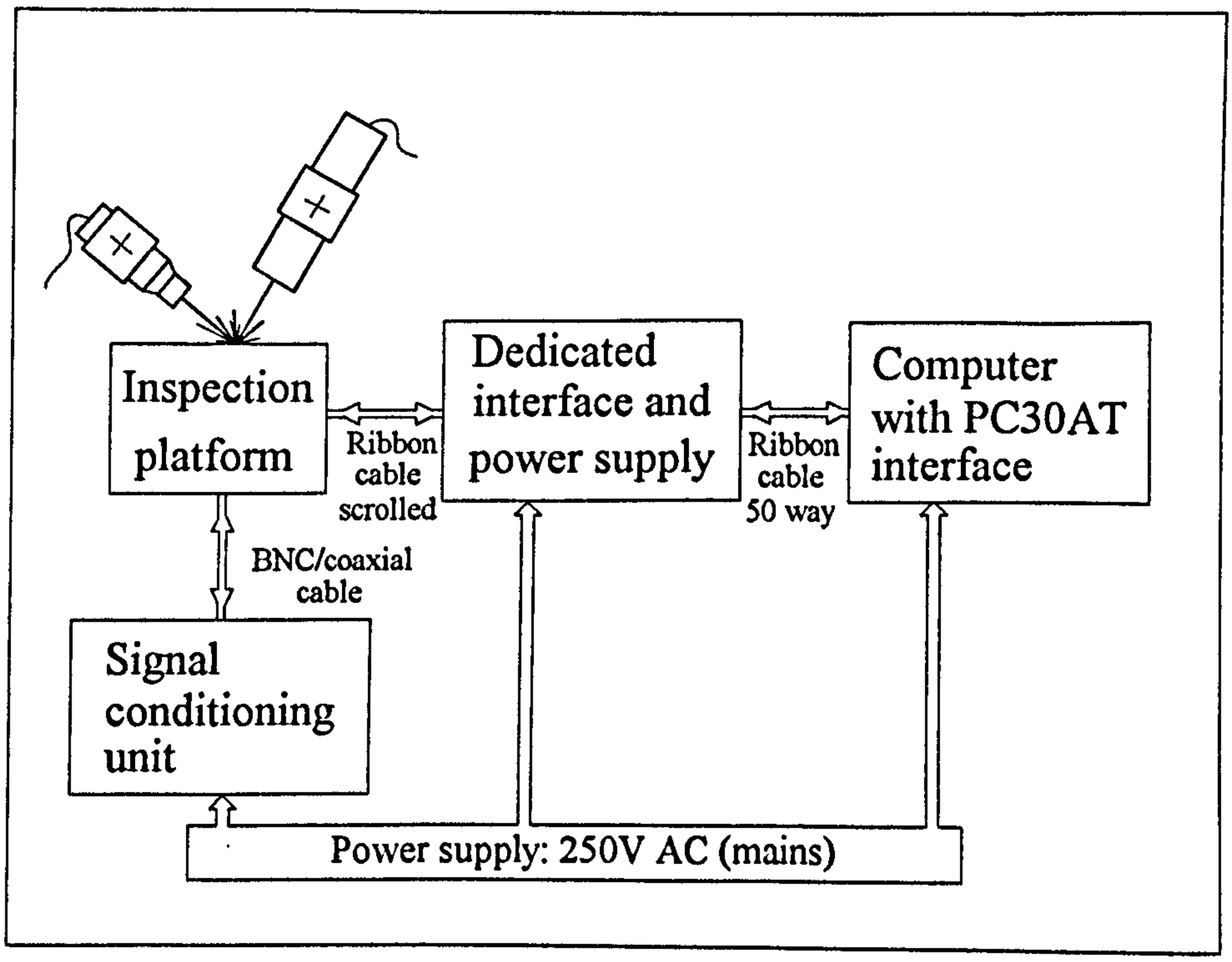

Figure 4-17 Two-axis inspection device, system structure

The control software run on the computer system was again written in Turbo Pascal. The main program (*workarea.exe*) was designed to be user friendly and thus was driven through a menu and windowing system. Due to the complexity and size of the program a number of include files were associated with the main program (by way of the compiler directive {$I}), they were given the following files designations;

- *TYPEDEF.INC*
- *VARIABLE.INC*
- *SETUPSCN.INC*
- *BASMOVES.INC*
- *TRANSDAT.INC*
- *FINDDATM.INC*

Cutting tool inspection data was presented on the screen prior to being written to disk in a file automatically linked to the inspected tool identification number. All data files were saved under a sub-directory *Scandata* below the root directory. Cutting tool move templates were stored as (ASCII) data files in a sub-directory *Tooldata*, again located under the root.

The laser and detector specifications for the general system are given below. Earlier work used a detector supplied by Phillips. A unit which is no longer available.

Laser Specification;

Supplier:	Imatronic, Castle Microwave Ltd., Willow Drive, Twyford, Berkshire. Tel (01734) 343838 Fax (01734) 342068
Size:	16 mm diameter x 50 mm length. Weight 50 g.
Wave length:	660 - 685 nm.
Output Power:	1 mW Class II. Output is preset to Class II requirements of 1 mW maximum.
Output Aperture:	5 mm.
Operational Temperature:	-10°C to + 30°C

Lens:	Single element aspheric. Adjustable focal length.
DC Supply:	3 V to 5.25 V at 80 mA to 120 mA.
Reliability Prediction:	10, 000 hours Mean Time Before Failure.

Detector Specification;

Supplier:	Hamamatsu, Hakuto International (UK) Ltd., Eleanor House, 33-35 Eleanor Road, Waltham Cross, Hertfordshire, EN8 7LF. Tel (01992) 769090.
Type:	Silicon Photodide.
Features:	Visible light to infrared, for precision photometry.
Spectral Range:	400 nm - 1100 nm
Peak wavelength:	900 nm
Package:	TO-18
Driver circuitary:	As per technical sales documentation.

Chapter 5.0

Presentation and Discussion of Results

5.0 Presentation and discussion of results

In the system under development surfaces were examined by illuminating them with visible laser light of wave length 670 nm. The surface interaction with the incident light causes a change in one or more of its characteristics. These changes were sensed by a photo-detector and then processed by computer to yield the desired information about the surface. This technique was applied initially to control samples and then to a restricted range of cutting tools. In this chapter of the thesis the results are presented and analysed.

5.1 Optimised surface interrogation and defect detection

Early work revolved around the simple V-scanner and plane inspection samples, which eliminated many of the complications of convoluted cutting-tool forms. Initially attention was focused upon understanding the functionality of the V-scanner and how the performance was affected by fundamental parameters such as the laser and detector angles, sampling interval and laser spot size. Details of the experimental procedures and apparatus used for each of the tests in the following series can be found in Chapter 4.0. However, the graphical results of these tests are presented and discussed in the sub-sections below.

5.1.1 Detector saturation

Like all analogue photo-detectors, the device used in the experimental work had upper and lower operational limits. When exposed to the full intensity of the laser light the detector was said to be saturated. At the opposite end of the scale, when in total darkness, the response signal was appropriately referred to as the dark signal. The analogue signal produced by the detector was initially processed by a current to voltage converter before being passed to the computer via an analogue-to-digital (A/D) converter interface. Due to this arrangement the succeeding values of reflected light intensity monitored by the photo-detector, were represented by a voltage in the range of 0 to 10 Volts. A direct relationship with the scattered light intensity was not considered necessary to this investigation. The rudimentary principle of the light signal being directly proportional to the computer-based

numerical representation was the key to this assumption. Thus values for the photo-detector output voltage were plotted against distance travelled in the scan cycle.

Figure 5-1 depicts the upper and lower operational limits for the photo-detector used in the preliminary laser V-scanner tests.

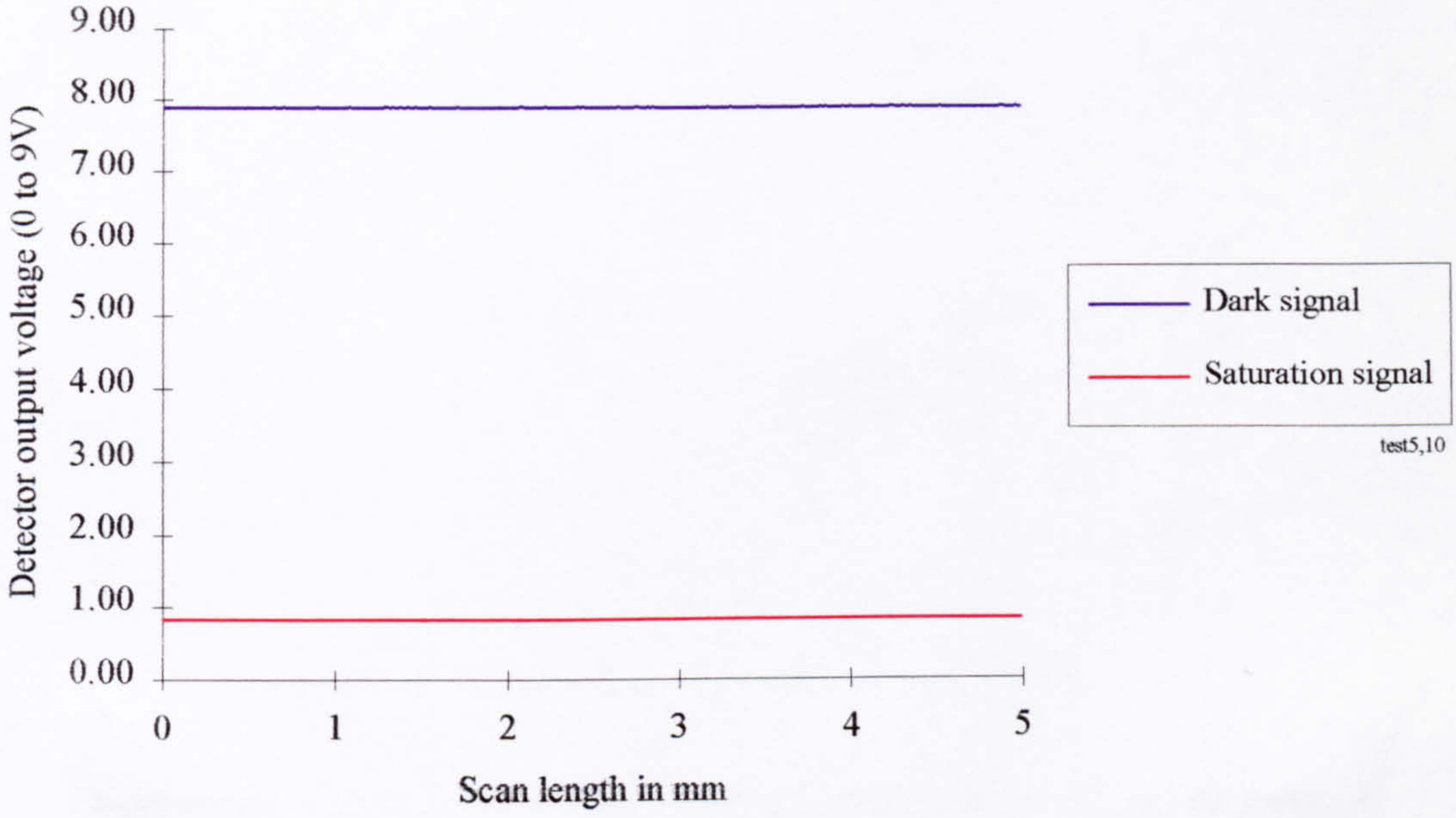

Figure 5-1 Dark and saturation signals for the photo-detector device

The limits shown above must be taken into consideration when developing a system based on light sampling for inspection purposes. This is reinforced in Figure 5-2 which shows three signals. The first possesses a square-wave form, with the detector initially saturated, then starved of any light and finally once again flooded with light causing it to saturate. The response signal, initially at the saturation limit, rises to meet the dark signal confine and then drops accordingly to the saturation confine. The second response signal clearly illustrates the problematic situation encountered when the detector is momentarily over-supplied (saturated) with light. In this situation the signal extending below the saturation limit of the detector is lost and as a consequence is represented by a straight, horizontal line at the saturation confine (light level of approximately 0.8 Volt, in this case). The true nature of this portion of signal, now represented by the straight line, is lost and the information it contained is irretrievable. In respect of this, the system must be configured

in such a way so as to avoid the occurrence of detector saturation on all accounts. The final signal (three) is typical of that for a full-form high contrast signal. This type of response signal is desirable as it contains detailed information about the surface and its topography.

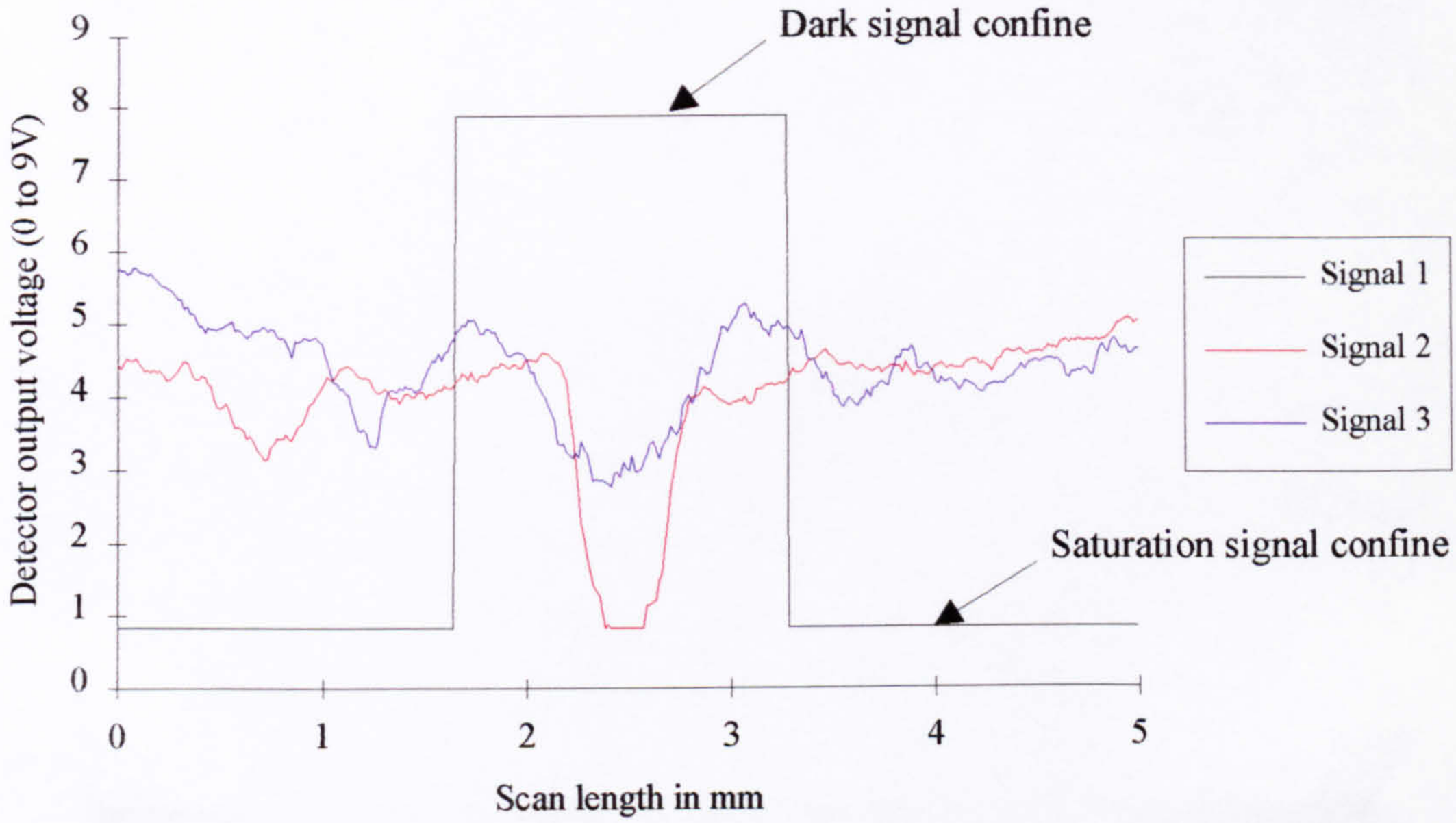

Figure 5-2 Response signals illustrating problems of saturation and starvation of light

5.1.2 Repeatability

Repeatability of the scanning system must also be understood and quantified so that the resolution and reliability can be optimised. In an effort to quantify the repeatability and define a resolution for the system a series of tests were undertaken. The analysis for repeatability was undertaken in the following way. A typical response signal for a built-up edge (BUE) was collected, (Figure 5-3). With the same set-up, a further seven successive response signals were gathered, which should have been identical in every detail. Each of the seven successive signals were subsequently subtracted from the original to produce a differential or deviance graph. The seven resultant graphs were then examined, with the maximum and minimum deviations at each step being recorded. These limiting

deviations, from the original trace, were then plotted to give two graphs, the maximum and minimum differences (deviations) at each location along the scan length.

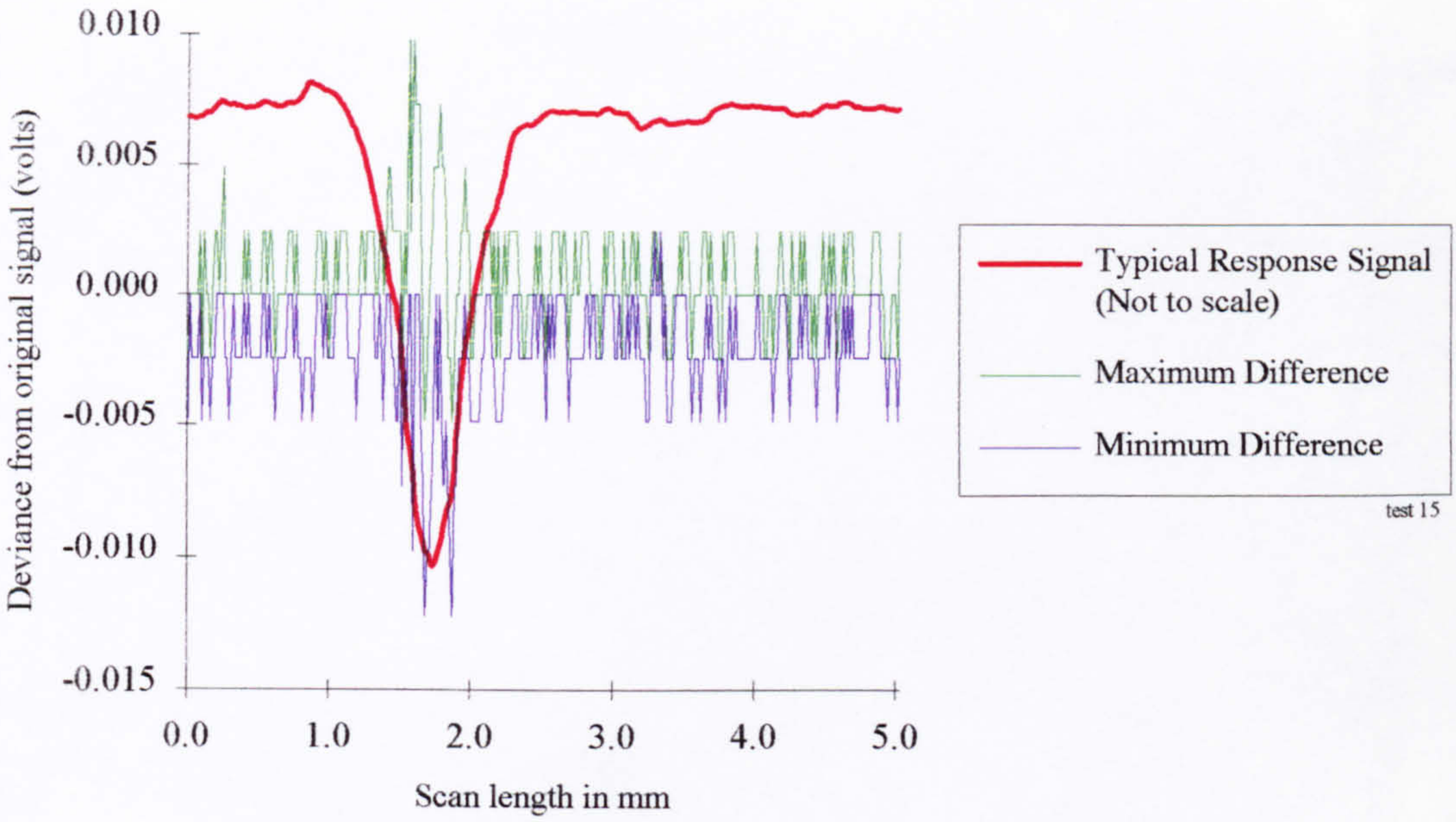

Figure 5-3 Repeatability test for a typical BUE defect response signal

With the V-scanner arrangement under test, it is immediately apparent that the detector output voltage can vary by up to ±0.005 Volts during the course of a typical repeat scan (at about 10% of the full scale detector output voltage, the near horizontal portion of the above master signal). Thus an absolute minimum repeatable resolution can not exceed this figure. With respect to this observation it is impractical and totally unreliable to attempt to distinguish response signal features which are less than 0.005 Volts at the detector output. A divergence is noted as the master signal falls away from the background (to a maximum 28% of the full scale detector output voltage, illustrated by the low trough in the above figure). The maximum and minimum differences are +0.01 and -0.013 Volts respectively. This further observation suggests that the previously suggested minimum repeatable resolution must be relaxed to a more generous figure of say ±0.015 Volts, to filter out any inconsistencies in the system and prevent rogue signals falsely triggering the screening sequence. A general relationship between the signal and the signal deviation can be proposed as a result of these simple tests. The deviance is approximately 0.05% of the

signal strength at that point. Thus the inspection system must not attempt to resolve the signal to a degree beyond this limit.

5.1.3 Optimisation of the incidence and reflection angles

Early general inspection work undertaken in the laser tooling laboratory revealed the sensitive nature of the V-scanner apparatus. This sensitivity was particularly noticeable for the orientation of the lighting source (laser) and viewing detector [50]. Furthermore, it was noted that these parameters were highly dependent upon the topography and nature of the surface being scanned. Thus, before the implications of optimised laser spot size and sampling interval could be investigated, the image quality/intensity resulting from a range of lighting (incidence) and viewing (reflection) angles had to be analysed. This work was a parallel, practical approch to the theoretical work and resultant model proposed by Dewhurst and Swift [35] in their paper *Recent Advances in Laser Tooling for Flexible Handling Systems* and the theoretical predictive work of Sweeney et al. [61].

It has been reported [35], [59] that the scattered light from the surface is made up of two components;

- A specular component, where there is a peak intensity of scattered light at the specular angle: Reflection angle = Incidence angle.
- A diffuse component where the peak intensity often occurs when:

  Reflection angle > Incidence angle.

Figure 5-4 below best illustrates the nature of the reflected and scattered laser light. The diffuse peak is broader than the specular peak; it broadens with increasing surface roughness, and it is dependent in part on the ratio σ_m/λ, where σ_m is the root-mean-square mechanical roughness of the surface and λ is the wavelength of the laser light. It is also reported to be dependent upon the angle of incidence of the laser light. The existance of off-specular peaks were observed as early as 1901 by Lord Rayleigh [51] but work in this area has been reported more recently by Torrance et al. [59] and Birkebak et al [60].

The response signals produced by a laser-based V-scanner arrangement are investigated and discussed below. Particular attention is given to the variation of signal quality in response to a prescribed range of laser and detector angles.

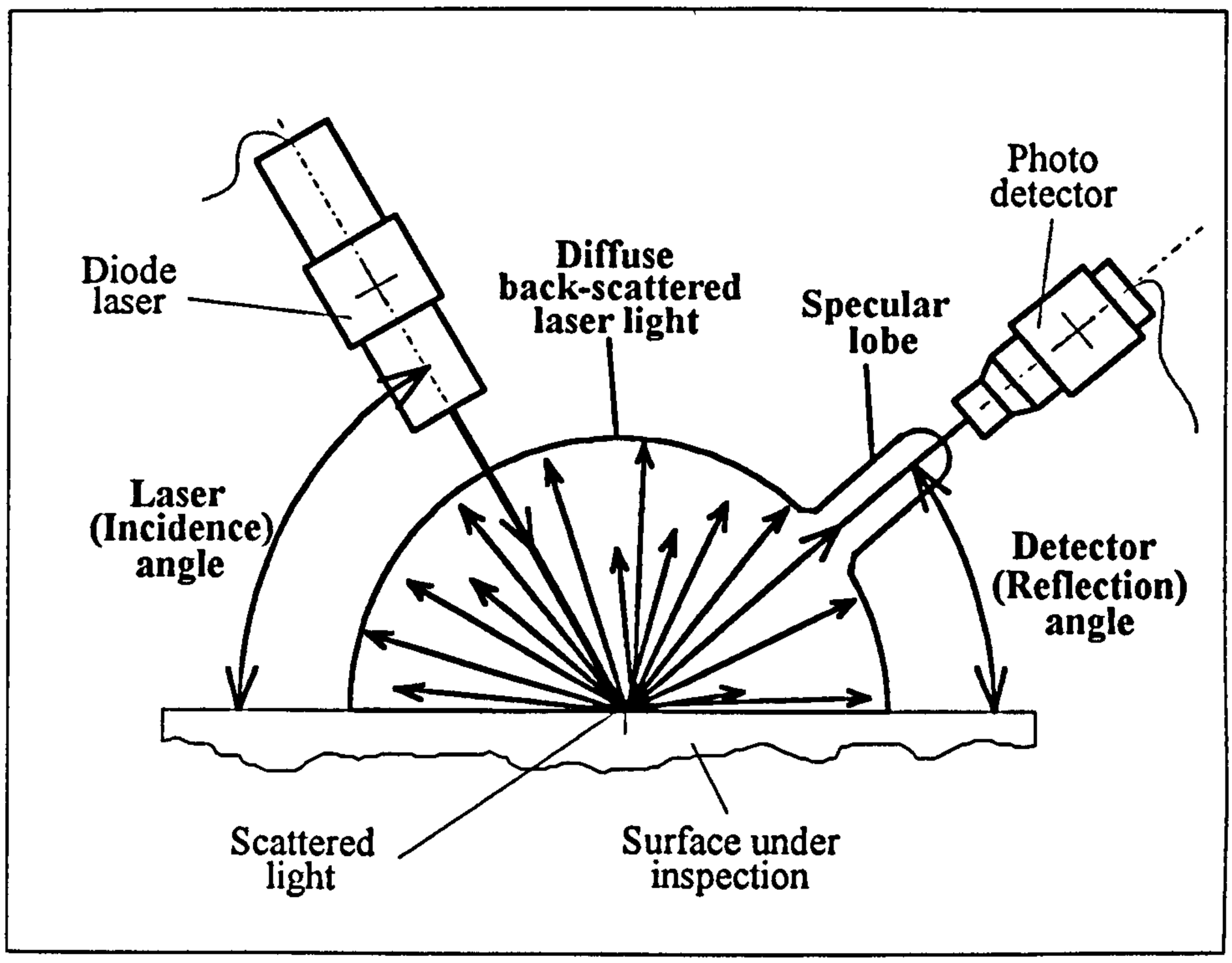

Figure 5-4 Light intensity profile for an incident beam onto a rough plane surface

The incidence and reflection optimisation tests adopted the following procedure;

- With the laser angle set at 80° and that for the detector fixed at 20° a 5 mm scan of a control sample was recorded.
- On the same sample, repeat scans were recorded for laser angles incrementally reduced by ten degrees, down to a minimum of 20° (seven scans in total), with the detector angle being maintained.
- The seven resultant graphs were then manipulated and superimposed on the same graphical axes. These results have been incorporated into the following discussions.
- The three stages described above were then repeated for a range of detector angles, increasing from 20° to 50° in steps of 10°, again for the same control sample.

- A range of control samples, representing different surface finishes (grinding, milling, shot blasting and polishing) and roughnesses (0.5 μm to 12.5 μm), were analysed using the same procedure as that defined above. Again the graphical output has been incorporated into the following discussion of results.

The results are presented in the following format;

- close-up photograph of the inspected surface,
- surface topography trace of the inspected surface,
- combined discussion of results comprising four graphs,
- summary of the results.

12.5 μm Plain end mill control sample

Photograph of inspected surface (12.5 μm Plain end mill sample)

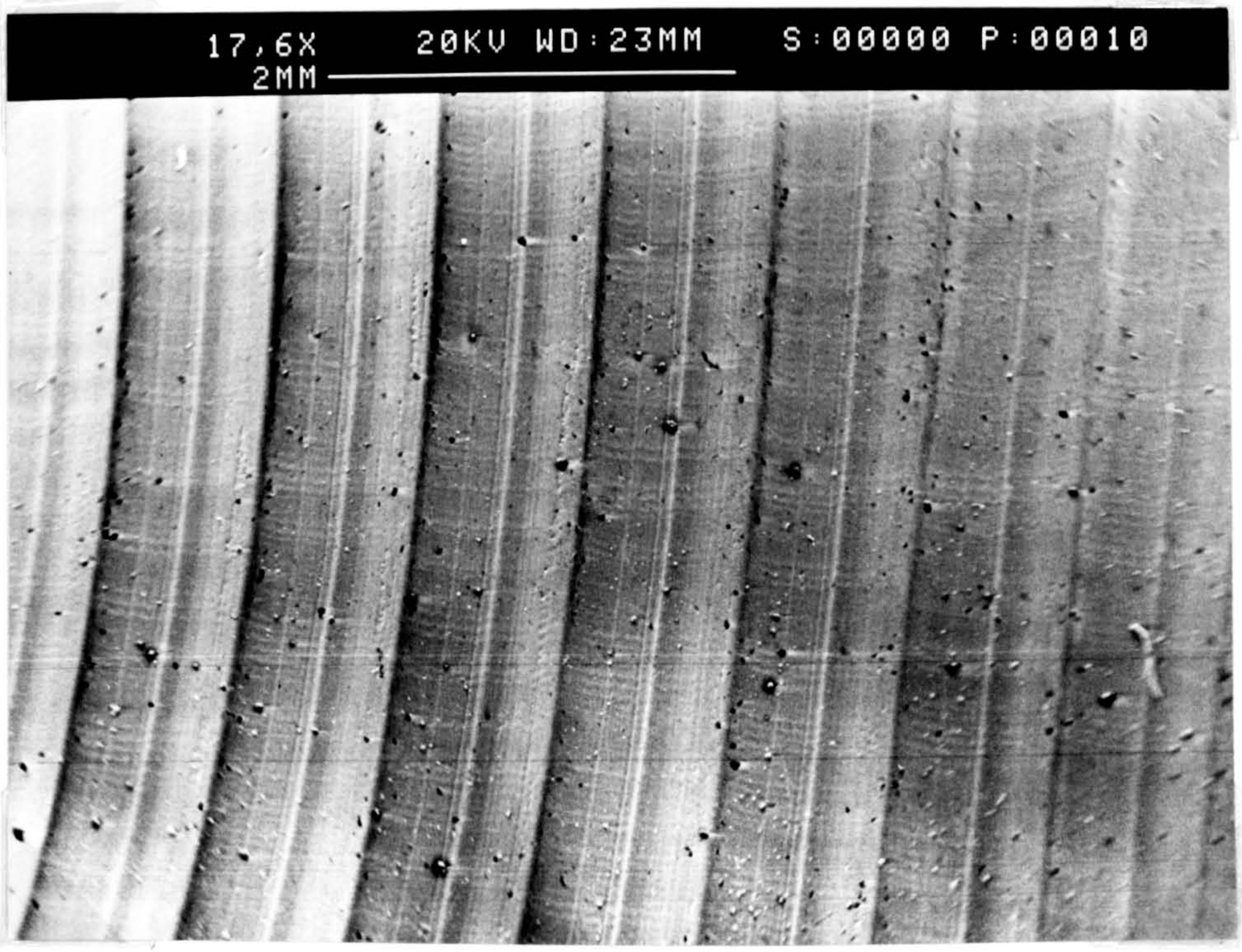

Figure 5-5 12.5 μm Plain end mill sample, surface photograph

Surface topography trace (12.5 μm Plain end mill sample)

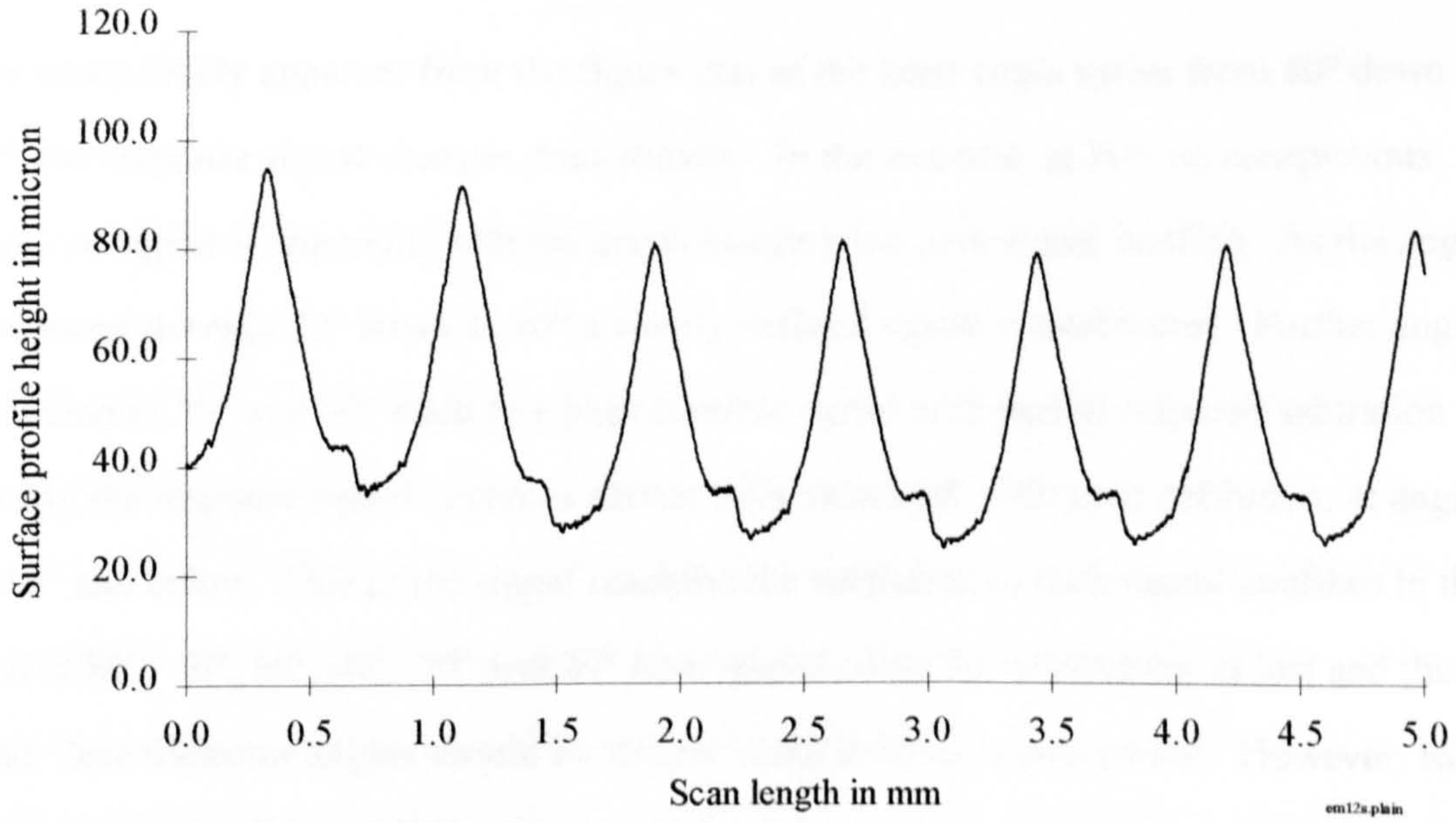

Figure 5-6 12.5 μm Plain end mill sample, surface profile

12.5 μm Plain end mill sample - 20° fixed detector angle

The clearly visible surface form of the 12.5 μm end milled control sample made it the obvious first choice for scanning. A strong correlation between the response signal and surface topography had been noted on earlier inspection test-runs. The graphical results of the seven scans, from the first test, are presented in figure 5-7 below.

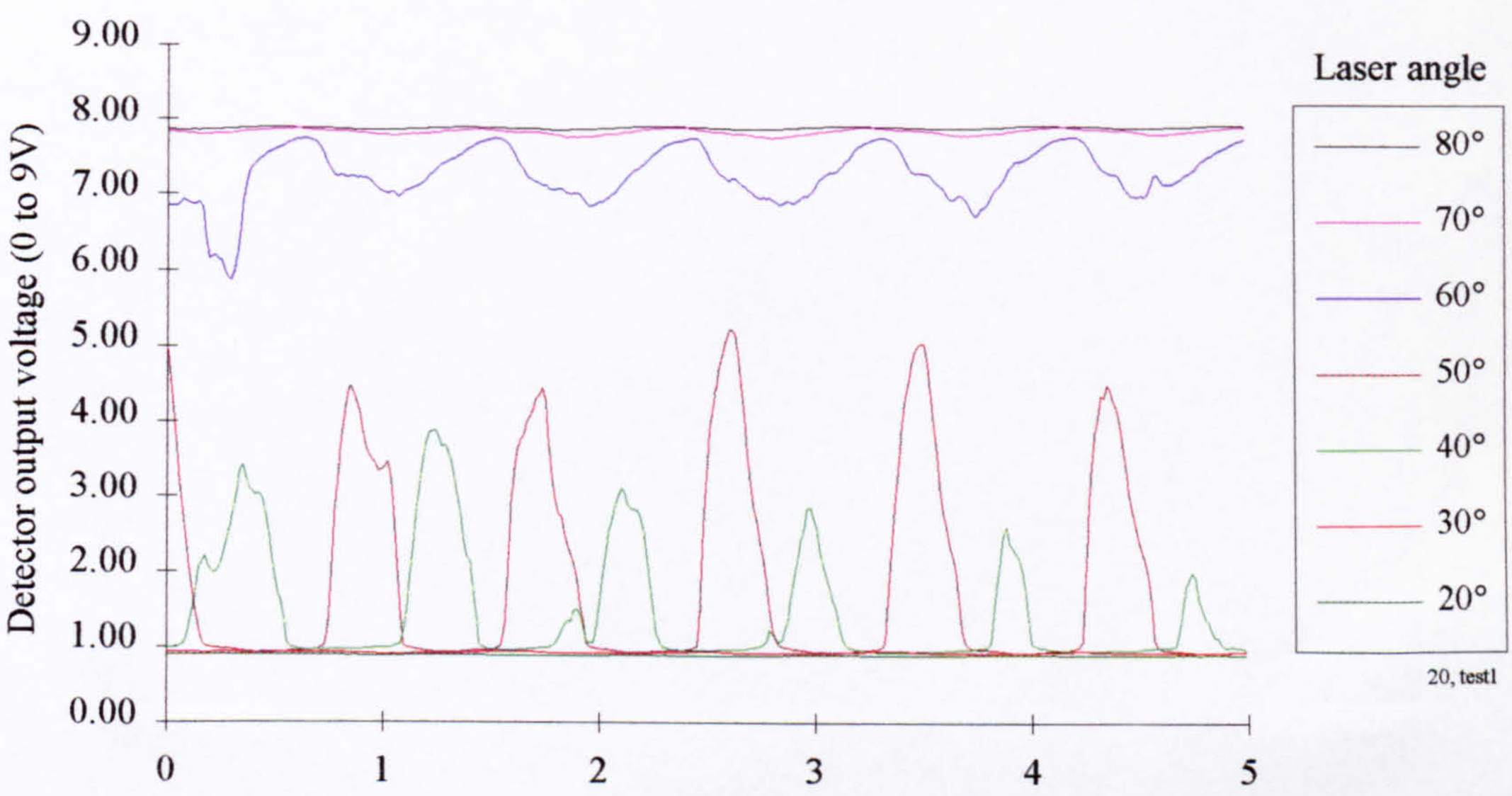

Figure 5-7 12.5 μm Plain end mill sample with fixed detector angle of 20°

It is immediately apparent from the figure that as the laser angle varies from 80° down to 20°, the response signal changes dramatically. In the extreme, at 80°, no conspicuous response signal is apparent, with the graph hugging the dark signal confine. As the angle is reduced through 70° down to 60° a clearly defined signal is established. Further angle reduction to 50° and 40° leads to a high contrast signal with partial response saturation. Finally the response signal becomes almost fully saturated, with poor definition, at angles of 30° and below. Due to the signal reaching the saturation or dark signal confines in the case of 80°, 70°, 50°, 40°, 30° and 20° laser angles, detailed information is lost and thus these laser/detector angles should be strictly considered as inappropriate. However, two of these signals (50° and 40°) contain meaningful information about the surface and due to their strength could be used to advantage in a scanning application. This observation will

be further deliberated as more results are presented. The full form of the response signal for a laser angle of 60° illustrates that it perhaps offers the most suitable settings under the imposed test conditions.

12.5 μm Plain end mill sample - 30° fixed detector angle

As in the previous case the basic form of the end milled control sample is immediately apparent from the signals presented in figure 5-8. The signals were gathered for a series of laser angles ranging from 80° down to 20°. Through-out the tests the detector angle was maintained at 30°.

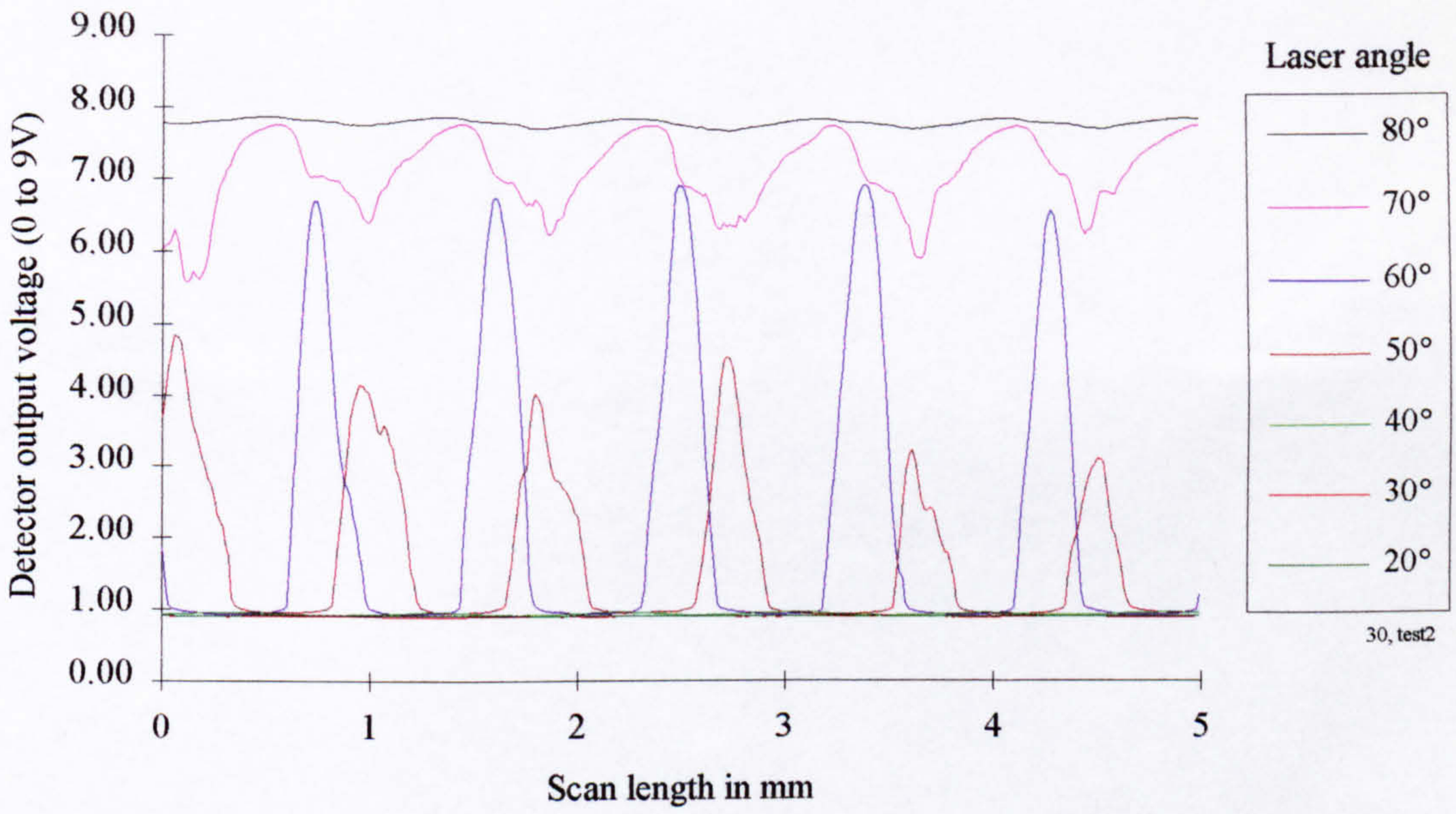

Figure 5-8 12.5 μm Plain end mill sample with fixed detector angle of 30°

When compared with the results of the first end mill test (figure 5-7) a noticeable downward shift of all the series, towards the saturation (bottom) confine, is apparent. Two distinguishing features which separate figure 5-8 from figure 5-7 are; only one response signal meets the dark signal (top) confine and the form of the signals which respond to the control surface undulations are fuller. For a laser angle of 80° the response signal is seen to meet the dark signal confine with little variation in strength. At 70° the laser set-up produces a full form signal with no saturation taking place. Notably the signal has

superior contrast when compared to the optimum signal of the previous figure. The following two series for laser angles of 60° and 50° again display enhanced contrast, though they exhibit saturation over part of the signal range. The remaining laser angles of 40°, 30° and 20° produce signals consistent with a completely saturated detector rendering them unsuitable.

12.5 μm Plain end mill sample - 40° fixed detector angle

In Figure 5-9 the distinguishing differences between the results for detector angles of 20° and 30° are again apparent for the further increase in detector angle from 30° to 40°. They are; a downward cascading displacement of the series and an increase in contrast of those signals responding to the form of the inspected surface. Only a laser angle of 80° produces a signal with full form and good contrast. 70° and 60° angles display increased contrast at the expense of partial saturation over a significant proportion of the signal. Complete saturation occurs for all angles of 50° and below.

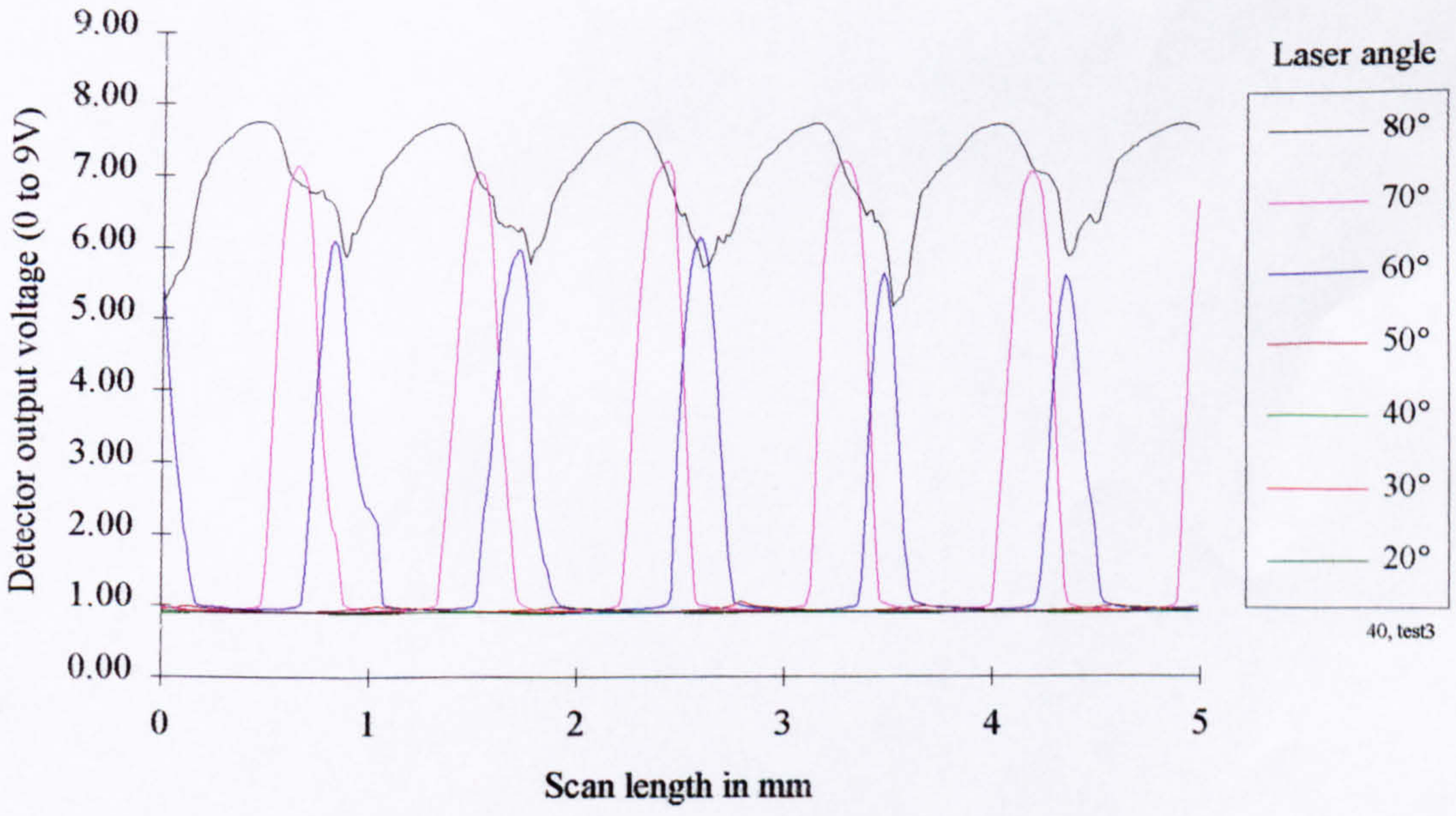

Figure 5-9 12.5 μm Plain end mill sample with fixed detector angle of 40°

12.5 μm Plain end mill sample - 50° fixed detector angle

For a detector angle of 50°, high contrast and the regular nature of the milled surface are the dominant response signal features for illumination angles of 80° and 70° (See Figure 5-10 below). A degree of saturation render the signals unsuitable for detailed information extraction. A laser angle of 60° results in the response signal tending towards saturation with narrow peaks representing each of the ridges on the control sample. Angles of 50° and below produce a completely saturated signal.

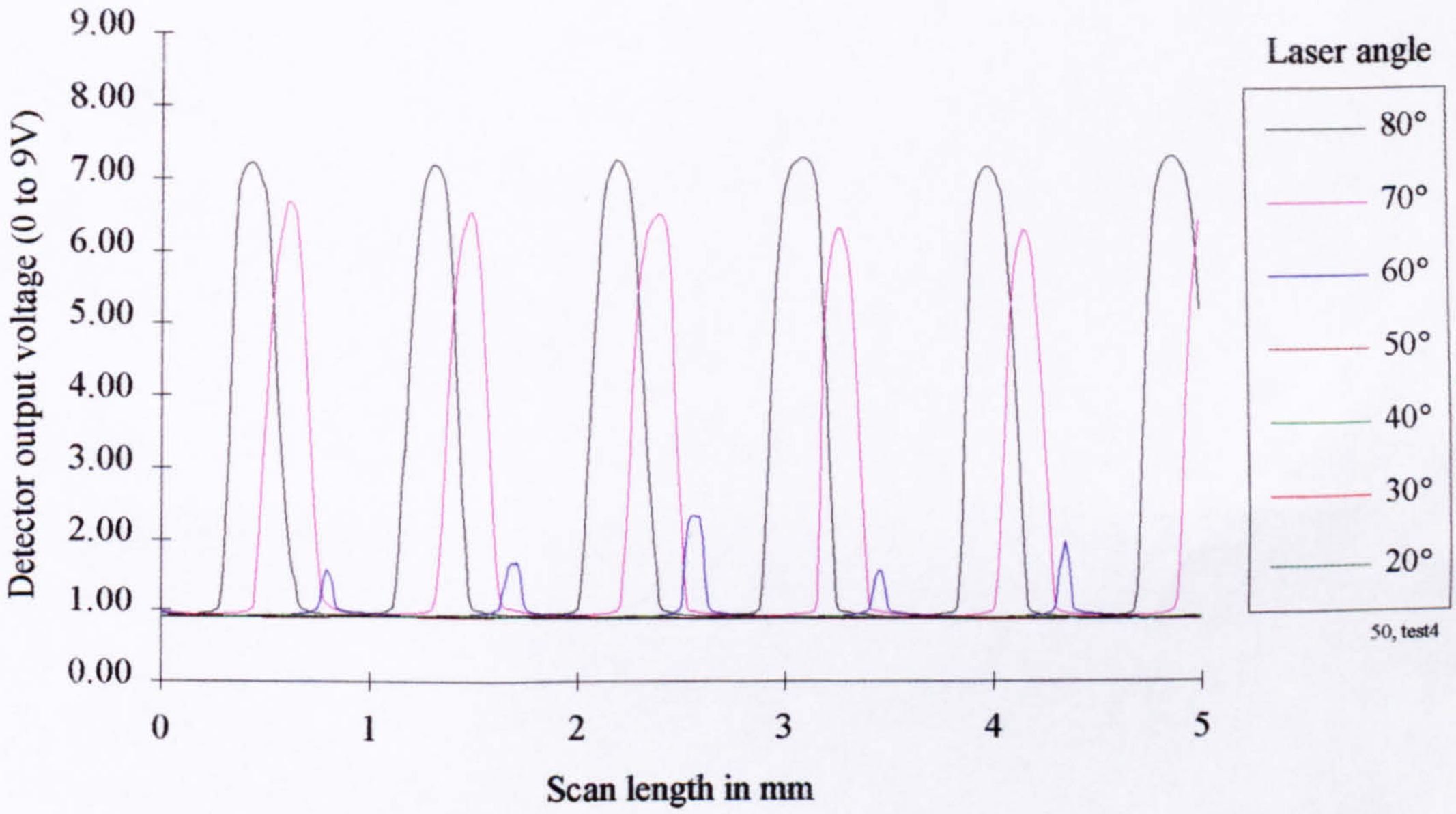

Figure 5-10 12.5 μm Plain end mill sample with fixed detector angle of 50°

12.5 μm Plain end mill sample - Summary

The results of the four end mill sample figures are summarised in the matrix below (Table 5-1), which indicate the optimum laser and detector angles for an end milled surface with roughness of 12.5 μm. The tick (✓) implies an optimum setting whereas the cross (✖) suggests a laser and detector angle arrangement which lead to response saturation or poor definition. A intermediary mark (o) indicates that the settings produced a response signal

which contained some basic information though detail could not be extracted due to the form or level of saturation.

Relative Laser/Detector Angle - Response Signal Suitability Matrix (12.5 μm Plain end mill sample)							
Detector Angle	Laser Angle						
	80°	70°	60°	50°	40°	30°	20°
20°	×	×	✓	o	o	×	×
30°	×	✓	o	o	×	×	×
40°	✓	o	o	×	×	×	×
50°	o	o	o	×	×	×	×

Table 5-1 12.5 μm Plain end mill sample response signal suitability matrix

Further to the specific observations already made, the end milled control sample response signal suitability matrix reveals additional general information. The nearest true form of the inspected surface is represented by those laser and detector settings marked by a tick (✓). The narrow, steep sided signals which experience partial saturation (o) clearly indicate the presence of the regularly undulating surface though some detail is lost. As the laser angle decreases a shift in spatial phase, of the response signal, is detected (left to right in every case). For shallow detection angles (20°) the shift is approximately 0.5 mm - for a 10° change in laser angle. At steeper detector angles (50°) the shift is considerably reduced, to approximately 0.2 mm, for the same change in laser angle.

12.5 μm End mill control sample with scratch defect

Photograph of inspected surface (12.5 μm end mill sample with scratch defect)

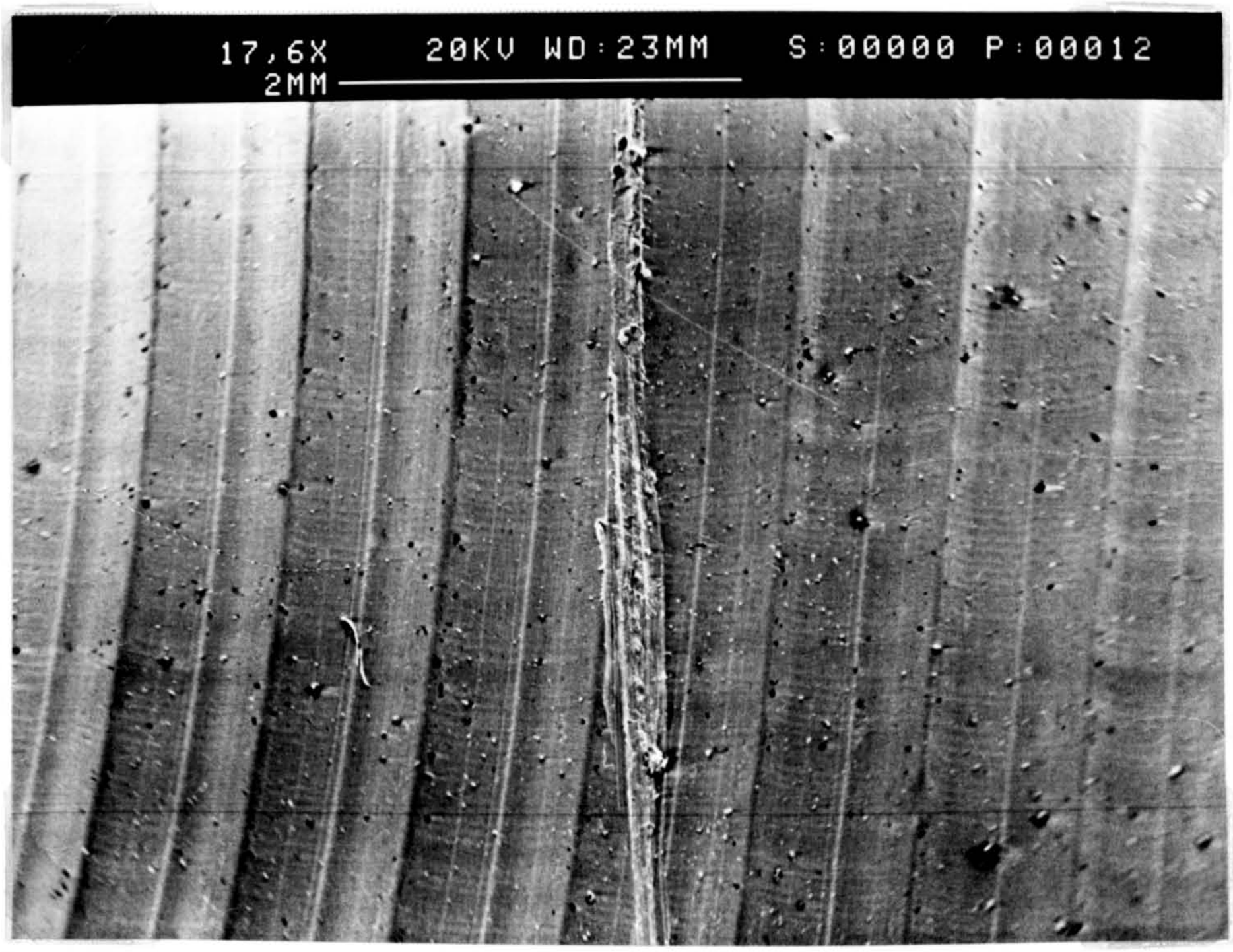

Figure 5-11 12.5 μm end mill sample with scratch defect, surface photograph

Surface topography trace (12.5 μm end mill sample with scratch defect)

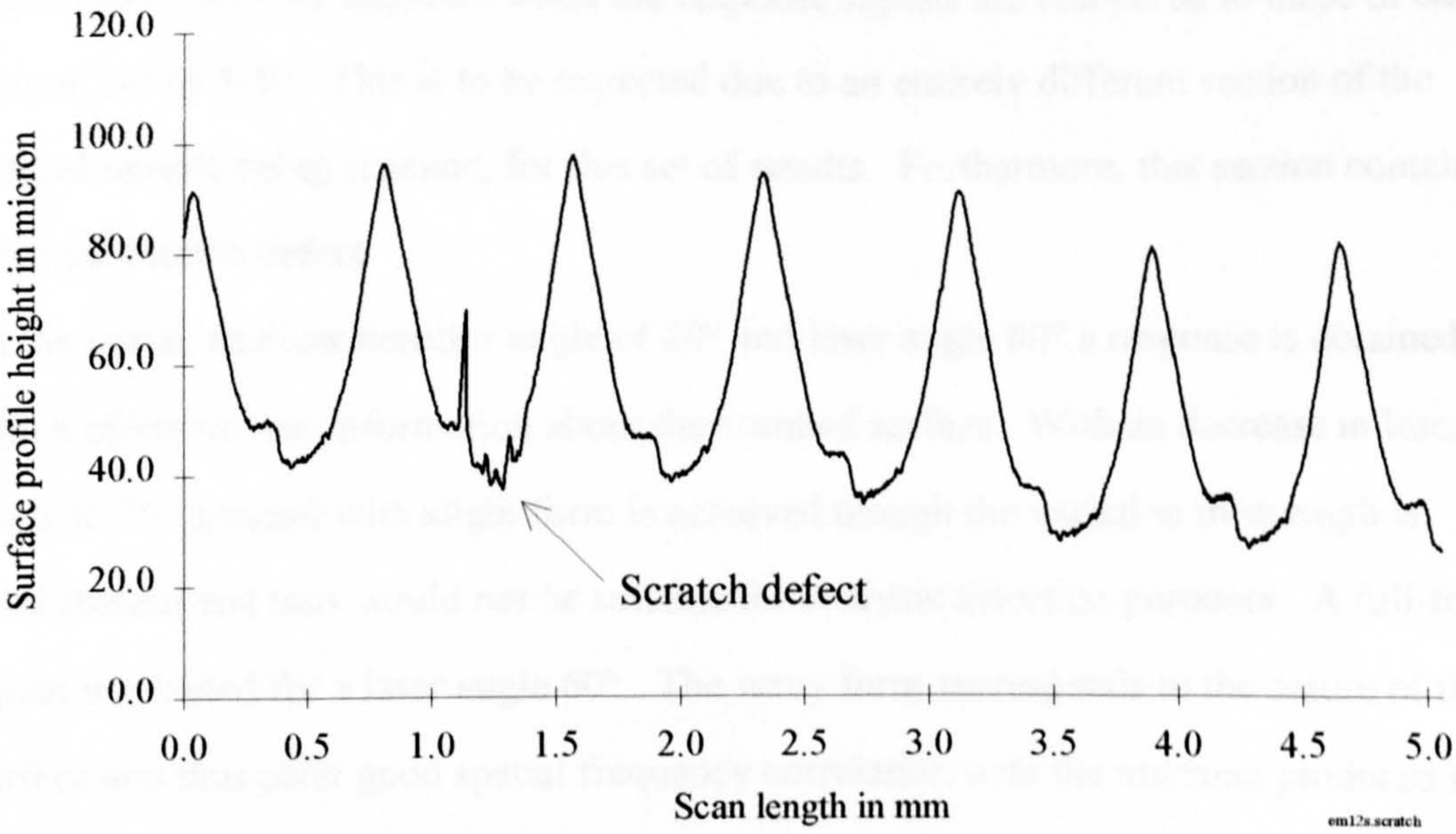

Figure 5-12 12.5 μm end mill sample with scratch defect, surface profile

12.5 μm end mill sample with scratch defect - 20° fixed detector angle

The characteristic end mill, steep sided peaks (See figures 5-11 and 5-12) are visible in the data sets displayed in the first figure of the result group, see figure 5-13 below.

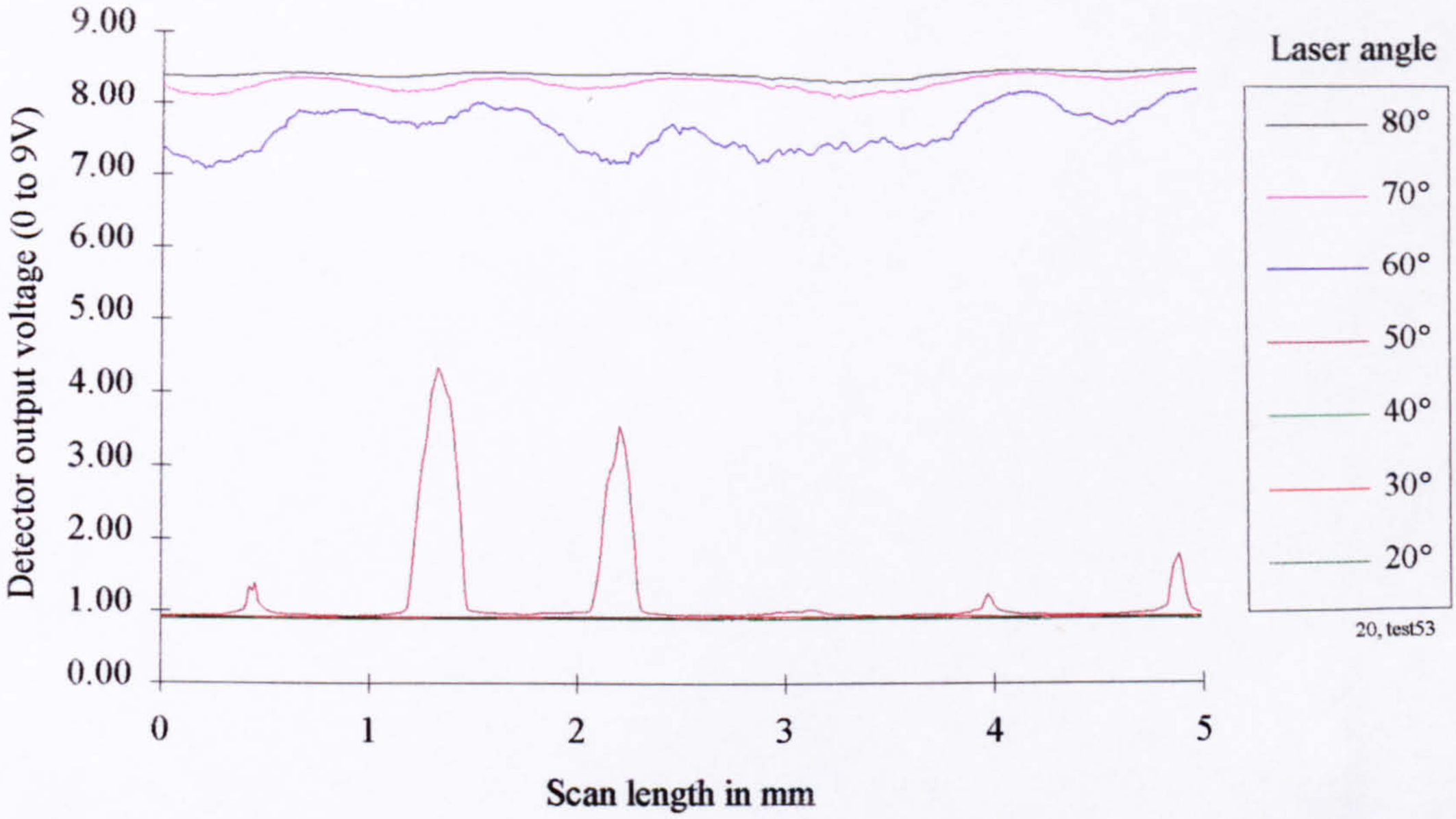

Figure 5-13 End mill sample with scratch defect and fixed detector angle of 20°

Though surface inspection was performed on the same sample form (12.5 μm end mill) slight differences are apparent when the response signals are compared to those of earlier figures 5-7 to 5-10. This is to be expected due to an entirely different section of the control sample being scanned, for this set of results. Furthermore, this section contains an artificial scratch defect.

At the initial, shallow detector angle of 20° and laser angle 80° a response is obtained which offers no real information about the scanned surface. With an decrease in laser angle to 70° a signal with slight form is achieved though the variation in strength is insubstantial and thus would not be suitable for analysis/detection purposes. A full-form signal is attained for a laser angle 60°. The wavy form corresponds to the nature of the surface and thus offer good spatial frequency correlation with the machine produced ridges on the control sample (approximately 1.3 peaks/mm). Though the peaks and troughs are not of regular form, sufficient disruption of the response signal trend occurs as a

consequence of the scratch defect for it to be detected. Presence of the scratch is further signified by an increase in amplitude of the low frequency signal component, of the order of 10 peaks/mm. Enhanced indication of the scratch presence is evident when the laser angle is reduced further to 50°. The steep sided characteristic peaks, of varying height, are clearly visible except at the site of the scratch (scan length 3 mm approximately). Here there is only a marginal variation in detector output voltage. However, information rendered by the response signal is limited as saturation occurs between the peaks, at the lower confine. For decreased laser angles (40°, 30° and 20°) the detector is saturated for the entire scan, so rendering the settings totally unsuitable.

12.5 µm end mill sample with scratch defect - 30° fixed detector angle

A low contrast (amplitude) variation of the response is attained for a detector angle of 30° and a laser angle 80°, making the settings unsuitable for detection or analysis purposes. With a decreased laser angle (70°) a full-form response is gained which offers encapsulated general and detailed information about the scanned surface, see figure 5-14 below.

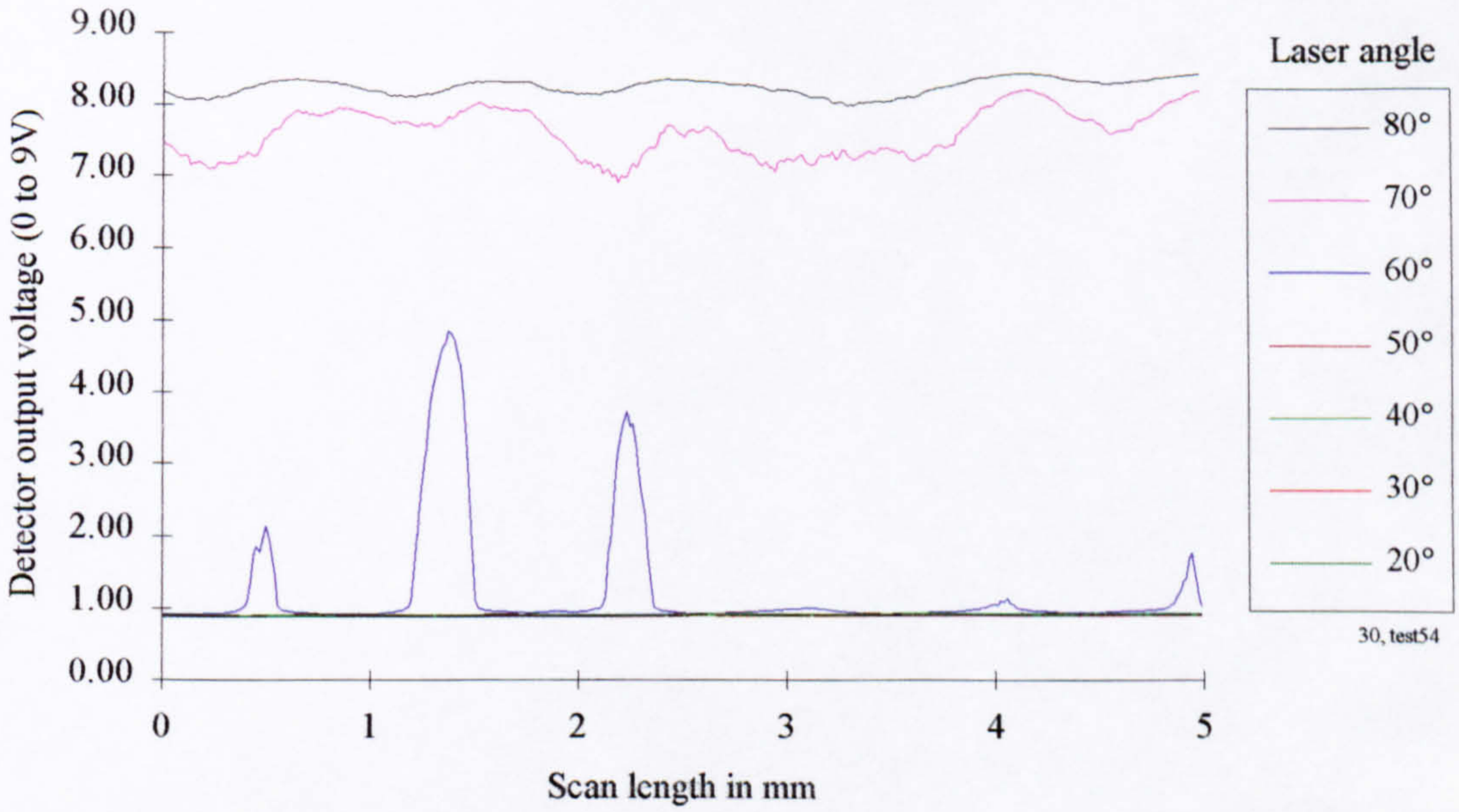

Figure 5-14 End mill sample with scratch defect and fixed detector angle of 30°

At the laser angle of 70° an increase in the higher frequency, low amplitude component of the signal is apparent at the scratch defect site (scan length 2.0 to 3.8 mm). This replaces one of the dominant response peaks at the site of the scratch defect. The steep characteristic peaks rising from an otherwise saturated signal are evident at a reduced laser angle of 60°. The high contrast achieved with this setting makes it ideally suited to scratch defect detection, despite the signal being partially saturated. Note the missing peak at the site of the scratch defect (scan length 3 mm). A further reduction in laser angle results in total response saturation in all cases (50°, 40°, 30° and 20°).

12.5 µm end mill sample with scratch defect - 40° fixed detector angle

The full-form signal exhibited by the 60° and 70° laser angles in the first and second graphs of this subsection is again displayed but at a laser angle of 80°. The Details of the signal are much the same as those mentioned above. At a lower angle of 70° the steep sided characteristic peaks once again form a distinguishing feature of end mill results. See figure 5-15 below.

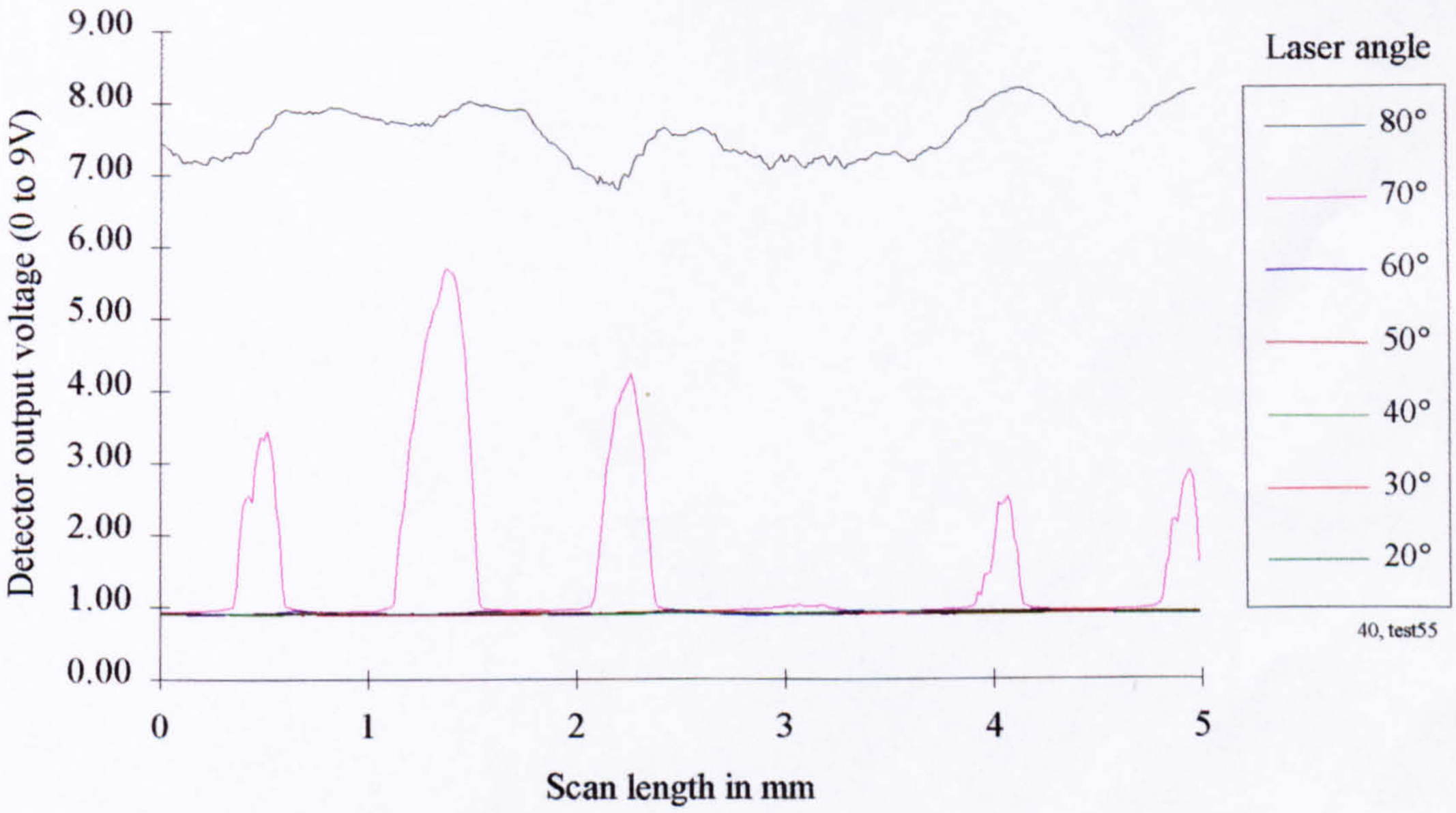

Figure 5-15 End mill sample with scratch defect and fixed detector angle of 40°

These high contrast peaks are more pronounced and uniform than for the previous settings, making them easier to detect. The distinct lack of a peak at the site of the scratch defect is also clearly evident, thus making defect detection possible. For laser angles of 60° down to 20° the detector remains saturated throughout.

12.5 μm end mill sample with scratch defect - 50° fixed detector angle

The final array of results for this end mill sample with scratch defect, figure 5-16, is dominated by the characteristic peaky response (laser angle of 80°). This was the only laser setting in the group (detector angle of 50°) which yielded results suitable for analysis purposes. All other investigated laser incidence angles (70° down to 20°) produced saturated, featureless responses.

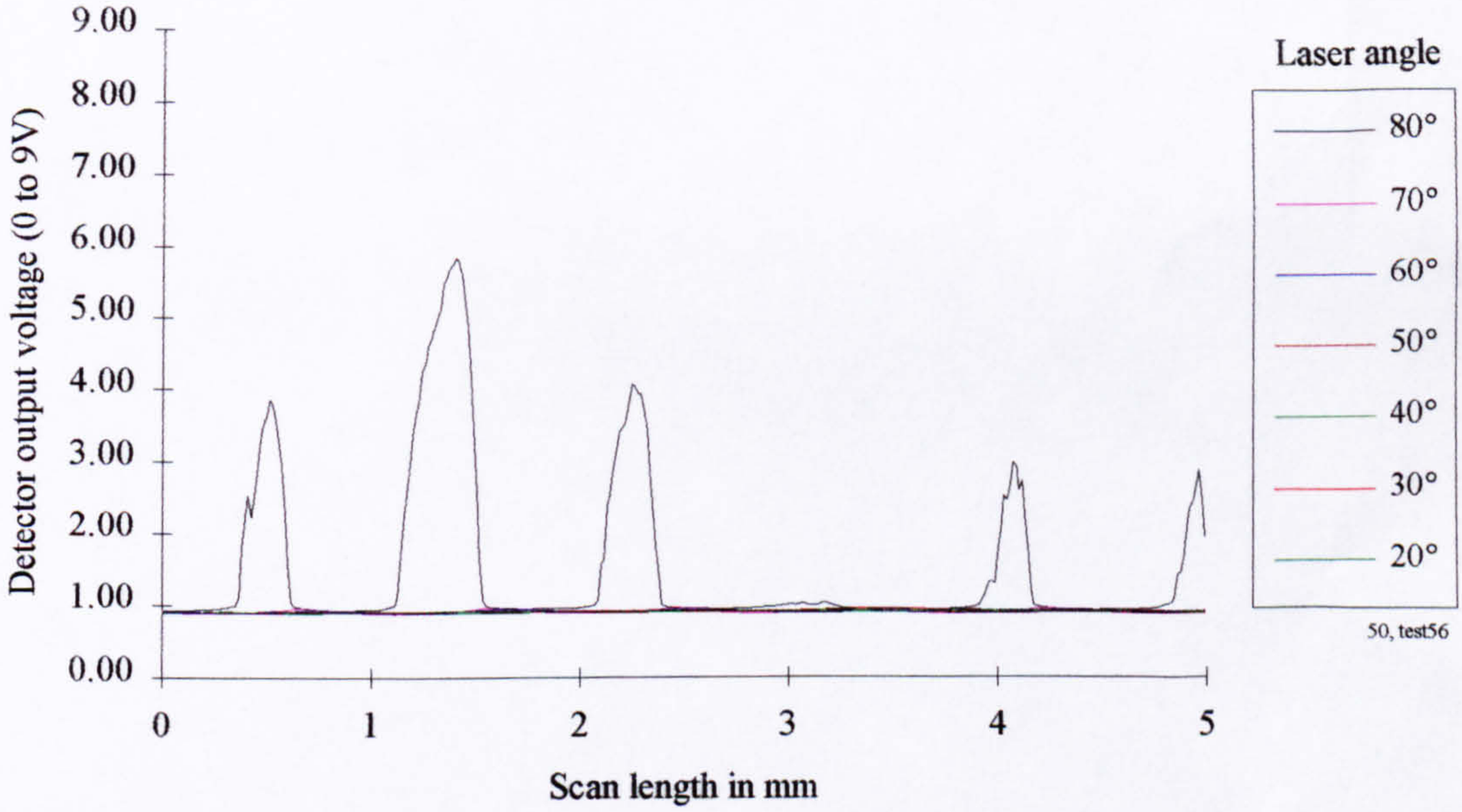

Figure 5-16 End mill sample with scratch defect and fixed detector angle of 50°

12.5 μm end mill sample with scratch defect - Summary

The results of the end mill sample with scratch defect are summarised in the matrix below. As before, optimum laser and detector angles can be easily identified using the following key. A tick (✓) indicates an optimum setting whereas the cross (✗) suggests a laser and

detector angle arrangement which lead to response saturation or poor definition. An intermediary mark (o) indicates that the settings produced a response signal which contained some basic information though detail could not be extracted due to the form or level of saturation.

Relative Laser/Detector Angle - Response Signal Suitability Matrix
(12.5 μm end mill sample with scratch defect)

Detector Angle	Laser Angle						
	80°	70°	60°	50°	40°	30°	20°
20°	×	×	✓	o	×	×	×
30°	×	✓	o	×	×	×	×
40°	✓	o	×	×	×	×	×
50°	o	×	×	×	×	×	×

Table 5-2 12.5 μm end mill sample with scratch defect, response signal suitability matrix

Identical tests to those described in the previous sub-sections were performed on a range of control samples resulting in excess of 560 data series being recorded. Due to the volume of the data involved (almost 200 000 discrete data items) the subsequent discussions and analyses of the remaining results are kept brief. The discussions revolve around the surface photograph, surface profile trace, suitability matrix and four graphs. This abridged approach will be adopted throughout with the exception of a few cases which reveal interesting or unexpected results. The presentation format is kept uniform throughout for ease of reference/cross reference, as it is intended that the results of this sub-section should be used as a guide to researchers who are actively working in closely related fields.

12.5 μm end mill control sample with built-up edge (BUE) defect

Photograph of inspected surface (12.5 μm end mill sample with BUE defect)

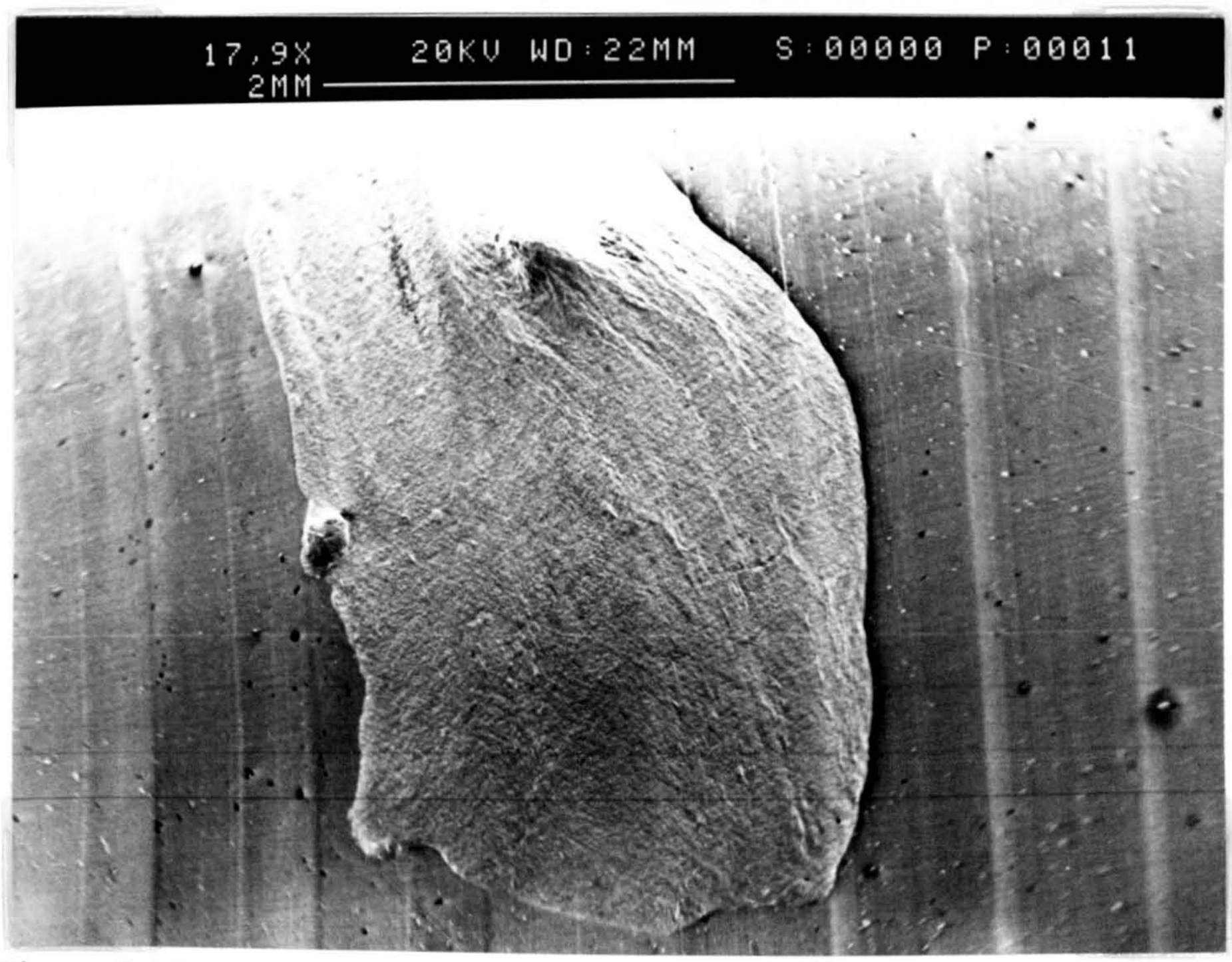

Figure 5-17 12.5 μm end mill sample with BUE defect, surface photograph

Surface topography trace (12.5 μm end mill sample with BUE defect)

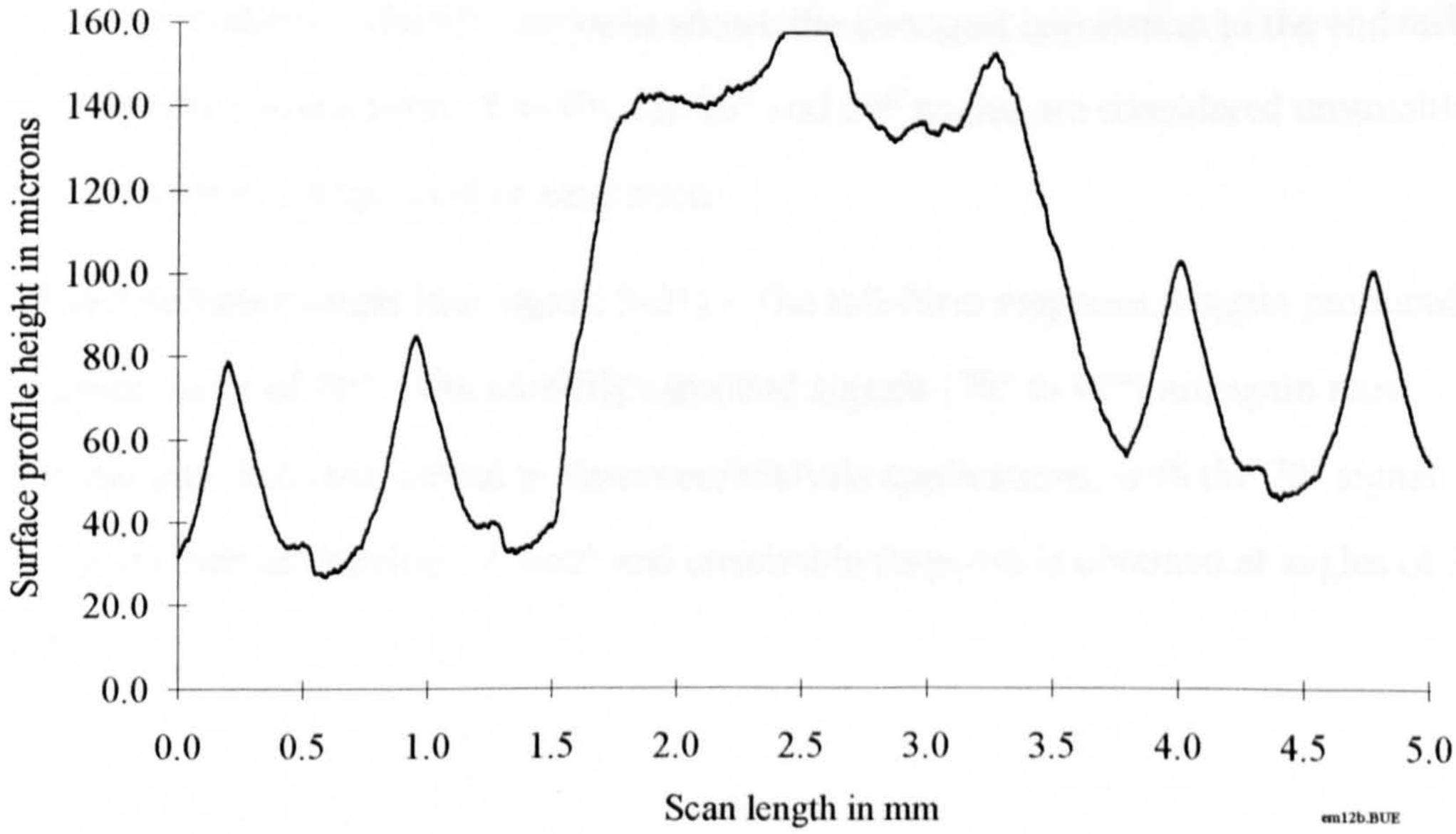

Figure 5-18 12.5 μm end mill sample with BUE defect, surface profile

Discussion of results (12.5 μm end mill sample with BUE defect)

The characteristic steep sided peaks clearly illustrated in figures 5-17 and 5-18 are visible in all four figures of the result group (figure 5-19 to 5-22 below).

20° fixed detector angle (See figure 5-19) - The high contrast signals for angles of 50°, 40° and 30° would be most suited to automatic defect detection, with the laser angle of 50° producing the best results of the three - the regular undulations of the end mill control sample being clearly visible. At the steeper laser angles of 80° to 60°, all resultant response signals contain sufficient information to act as a trigger in an automatic defect screening operation/system but would require a more sensitive analysis procedure than those mention previously. Thus the system would be more prone to false triggering. However, additional surface form information is contained in the 70° and 60° results which suggests that they are of higher analytical value. A totally unsuitable signal (saturated) is produced at the common laser/detector angle of 20°.

30° fixed detector angle (See figure 5-20) - Full-form signals are produced at angles of 80° and 70° which contain surface form information. The high contrast signals produced at shallower angles of 60° down to 40° are well suited for automated analysis and detection procedures. The 60° response shows the strongest correlation to the end mill control sample surface form. Finally, the 30° and 20° angles are considered unsuitable due to low contrast or a high level of saturation.

40° fixed detector angle (See figure 5-21) - The full-form response is again produced at the highest angle of 80°. The partially saturated signals (70° to 40°) are again most prominent and thus most suited to detection/analysis applications, with the 70° signal offering the best correlation. A poor and unsuitable response is obtained at angles of 30° and 20°.

50° fixed detector angle (See figure 5-22) - The first data set in this group of four which contains no full-form or fully saturated response signals. Partially saturated signals dominate the figure with the highest contrast and most suitable form being produced with laser angle of 80°.

Suitability matrix (12.5 μm end mill sample with BUE defect)

Relative Laser/Detector Angle - Response Signal Suitability Matrix (12.5 μm end mill sample with BUE defect)							
Detector Angle	Laser Angle						
	80°	70°	60°	50°	40°	30°	20°
20°	o	✓	✓	o	o	o	×
30°	✓	✓	o	o	o	×	×
40°	✓	o	o	o	o	×	×
50°	o	o	o	o	o	o	o

Table 5-3 12.5 μm end mill sample with BUE defect, response signal suitability matrix

Graphical results (12.5 μm end mill sample with BUE defect)

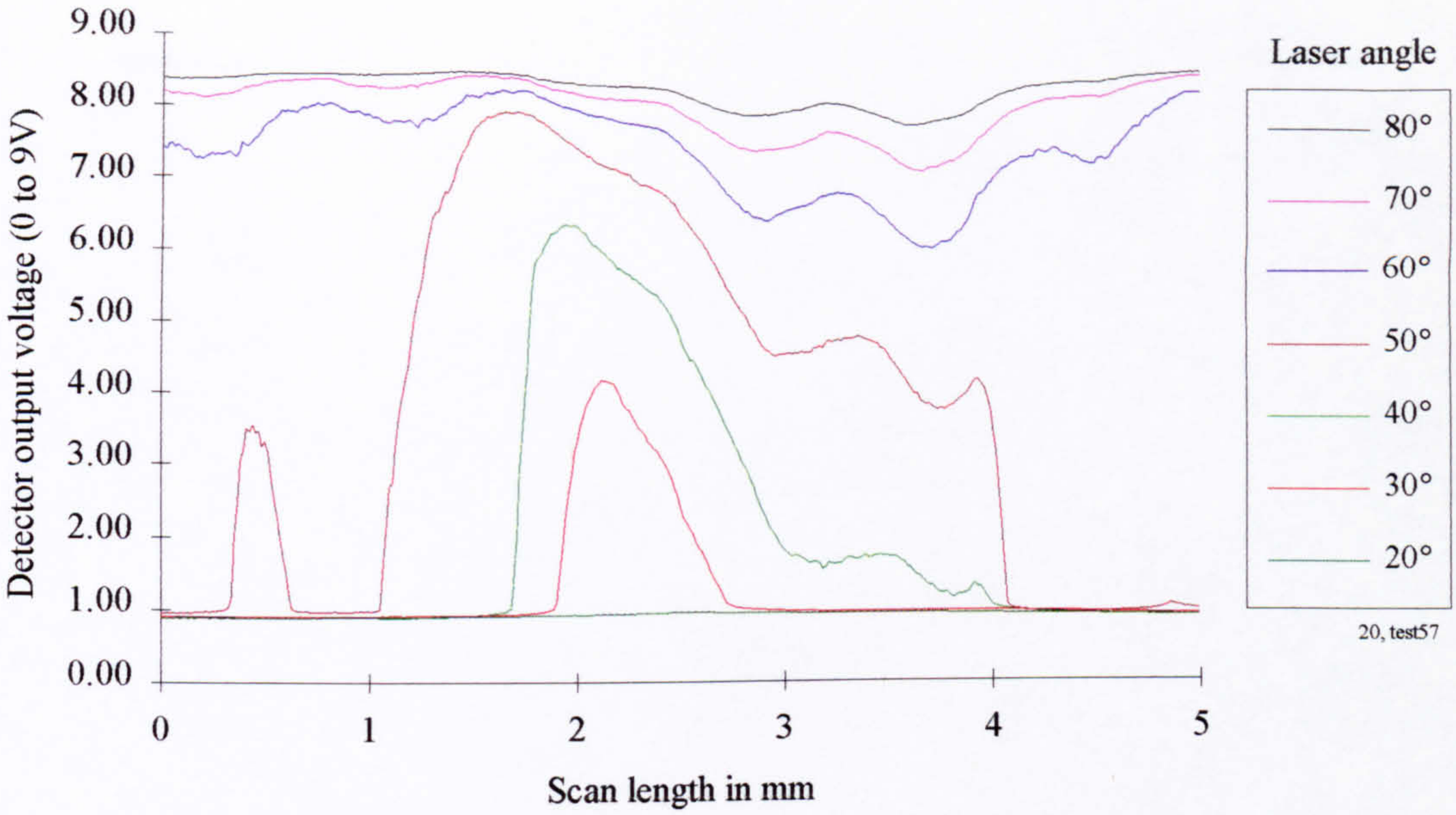

Figure 5-19 End mill sample with BUE defect and fixed detector angle of 20°

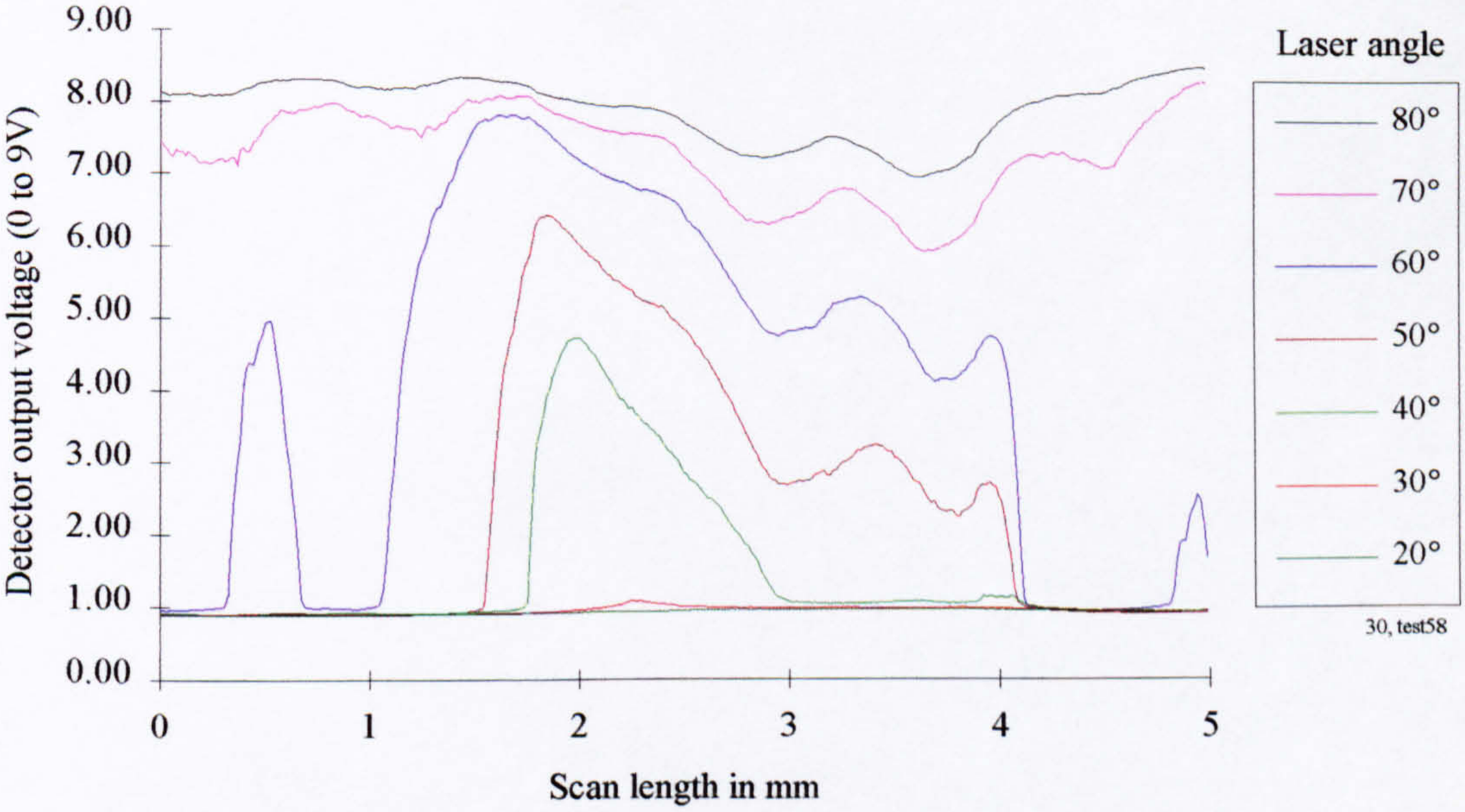

Figure 5-20 End mill sample with BUE defect and fixed detector angle of 30°

Graphical results continued (12.5 μm end mill sample with BUE defect)

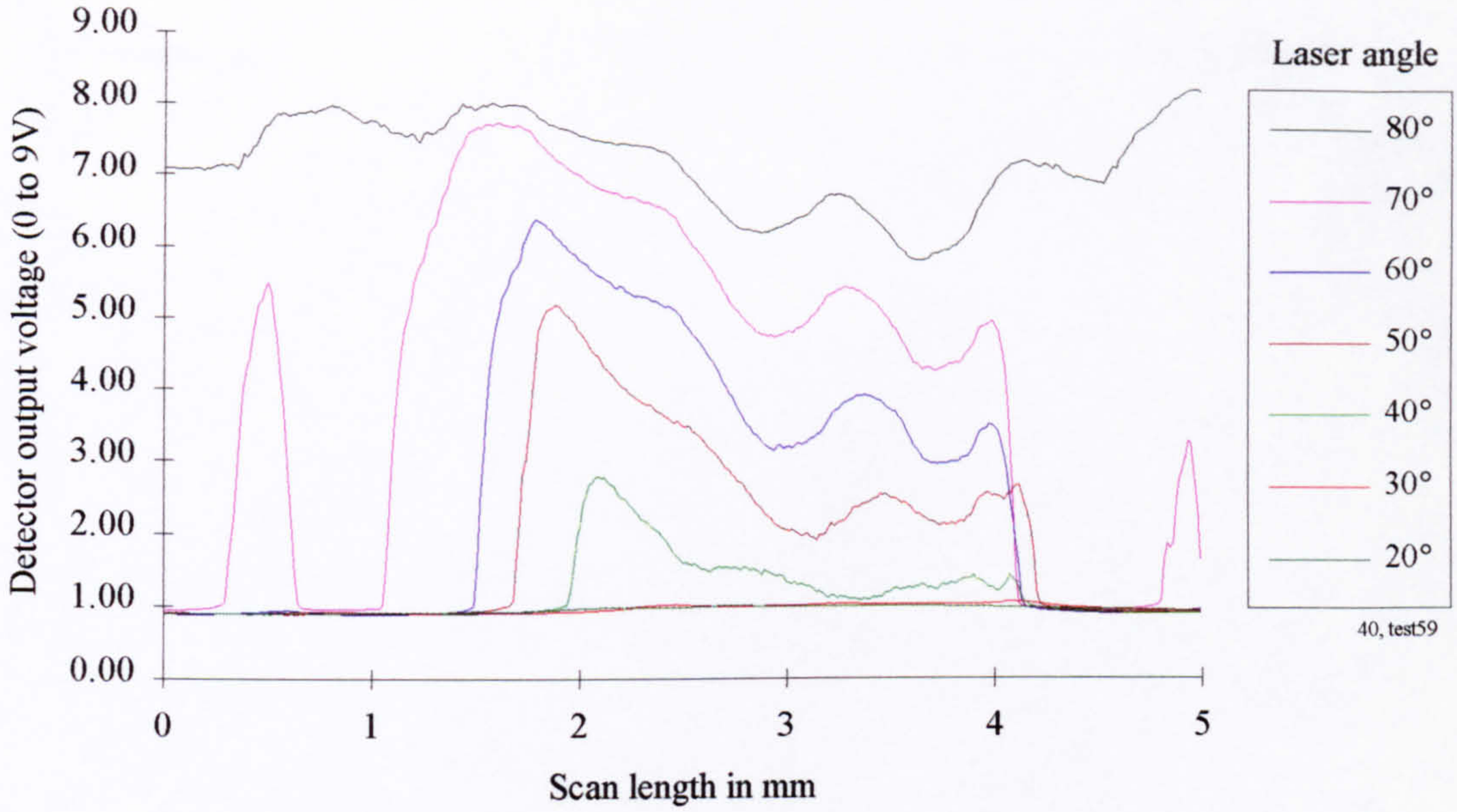

Figure 5-21 End mill sample with BUE defect and fixed detector angle of 40°

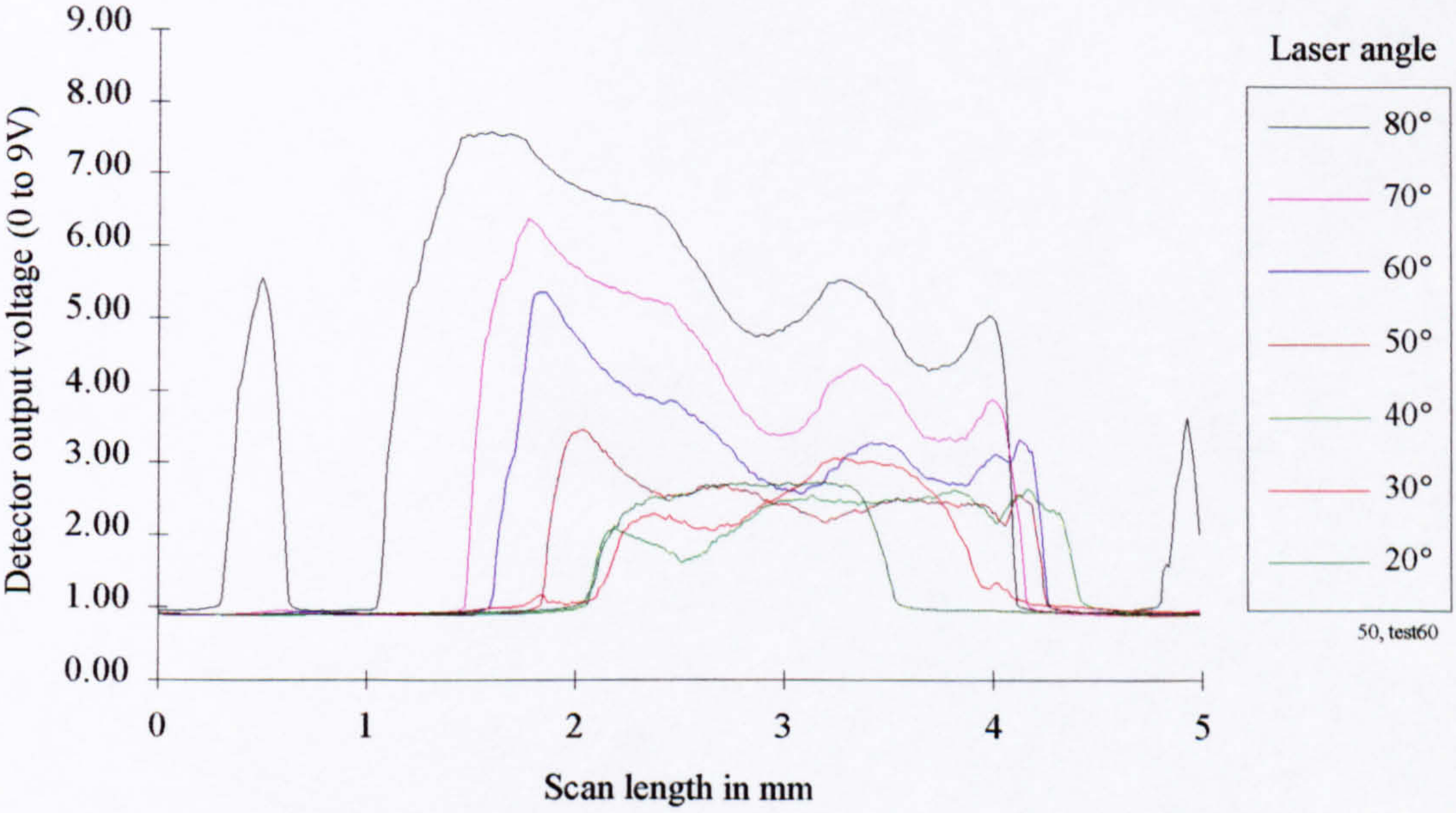

Figure 5-22 End mill sample with BUE defect and fixed detector angle of 50°

Further comments and general observations (12.5 μm end mill sample)

During data collection and general testing it was noted on several occasions that the response signal underwent a dramatic variation (step change) for small changes in laser/detector angles. To verify the results and confirm that the apparatus was functioning correctly a simple test was performed on a sample which exhibited such a step change. The graph below illustrates laser angle settings of 70° and 58° in the extremes. These two signals could thus encompass a change in response typical of those encountered during the normal course of an image acquisition session, where 10° step changes in laser/detector angle were used consistently. Between these extremes the response signals for laser angles decremented at 2° are shown. This clarifies the nature of the response and justifies the occurence of the step changes encountered.

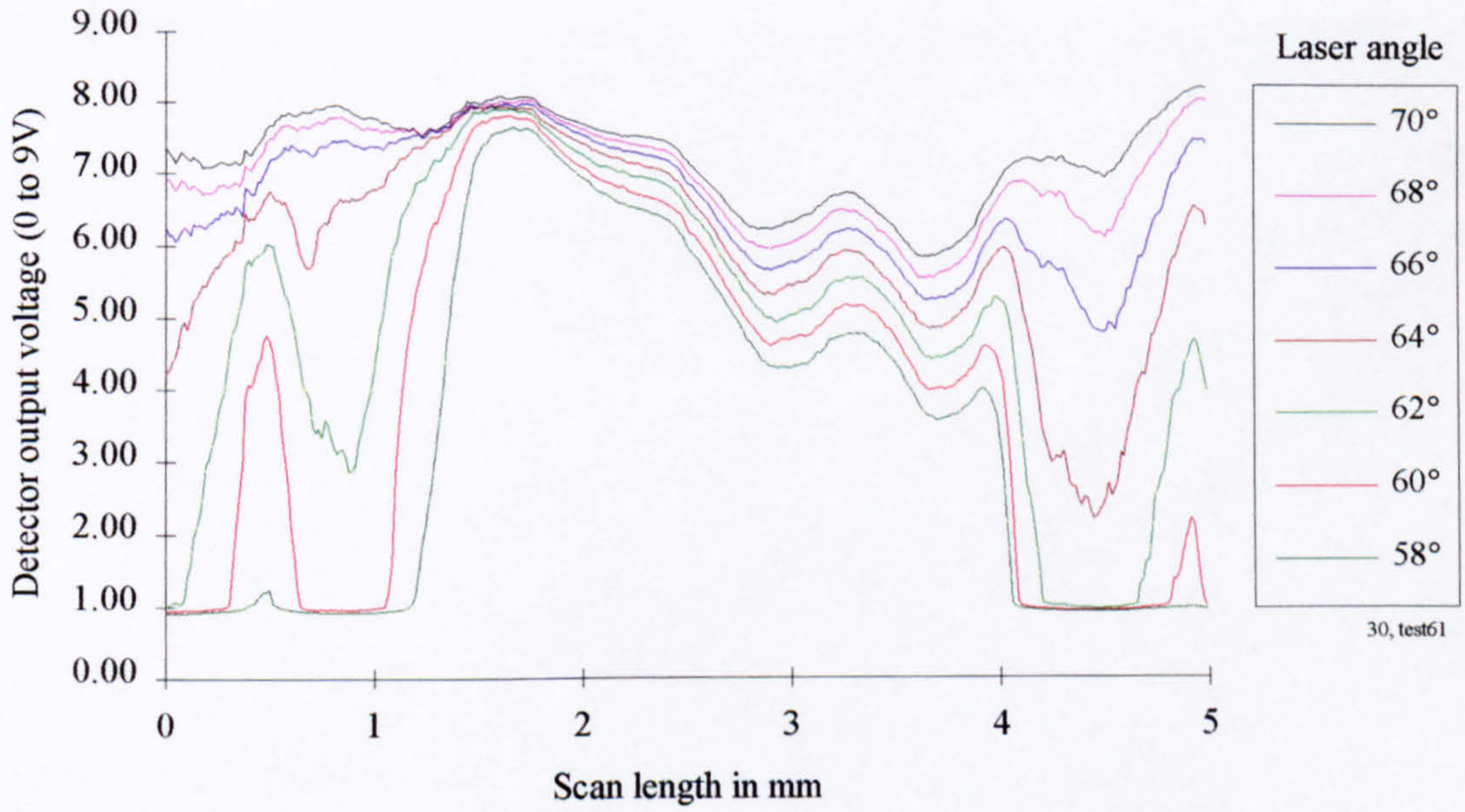

Figure 5-23 A detailed analysis of a typical step change experienced in early tests

General observation of the presented results suggests that a strong relationship exists between the laser and detector angles. Initially it was thought that similar signals may be produced with a constant included angle (see Figure 5-25). However, the results that were obtained did not support this theory.

Over a range of inspection tests a pattern was found to exist; a cascading nature of the response signals as the detector/laser angles were varied produced a striking trend. However, it was noted that consistent results could be obtained for a range of laser/detector angles. A rule was subsequently proposed which predicted system behaviour and could thus be used to determine optimum laser/detector angles for near consistent response signal output. Figure 5-24 below, which contains response signals extracted from the last four sets of results (12.5 μm end mill sample with BUE defect), illustrates this point;

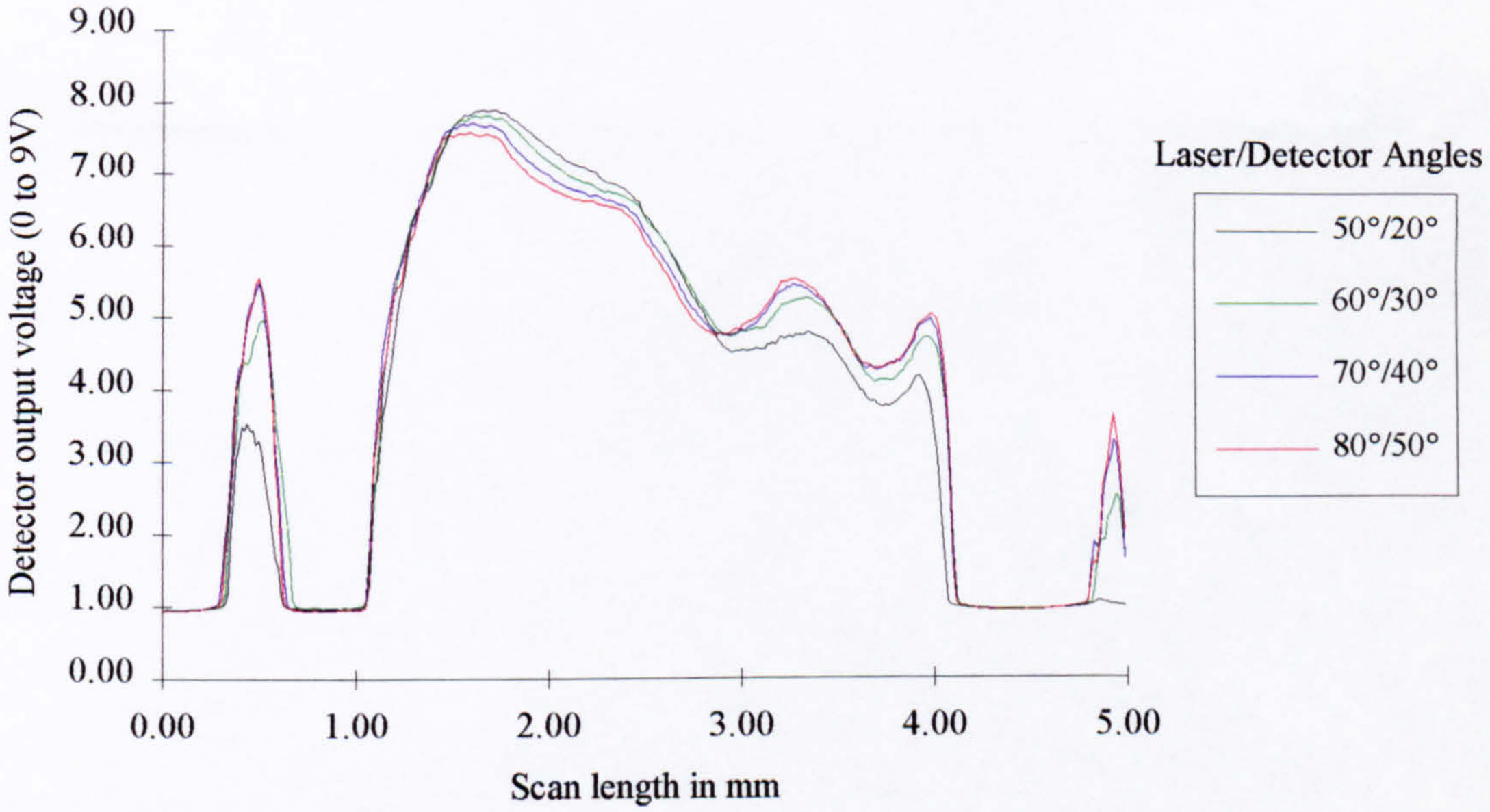

Figure 5-24 Near consistent response results for a range of laser/detector angles

A consistent image was seen to exist (not including saturated response signals) across the grouped tests, for a certain range of laser/detector angle settings. The figure above indicates that as the laser angle was increased the detector angle had to be increased by an

equal amount for the response to remain almost constant. Figure 5-25 depicts how the relative angles were measured during the tests.

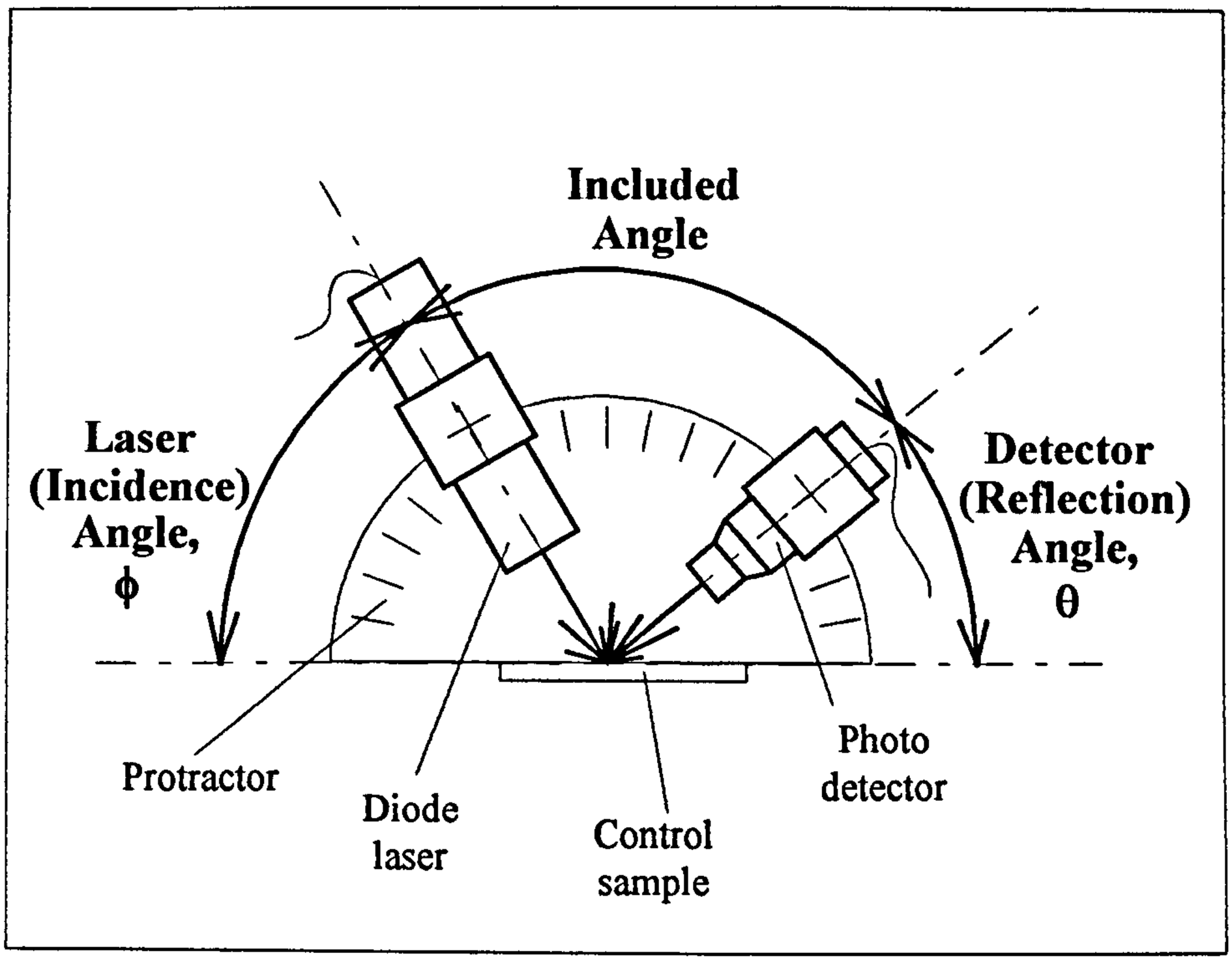

Figure 5-25 Relative measurement of laser and detector angles

Drawing from the graphical information of figure 5-24 (graph) above and with further reference to figure 5-25 the following rule was proposed:

> The sum of the laser angle (ϕ) plus the difference of 90° less the detector angle (θ) must be constant to obtain similar response results.

or conversely,

> The sum of the detector angle (θ) plus the difference of 90° less the laser angle (ϕ), must be constant to obtain similar response results,

Algebraically, for near constant response signals;

> The *consistent image angle*, $\delta = \phi + (90 - \theta) =$ a constant

Thus a newly defined term, the *consistent image angle*, was proposed for use throughout the remainder of this thesis in an attempt to simplify the discussion of results.

In all cases of detector angle under investigation, for the end mill control samples (plain, scratch and built-up-edge defects), a consistent image angle (δ) of 130° produced a good full-form signal. Whereas a consistent image angle of 120° would provide partially saturated results with high contrast though generally more suited to defect detection.

0.1 μm Plain ground control sample

Photograph of inspected surface (0.1 μm plain ground sample)

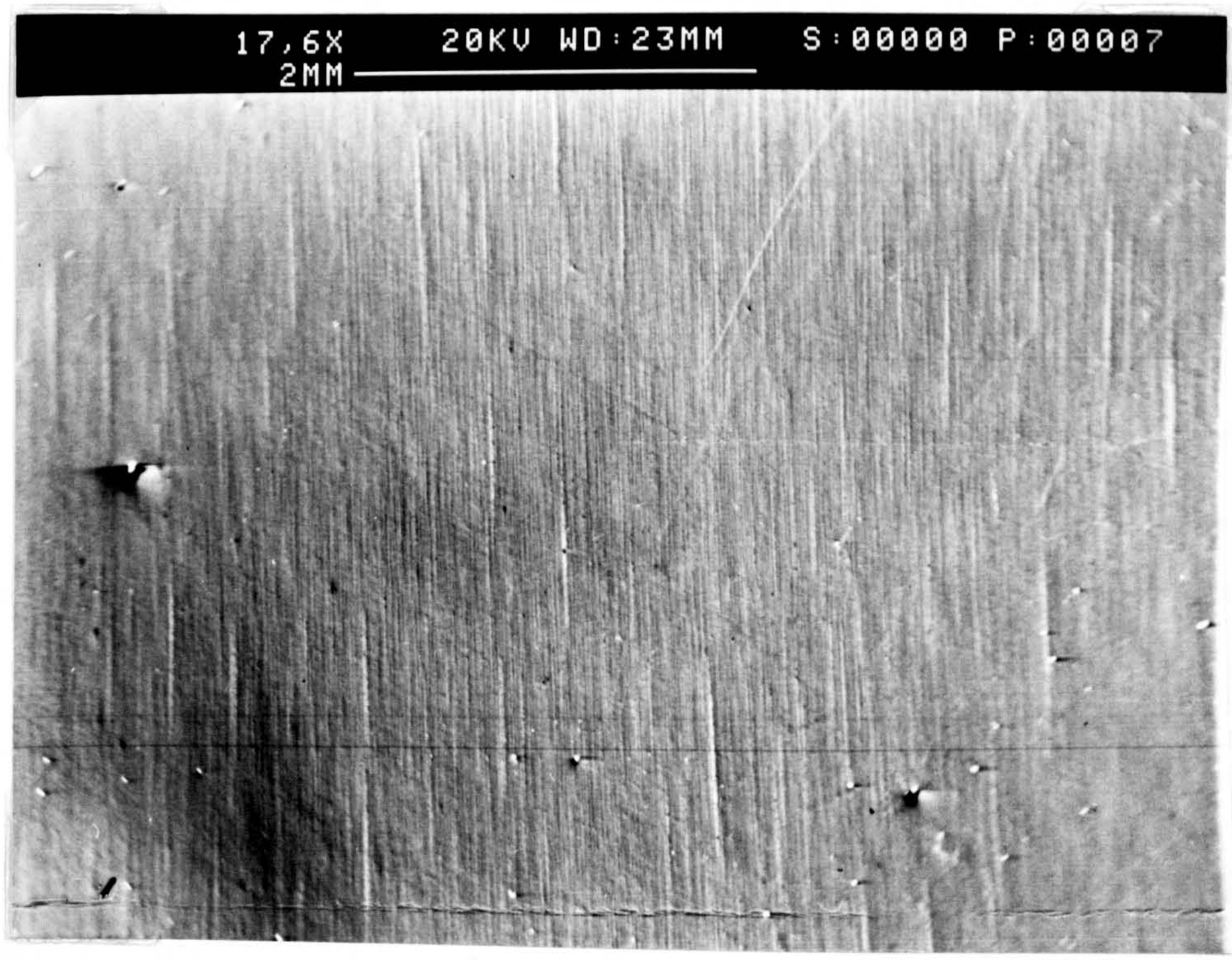

Figure 5-26 0.1 μm plain ground sample, surface photograph

Surface topography trace (0.1 μm plain ground sample)

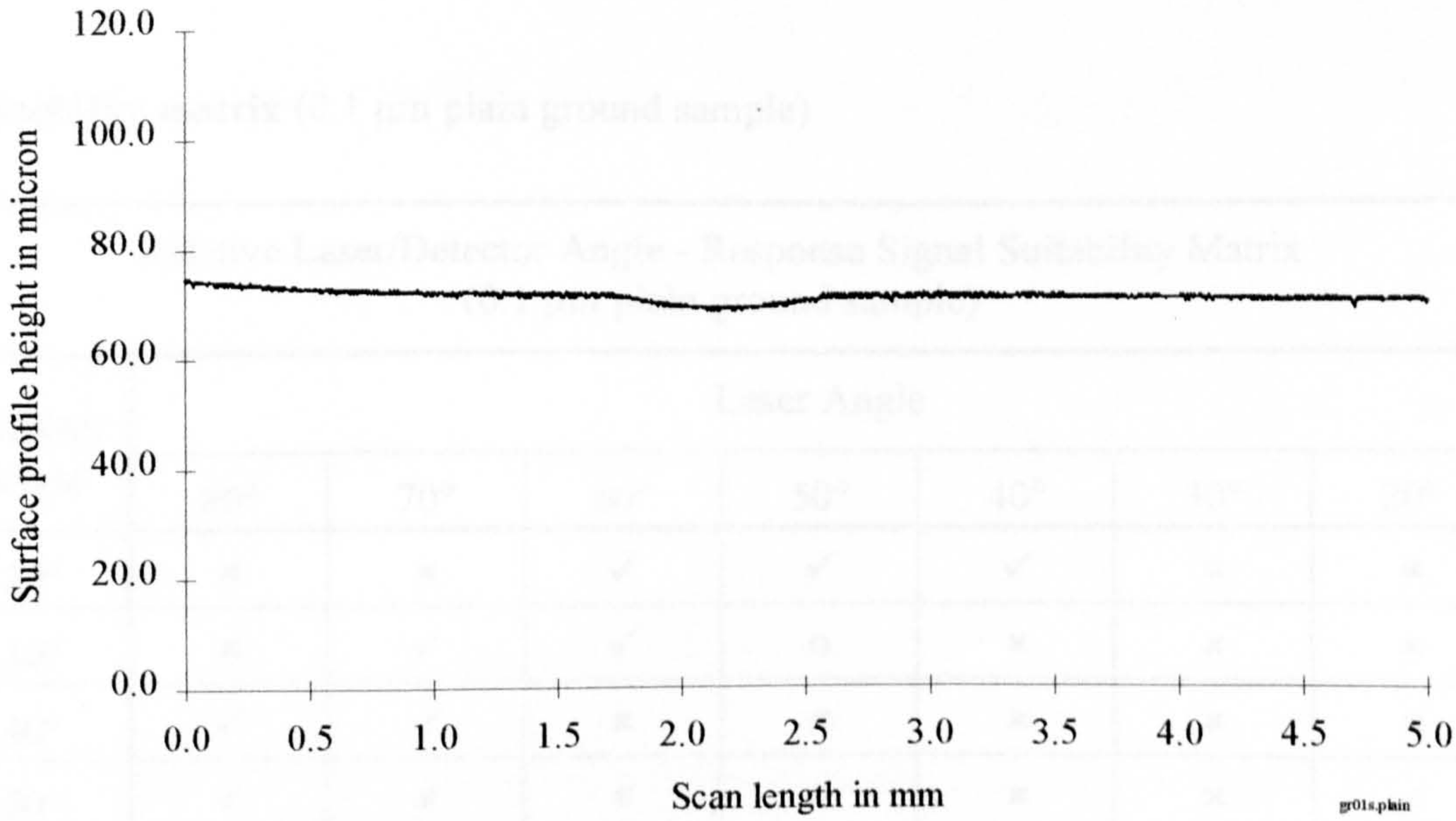

Figure 5-27 0.1 μm plain ground sample, surface profile

Discussion of results (0.1 μm plain ground sample)

20° fixed detector angle (See figure 5-28) - At the steeper laser angles the response signal is seen to tend towards the dark signal confine. Thus the laser angles of 80° and 70° must be considered unsuitable. Information contained in the full-form response signals for laser angles of 60°, 50° and 40° make them highly suited to surface interrogation, with signal contrast and therefore applicability increasing with a decrease in laser angle. The shallow angles of 30° and 20° are inappropriate due to detector saturation.

30° fixed detector angle (See figure 5-29) - An 80° laser configuration yields a response with some embedded detail though the overall result is thought to be too weak for interrogation purposes. However, the general surface form is apparent in the signals resulting from the high laser angles of 70° and 60°. Partial or full saturation at lower angles renders the signals unusable.

40° fixed detector angle (See figure 5-30) - The typical cascading trend is apparent in this series by this stage, with only the top two angles (80° and 70°) being appropriate and effectively one signal transferring from the dark to the saturation confine.

50° fixed detector angle (See figure 5-31) - Detector saturation is seen to occur for all but the extreme angles of 80° and 20°. Satisfactory signals are obtained for these two settings.

Suitability matrix (0.1 μm plain ground sample)

Relative Laser/Detector Angle - Response Signal Suitability Matrix
(0.1 μm plain ground sample)

Detector Angle	Laser Angle						
	80°	70°	60°	50°	40°	30°	20°
20°	✗	✗	✓	✓	✓	✗	✗
30°	✗	✓	✓	o	✗	✗	✗
40°	✓	✓	✗	✗	✗	✗	✗
50°	✓	✗	✗	✗	✗	✗	✓

Table 5-4 0.1 μm plain ground sample, response signal suitability matrix

Graphical results (0.1 μm plain ground sample)

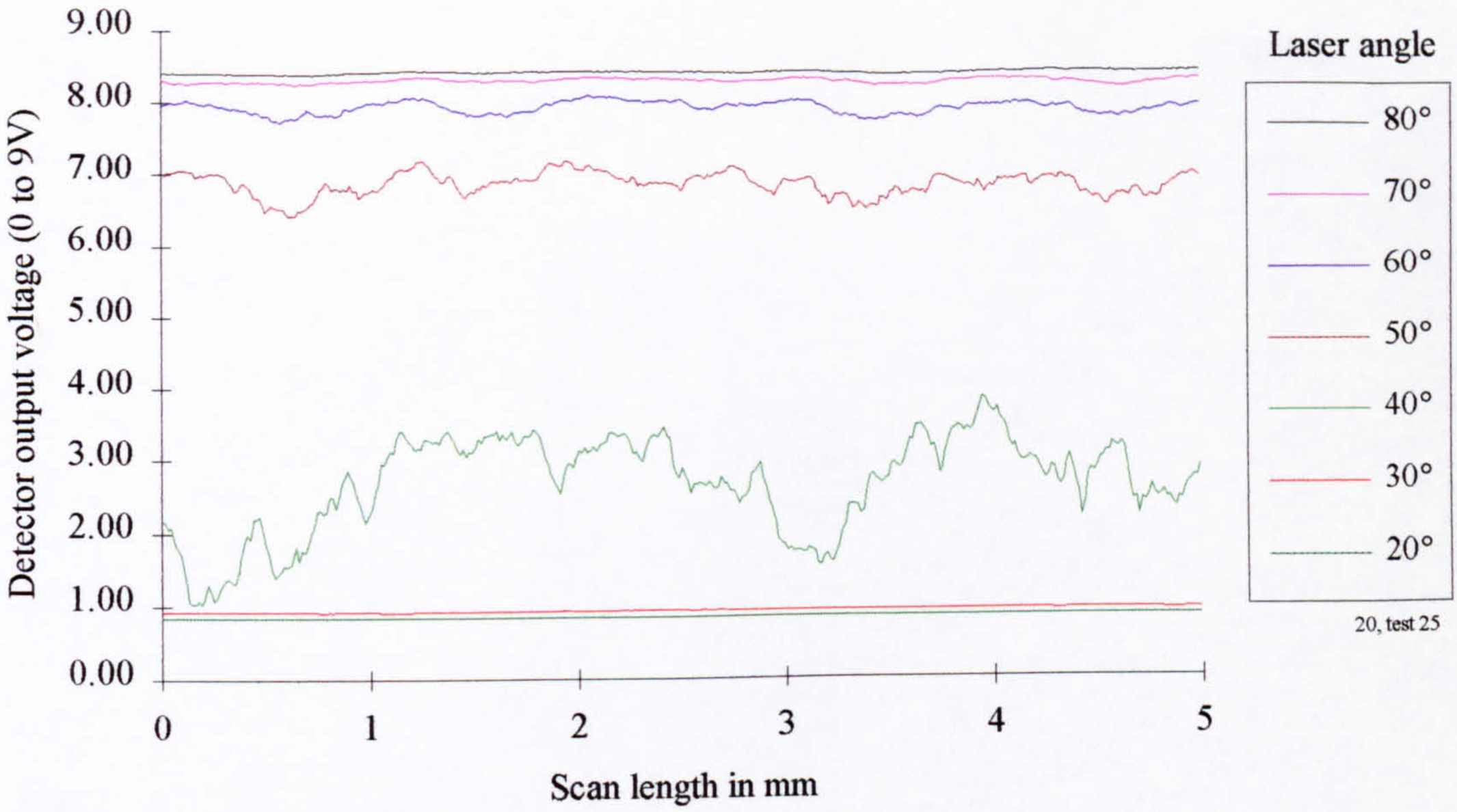

Figure 5-28 0.1 μm plain ground sample with fixed detector angle of 20°

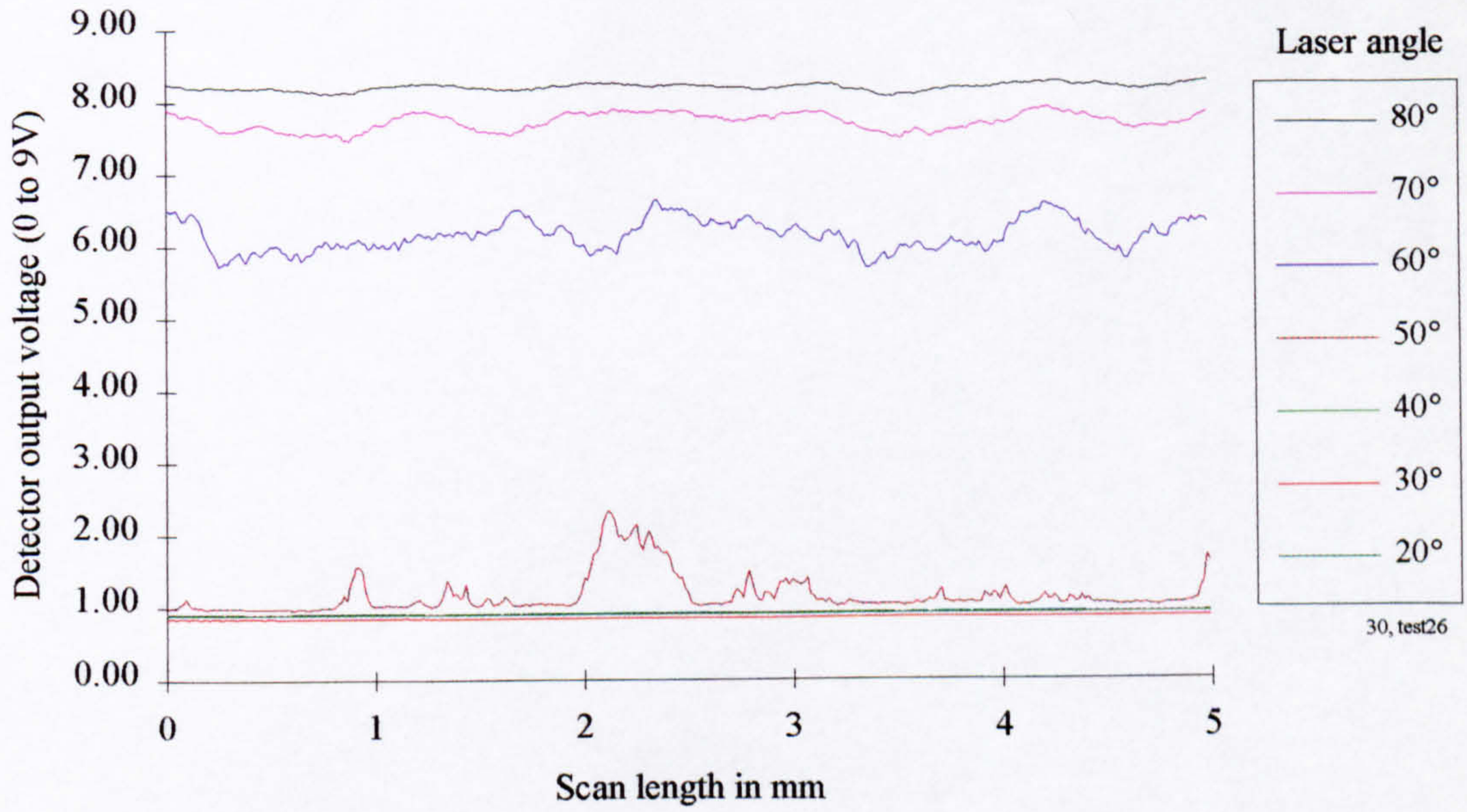

Figure 5-29 0.1 μm plain ground sample with fixed detector angle of 30°

Graphical results continued (0.1 μm plain ground sample)

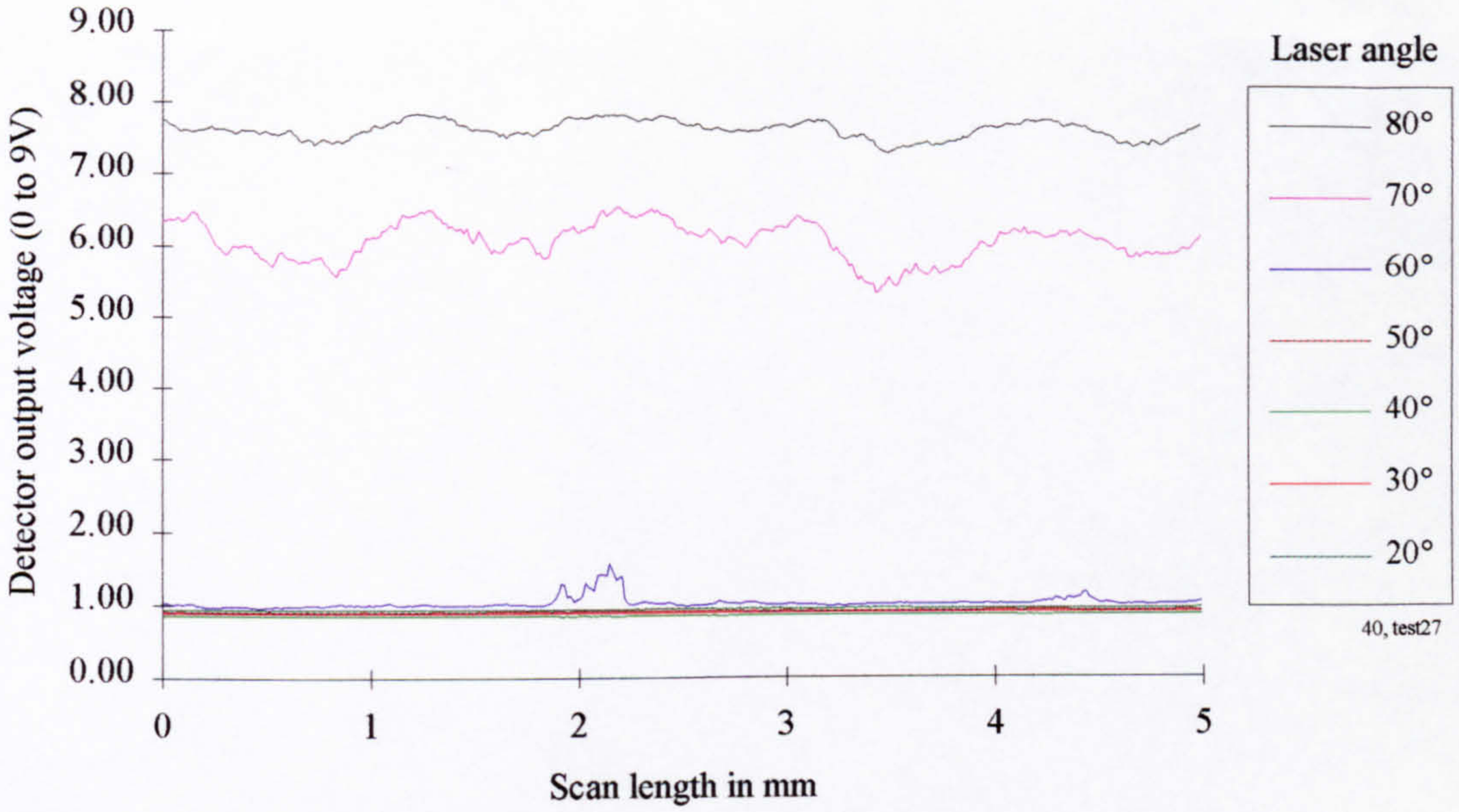

Figure 5-30 0.1 μm plain ground sample with fixed detector angle of 40°

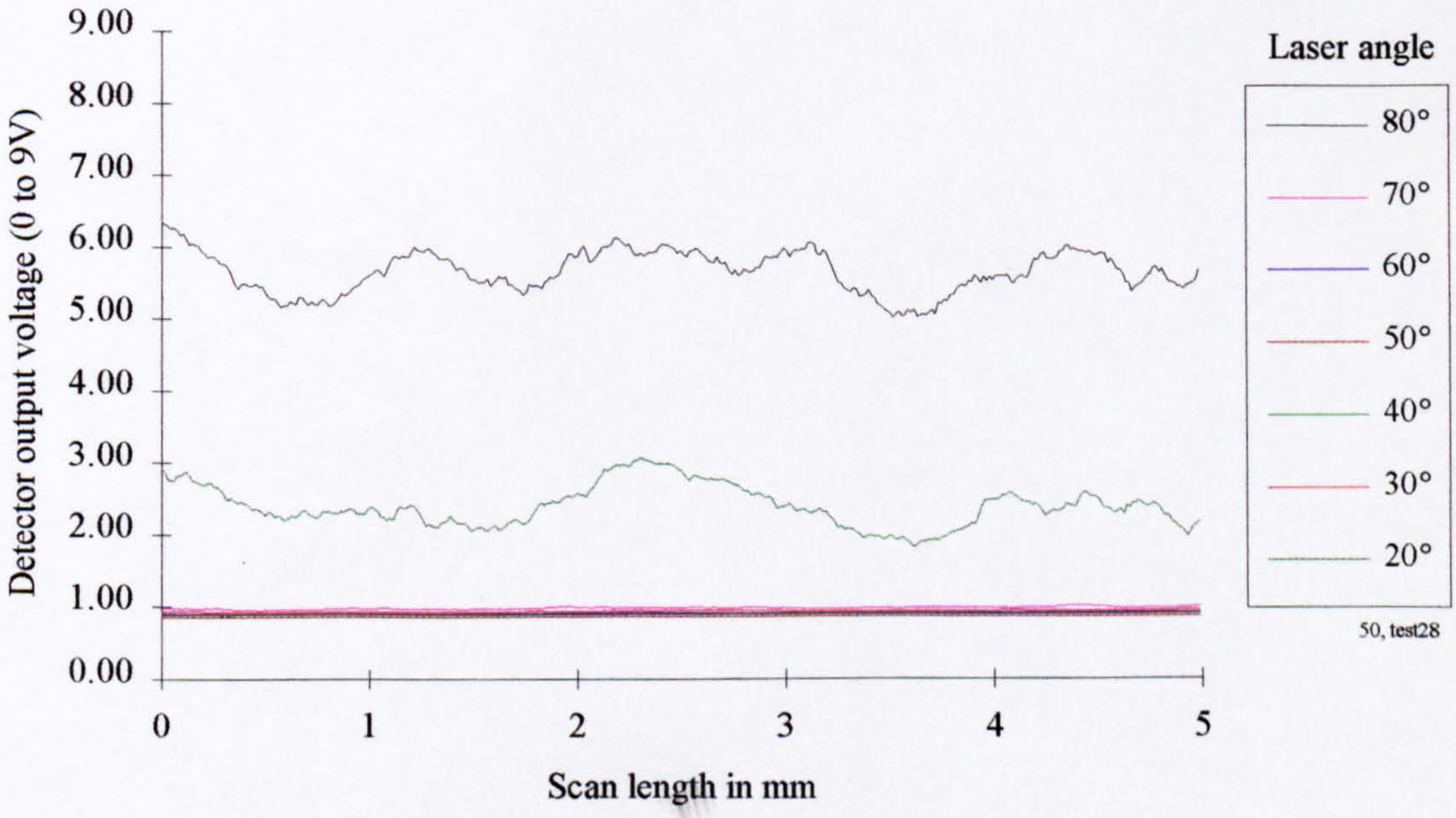

Figure 5-31 0.1 μm plain ground sample with fixed detector angle of 50°

0.1 μm Ground control sample with scratch defect

Photograph of inspected surface (0.1 μm ground sample with scratch defect)

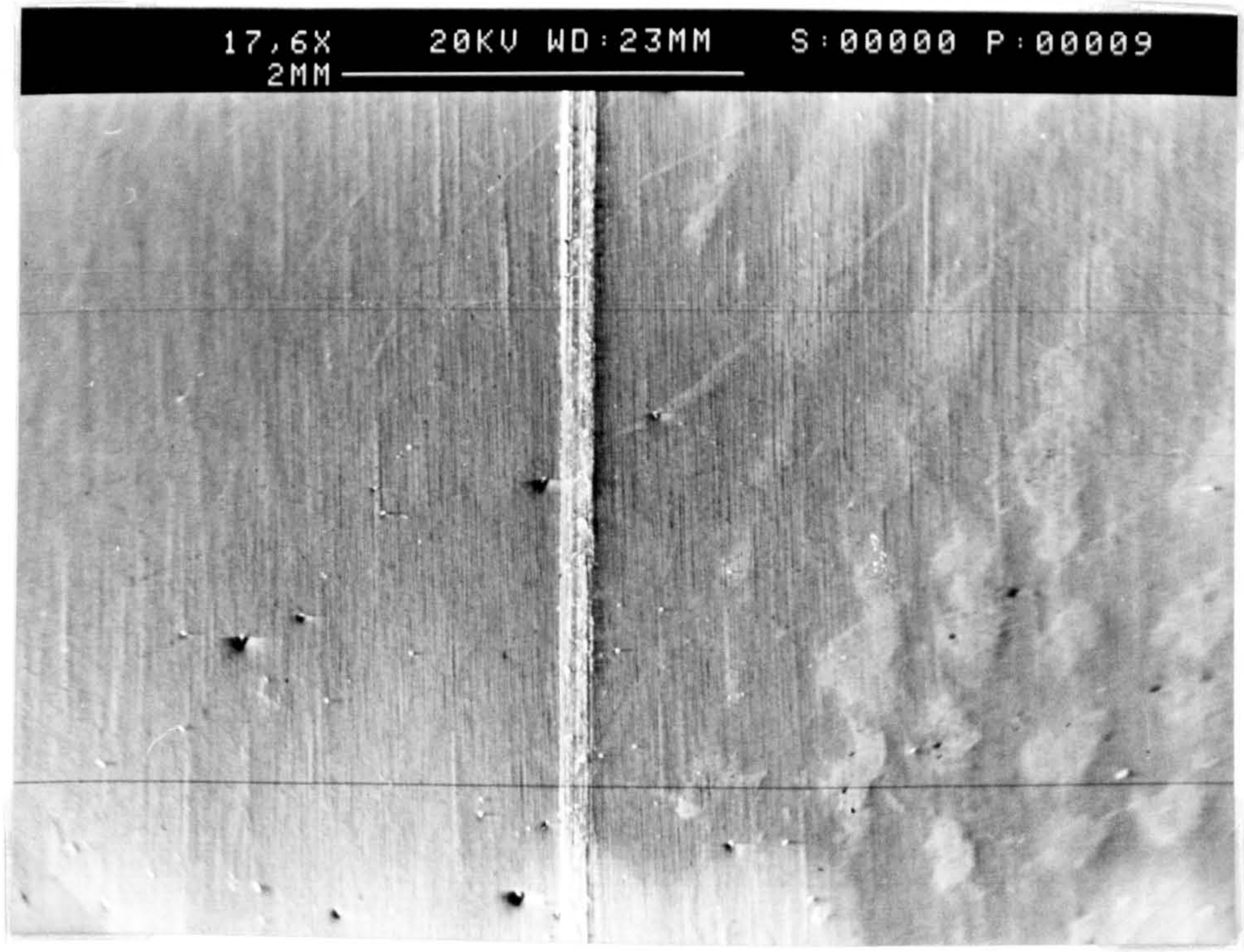

Figure 5-32 0.1 μm ground sample with scratch defect, surface photograph

Surface topography trace (0.1 μm ground sample with scratch defect)

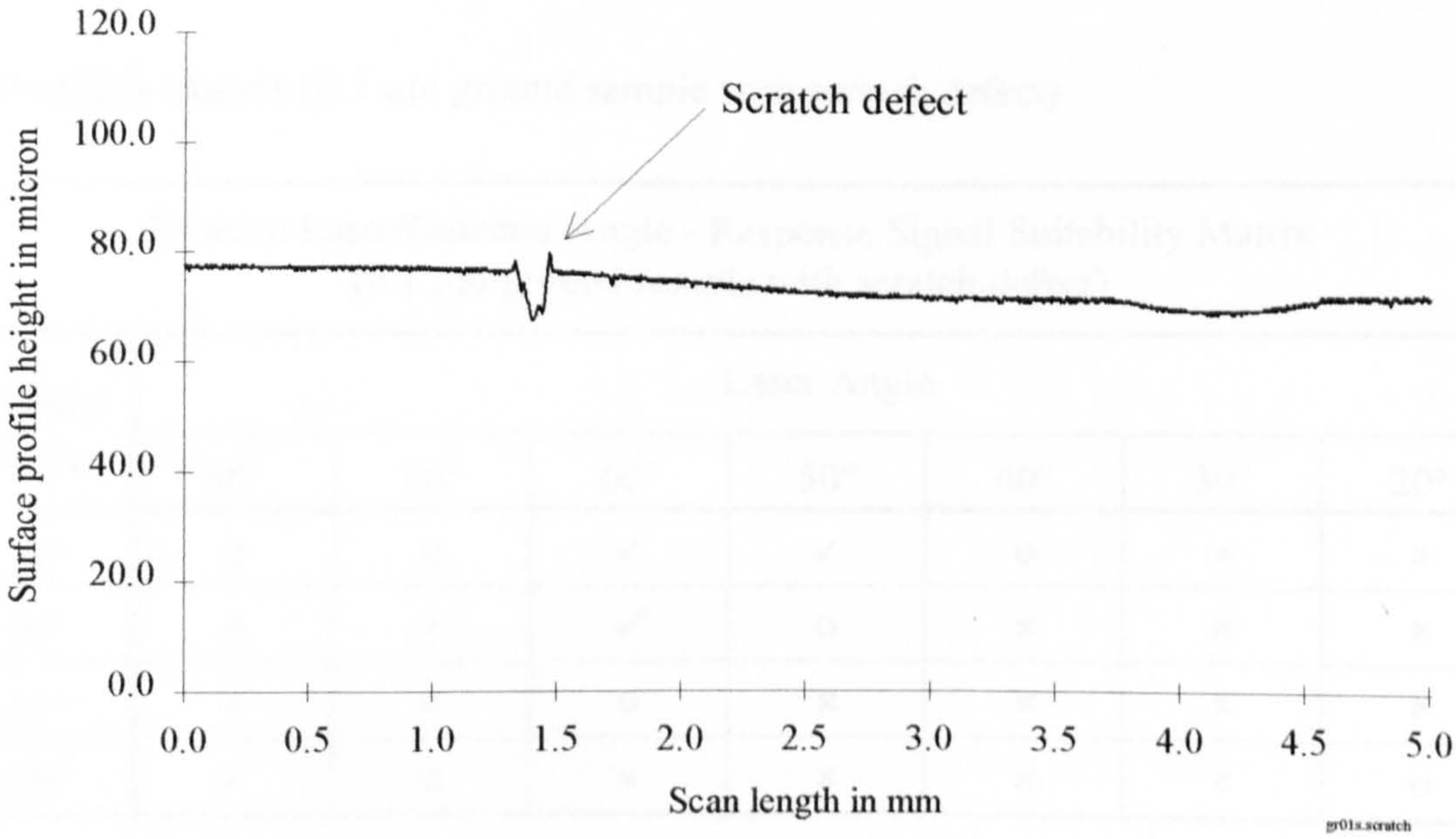

Figure 5-33 0.1 μm ground sample with scratch defect, surface profile

Discussion of results (0.1 μm ground sample with scratch defect)

20° fixed detector angle (See figure 5-34) - The spread and suitability of the results are much the sames as those for the plain ground sample discussed in the previous subsection. One noticable difference is that the scratch defect causes the marginal signals of the previous analysis to be of some use in defect/feature detection and thus are marked with a naught (o) as opposed to a cross (✖) in the summary matrix below (Table 5-5). A strong contrast is most apparent for a laser angle of 50°.

30° fixed detector angle (See figure 5-35) - Again the basic form of the suitability matrix is preserved in this section of the analysis, when compared to that for the plain 0.1 μm ground surface. Naturally, this was anticipated. The most suitable laser setting was identified as 60° in this test series. For this scanning application an optimum consistent image angle of 120° was identified.

40° fixed detector angle (See figure 5-36) - High laser angles of 80° and 70° offer full-form resonses. As the angle is decreased is is apparent form the graphical results that the response signals contain more detail, relating to the microscopic surface structure.

50° fixed detector angle (See figure 5-37) - The high and low angles produce the optimum results for this configuration with a broad band of saturation occuring between.

Suitability matrix (0.1 μm ground sample with scratch defect)

Relative Laser/Detector Angle - Response Signal Suitability Matrix (0.1 μm ground sample with scratch defect)							
Detector Angle	Laser Angle						
	80°	70°	60°	50°	40°	30°	20°
20°	o	o	✓	✓	o	✖	✖
30°	o	✓	✓	o	✖	✖	✖
40°	✓	✓	o	✖	✖	✖	✖
50°	✓	o	✖	✖	✖	✖	o

Table 5-5 0.1 μm ground sample with scratch defect, response signal suitability matrix

Graphical results (0.1 μm ground sample with scratch defect)

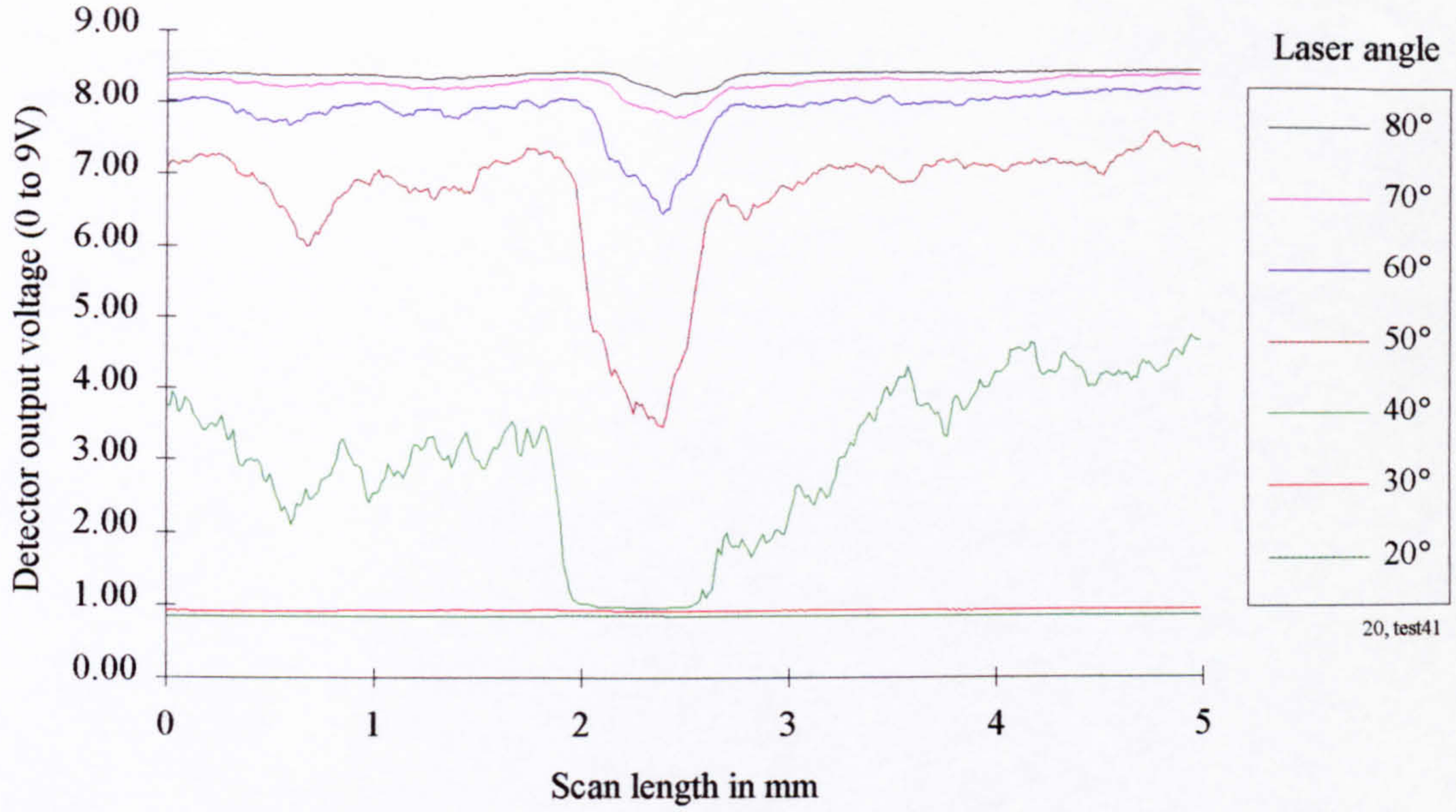

Figure 5-34 0.1 μm ground sample with scratch defect and fixed detector angle of 20°

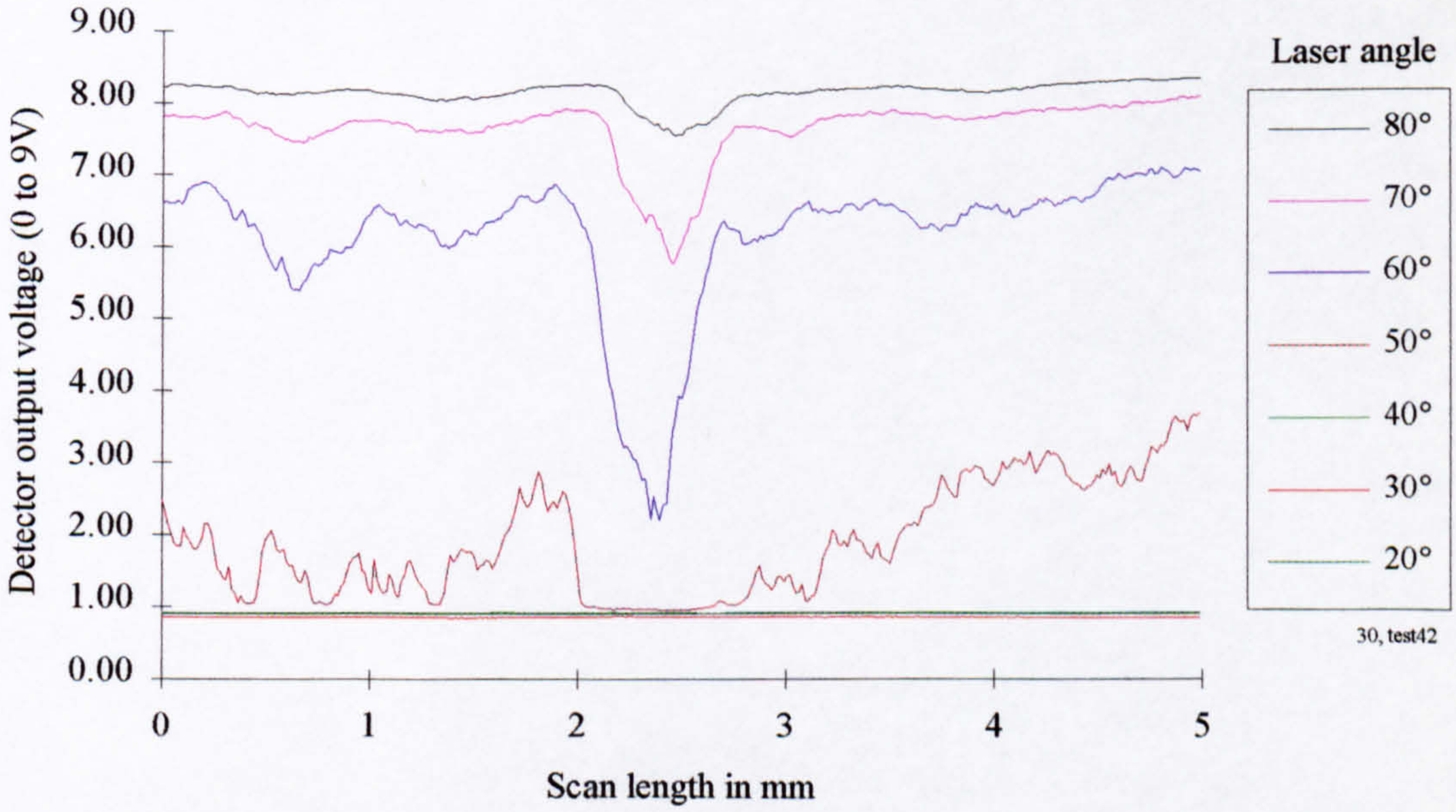

Figure 5-35 0.1 μm ground sample with scratch defect and fixed detector angle of 30°

Graphical results continued (0.1 μm ground sample with scratch defect)

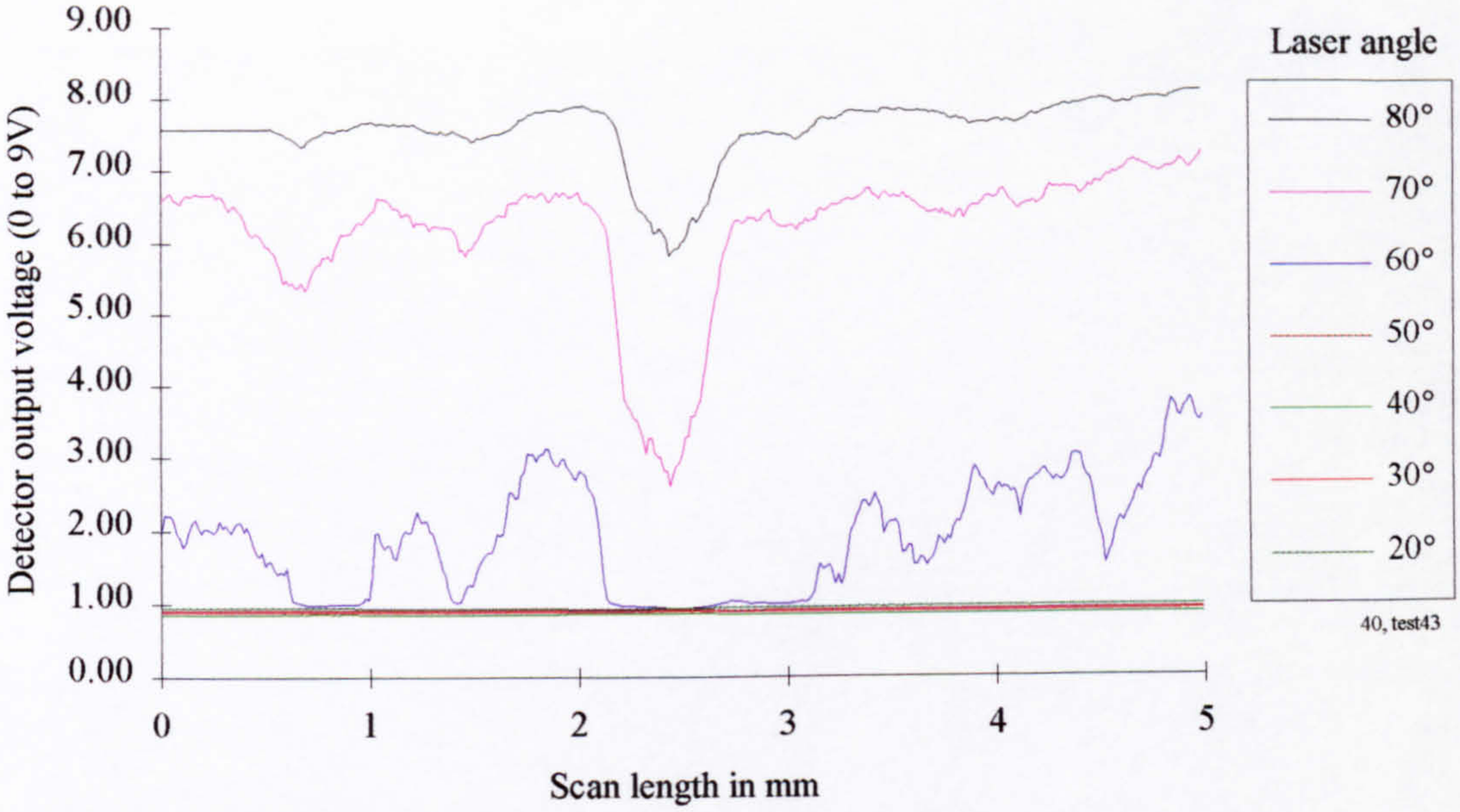

Figure 5-36 0.1 μm ground sample with scratch defect and fixed detector angle of 40°

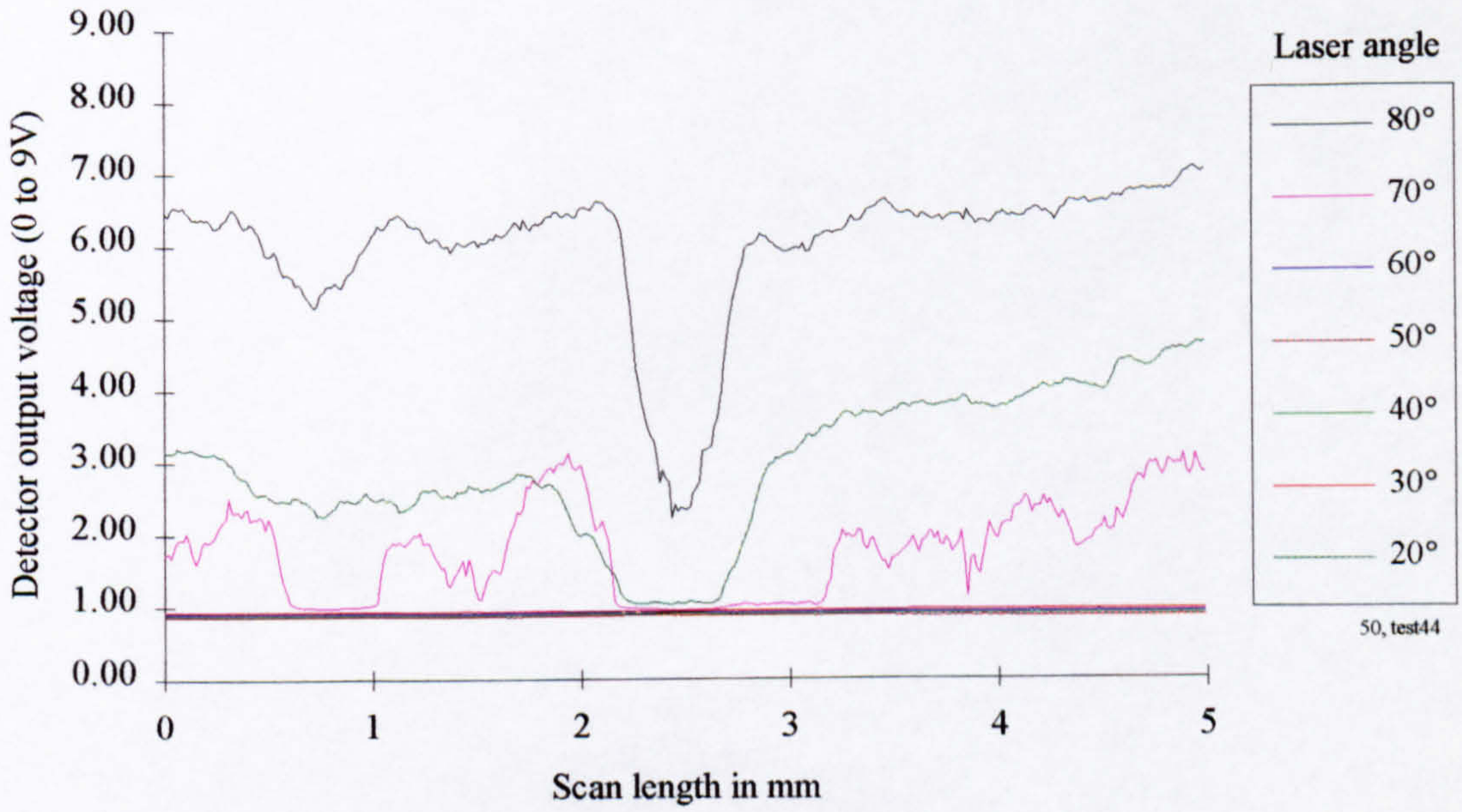

Figure 5-37 0.1 μm ground sample with scratch defect and fixed detector angle of 50°

0.1 μm Ground control sample with built-up edge (BUE) defect

Photograph of inspected surface (0.1 μm ground sample with BUE defect)

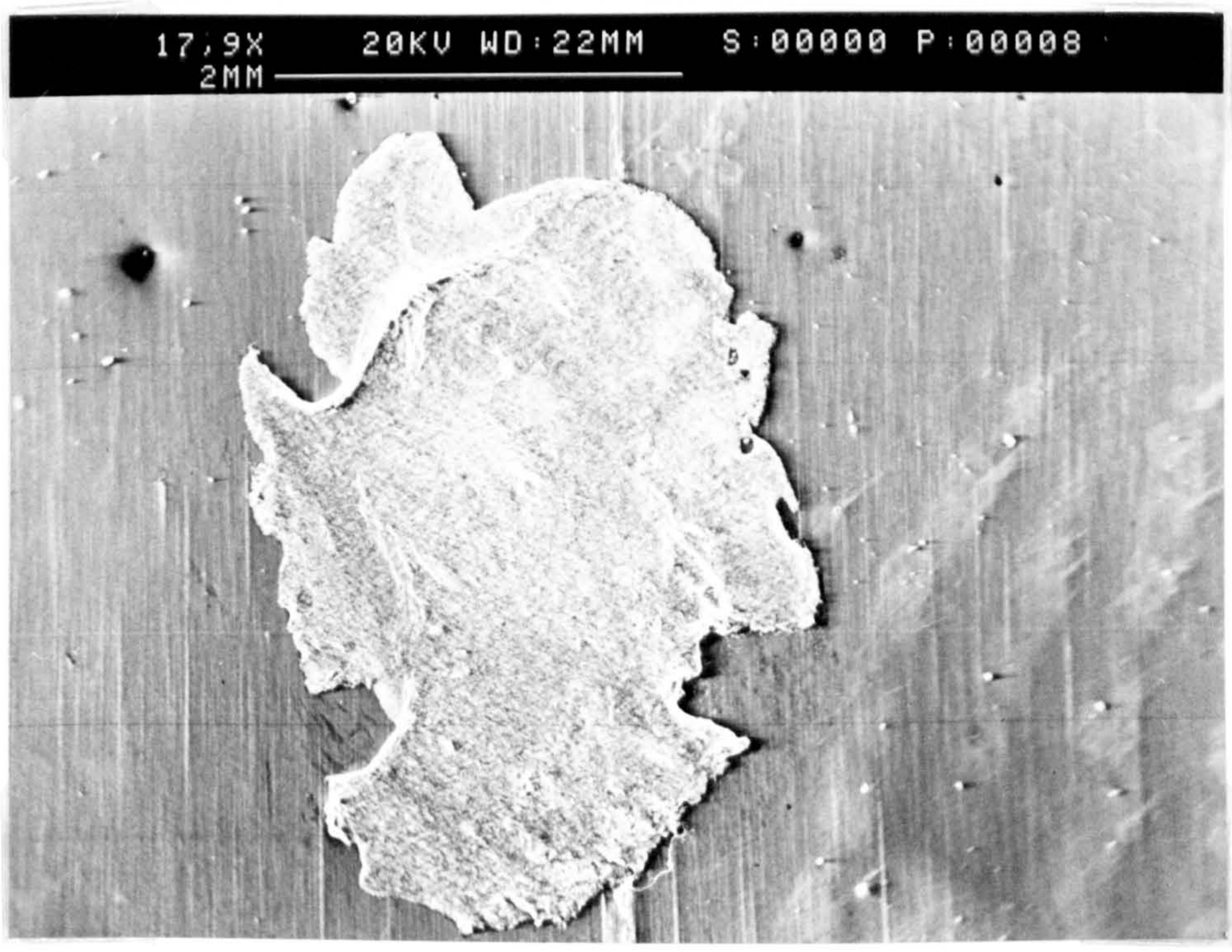

Figure 5-38 0.1 μm ground sample with BUE defect, surface photograph

Surface topography trace (0.1 μm ground sample with BUE defect)

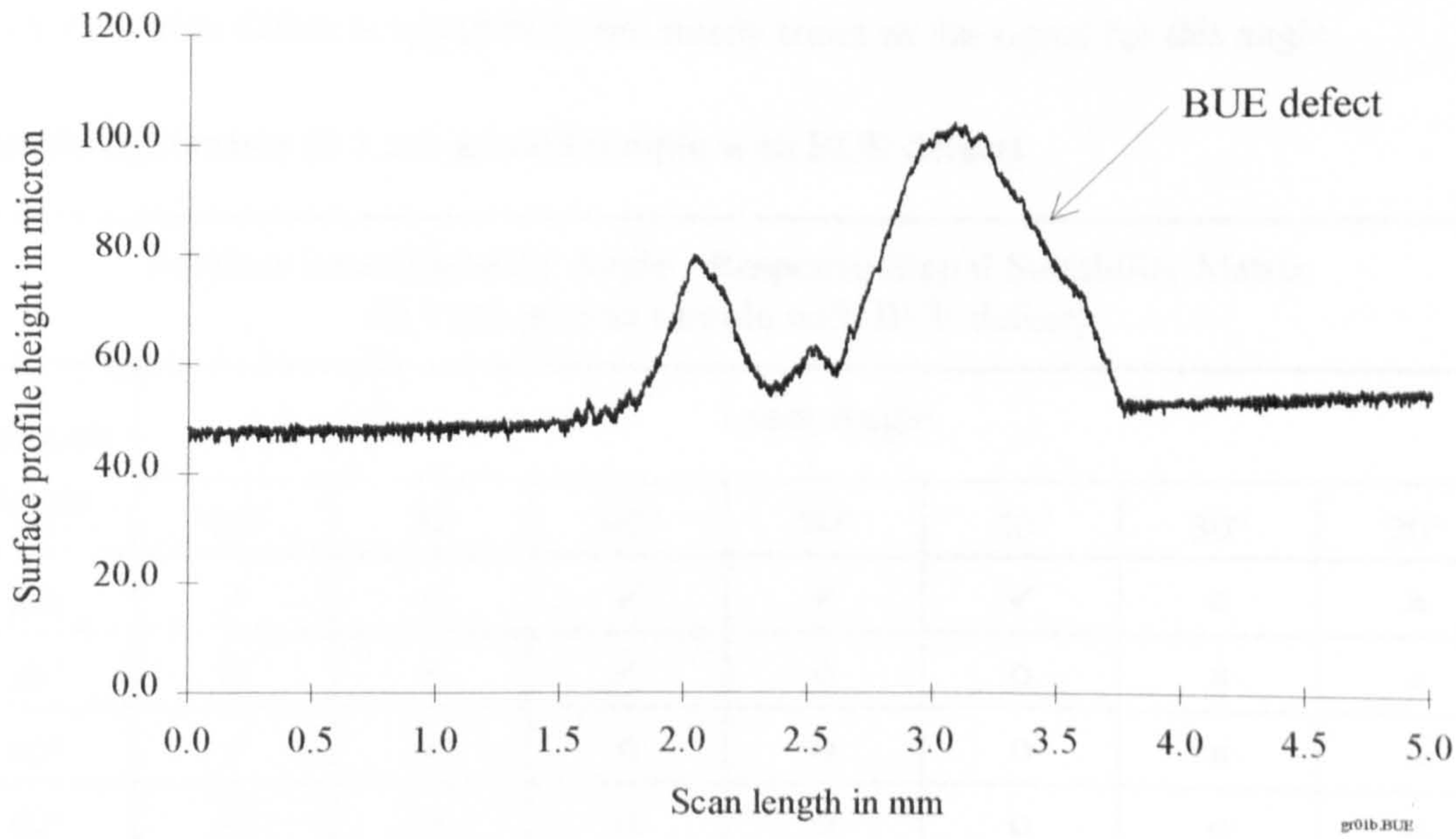

Figure 5-39 0.1 μm ground sample with BUE defect, surface profile

Discussion of results (0.1 μm ground sample with BUE defect)

20° fixed detector angle (See figure 5-40) - The full-form signal obtained for a laser setting 40° indicates the presence of a sizeable defect though. A noticable variation in the high frequency component of the signal, relating to micro-surface structure, is apparent at the site of the defect (between 1 and 4 mm).

30° fixed detector angle (See figure 5-41) - The strongest signals which clearly illustrates the presence of a BUE defect tend to poses a significant proportion of saturation. Thus dual laser/detector settings would be essential to detect BUE type defects (of the scale under review) and to furthermore gain some insight into the general form of the surface. For this arrangement a laser angle of 60° would produce a signal with enhanced surface form whereas a lower angle of 50° or 40° would be solely suited to defect detection.

40° fixed detector angle (See figure 5-42) - The problem of accurate signal delineation becomes clearly apparent when the graphical results from this series of tests is reffered to. For laser angles of 60° to 40° the defect is seen to centre on 2.8 mm, with the defect width varying from about 3 mm down to 1 mm.

50° fixed detector angle (See figure 5-43) - The main difference when compared to the results already discussed in this section can be seen in the signal for a laser angle of 20°. No discernable defect is apparent in the steady trend of the signal for this angle.

Suitability matrix (0.1 μm ground sample with BUE defect)

Relative Laser/Detector Angle - Response Signal Suitability Matrix
(0.1 μm ground sample with BUE defect)

Detector Angle	Laser Angle						
	80°	70°	60°	50°	40°	30°	20°
20°	o	o	✓	✓	✓	o	×
30°	o	✓	✓	o	o	×	×
40°	✓	✓	o	o	o	×	o
50°	✓	o	o	o	o	o	o

Table 5-6 0.1 μm ground sample with BUE defect, response signal suitability matrix

Graphical results (0.1 μm ground sample with BUE defect)

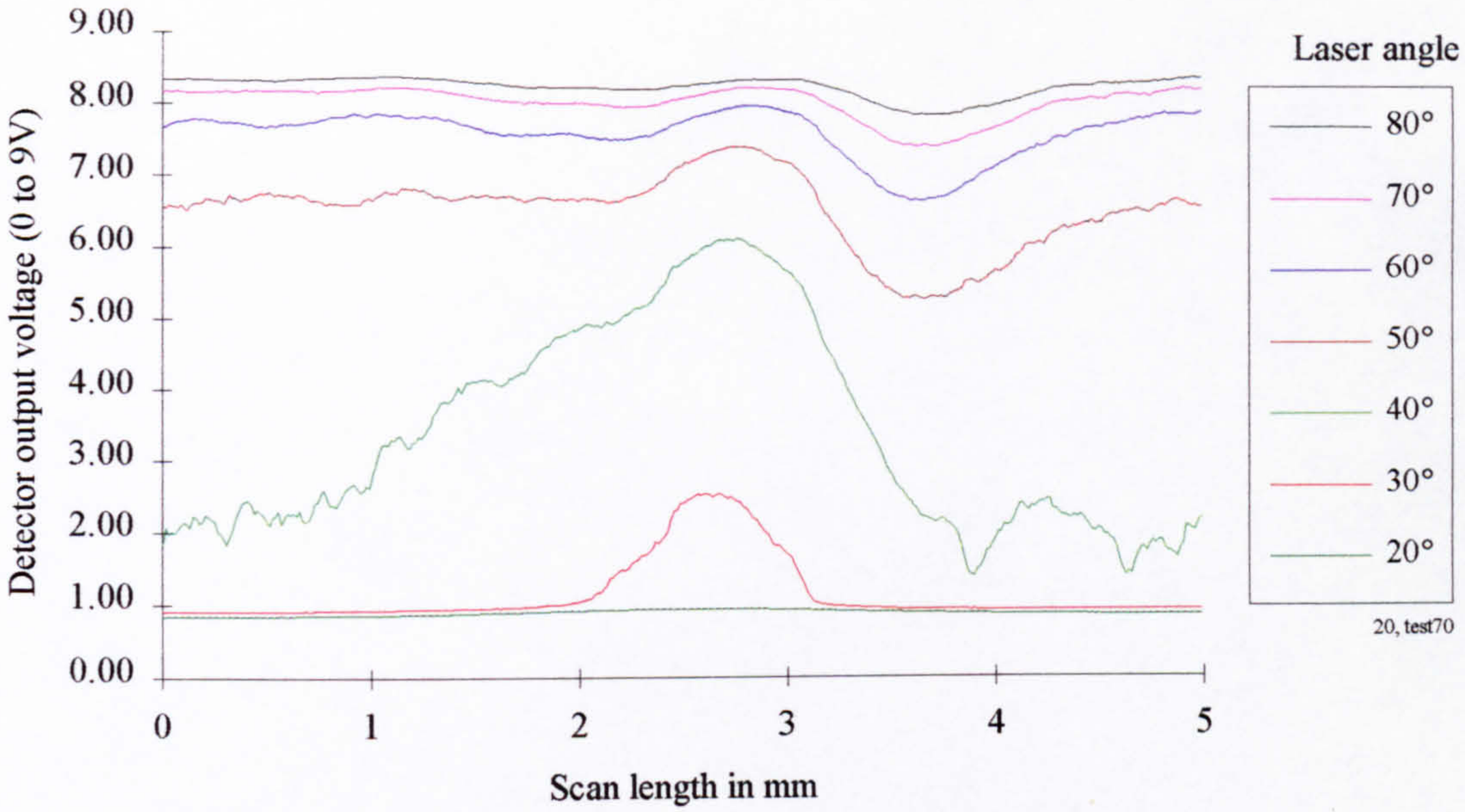

Figure 5-40 0.1 μm ground sample with BUE defect and fixed detector angle of 20°

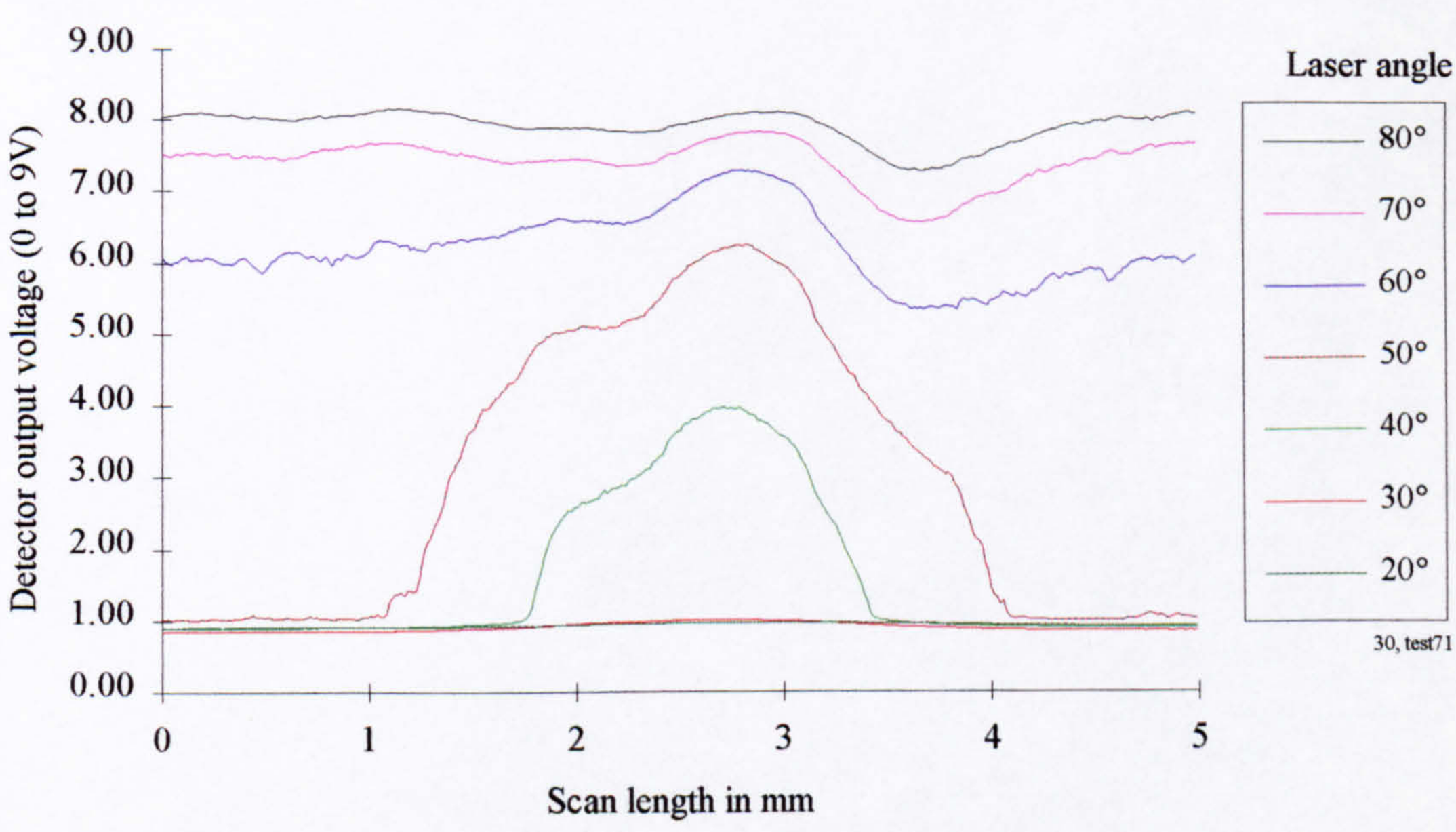

Figure 5-41 0.1 μm ground sample with BUE defect and fixed detector angle of 30°

Graphical results continued (0.1 μm ground sample with BUE defect)

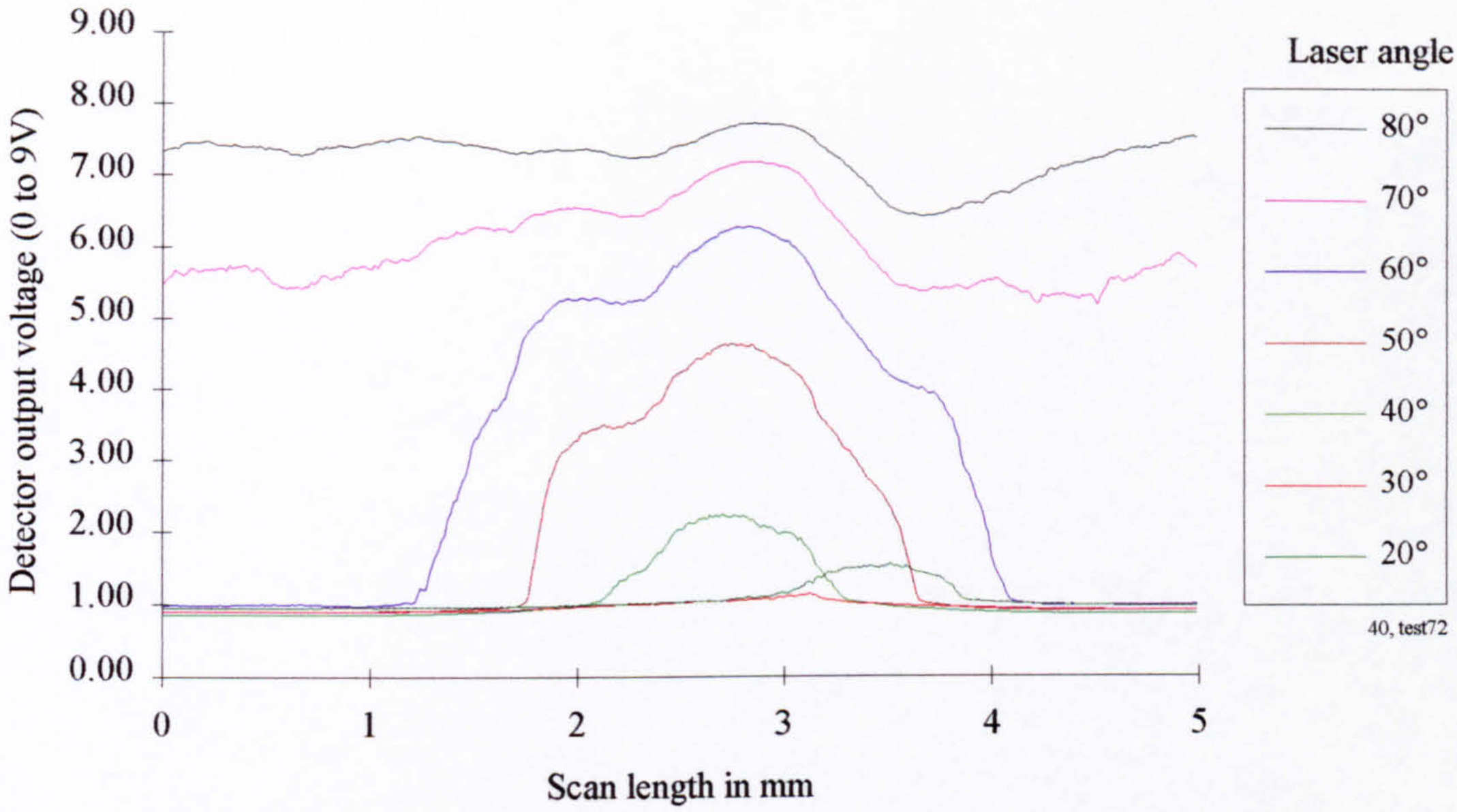

Figure 5-42 0.1 μm ground sample with BUE defect and fixed detector angle of 40°

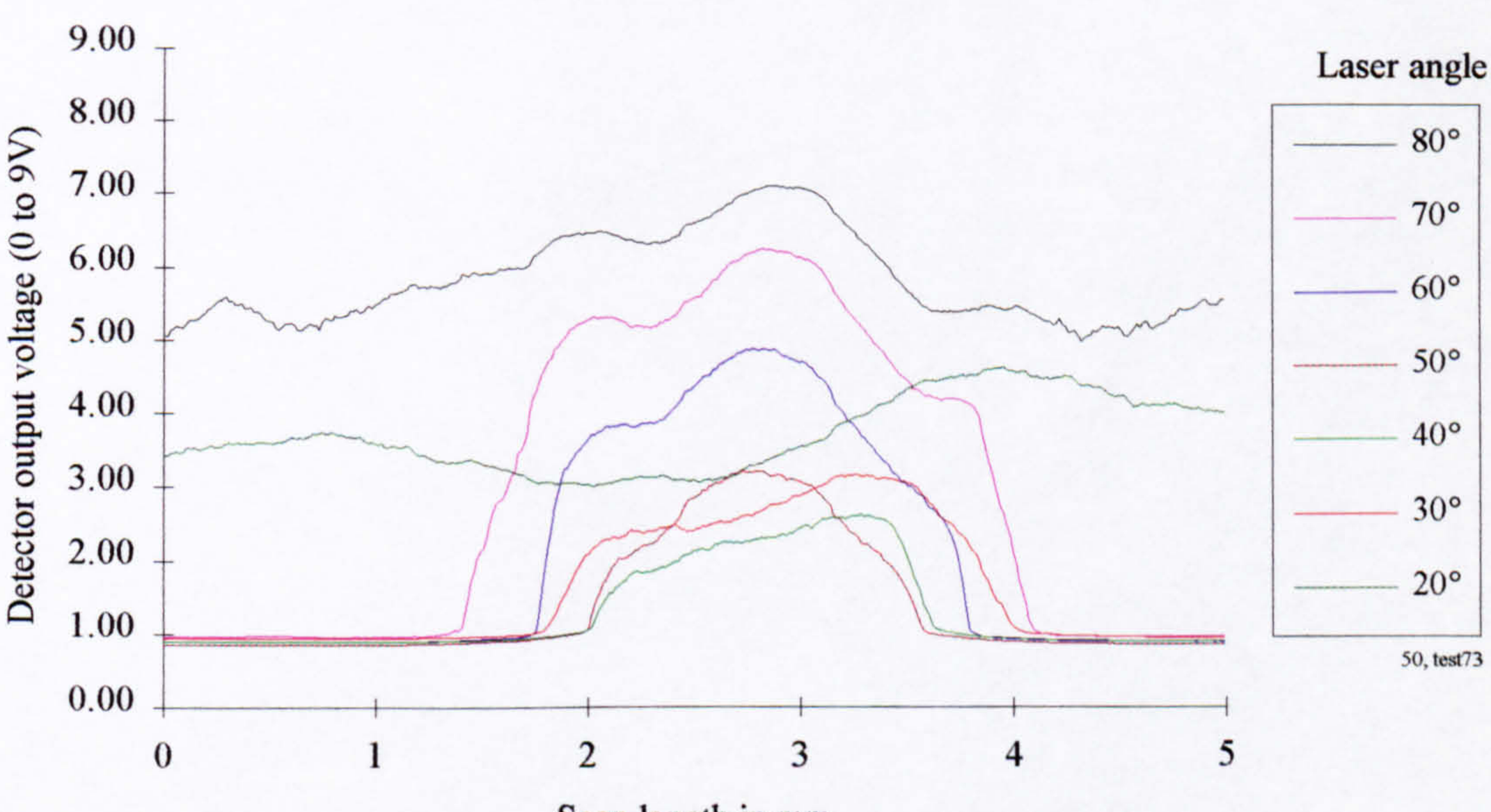

Figure 5-43 0.1 μm ground sample with BUE defect and fixed detector angle of 50°

1.6 µm Plain ground control sample

Photograph of inspected surface (1.6 µm Plain ground sample)

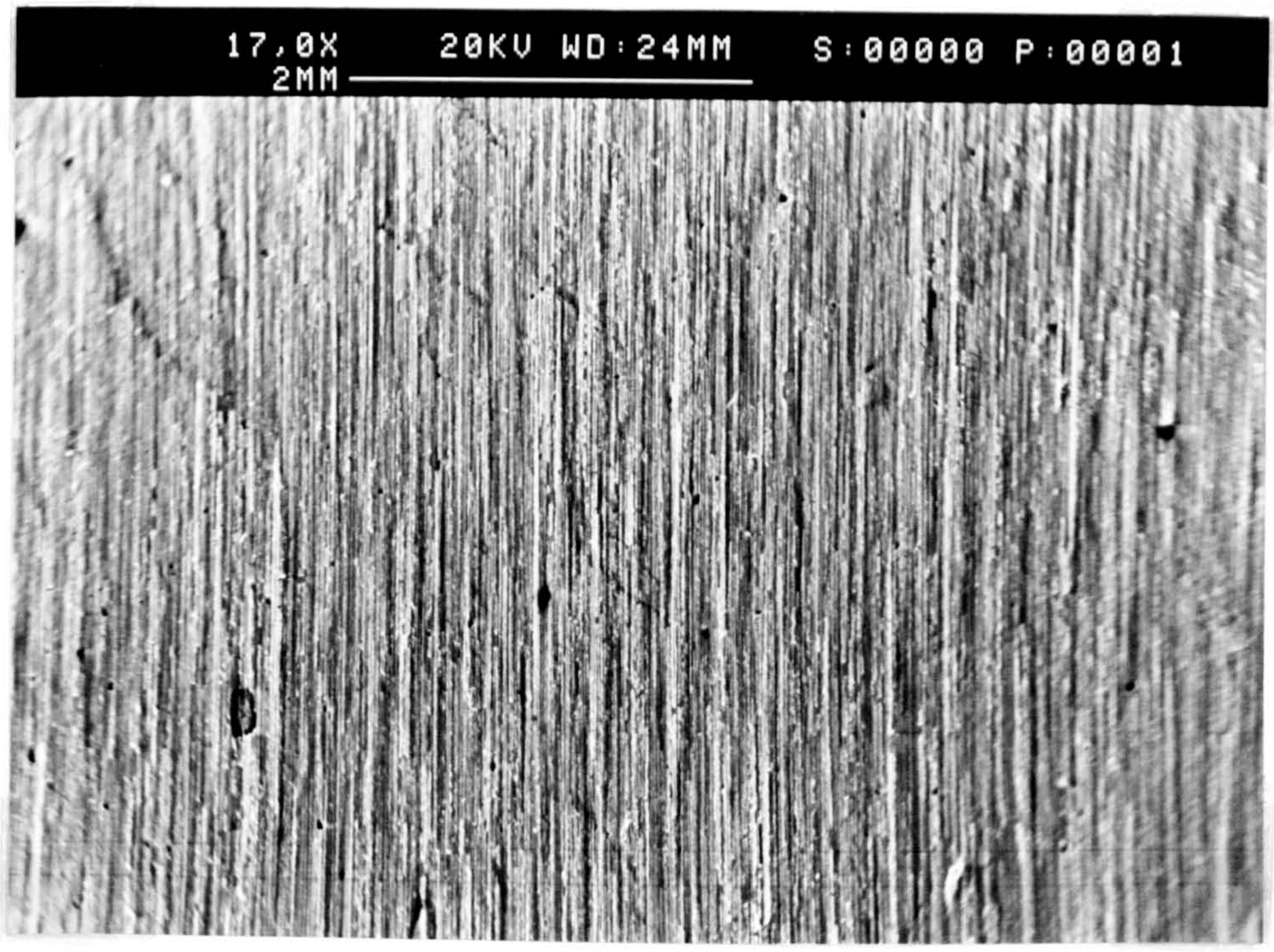

Figure 5-44 1.6 µm Plain ground sample, surface photograph

Surface topography trace (1.6 µm Plain ground sample)

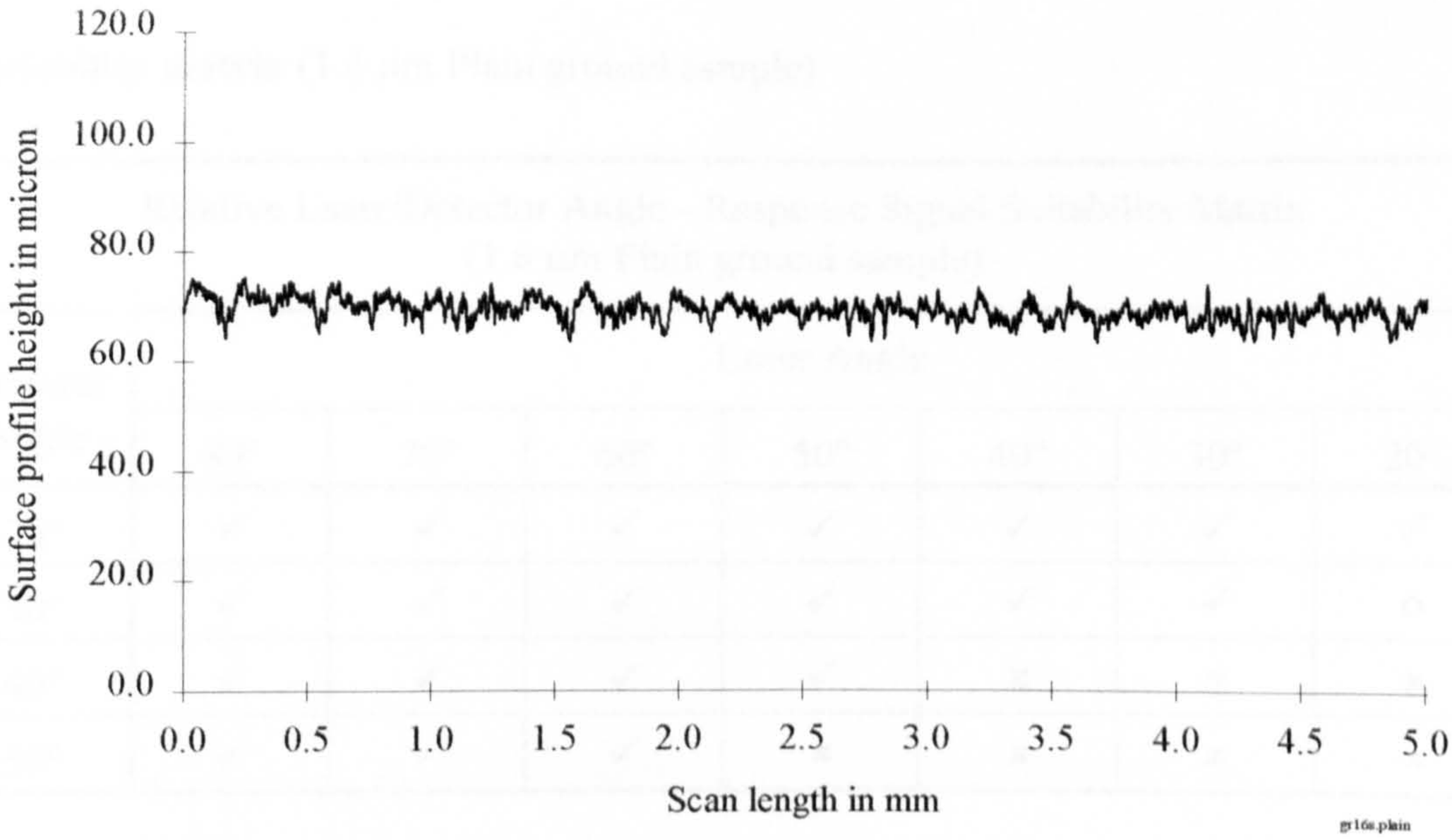

Figure 5-45 1.6 µm Plain ground sample, surface profile

Discussion of results (1.6 μm Plain ground sample)

Typical, ground sample response signals are apparent in all of the non-saturated sections of the graphs illustrated over leaf (Figures 5-46 to 5-49). The high frequency jagged nature of the signals is a characteristic of the ground samples. It should be noted that the 1.6 μm sample currently being reviewed has a higher amplitude, low frequency signal than the 0.1 μm samples analysed earlier, as expected. However, the signal is approximately the same as the 3.2 μm ground samples yet to be examined. The high frequency component is obviously heavily dependent on the laser spot size, as is any surface defect. Thus the response to the micro surface structure can be controlled by modulating the laser spot size and effectively filtering the signal obtained. This topic is addressed later in the work.

From the results summary (suitability matrix) it is apparent that the shallow detector angle (20°) combined with laser angles test (80°down to 20°) are suited to image acquisition, giving a full-form response. As the detector angle is increased and/or the laser angle is decreased, detector saturation soon occurs. A consistent image angle of 100° or greater is ultimately required to ensure that good, full-form response signals are produced. Other angle combinations result in partial/complete response saturation, for almost every case under investigation.

Suitability matrix (1.6 μm Plain ground sample)

Relative Laser/Detector Angle - Response Signal Suitability Matrix (1.6 μm Plain ground sample)							
Detector Angle	Laser Angle						
	80°	70°	60°	50°	40°	30°	20°
20°	✓	✓	✓	✓	✓	✓	✓
30°	✓	✓	✓	✓	✓	✓	o
40°	✓	✓	✓	✓	×	×	×
50°	✓	✓	✓	×	×	×	×

Table 5-7 1.6 μm Plain ground sample, response signal suitability matrix

Graphical results (1.6 μm Plain ground sample)

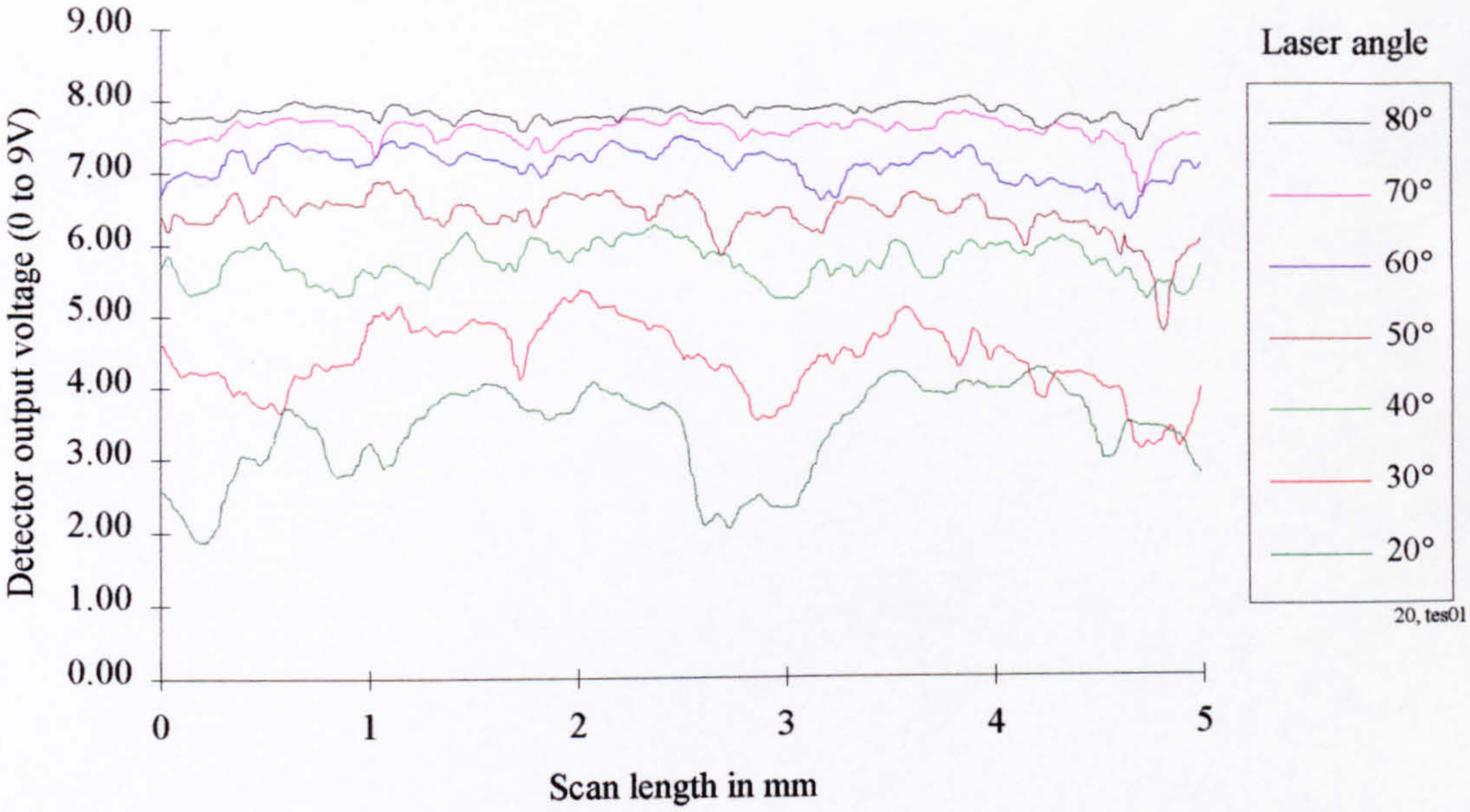

Figure 5-46 1.6 μm Plain ground sample with fixed detector angle of 20°

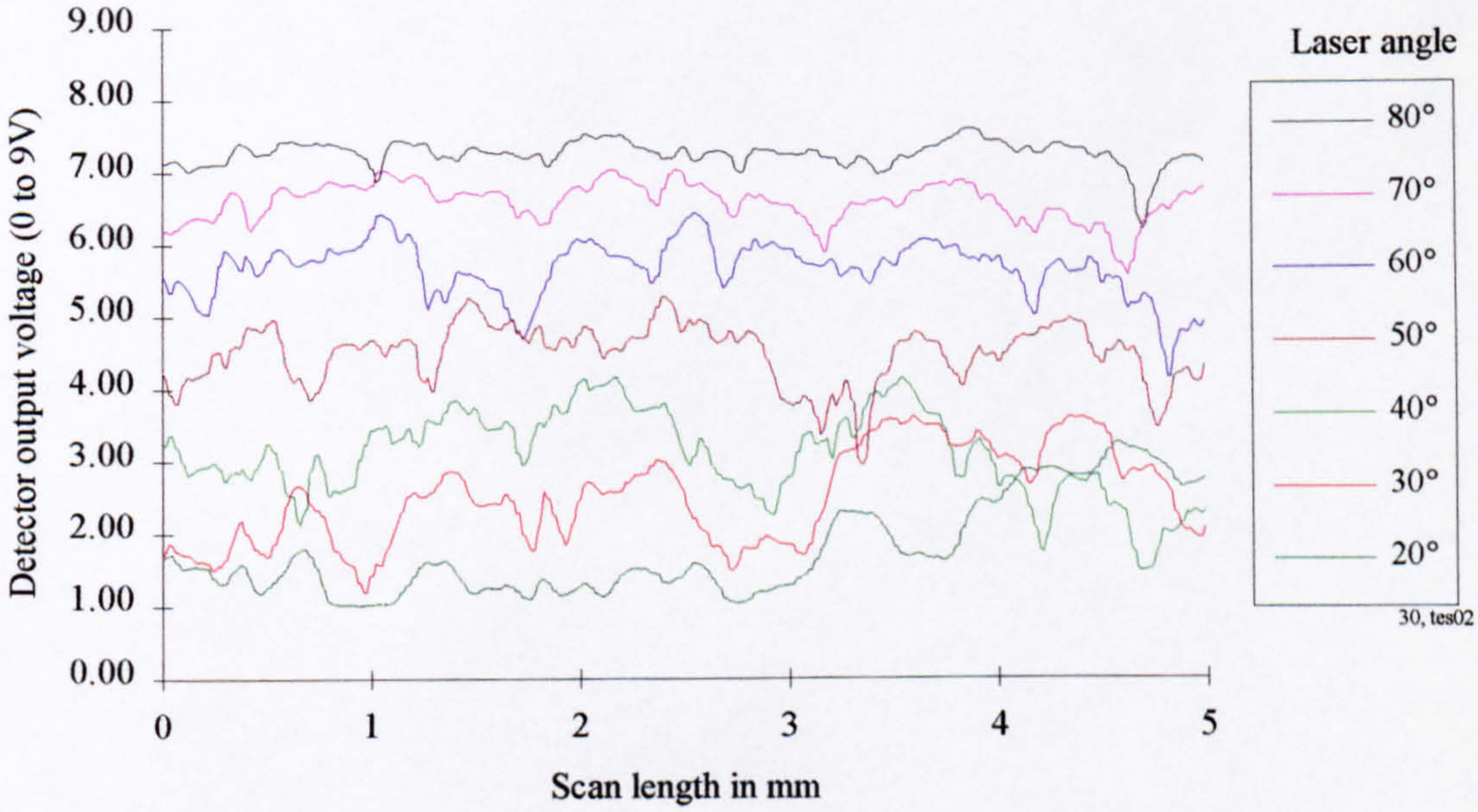

Figure 5-47 1.6 μm Plain ground sample with fixed detector angle of 30°

Graphical results continued (1.6 μm Plain ground sample)

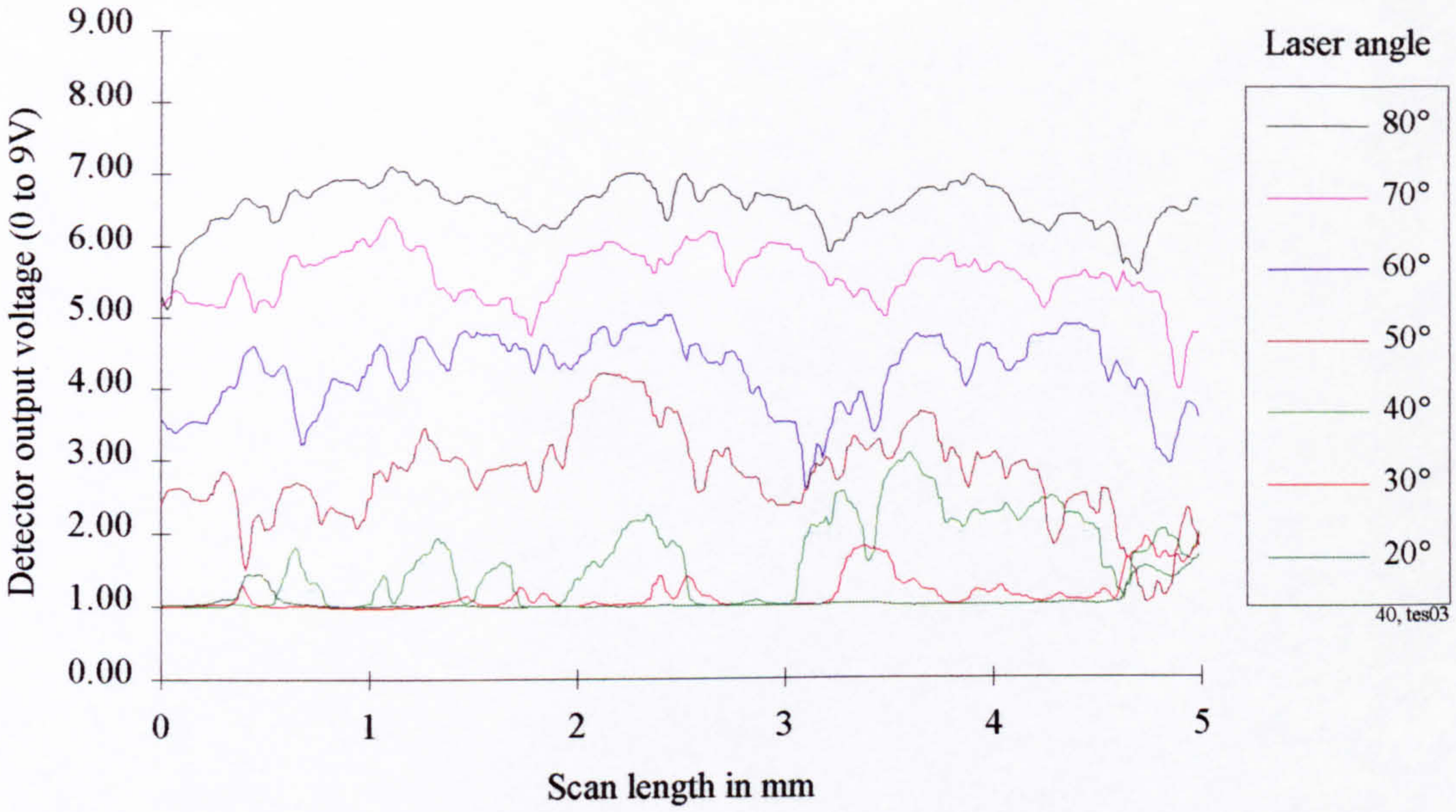

Figure 5-48 1.6 μm Plain ground sample with fixed detector angle of 40°

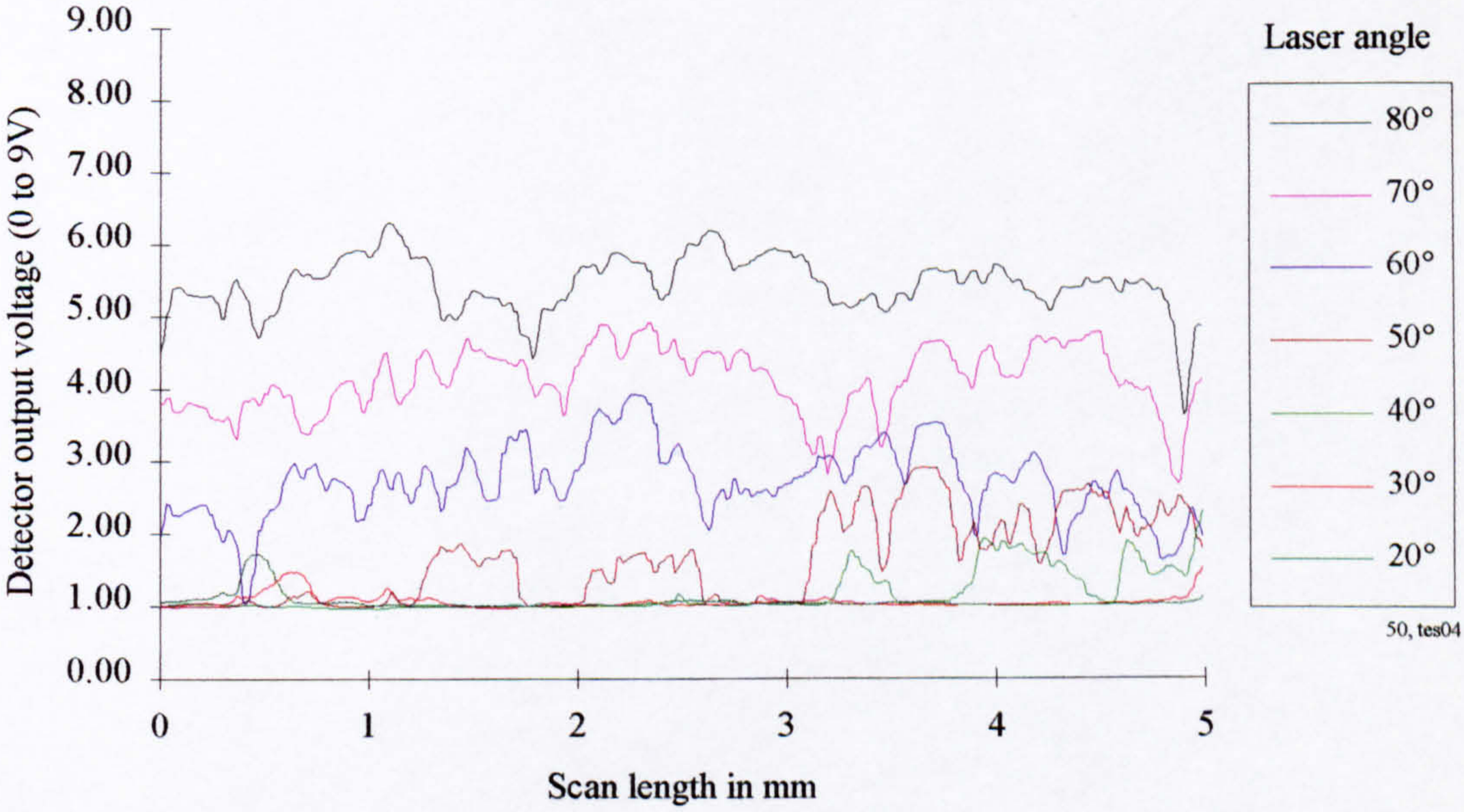

Figure 5-49 1.6 μm Plain ground sample with fixed detector angle of 50°

1.6 μm Ground control sample with scratch defect

Photograph of inspected surface (1.6 μm Ground sample with scratch defect)

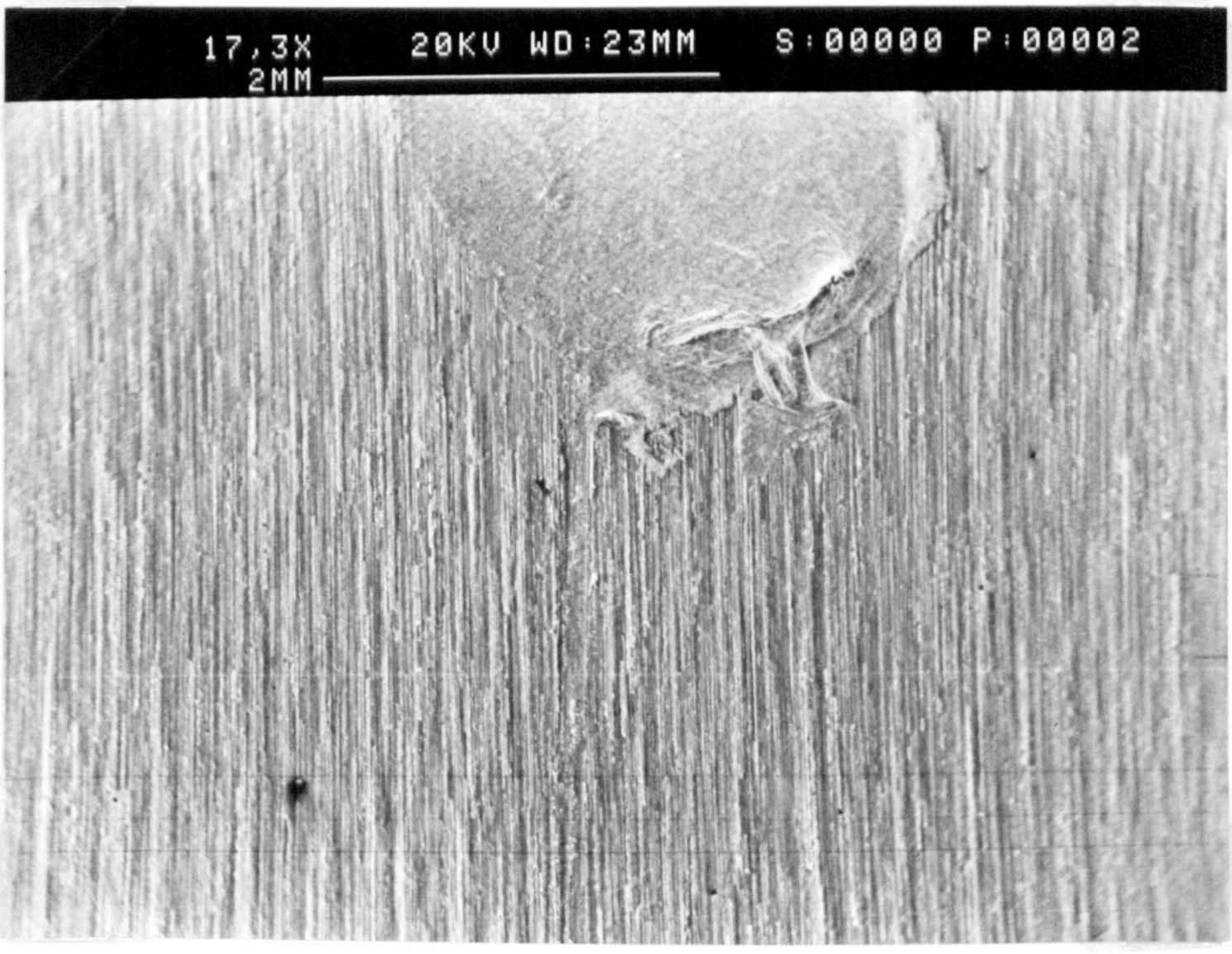

Figure 5-50 1.6 μm Ground sample with scratch defect, surface photograph

Surface topography trace (1.6 μm Ground sample with scratch defect)

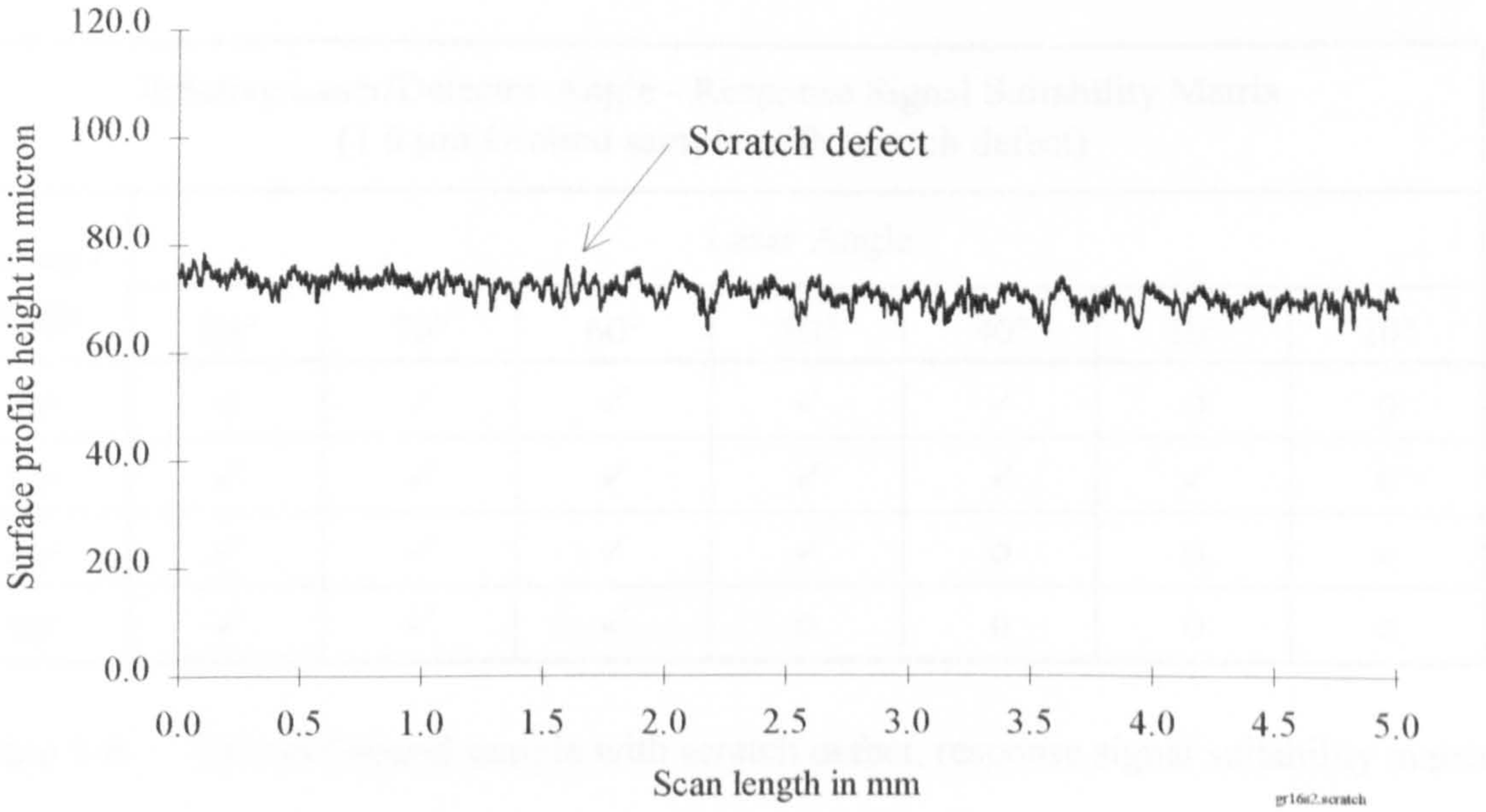

Figure 5-51 1.6 μm Ground sample with scratch defect, surface profile

Discussion of results (1.6 μm Ground sample with scratch defect)

As expected the graphs produce a similar pattern of suitability to that for the 1.6 μm plain ground samples. The table below suggests that a consistent image angle of 110° or greater but less than 150° must be used so as to render workable, full-form signals. Other angle combinations yield fully saturated or near fully saturated response signals. Such conditions obviously cause the signal to be unsuitable for any form of post-processing.

The presence of the scratch defect is clearly perceptible in the general form of the ground surface signal. A detector angle of 30° is seen to give the broadest band of acceptable results.

Suitability matrix (1.6 μm Ground sample with scratch defect)

Relative Laser/Detector Angle - Response Signal Suitability Matrix (1.6 μm Ground sample with scratch defect)							
Detector Angle	Laser Angle						
	80°	70°	60°	50°	40°	30°	20°
20°	o	✓	✓	✓	✓	o	o
30°	✓	✓	✓	✓	✓	✓	o
40°	✓	✓	✓	✓	o	o	o
50°	✓	✓	✓	o	o	o	o

Table 5-8 1.6 μm Ground sample with scratch defect, response signal suitability matrix

Graphical results (1.6 μm Ground sample with scratch defect)

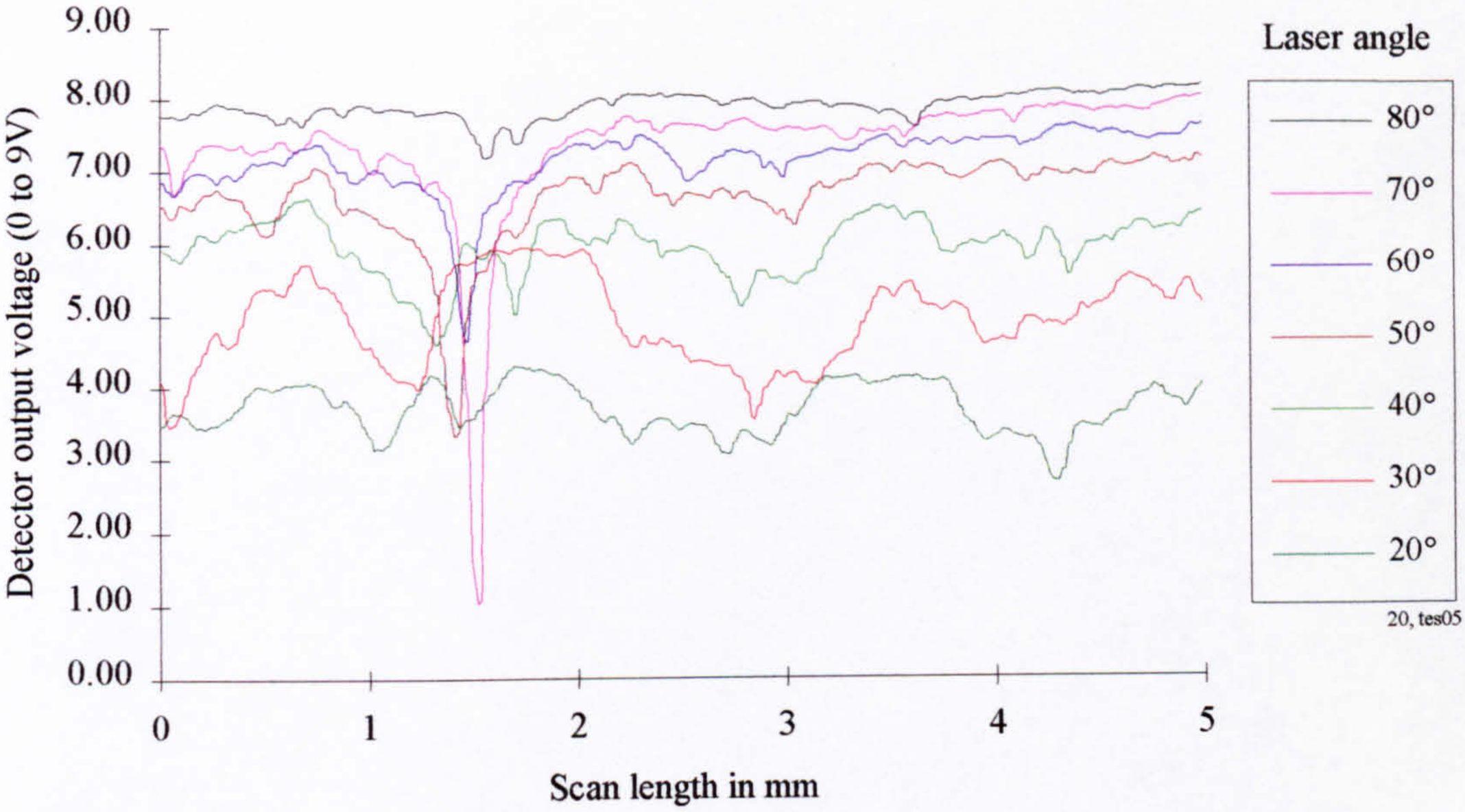

Figure 5-52 1.6 μm Ground sample with scratch defect and fixed detector angle of 20°

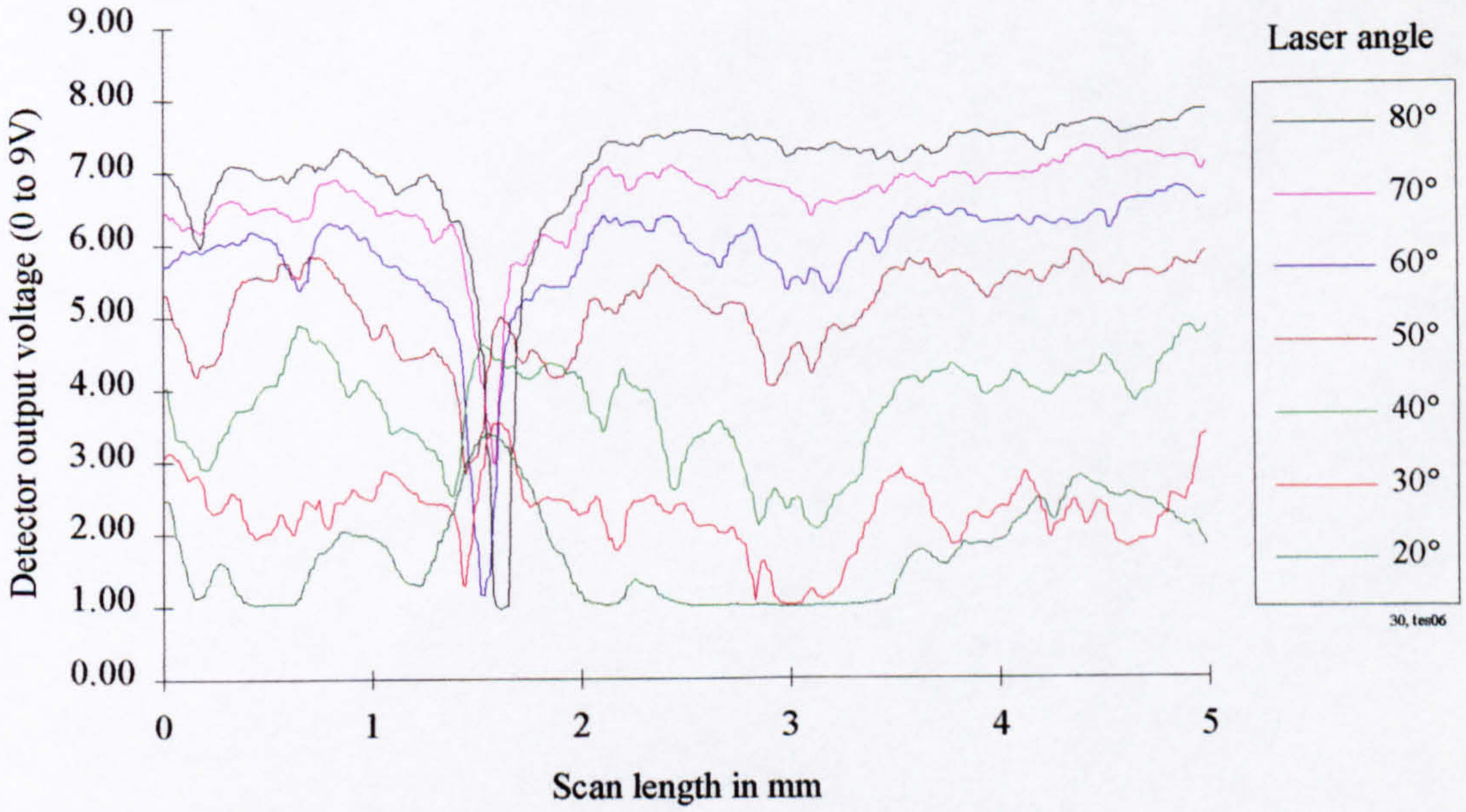

Figure 5-53 1.6 μm Ground sample with scratch defect and fixed detector angle of 30°

Graphical results continued (1.6 μm Ground sample with scratch defect)

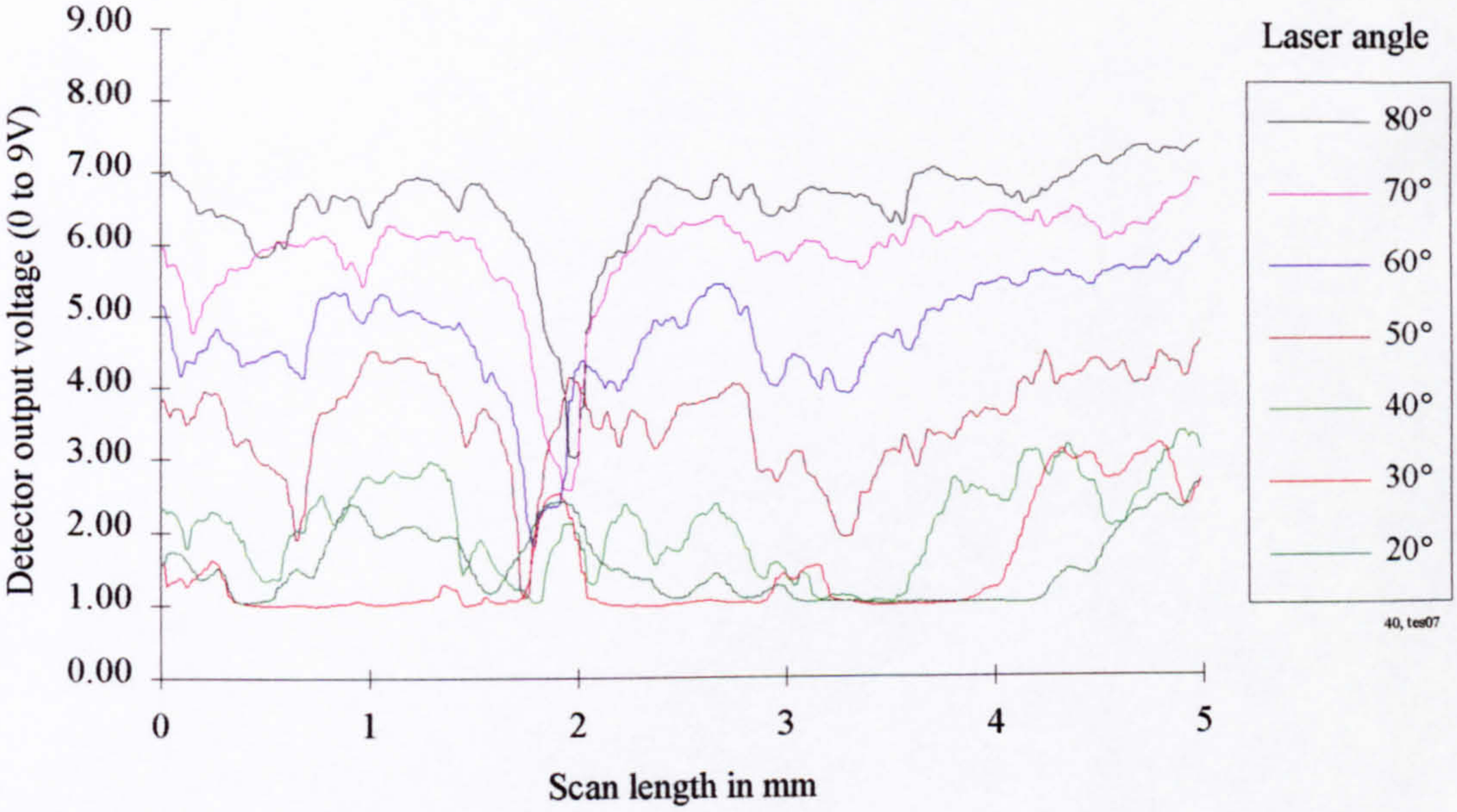

Figure 5-54 1.6 μm Ground sample with scratch defect and fixed detector angle of 40°

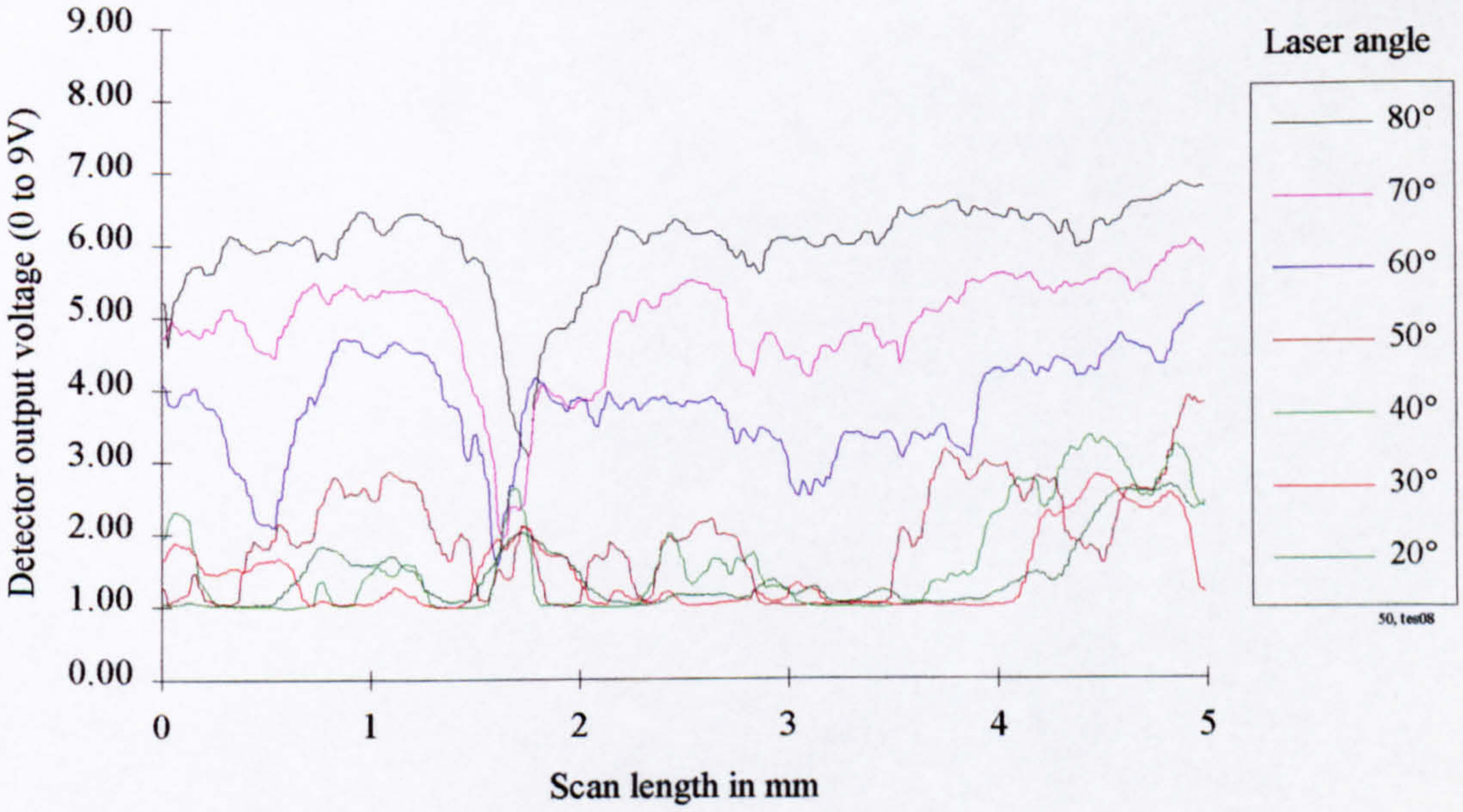

Figure 5-55 1.6 μm Ground sample with scratch defect and fixed detector angle of 50°

1.6 µm Ground control sample with built-up edge (BUE) defect

Photograph of inspected surface (1.6 µm Ground sample with BUE defect)

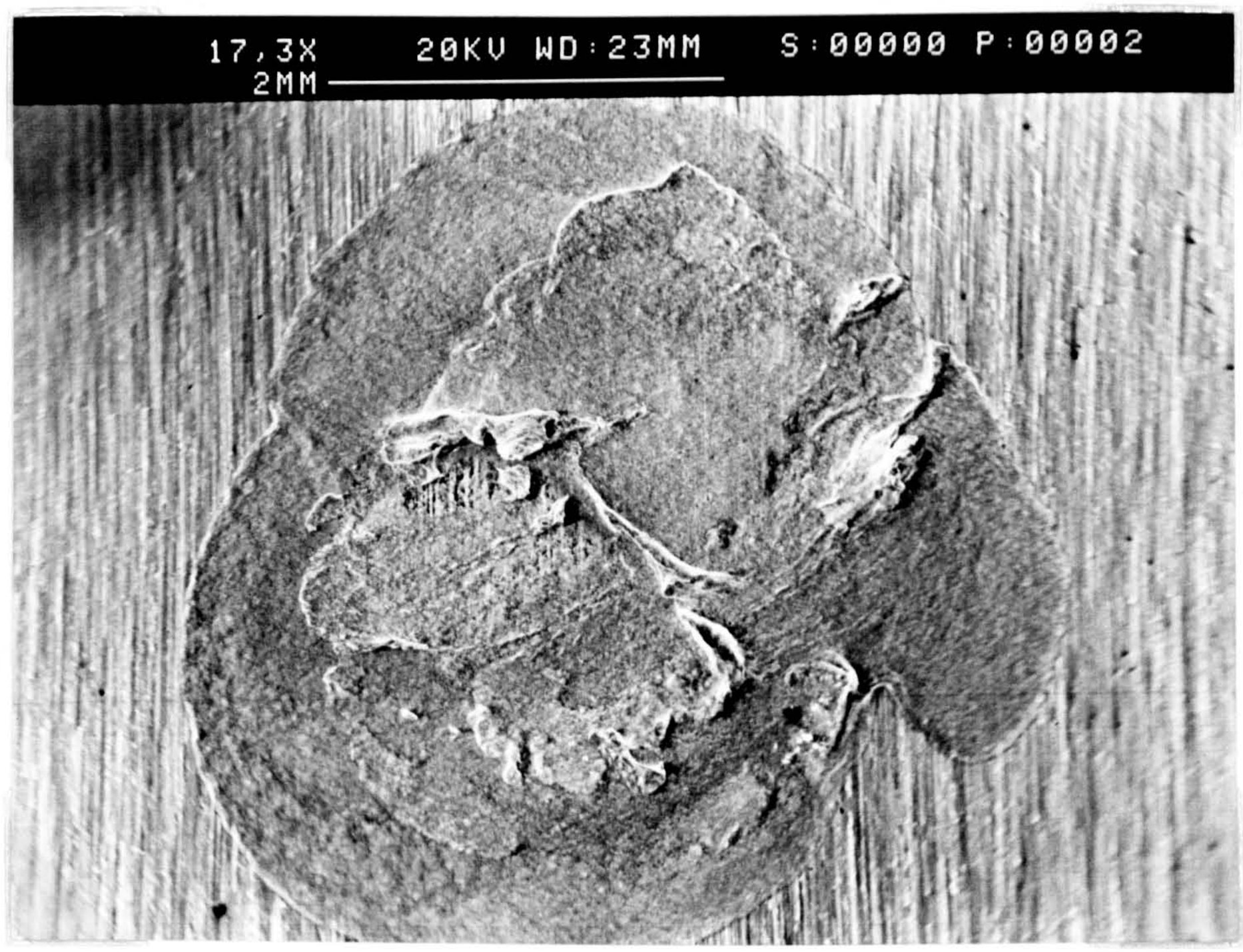

Figure 5-56 1.6 µm Ground sample with BUE defect, surface photograph

Surface topography trace (1.6 µm Ground sample with BUE defect)

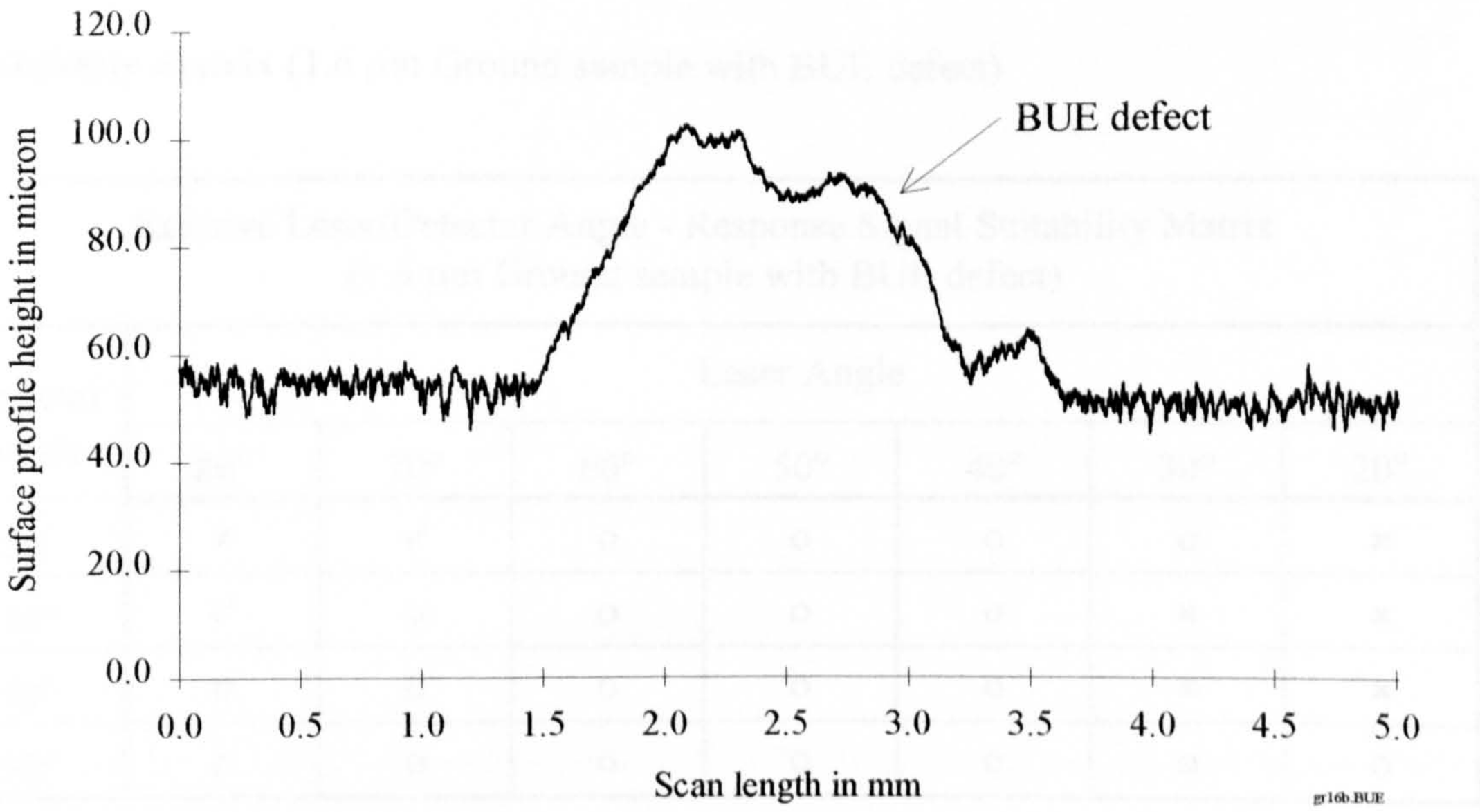

Figure 5-57 1.6 µm Ground sample with BUE defect, surface profile

Discussion of results (1.6 μm Ground sample with BUE defect)

The influence of the BUE defect is immediately apparent in all four of the related figures (5-58 to 5-61). Despite the full-form results (✓) once again adopting a similar pattern to those for the previous 1.6 μm ground samples tests, other combinations of laser/detector angle are nearly as well suited (o). Full-form signals which contain information about the general surface nature as well as the BUE defect are achieved for a consistent image angle of 140° and greater. Good defect detection signals can still be acquired at consistent image angles as low as 100°. Furthermore, the compiled results presented in the table below, yield an interesting phenomenon. At a steep detector angle (50° in this case) all laser angles under evaluation (20° to 80°) produced a response which contained sufficient information to support BUE defect detection. This is evident from the naughts on the bottom row of the table.

A stark contrast exists between the system's ability to detect the BUE but not the scratch defect. Close observation indicates that the compound used to produce the synthetic BUE defects has considerably lower reflectance properties than the parent substrate. This condition would most certainly cause the detector output voltage to rise (decreased light level), which is clearly the case for all associated response signals.

Suitability matrix (1.6 μm Ground sample with BUE defect)

Relative Laser/Detector Angle - Response Signal Suitability Matrix (1.6 μm Ground sample with BUE defect)							
Detector Angle	Laser Angle						
	80°	70°	60°	50°	40°	30°	20°
20°	✓	✓	o	o	o	o	×
30°	✓	o	o	o	o	×	×
40°	o	o	o	o	o	×	×
50°	o	o	o	o	o	o	o

Table 5-9 1.6 μm Ground sample with BUE defect, response signal suitability matrix

Graphical results (1.6 μm Ground sample with BUE defect)

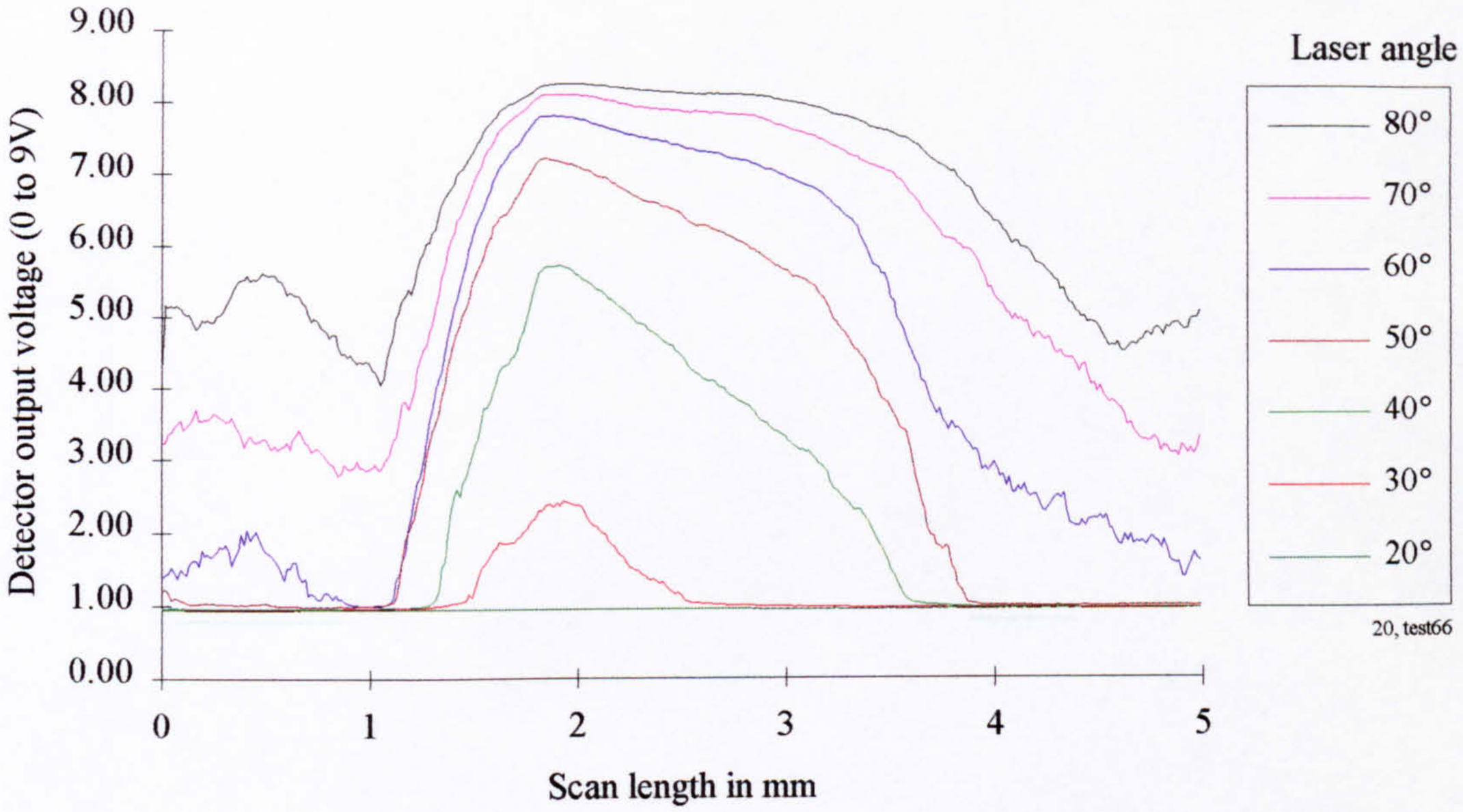

Figure 5-58 1.6 μm Ground sample with BUE defect and fixed detector angle of 20°

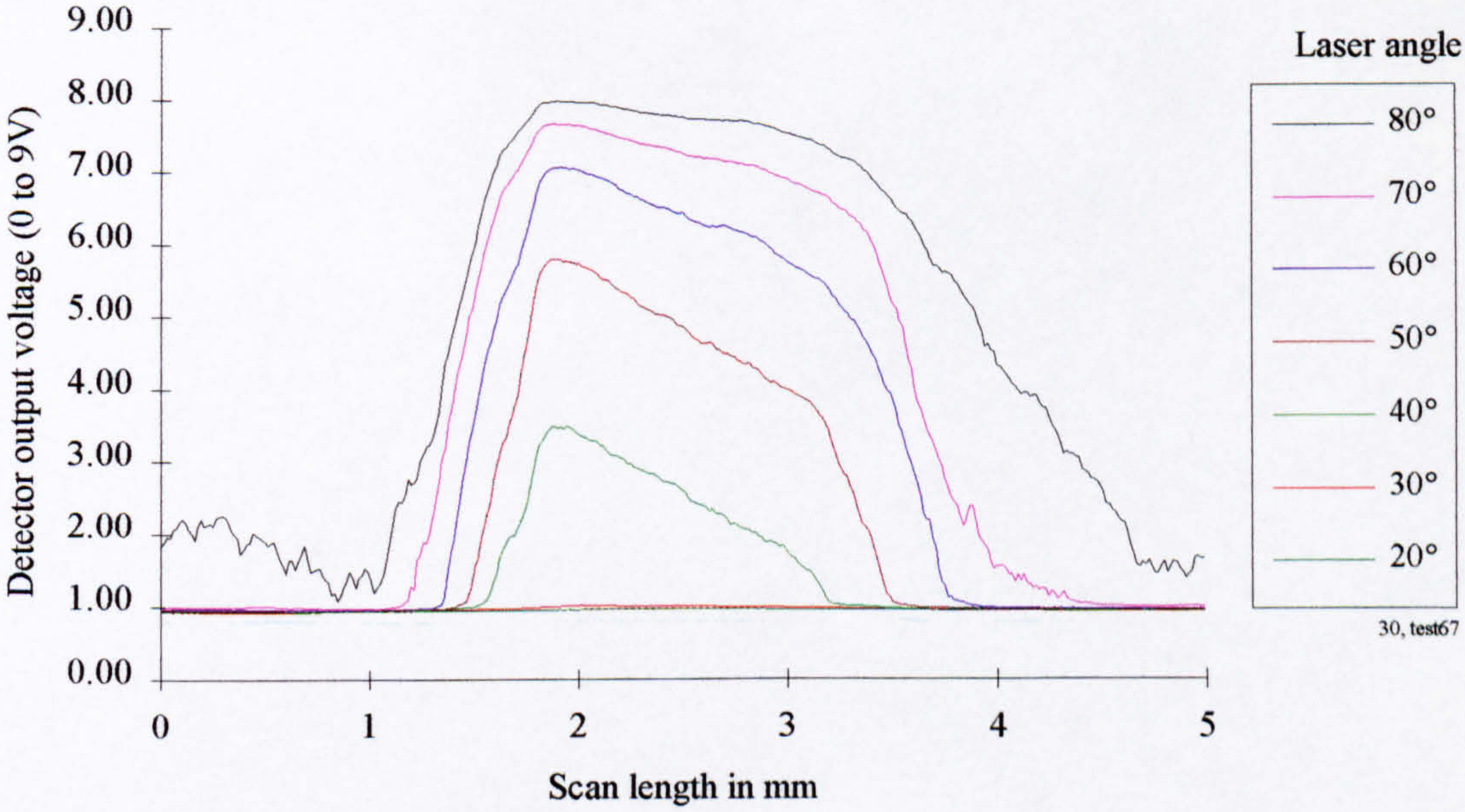

Figure 5-59 1.6 μm Ground sample with BUE defect and fixed detector angle of 30°

Graphical results continued (1.6 µm Ground sample with BUE defect)

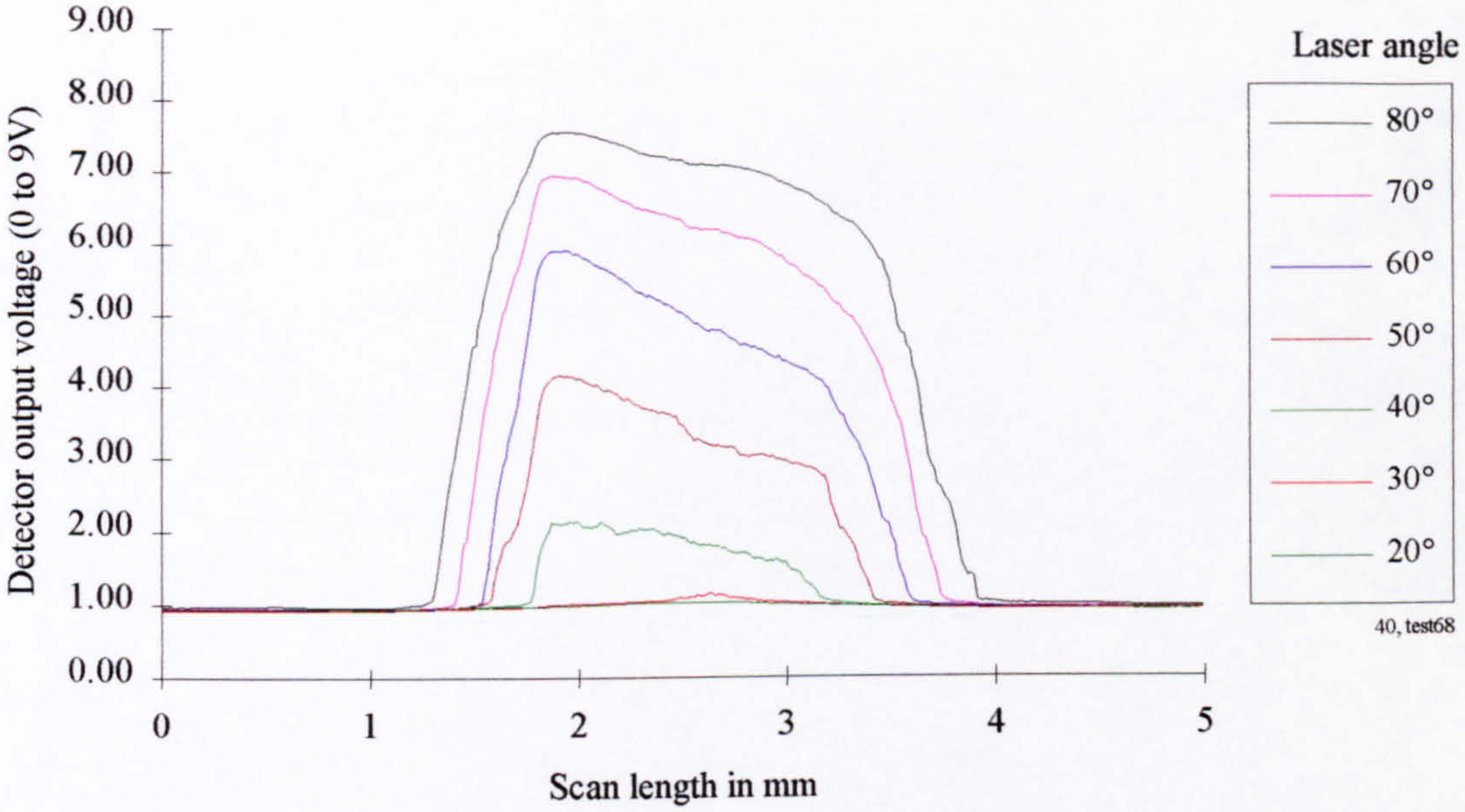

Figure 5-60 1.6 µm Ground sample with BUE defect and fixed detector angle of 40°

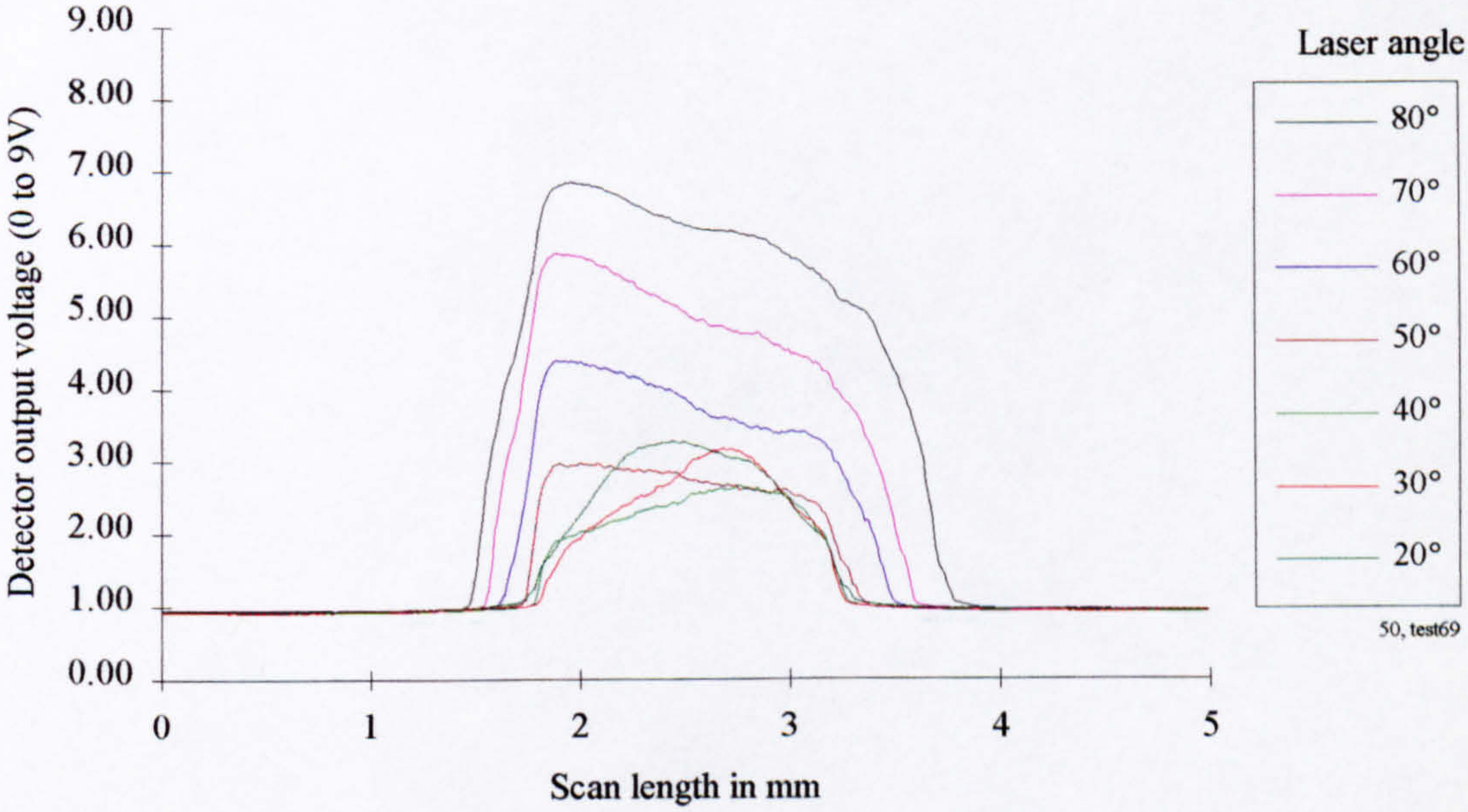

Figure 5-61 1.6 µm Ground sample with BUE defect and fixed detector angle of 50°

3.2 μm Plain ground control sample

Photograph of inspected surface (3.2 μm Plain ground sample)

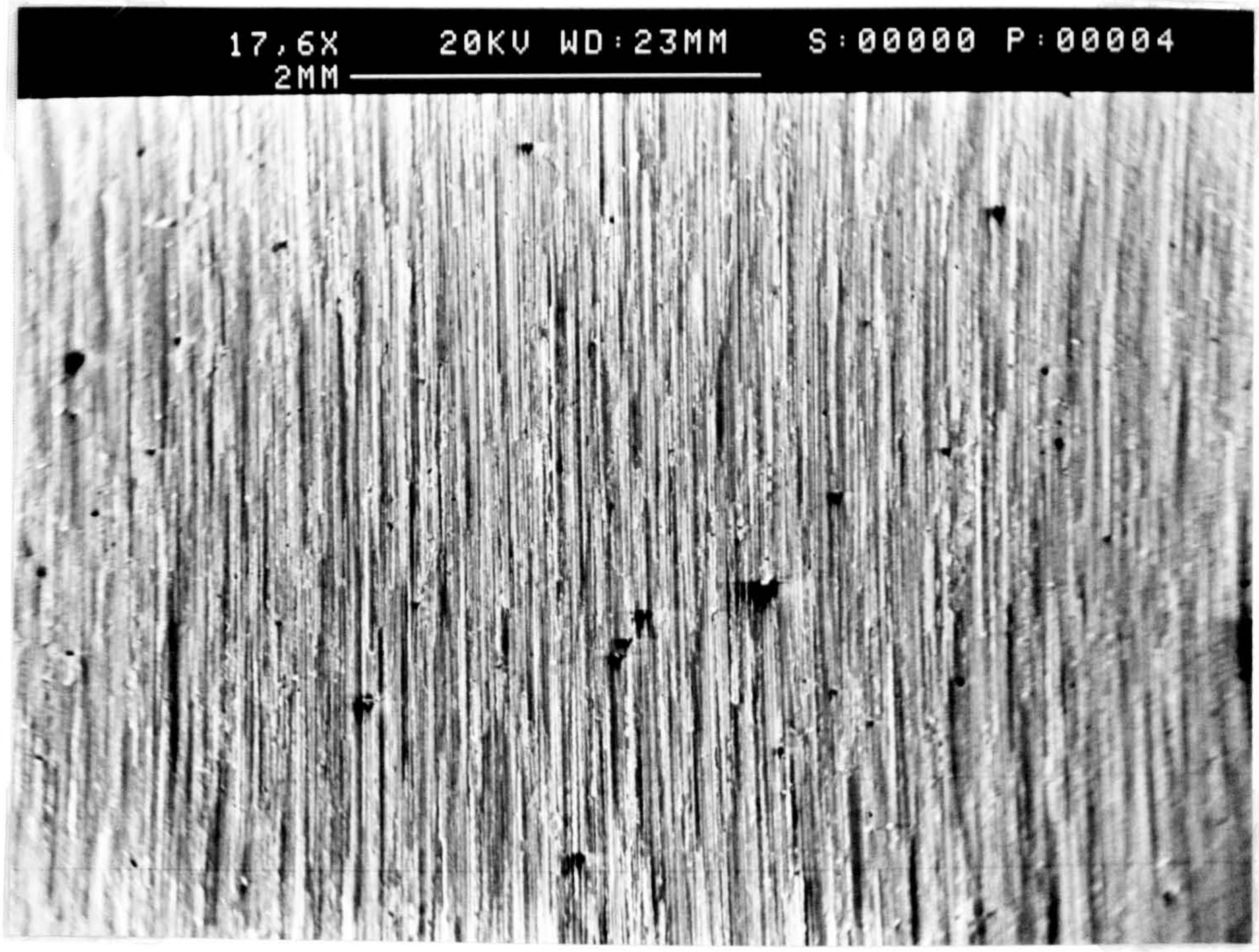

Figure 5-62 3.2 μm Plain ground sample, surface photograph

Surface topography trace (3.2 μm Plain ground sample)

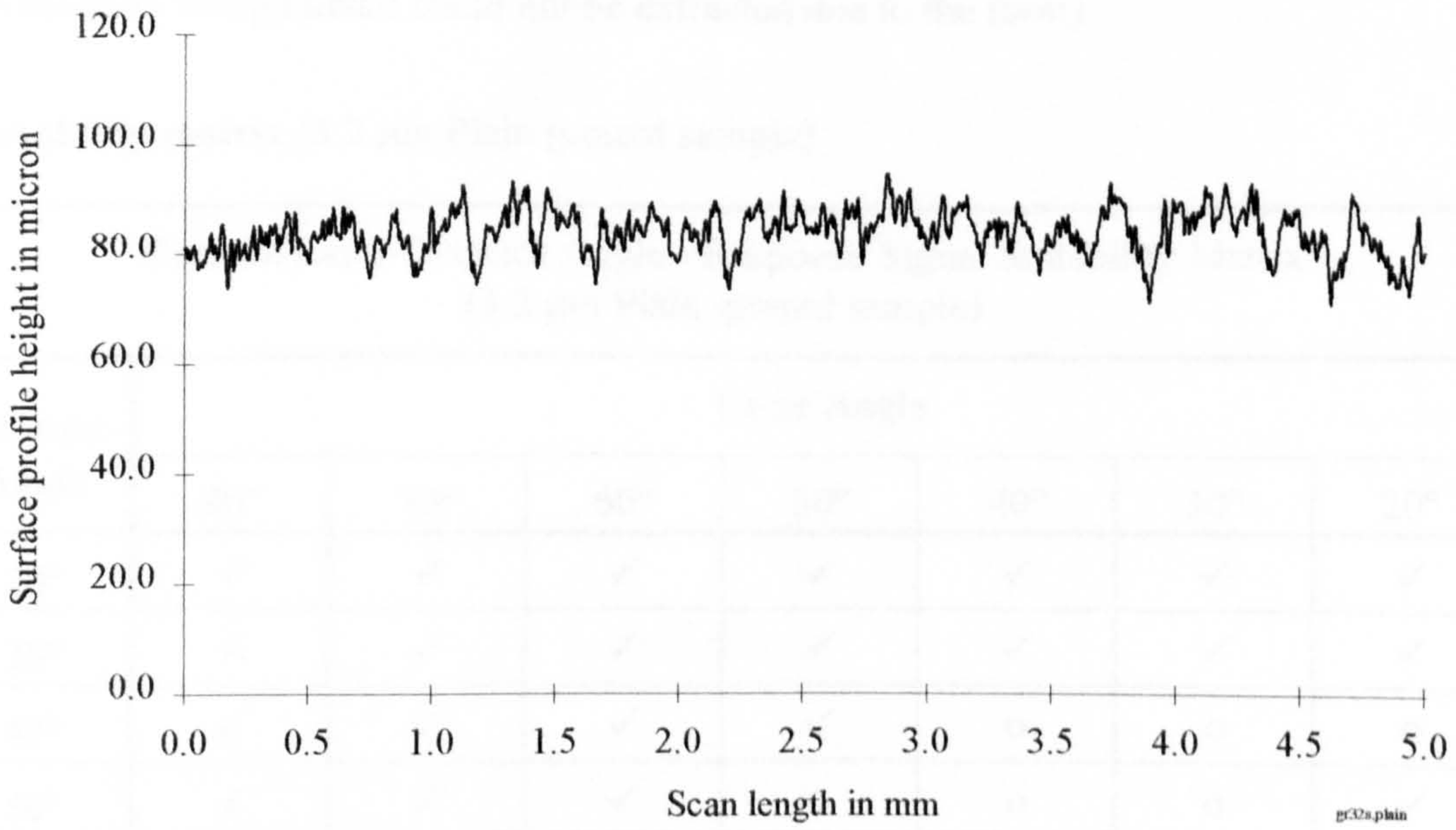

Figure 5-63 3.2 μm Plain ground sample, surface profile

Discussion of results (3.2 μm Plain ground sample)

It is immediately apparent from all of the displayed graphical results that the system configuration is sensitive to the surface topography of the 3.2 μm plain ground sample. Despite being ground flat the surface carries no defects, however undulations and sharp peaks/troughs are registered at locations along the length of some scans. The notable peak and trough features are reproduced across the range of tests thus eliminating the possibility of rogue signals/interference. The rapidly varying nature of the signals can be put down to one or two things at this stage. A critical relationship which exists between the surface roughness of the control sample and; the laser spot size, the wavelength of the laser light, 670 nm [35]. Furthermore, the signal undulations could be partly due to watermarks which were noted on the surface of the sample. The samples were prone to pronounced watermarking through oxidation and handling. Early tests indicated the sensitive nature of the laser inspection deveice and the ability to detect such features, with ease [47].

The suitability matrix suggests that a great number of the laser/detector settings are appropriate for interrogation purposes (denoted by a ✓ in the matrix below). It could be argued that the signals are not entirely suitable due to their spikey nature and so should be represented by a naught in the matrix (indicating that the signal contained some basic information though detail could not be extracted due to the form).

Suitability matrix (3.2 μm Plain ground sample)

Relative Laser/Detector Angle - Response Signal Suitability Matrix (3.2 μm Plain ground sample)							
Detector Angle	Laser Angle						
	80°	70°	60°	50°	40°	30°	20°
20°	✓	✓	✓	✓	✓	✓	✓
30°	✓	✓	✓	✓	✓	✓	✓
40°	✓	✓	✓	✓	o	o	o
50°	✓	✓	✓	o	o	o	✓

Table 5-10 3.2 μm Plain ground sample, response signal suitability matrix

Graphical results (3.2 μm Plain ground sample)

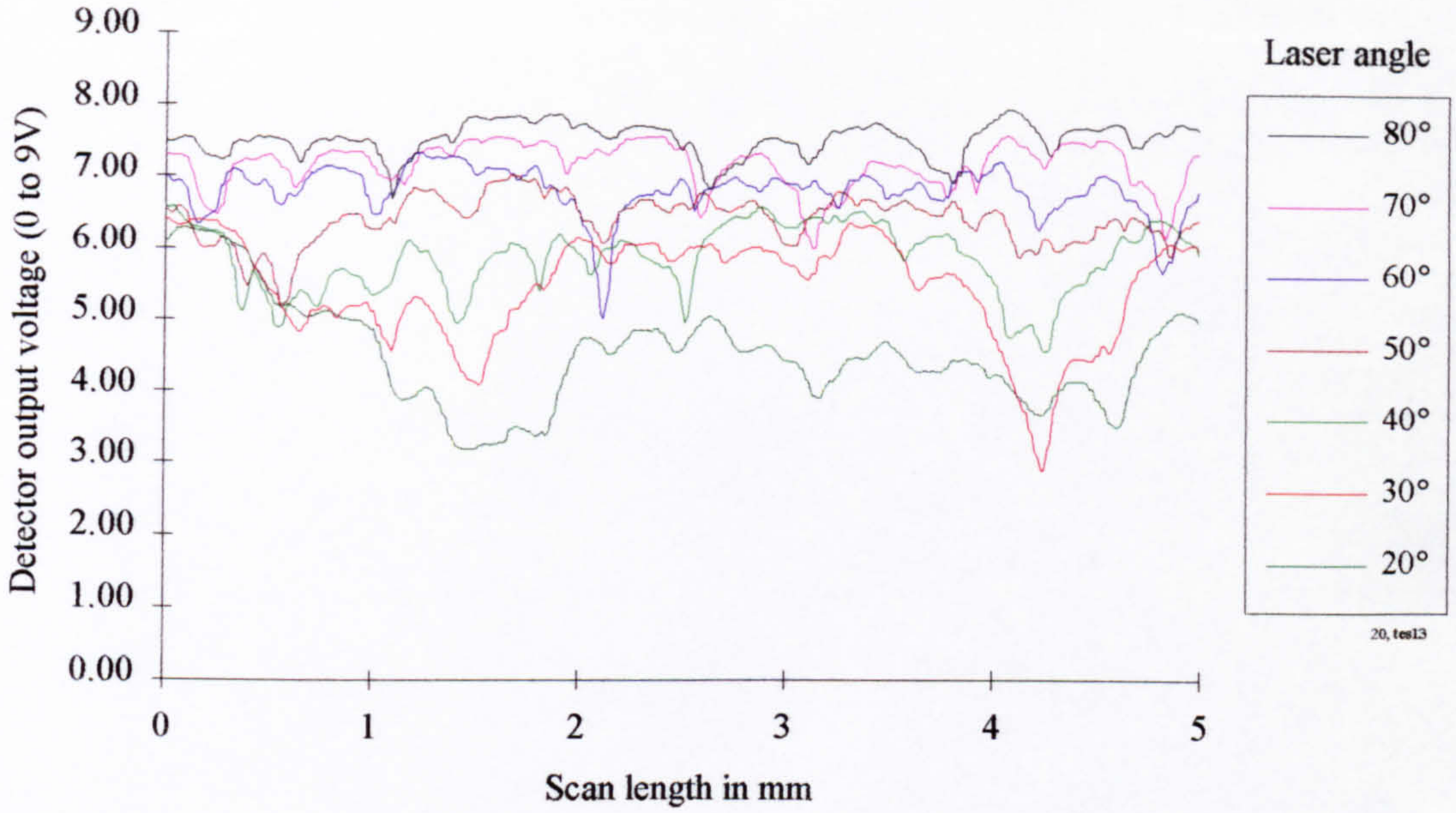

Figure 5-64 3.2 μm Plain ground sample with fixed detector angle of 20°

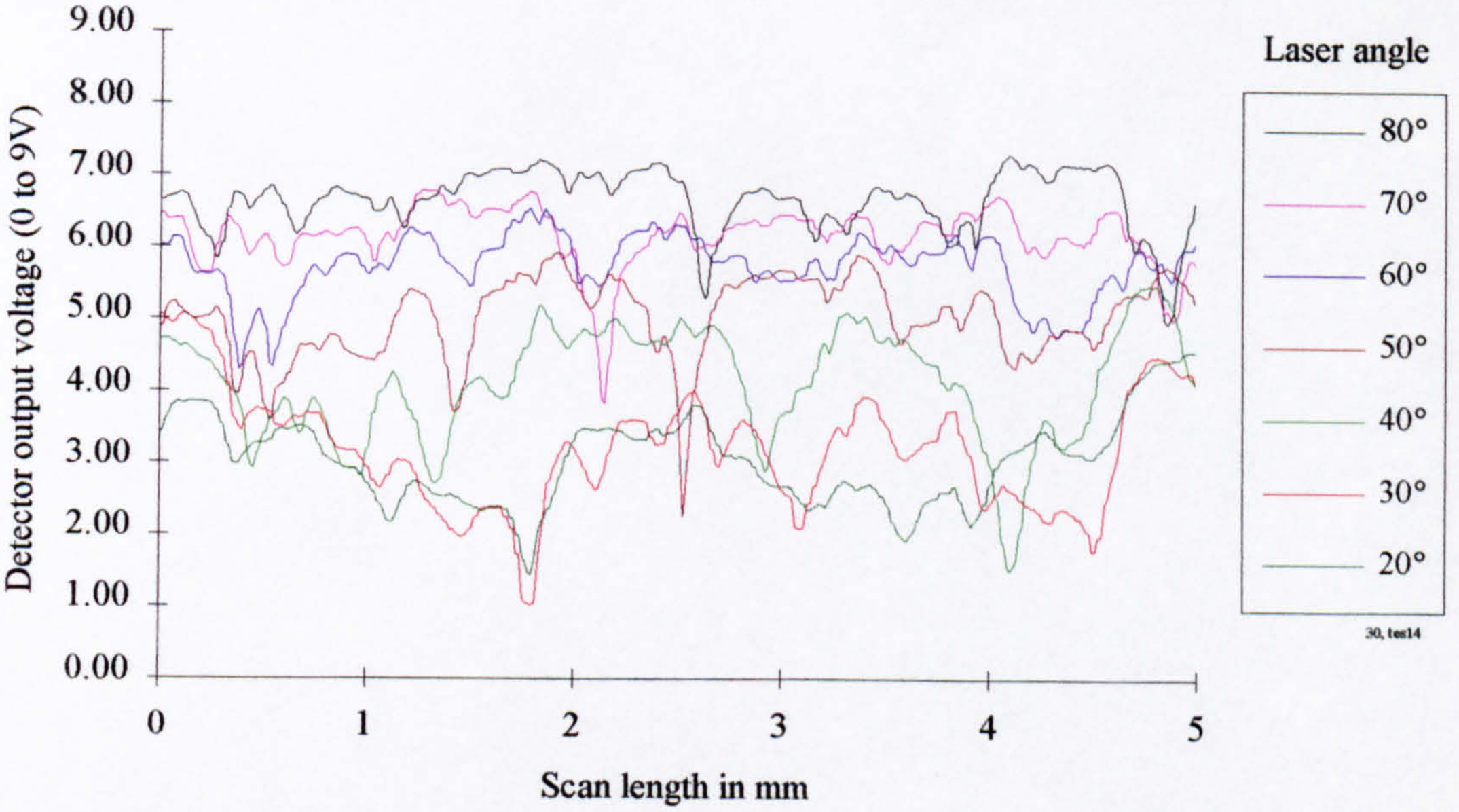

Figure 5-65 3.2 μm Plain ground sample with fixed detector angle of 30°

Graphical results continued (3.2 μm Plain ground sample)

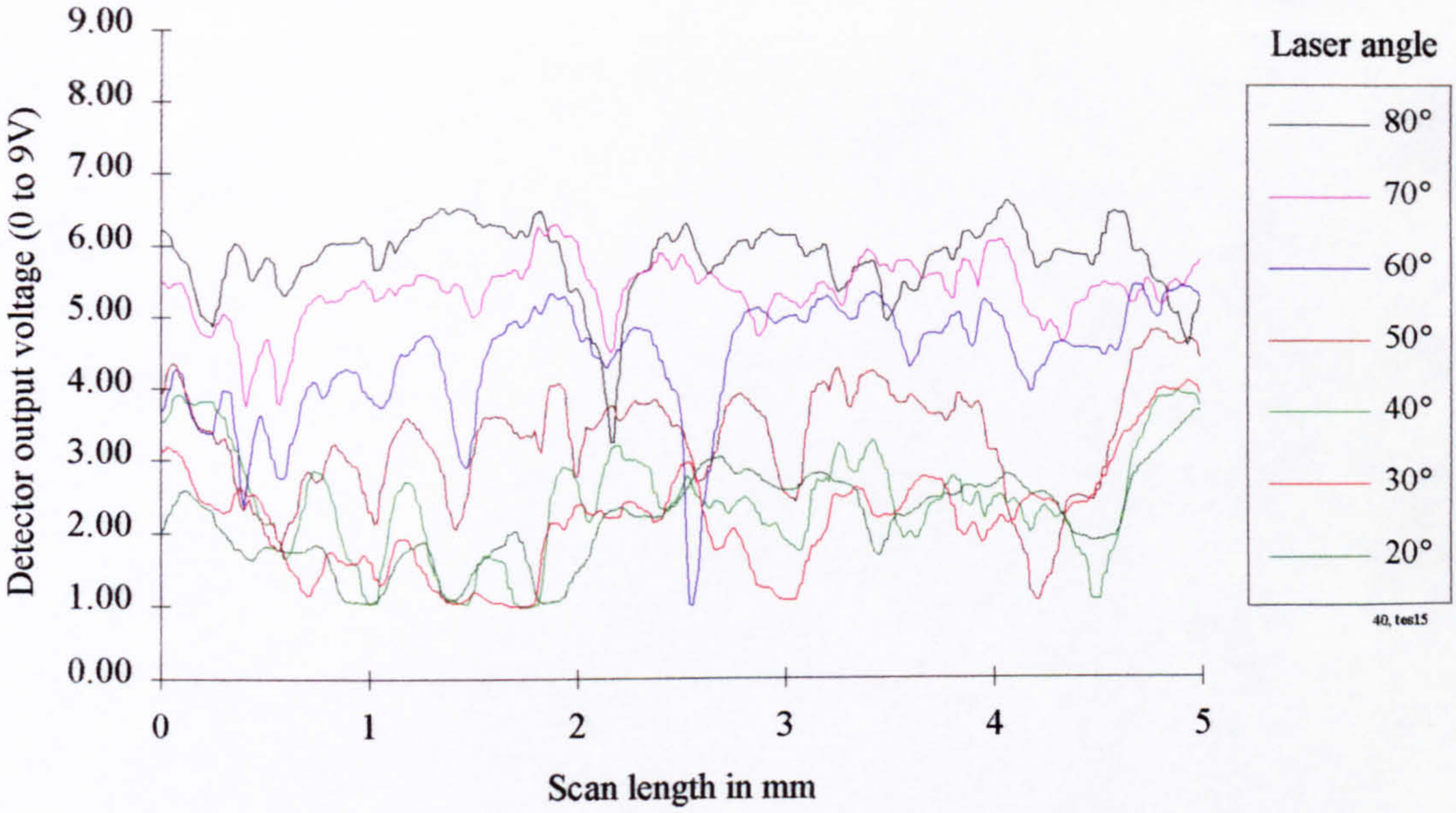

Figure 5-66 3.2 μm Plain ground sample with fixed detector angle of 40°

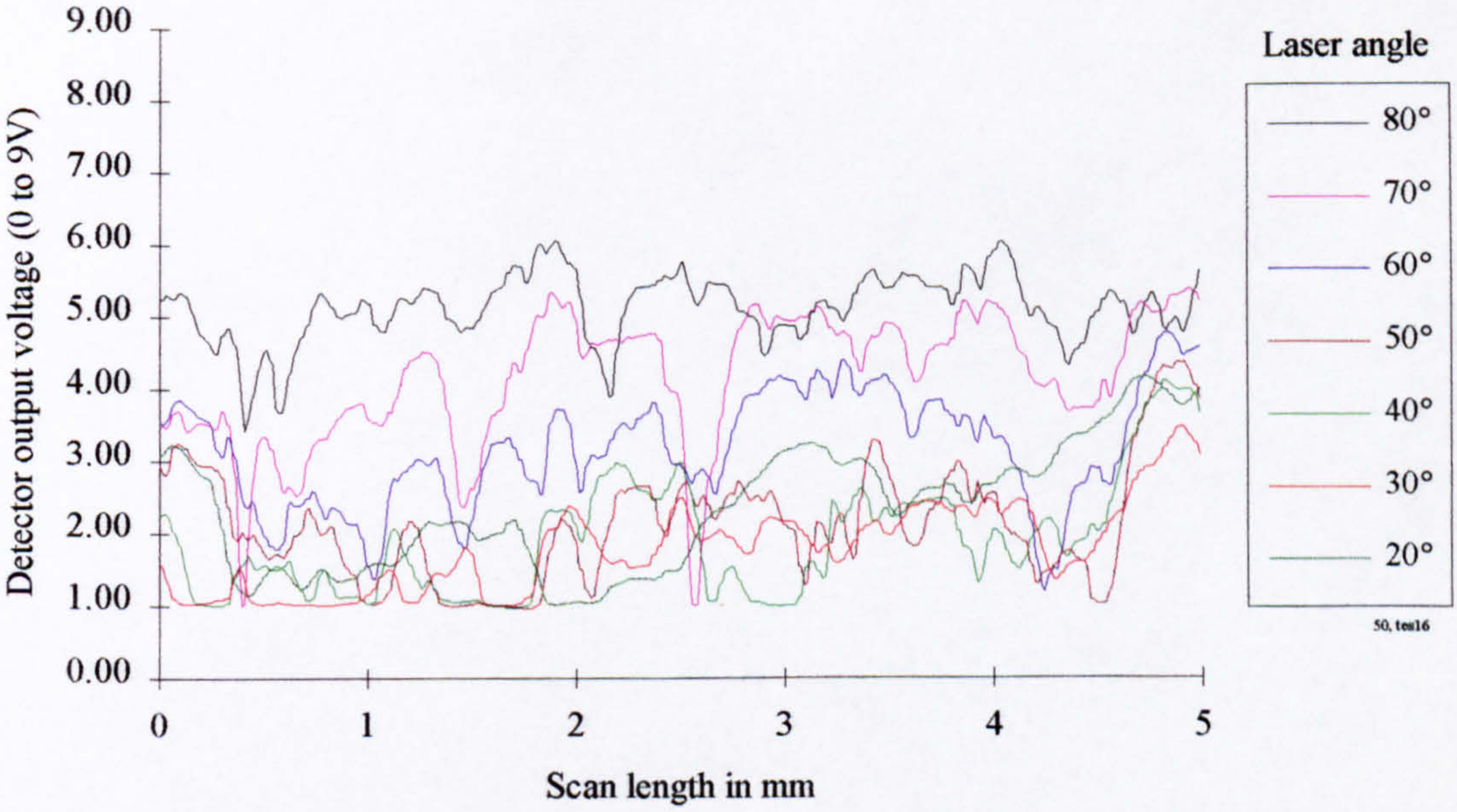

Figure 5-67 3.2 μm Plain ground sample with fixed detector angle of 50°

3.2 μm Ground control sample with scratch defect

Photograph of inspected surface (3.2 μm Ground sample with scratch defect)

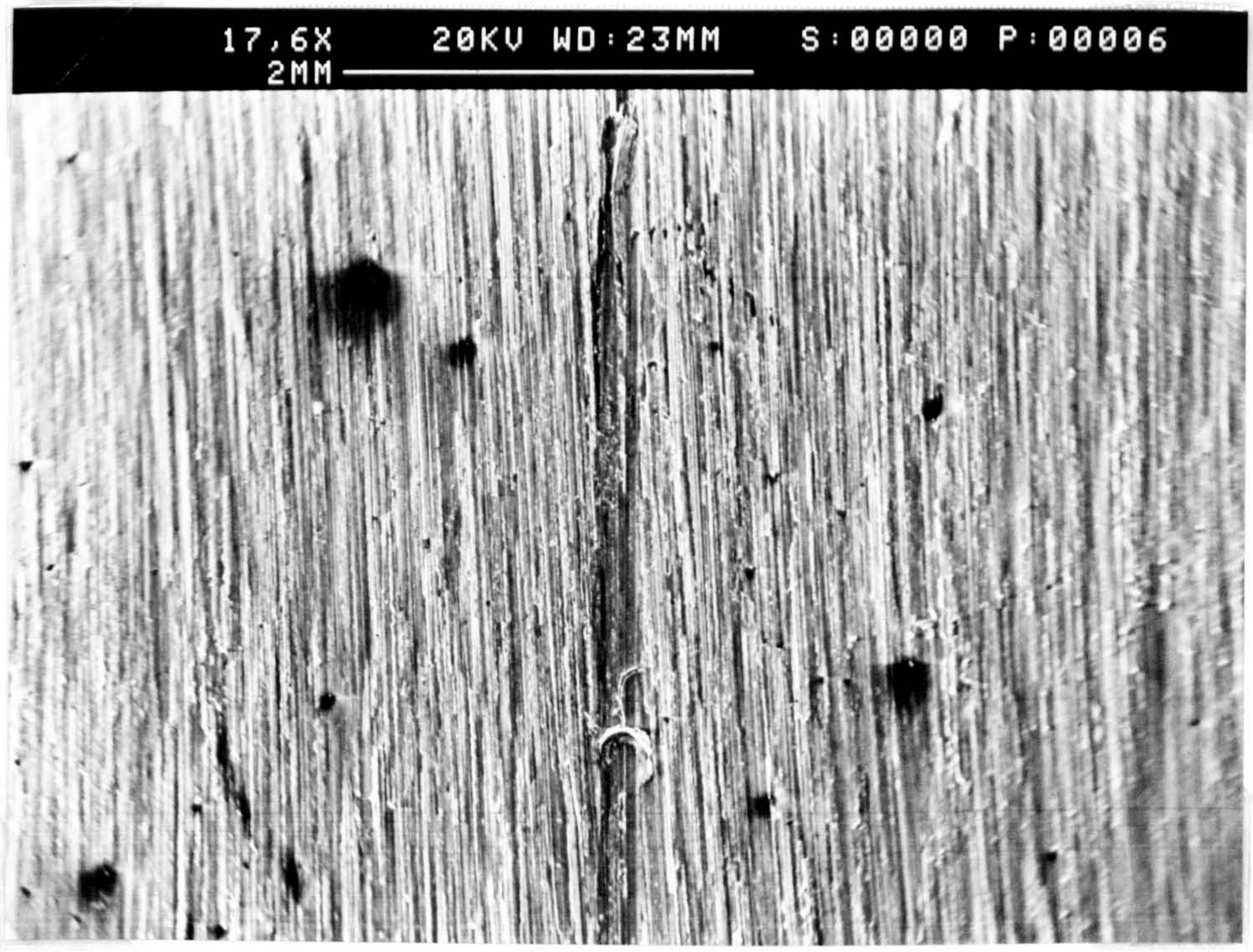

Figure 5-68 3.2 μm Ground sample with scratch defect, surface photograph

Surface topography trace (3.2 μm Ground sample with scratch defect)

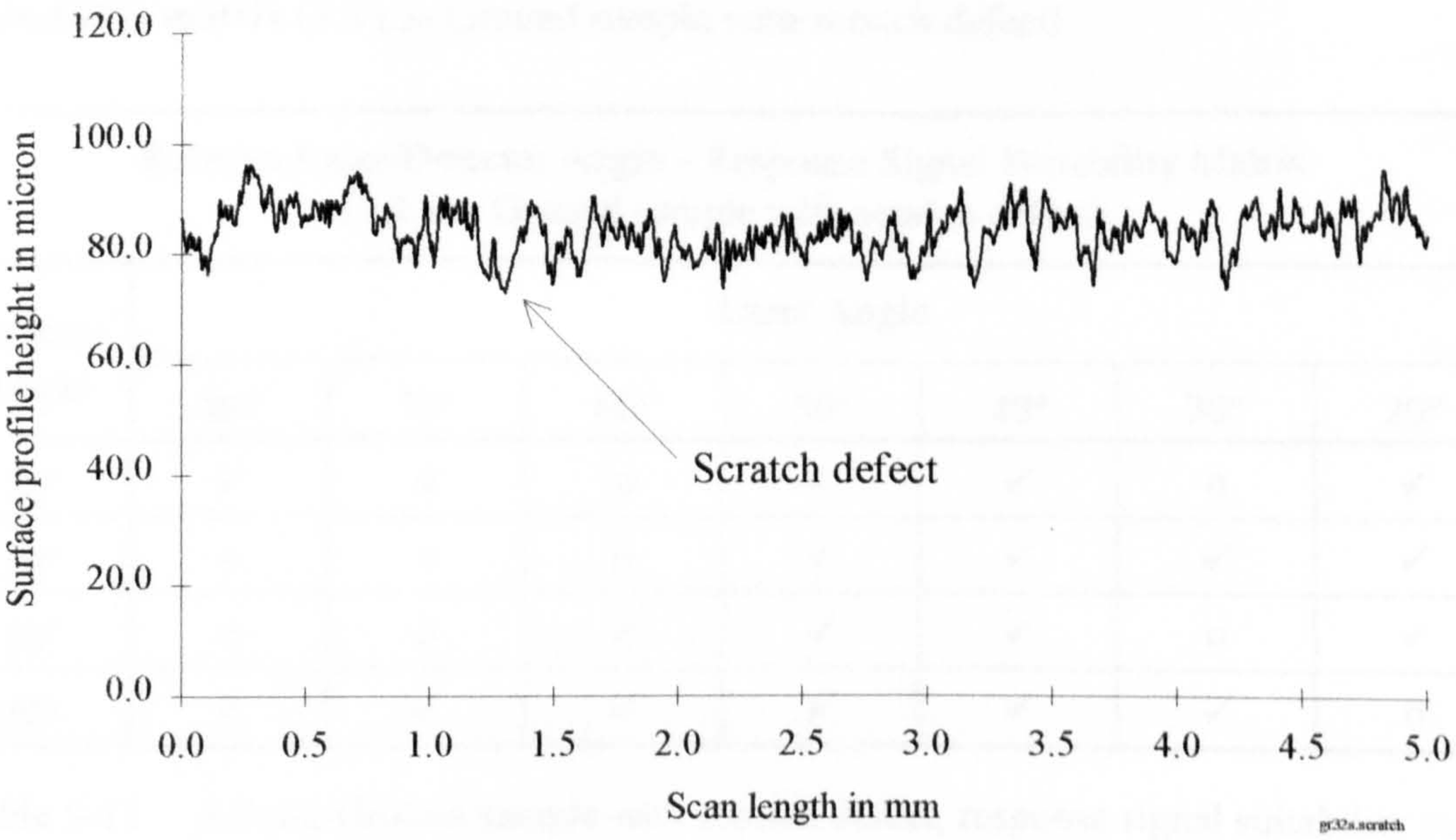

Figure 5-69 3.2 μm Ground sample with scratch defect, surface profile

Discussion of results (3.2 μm Ground sample with scratch defect)

The scratch defect is clearly apparent in each of the four groups of graphical data (figures 5-70 to 5-74). The scratch seen to centre on 2 mm is most pronounced for the shallower laser angles in each case. For a consistent image angle of 100° - 110° the best results are obtained for scratch defect detection, under the applied test conditions. It can be seen that for angles less than this, general trends and undulations in the basic signal could give rise to false defect detection triggering. This situation is illustrated in figure 5-70 with a laser angle of 60° where four distinct spikes in the signal are evident. It should be noted that the scratch is of a similar order to the surface marks produced during the grinding process, see figure 5-69. Thus defect detection and discrimination from the general surface signal understandably presented difficulties for certain configurations.

Further testing is necessary in an attempt to optimise the system configuration when applied to this type and grade of surface defect. The laser spot size is thought to exert a major influence, due to its integrating nature. A reduced laser spot size would offer more sensitivity towards small scale variations like the scratch defect and less towards gradual variations like the watermarks.

Suitability matrix (3.2 μm Ground sample with scratch defect)

Relative Laser/Detector Angle - Response Signal Suitability Matrix (3.2 μm Ground sample with scratch defect)							
Detector Angle	Laser Angle						
	80°	70°	60°	50°	40°	30°	20°
20°	✓	o	o	o	✓	o	✓
30°	o	o	o	✓	✓	✓	✓
40°	o	o	✓	✓	✓	o	✓
50°	o	✓	✓	✓	✓	✓	o

Table 5-11 3.2 μm Ground sample with scratch defect, response signal suitability matrix

Graphical results (3.2 μm Ground sample with scratch defect)

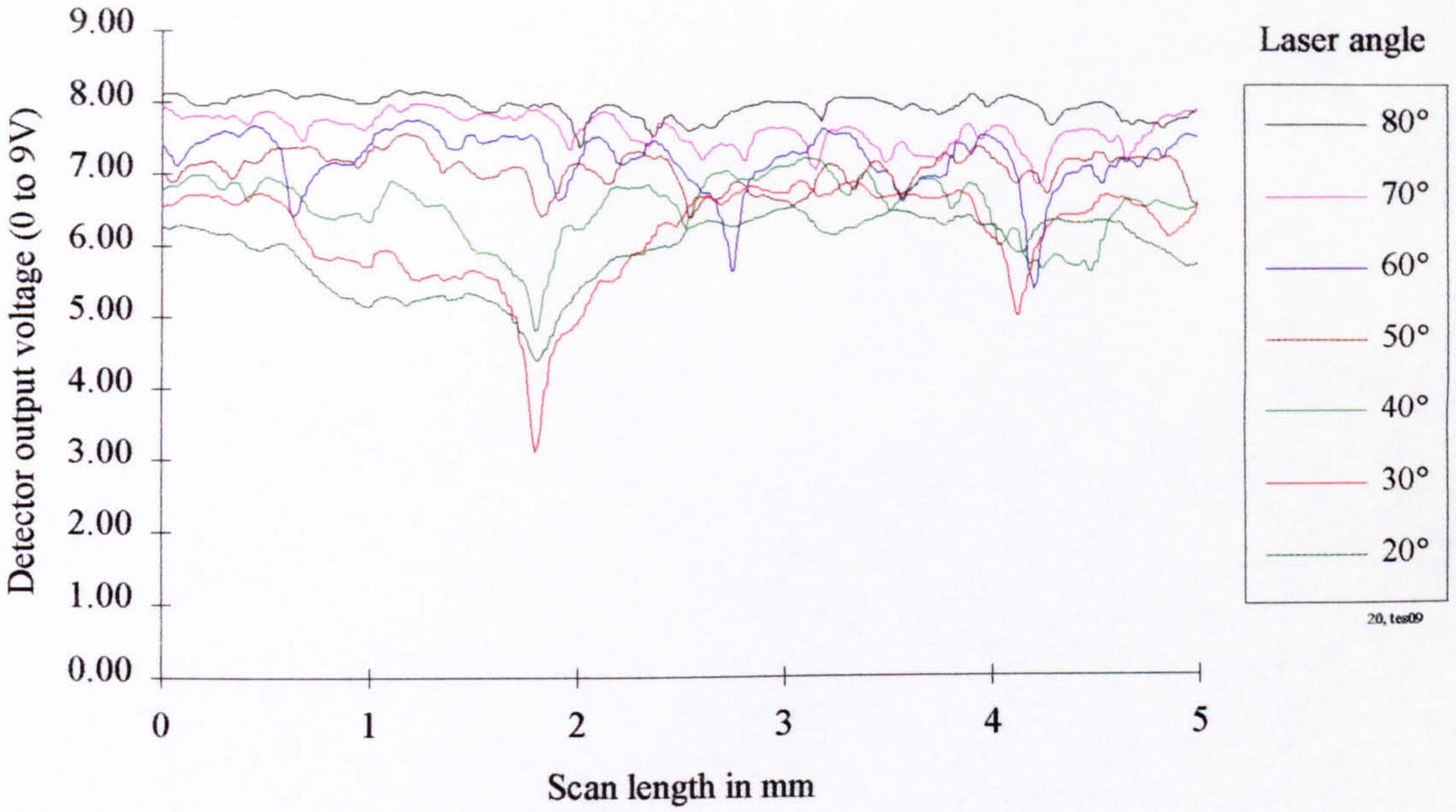

Figure 5-70 3.2 μm Ground sample with scratch defect and fixed detector angle of 20°

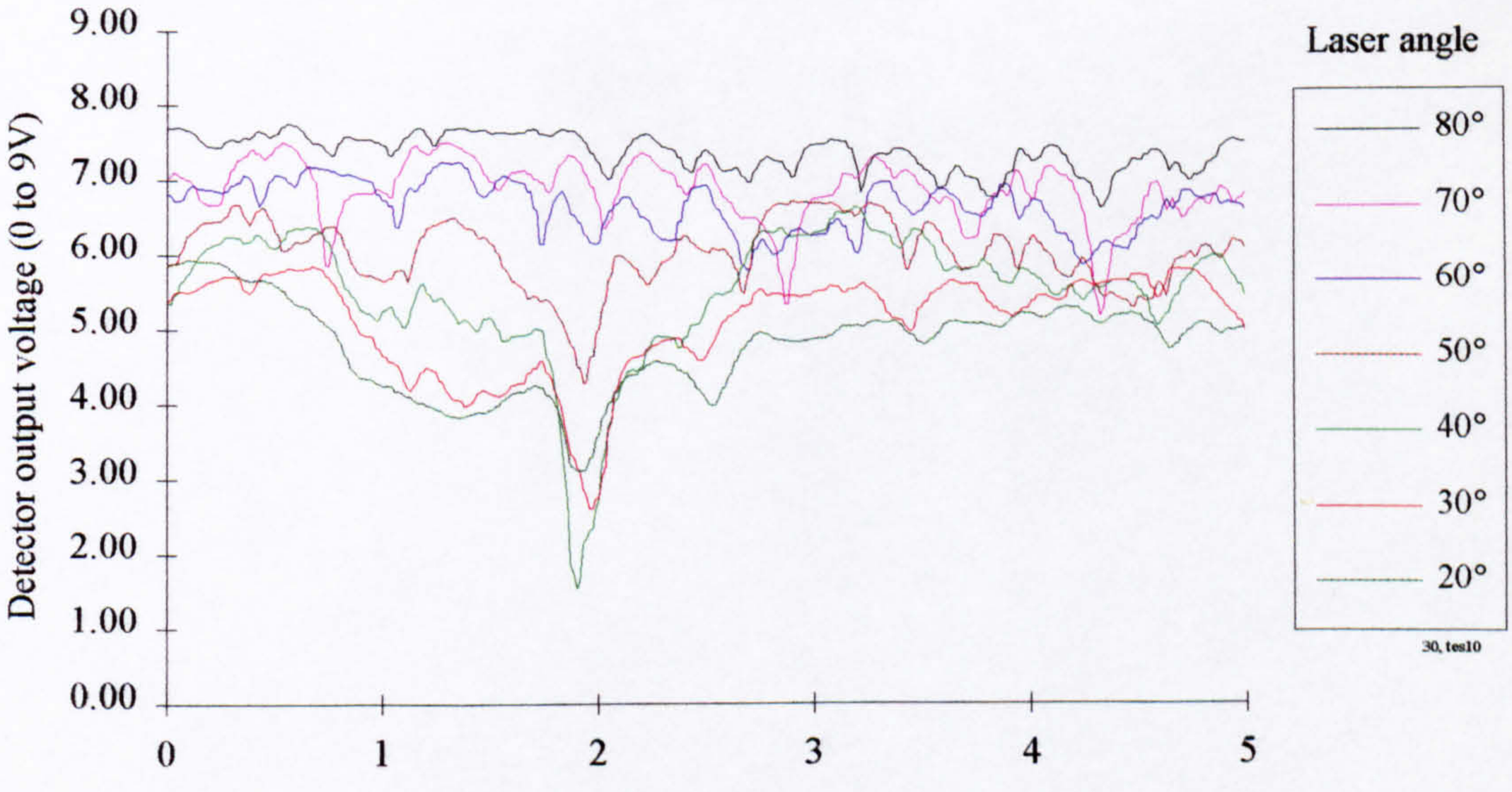

Figure 5-71 3.2 μm Ground sample with scratch defect and fixed detector angle of 30°

Graphical results continued (3.2 μm Ground sample with scratch defect)

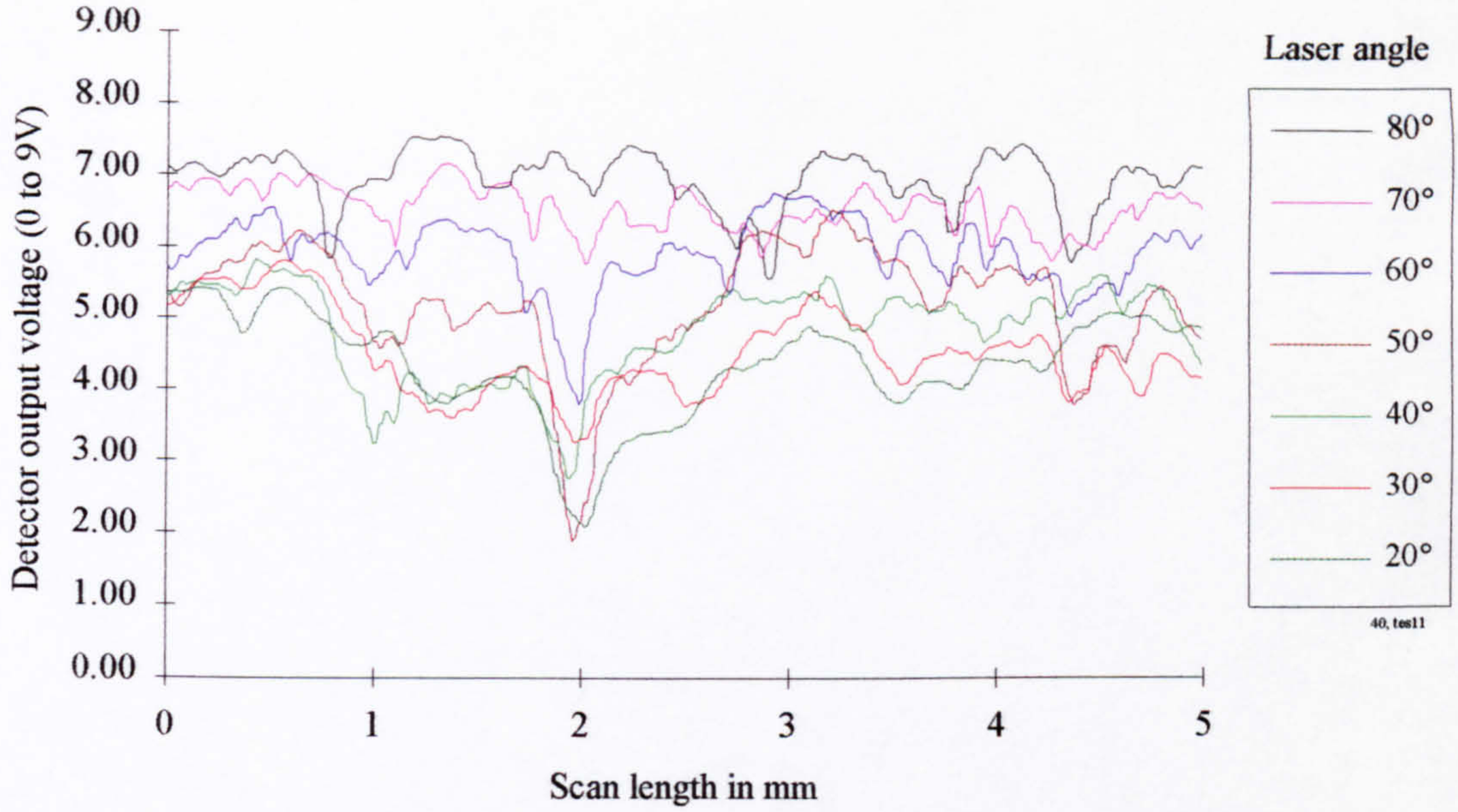

Figure 5-72 3.2 μm Ground sample with scratch defect and fixed detector angle of 40°

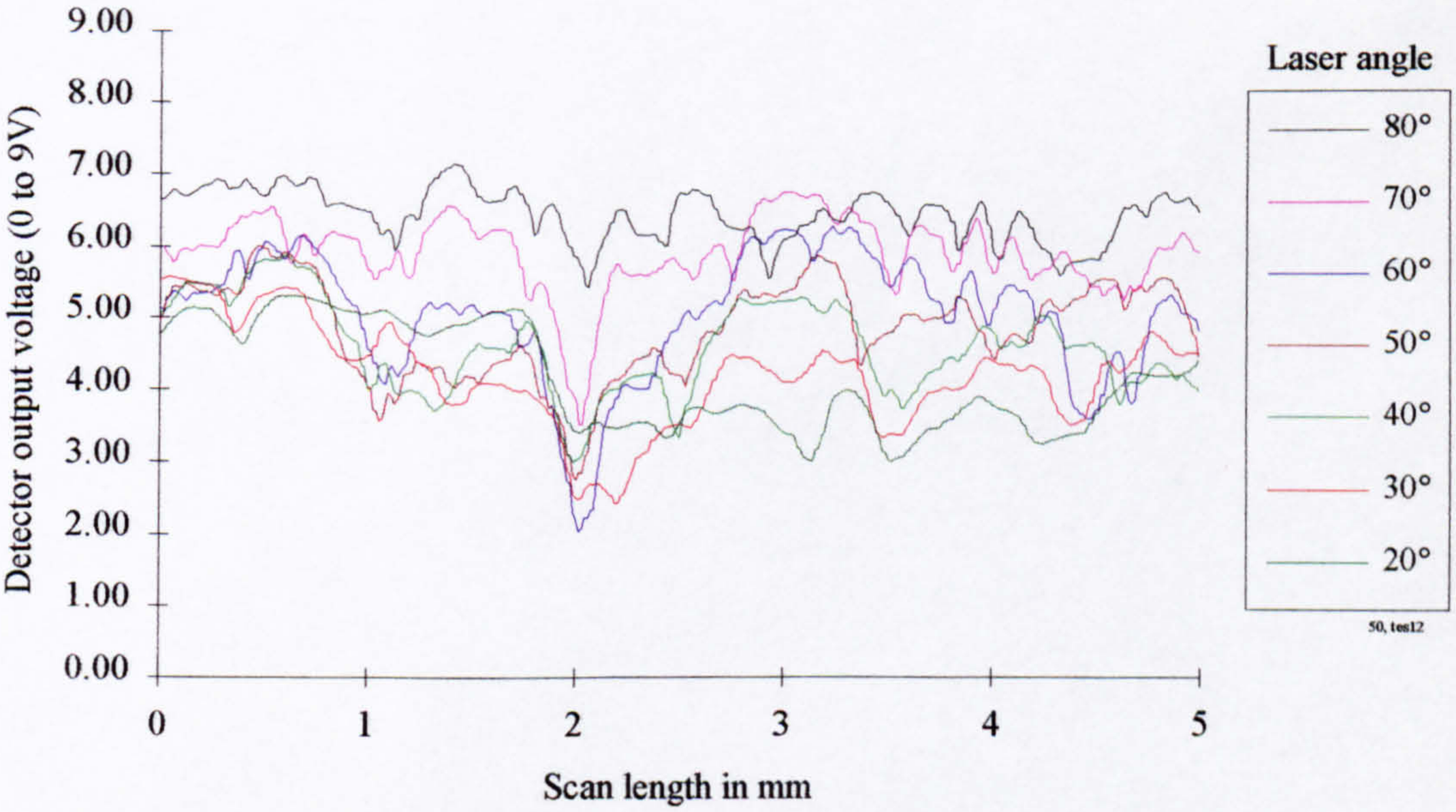

Figure 5-73 3.2 μm Ground sample with scratch defect and fixed detector angle of 50°

3.2 μm Ground control sample with built-up edge (BUE) defect

Photograph of inspected surface (3.2 μm Ground sample with BUE defect)

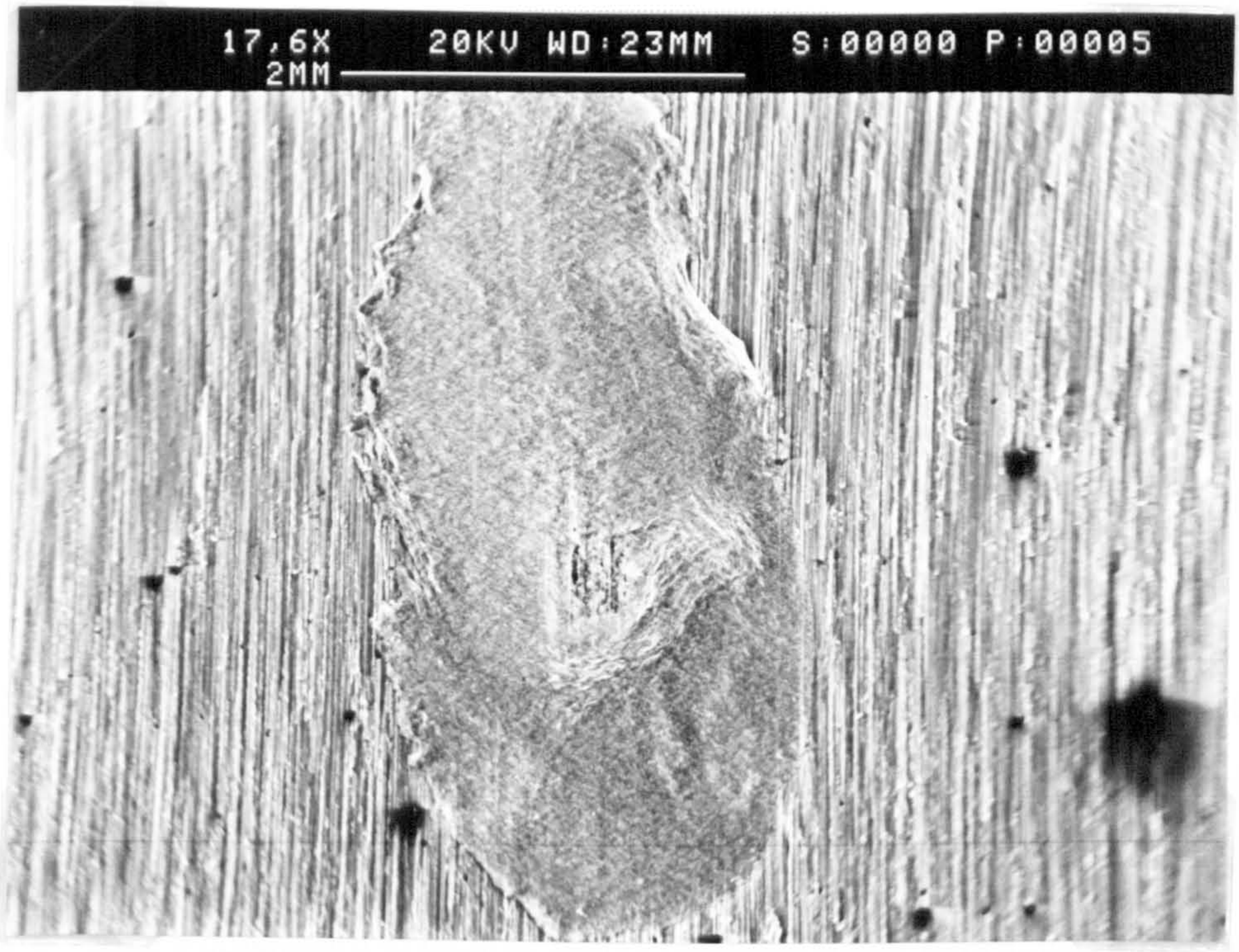

Figure 5-74 3.2 μm Ground sample with BUE defect, surface photograph

Surface topography trace (3.2 μm Ground sample with BUE defect)

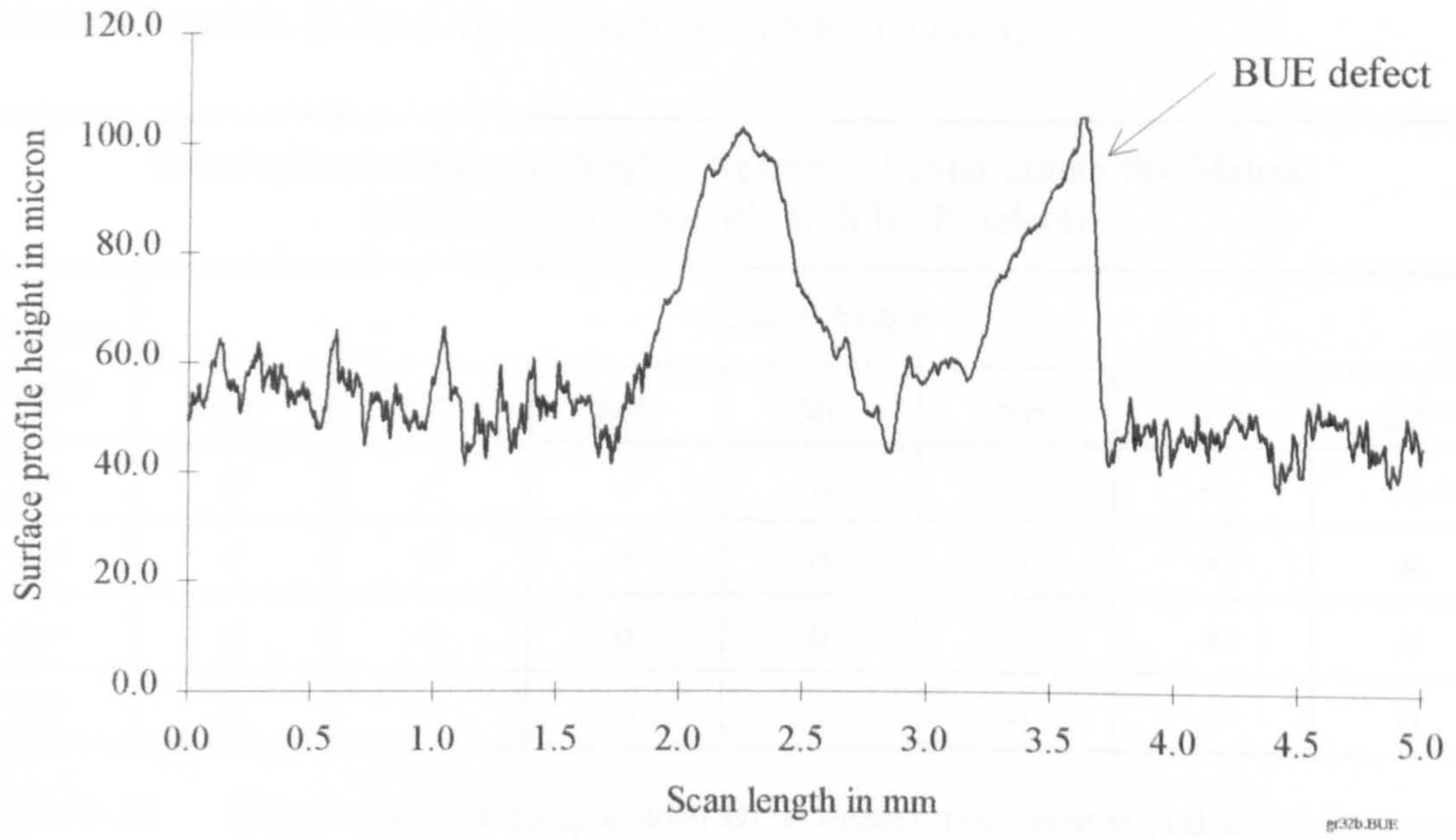

Figure 5-75 3.2 μm Ground sample with BUE defect, surface profile

Discussion of results (3.2 μm Ground sample with BUE defect)

The pronounced effect of the built up edge is apparent in all of the test results across the four figures (5-76 to 5-79). The fuller form results are obtained for shallow detector angles particularly 20° and 30°. The double peak form of the defect which is apparent in the surface topography trace (figure 5-75) is also evident in many of the response signals, for consistent image angles of 110° or greater. A distinct change in response signal is also seen to occur for consistent image angles of typically 100° and less. The general shape of the defect signal transforms from a double to a single peak response. Furthermore the peak centre shifts. It is considered that this is due to shadowing or a related effect.

The BUE defect produces a decrease in light level at the detector. As a consequence the response signal is seen to rise in each case at the site of the BUE. This situation applies to all BUE defects encountered during this program of work. In contrast the scratch defects tended to produce a downward extending defect response signal indicating an increased level of light at the detector.

Suitability matrix (3.2 μm Ground sample with BUE defect)

Relative Laser/Detector Angle - Response Signal Suitability Matrix (3.2 μm Ground sample with BUE defect)							
Detector Angle	Laser Angle						
	80°	70°	60°	50°	40°	30°	20°
20°	✓	✓	✓	o	o	o	×
30°	✓	o	o	o	o	×	×
40°	o	o	o	o	o	×	×
50°	o	o	o	o	o	o	o

Table 5-12 3.2 μm Ground sample with BUE defect, response signal suitability matrix

Graphical results (3.2 μm Ground sample with BUE defect)

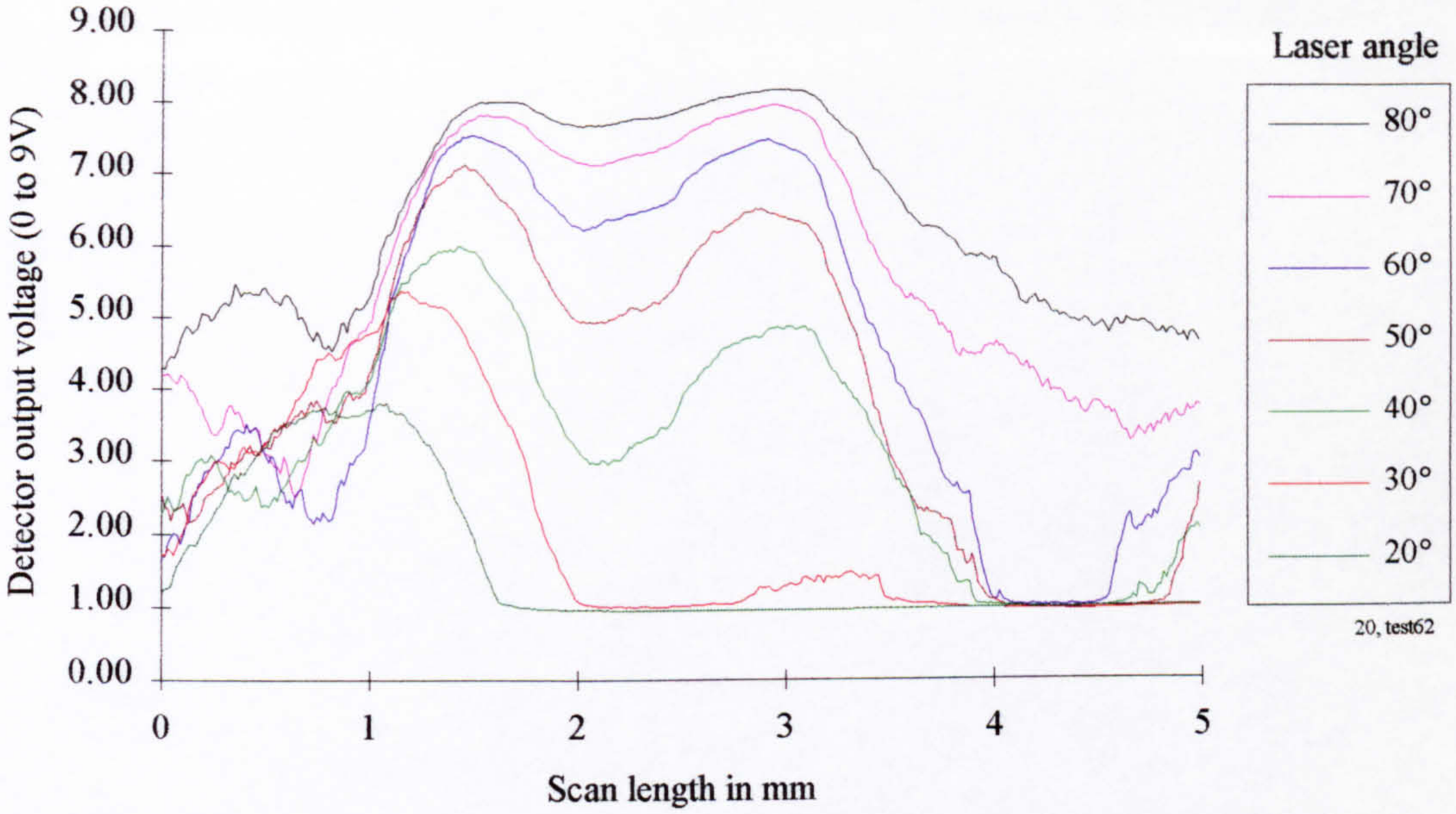

Figure 5-76 3.2 μm Ground sample with BUE defect and fixed detector angle of 20°

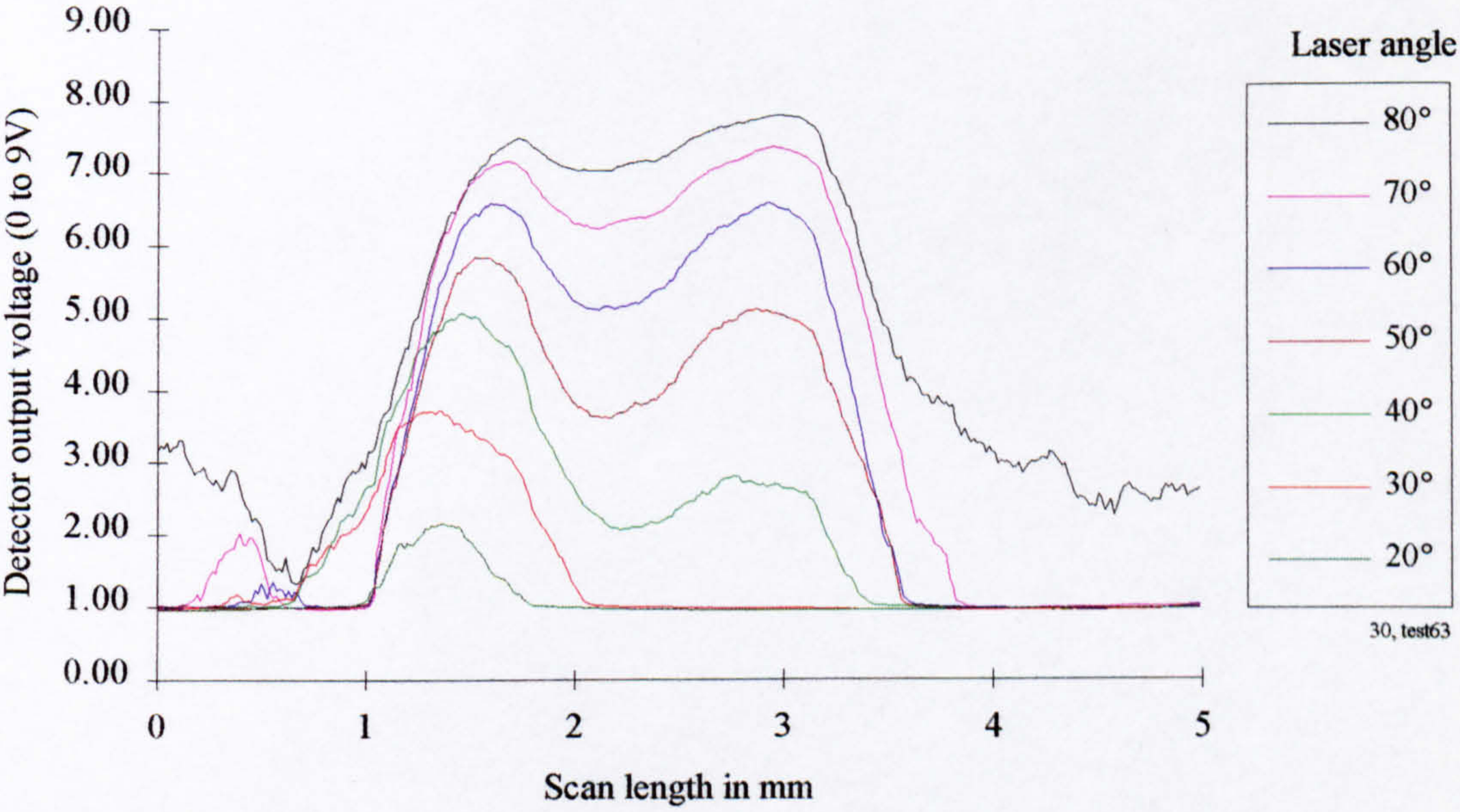

Figure 5-77 3.2 μm Ground sample with BUE defect and fixed detector angle of 30°

Graphical results continued (3.2 μm Ground sample with BUE defect)

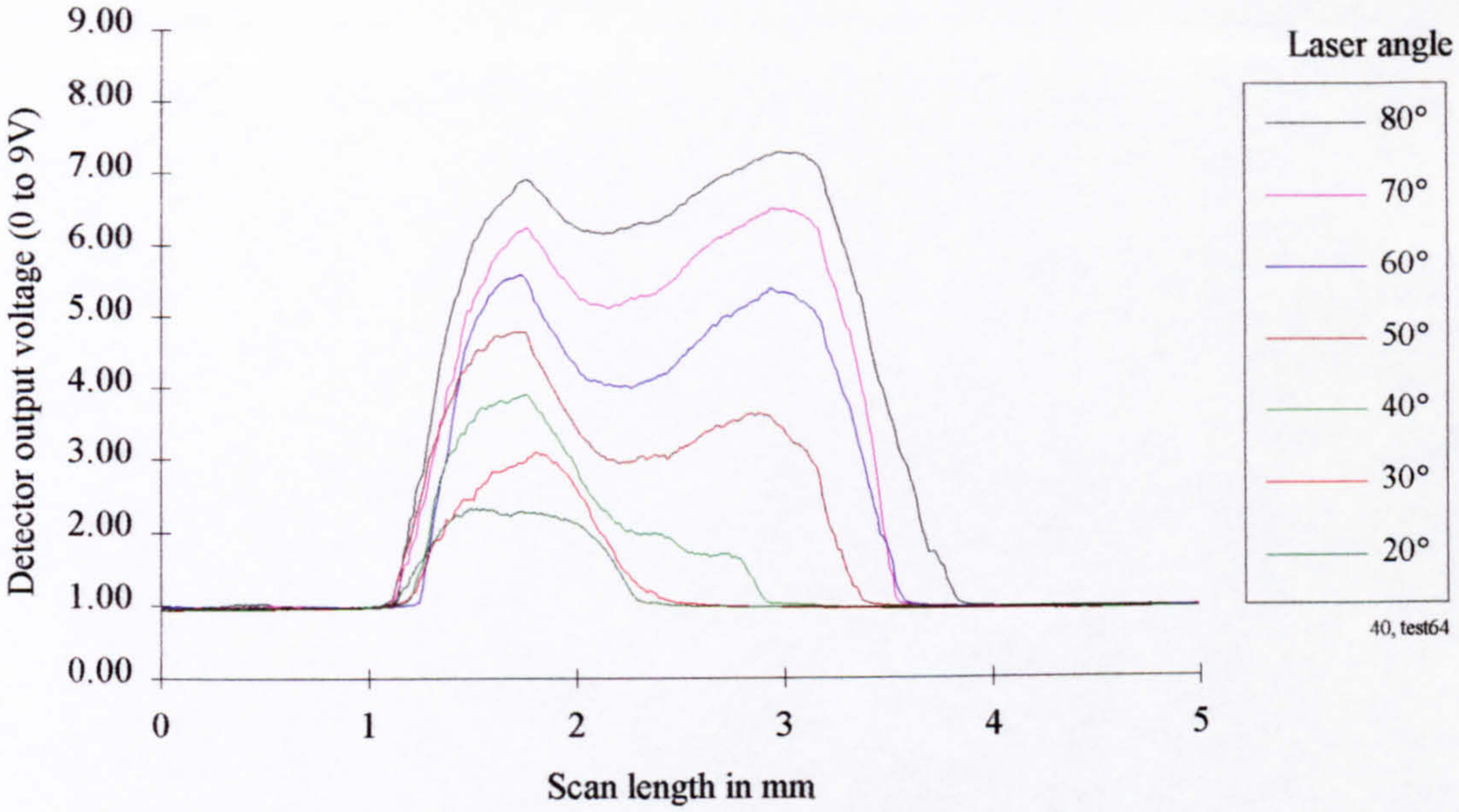

Figure 5-78 3.2 μm Ground sample with BUE defect and fixed detector angle of 40°

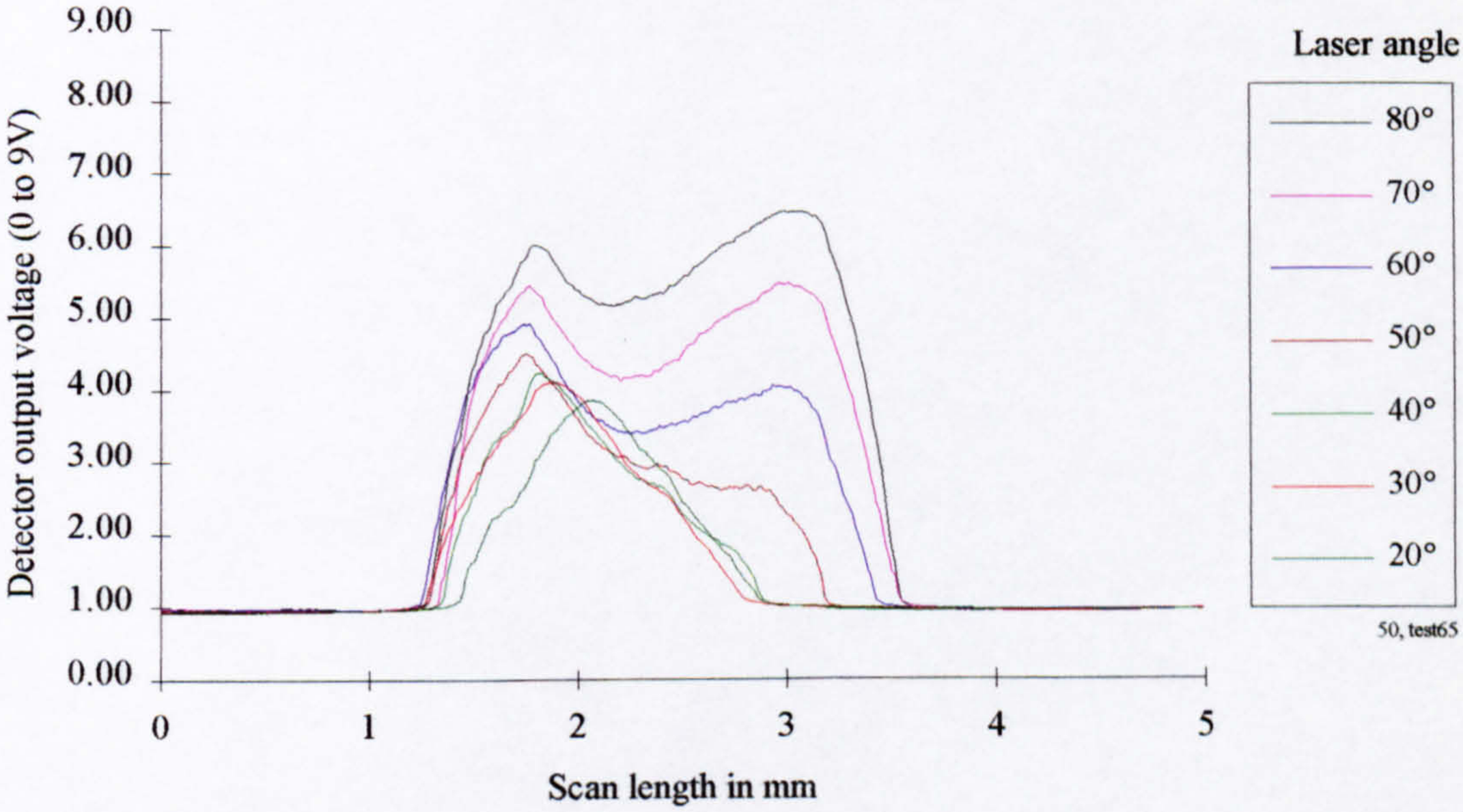

Figure 5-79 3.2 μm Ground sample with BUE defect and fixed detector angle of 50°

3.2 μm Plain shot blast control sample

Photograph of inspected surface (3.2 μm Plain shot blast sample)

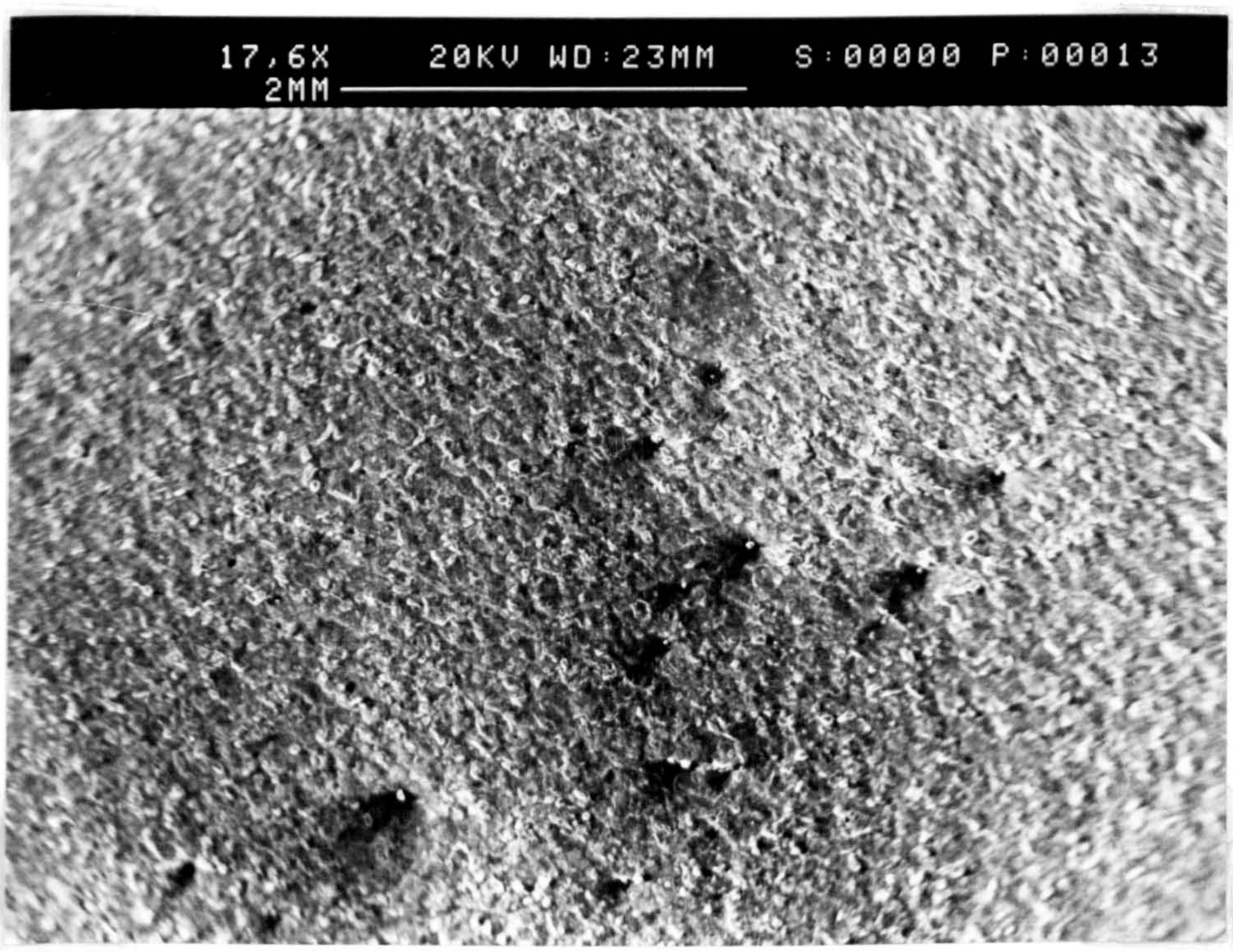

Figure 5-80 3.2 μm Plain shot blast sample, surface photograph

Surface topography trace (3.2 μm Plain shot blast sample)

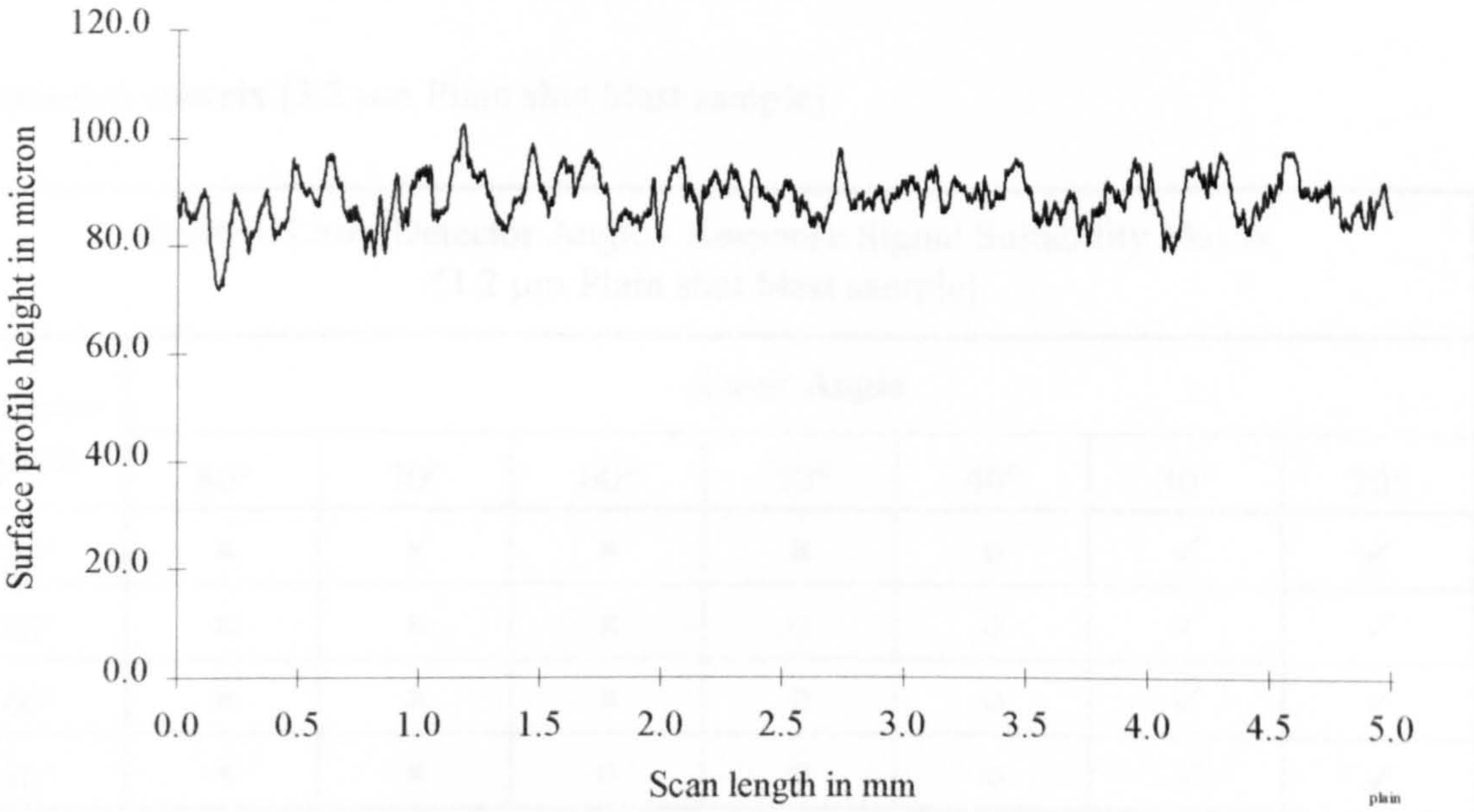

Figure 5-81 3.2 μm Plain shot blast sample, surface profile

Discussion of results (3.2 μm Plain shot blast sample)

The results shown in figures 5-82 to 5-85 represent the response signals acquired during tests on 3.2 μm plain shot blast samples. The results are summarised in the table below.

The pitted surface of the plain shot blast sample produces a spread of results which has a degree of contrast to those already presented for other surface textures. This is made apparent by the two vertical columns of ticks running down the right hand side of the table. The results to the left of the table conform with earlier findings - the crosses and naughts being separated by a diagonal line.

It is interesting to note that for a laser angle of 30° a near constant strength of signal is captured for a range of detector angles (20° to 40° inclusive). This signal is suitable for surface interrogation. However, the response signal strength starts to fade as the detector angle exceeds 40°. At a lower incidence (laser) angle the response fades consistently as the detection angle is increased from 20° up to 50°, apparent by the tighter grouping of the response results. Surface form information is contained in the response signal for the range of angles adopted in the tests.

A consistent image angle of 110° or less would produce signals with a degree of encapsulated surface nature/topography information.

Summary matrix (3.2 μm Plain shot blast sample)

Relative Laser/Detector Angle - Response Signal Suitability Matrix
(3.2 μm Plain shot blast sample)

Detector Angle	Laser Angle						
	80°	70°	60°	50°	40°	30°	20°
20°	x	x	x	x	o	✓	✓
30°	x	x	x	o	o	✓	✓
40°	x	x	x	o	o	✓	✓
50°	x	x	o	o	o	✓	✓

Table 5-13 3.2 μm Plain shot blast sample, response signal suitability matrix

Graphical results (3.2 μm Plain shot blast sample)

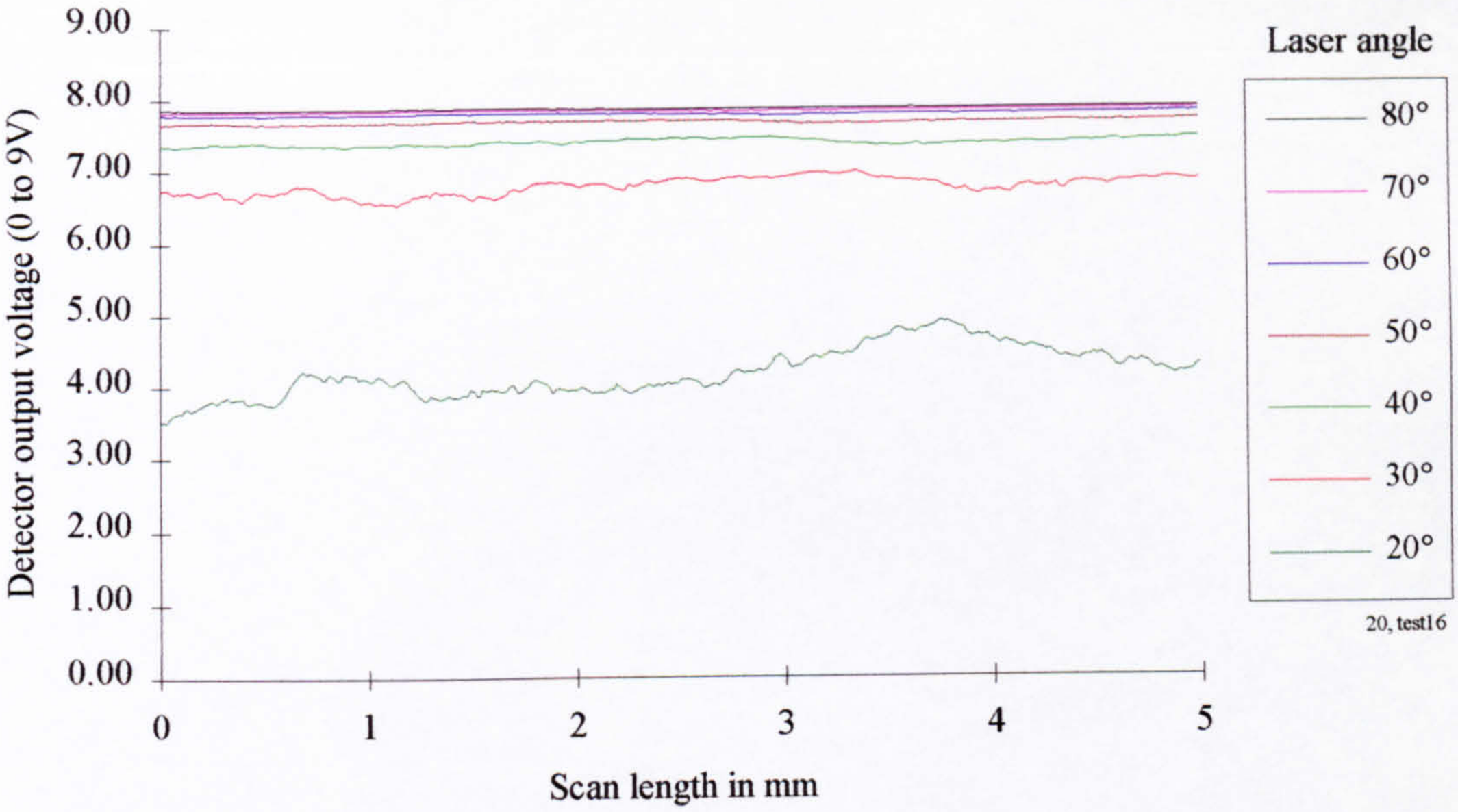

Figure 5-82 3.2 μm Plain shot blast sample with fixed detector angle of 20°

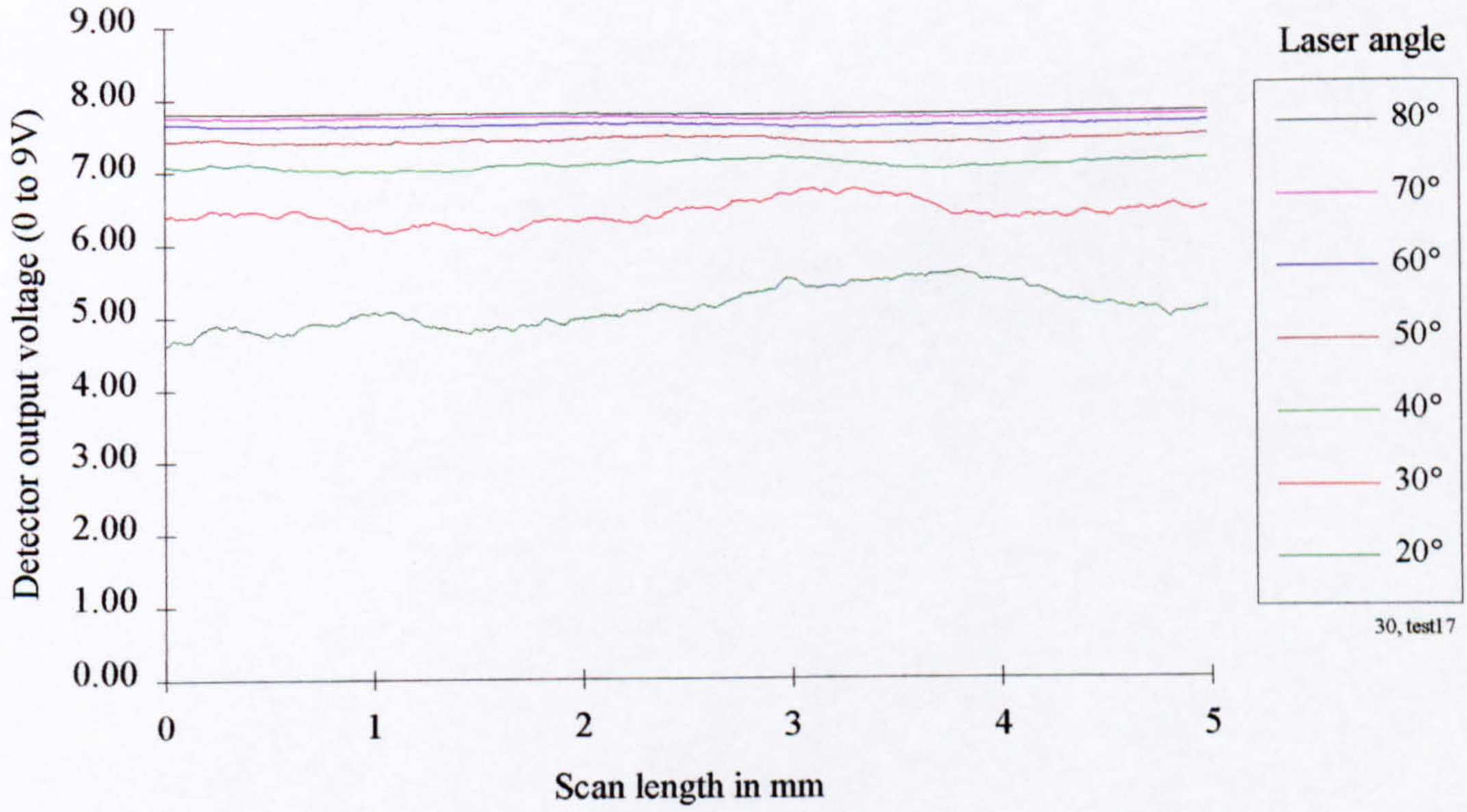

Figure 5-83 3.2 μm Plain shot blast sample with fixed detector angle of 30°

Graphical results continued (3.2 μm Plain shot blast sample)

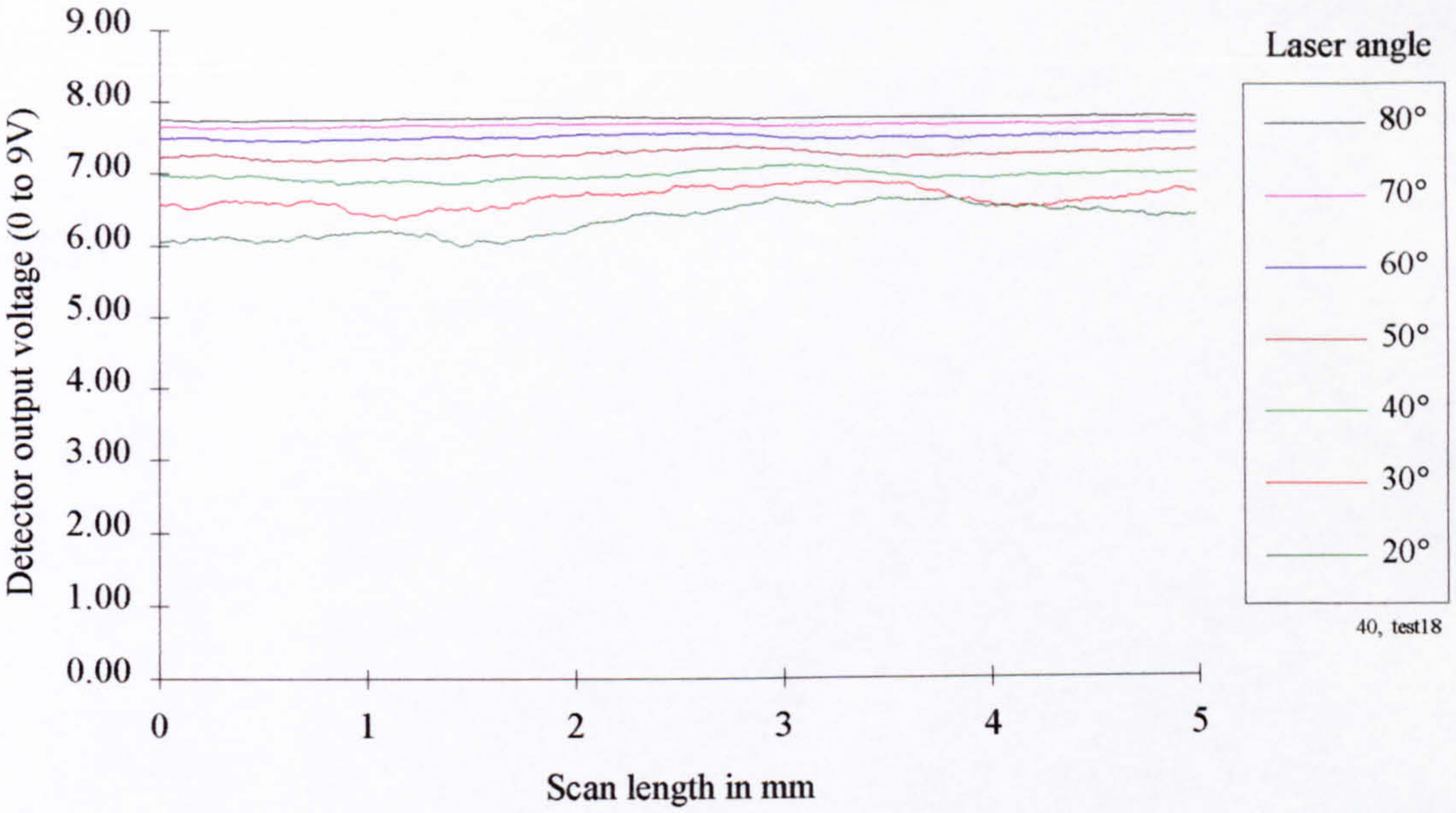

Figure 5-84 3.2 μm Plain shot blast sample with fixed detector angle of 40°

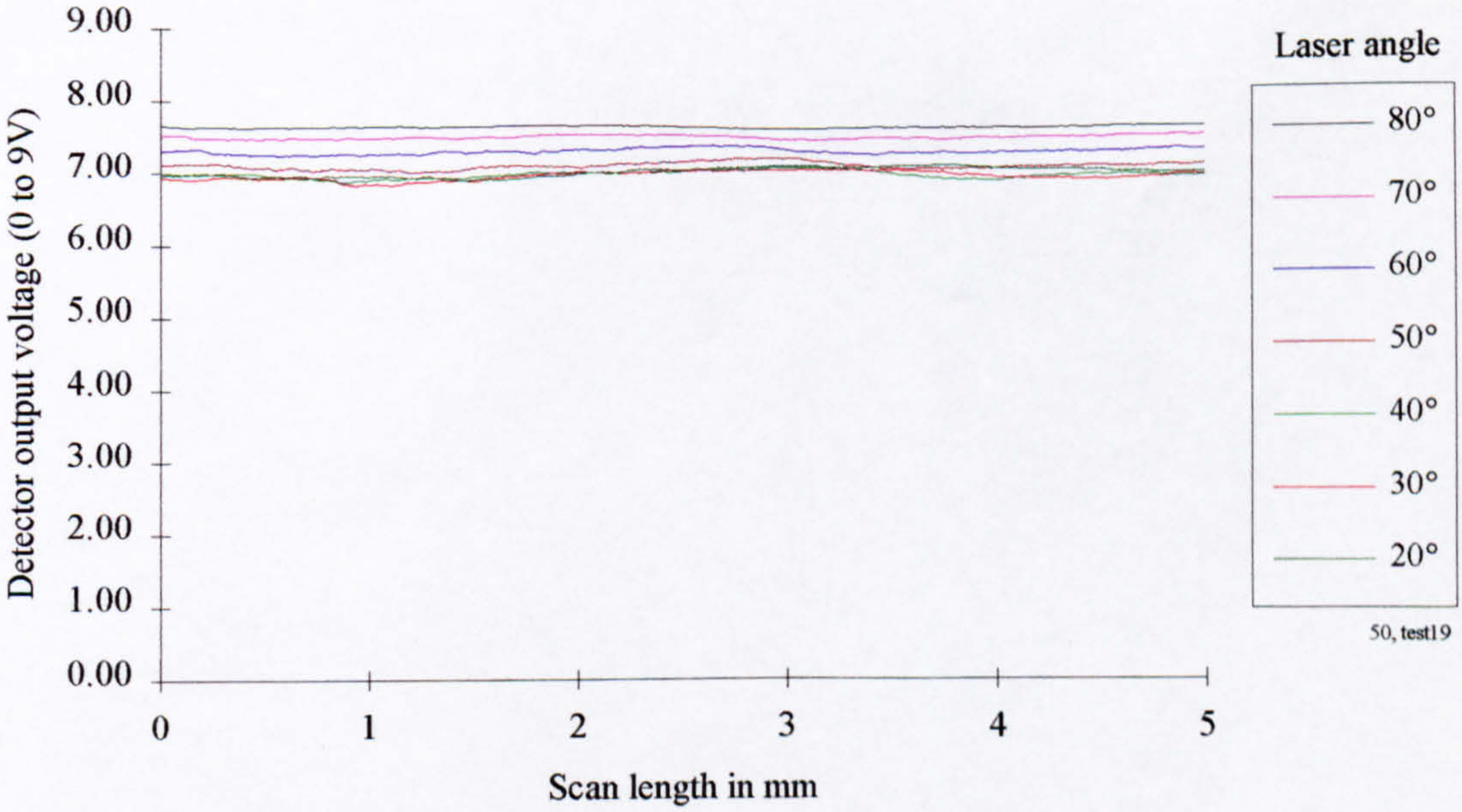

Figure 5-85 3.2 μm Plain shot blast sample with fixed detector angle of 50°

3.2 μm Shot blast control sample with scratch defect

Photograph of inspected surface (3.2 μm Shot blast sample with scratch defect)

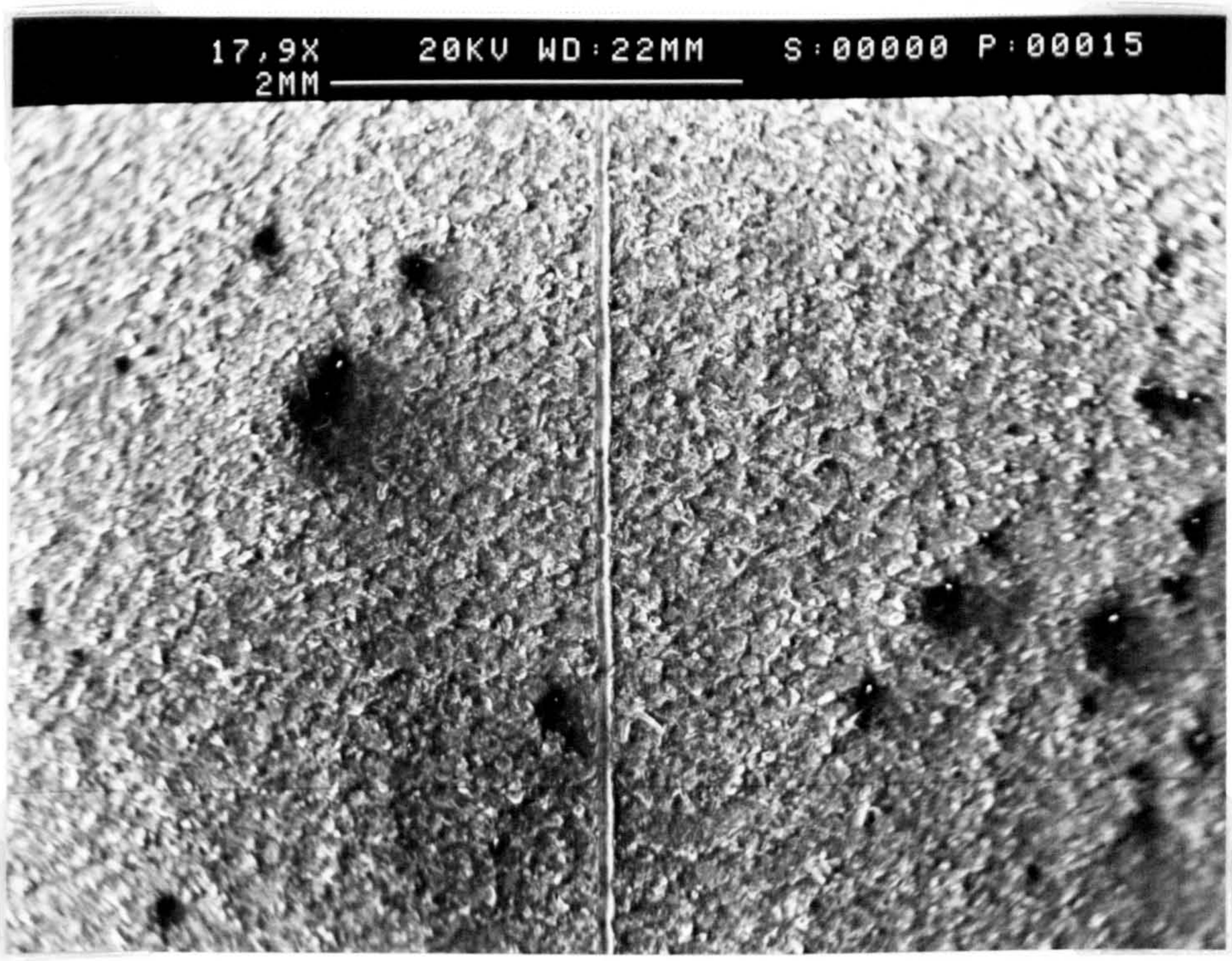

Figure 5-86 3.2 μm Shot blast sample with scratch defect, surface photograph

Surface topography trace (3.2 μm Shot blast sample with scratch defect)

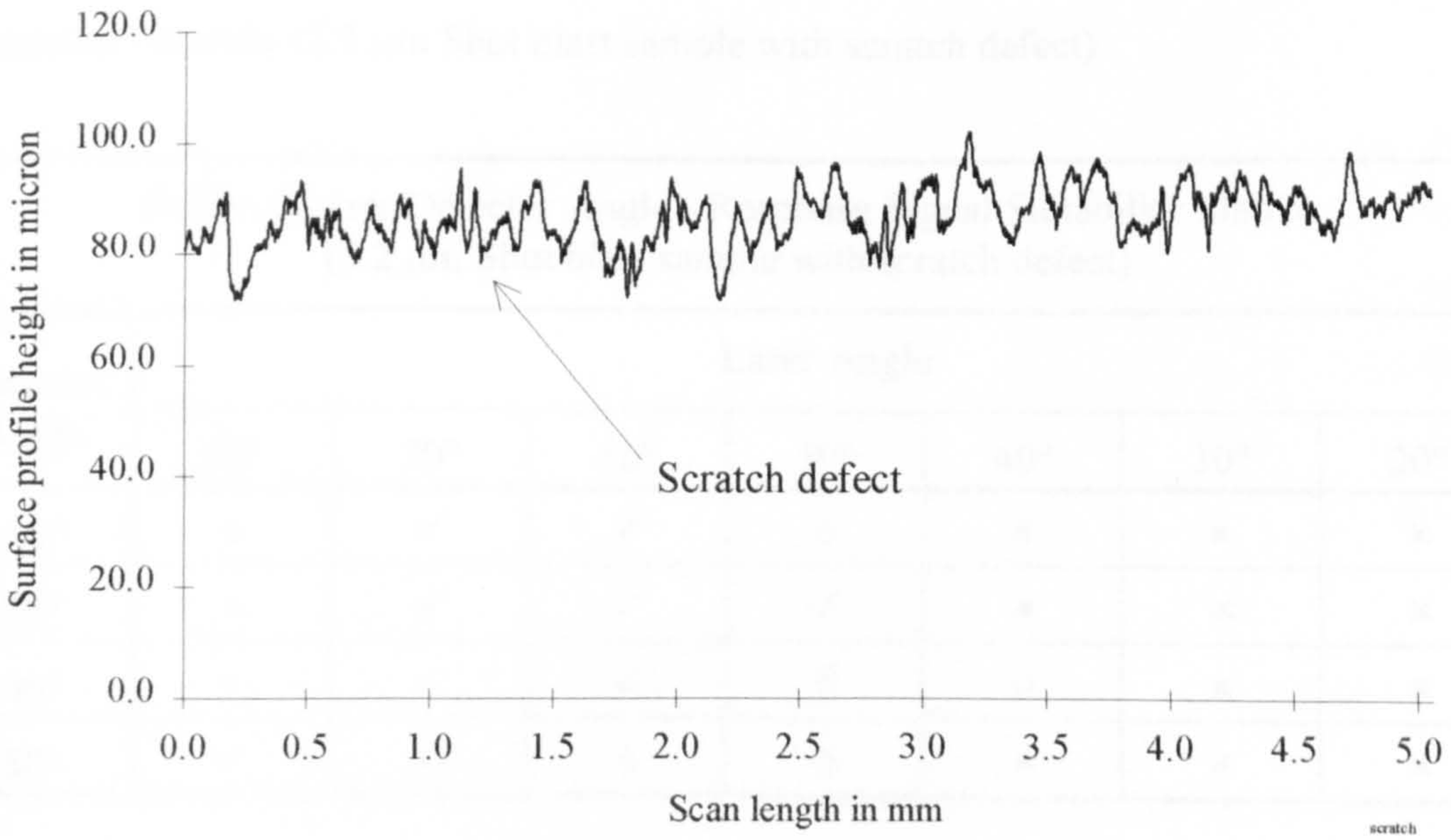

Figure 5-87 3.2 μm Shot blast sample with scratch defect, surface profile

Discussion of results (3.2 μm Shot blast sample with scratch defect)

The summary table below again illustrates the contrasting nature of the shot blast samples to those previously tested. The three columns of crosses which dominate the right hand portion of the tables is intercepted by a single naught. This stray result under-pins a discussion in Chapter 6.0 which suggests a more precise demarcation (quantitative not qualitative) is required to screen the suitable and unsuitable signals.

No general rule seems to exist but a consistent image angle of 130° would produce consistent results with the defect being detectable as well surface information being contained in the response results. Other settings are suitable for detection purposes as can be seen by the graphical and tabulated results. It is worth noting (figure 5-87) that the scratch defect is not significnantly prominent when compared to the general surface topography.

Loss of scratch defect signal for lower laser angles could be due to the laser spot size increasing (an effect produced as the laser angle decreases). Further tests should be carried out using a smaller and perhaps more appropriate spot size. See later test results on spot size optimisation.

Summary matrix (3.2 μm Shot blast sample with scratch defect)

Relative Laser/Detector Angle - Response Signal Suitability Matrix (3.2 μm Shot blast sample with scratch defect)							
Detector Angle	Laser Angle						
	80°	70°	60°	50°	40°	30°	20°
20°	o	✓	✓	o	×	×	×
30°	o	✓	✓	✓	×	×	×
40°	✓	✓	✓	o	o	×	×
50°	✓	✓	o	o	×	×	×

Table 5-14 3.2 μm Shot blast sample with scratch defect, response signal suitability matrix

Graphical results (3.2 μm Shot blast sample with scratch defect)

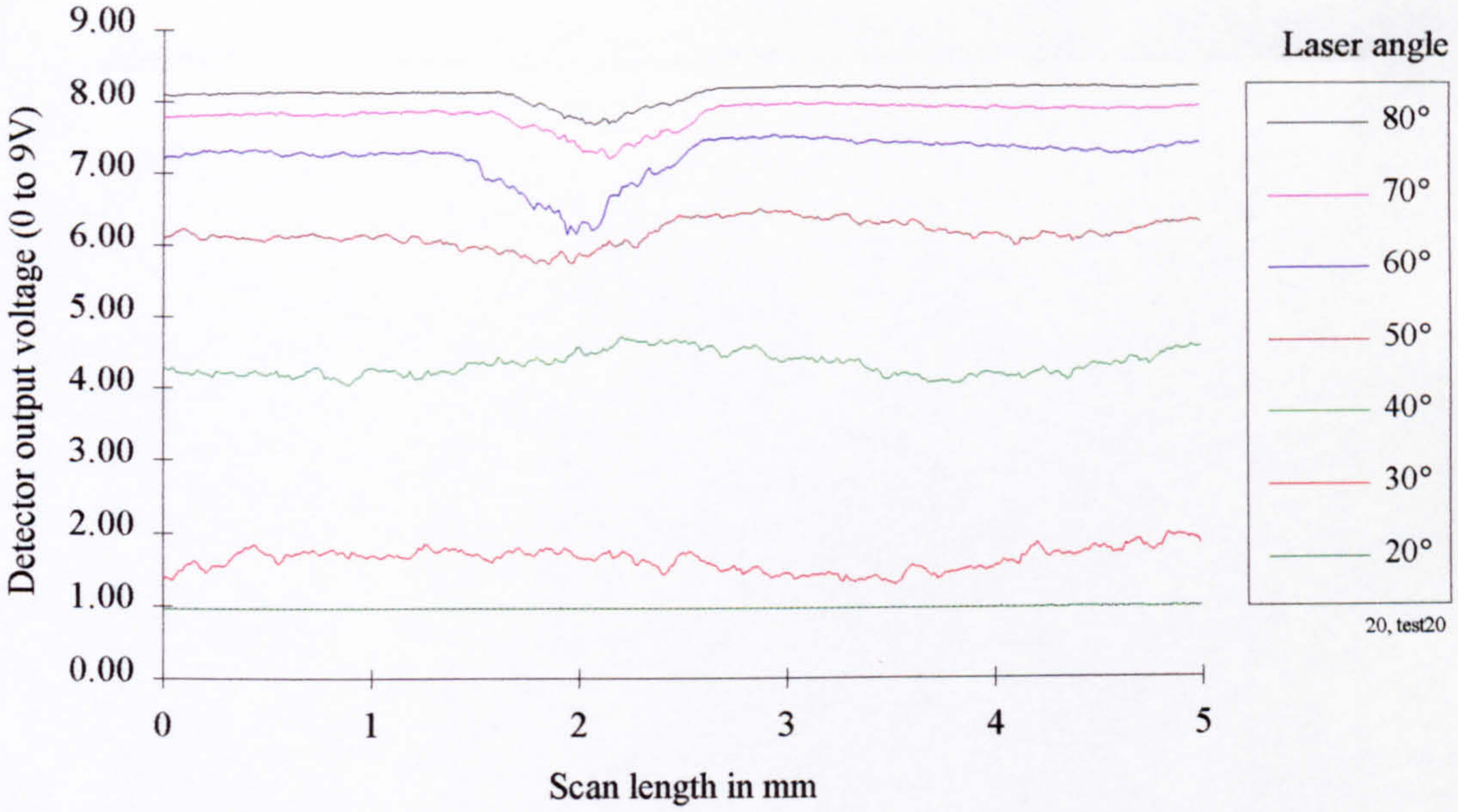

Figure 5-88 3.2 μm Shot blast sample with scratch defect and fixed detector angle of 20°

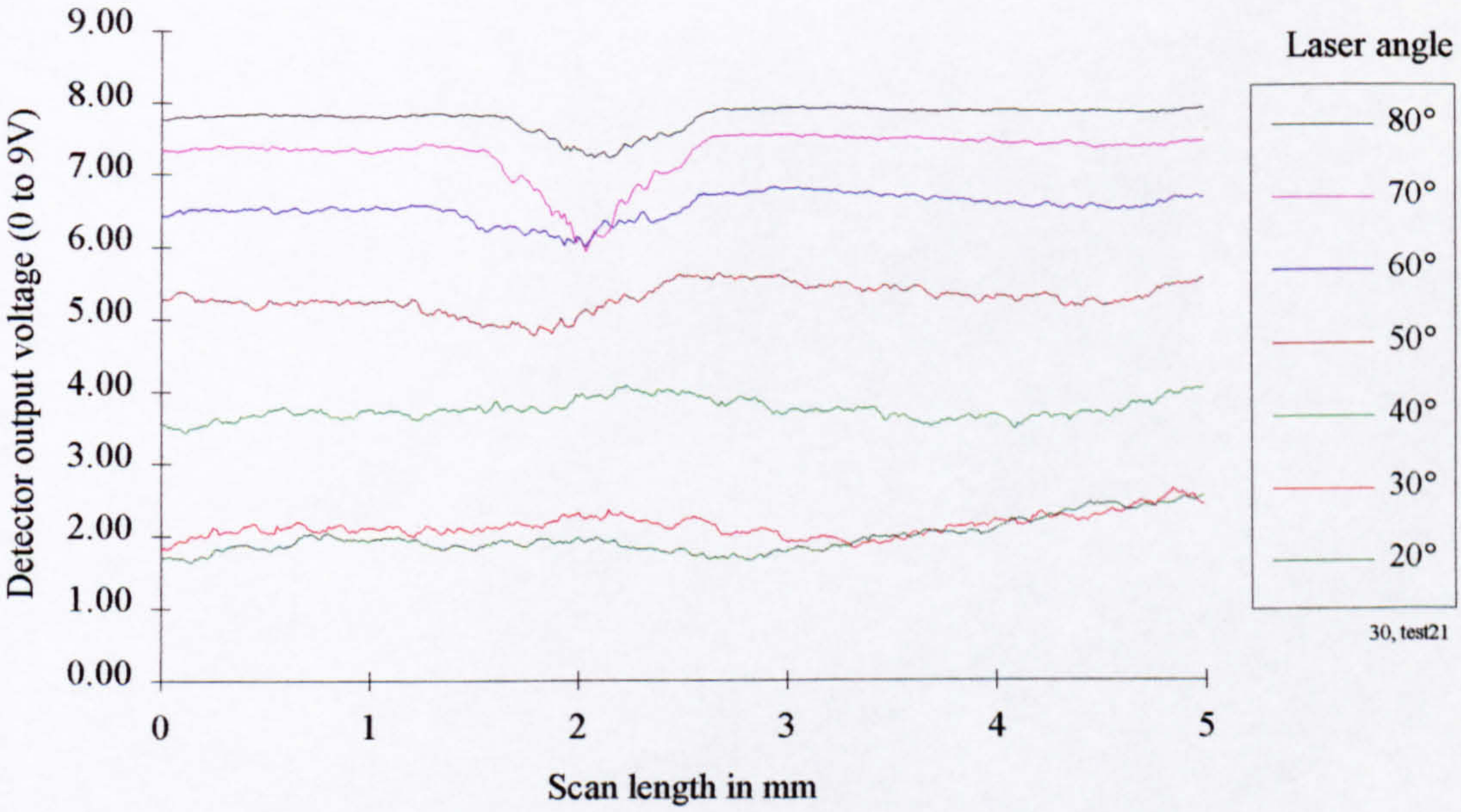

Figure 5-89 3.2 μm Shot blast sample with scratch defect and fixed detector angle of 30°

Graphical results continued (3.2 μm Shot blast sample with scratch defect)

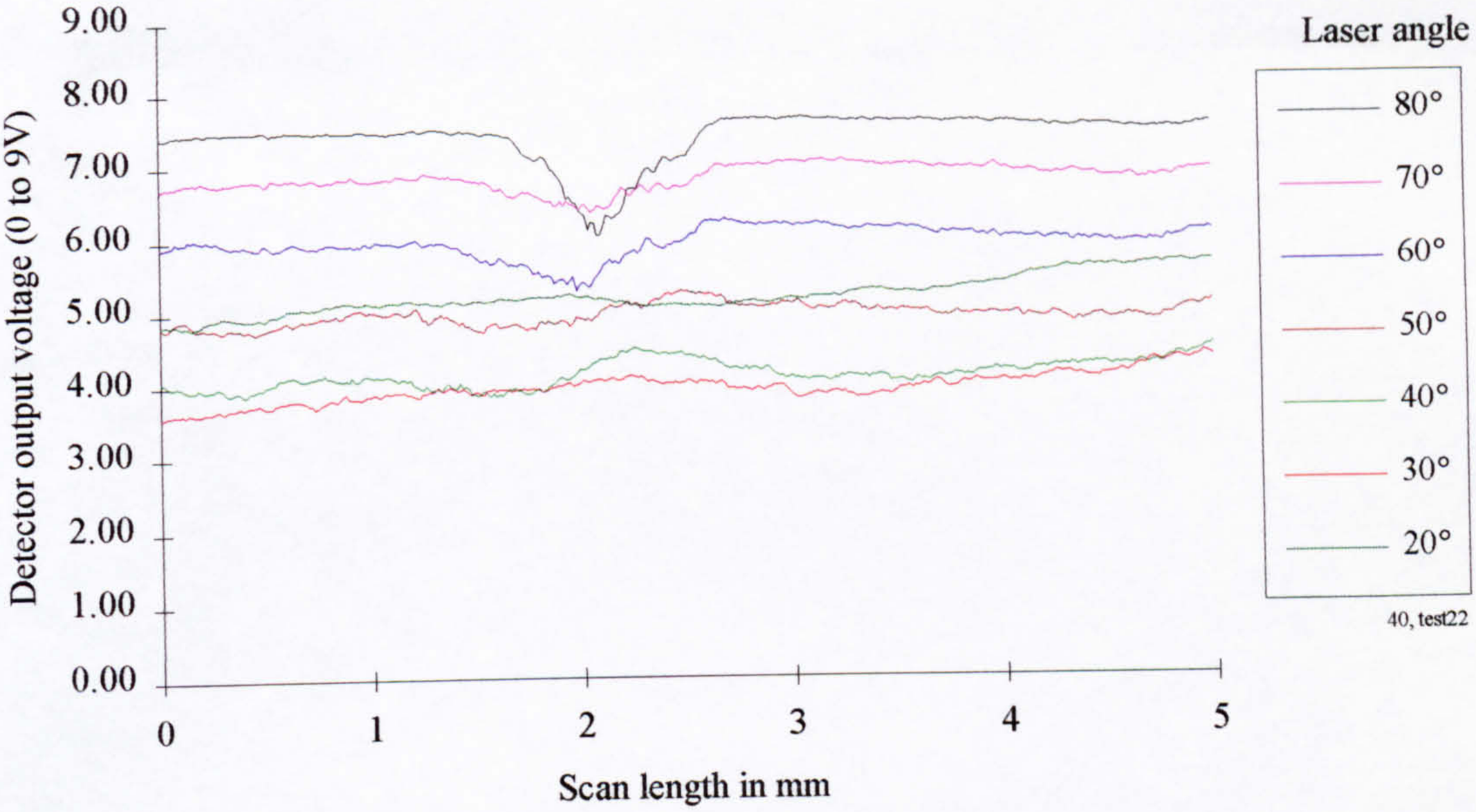

Figure 5-90 3.2 μm Shot blast sample with scratch defect and fixed detector angle of 40°

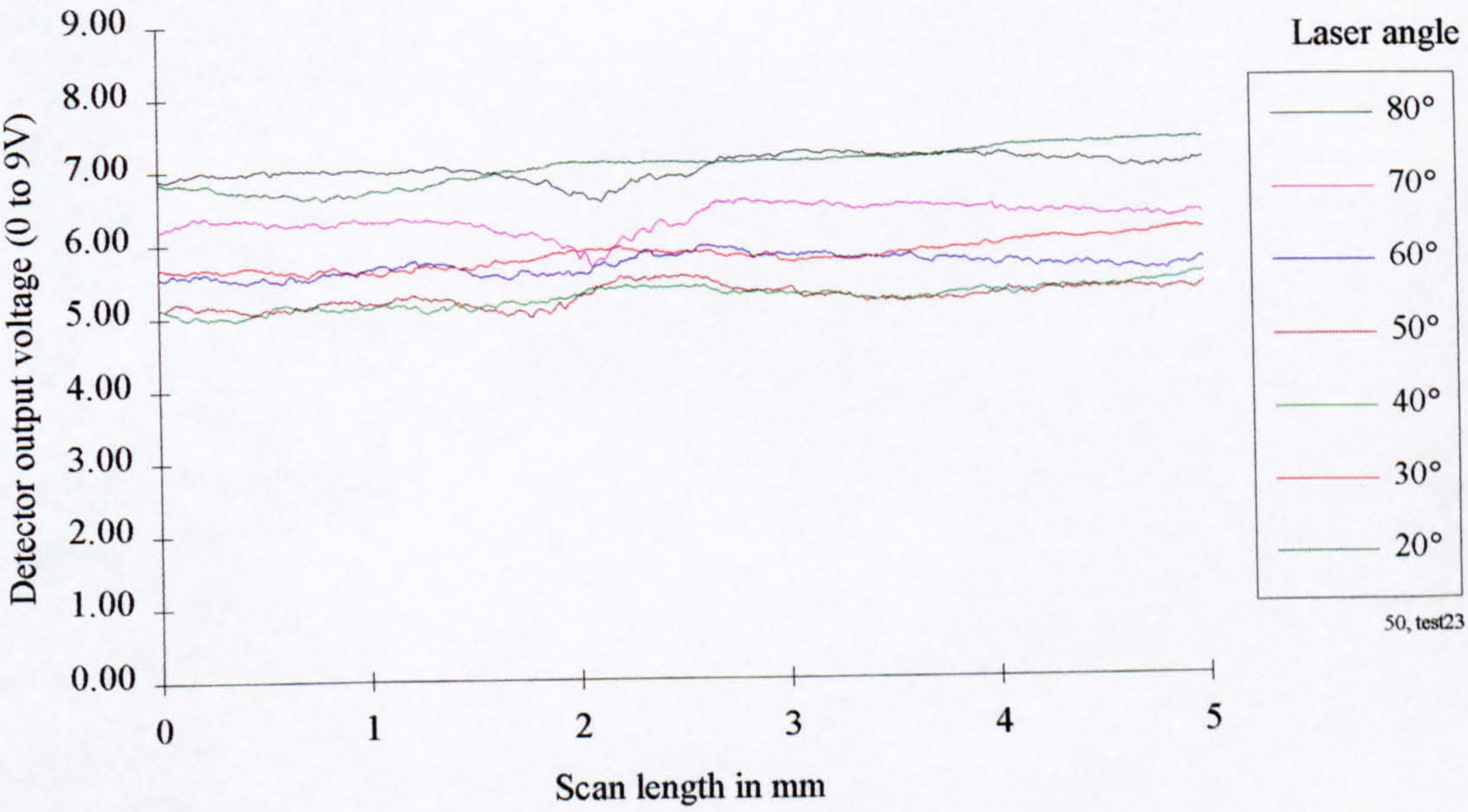

Figure 5-91 3.2 μm Shot blast sample with scratch defect and fixed detector angle of 50°

3.2 μm Shot blast control sample with built-up edge (BUE) defect

Photograph of inspected surface (3.2 μm Shot blast sample with BUE defect)

Figure 5-92 3.2 μm Shot blast sample with BUE defect, surface photograph

Surface topography trace (3.2 μm Shot blast sample with BUE defect)

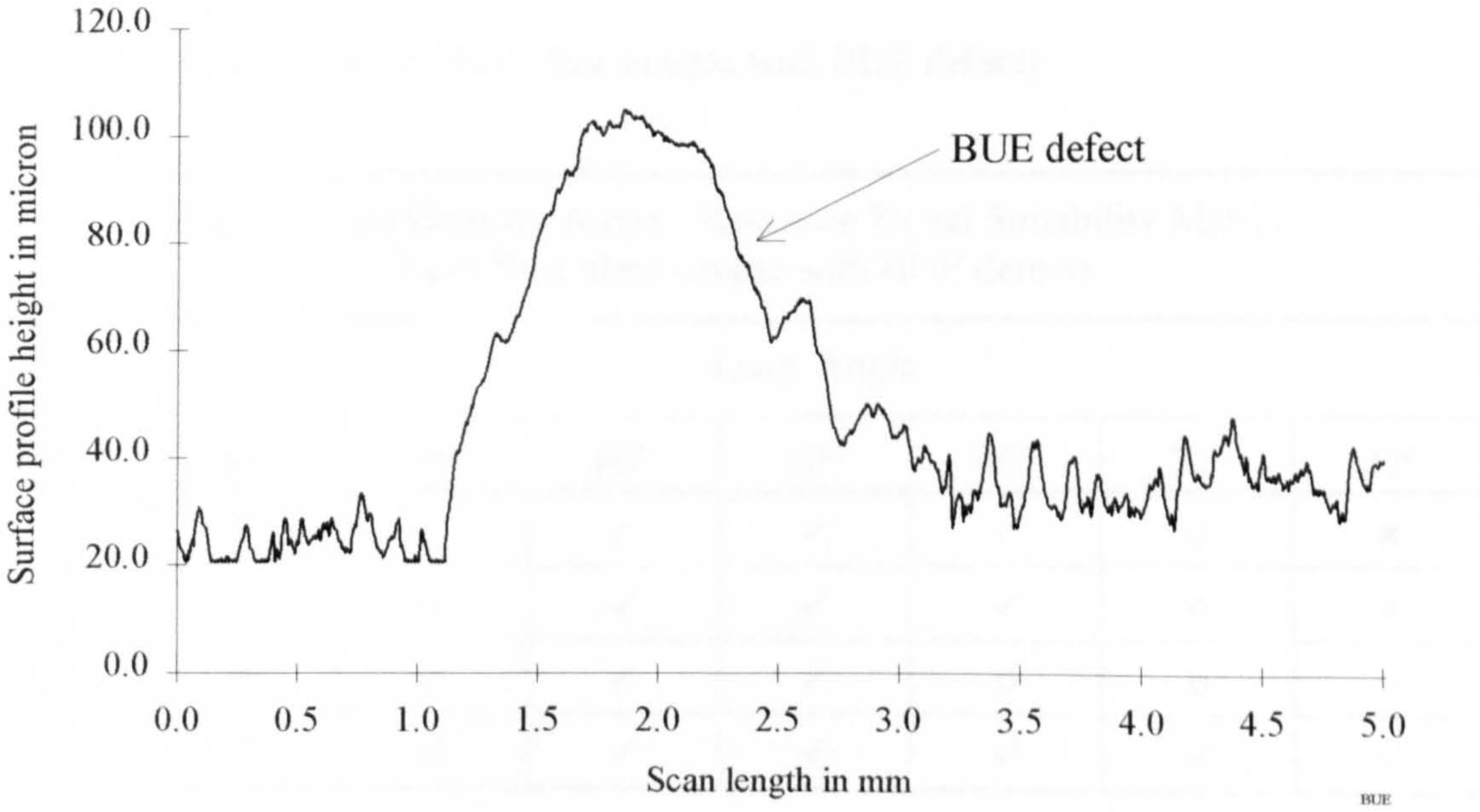

Figure 5-93 3.2 μm Shot blast sample with BUE defect, surface profile

Discussion of results (3.2 μm Shot blast sample with BUE defect)

The well defined graphical results of figures 5-94 to 5-97 which are summarised in the table below correspond with the distinct built up edge (BUE) defect they represent. For a steep detection angle of 50° the entire range of assessed incidence angles produced suitable results (line of ticks along the bottom edge of the summary table). For a reduced detection angle the recognised, regular pattern begins to form across the table array. Thus, for detection angles of 40° and less a consistent image angle of 120° can be used to attain good response results with no detector saturation. However, consistent image angles ranging from 140° down to 100° could be used to good effect when defect detection is the main concern.

The step change in response results apparent in the table below (line of ticks) would make this specimen a suitable candidate for subsequent dual detector tests discussed later in Chapter 6.0. When comparing the tabulated results below with those of Table 5-14 the contrast of the bottom lines (detection angle of 50°) could be used to advantage in distinguishing between scratch and BUE defects. Common laser and detector angles 60° and 30°, respectively, could be used to initially screen the surface for the presence of a defect. Thus minimising the number of laser and detector settings.

Summary matrix (3.2 μm Shot blast sample with BUE defect)

Relative Laser/Detector Angle - Response Signal Suitability Matrix (3.2 μm Shot blast sample with BUE defect)							
Detector Angle	Laser Angle						
	80°	70°	60°	50°	40°	30°	20°
20°	×	o	o	✓	✓	o	×
30°	o	o	✓	✓	✓	o	×
40°	o	✓	✓	✓	o	o	o
50°	✓	✓	✓	✓	✓	✓	✓

Table 5-15 3.2 μm Shot blast sample with BUE defect, response signal suitability matrix

Graphical results (3.2 μm Shot blast sample with BUE defect)

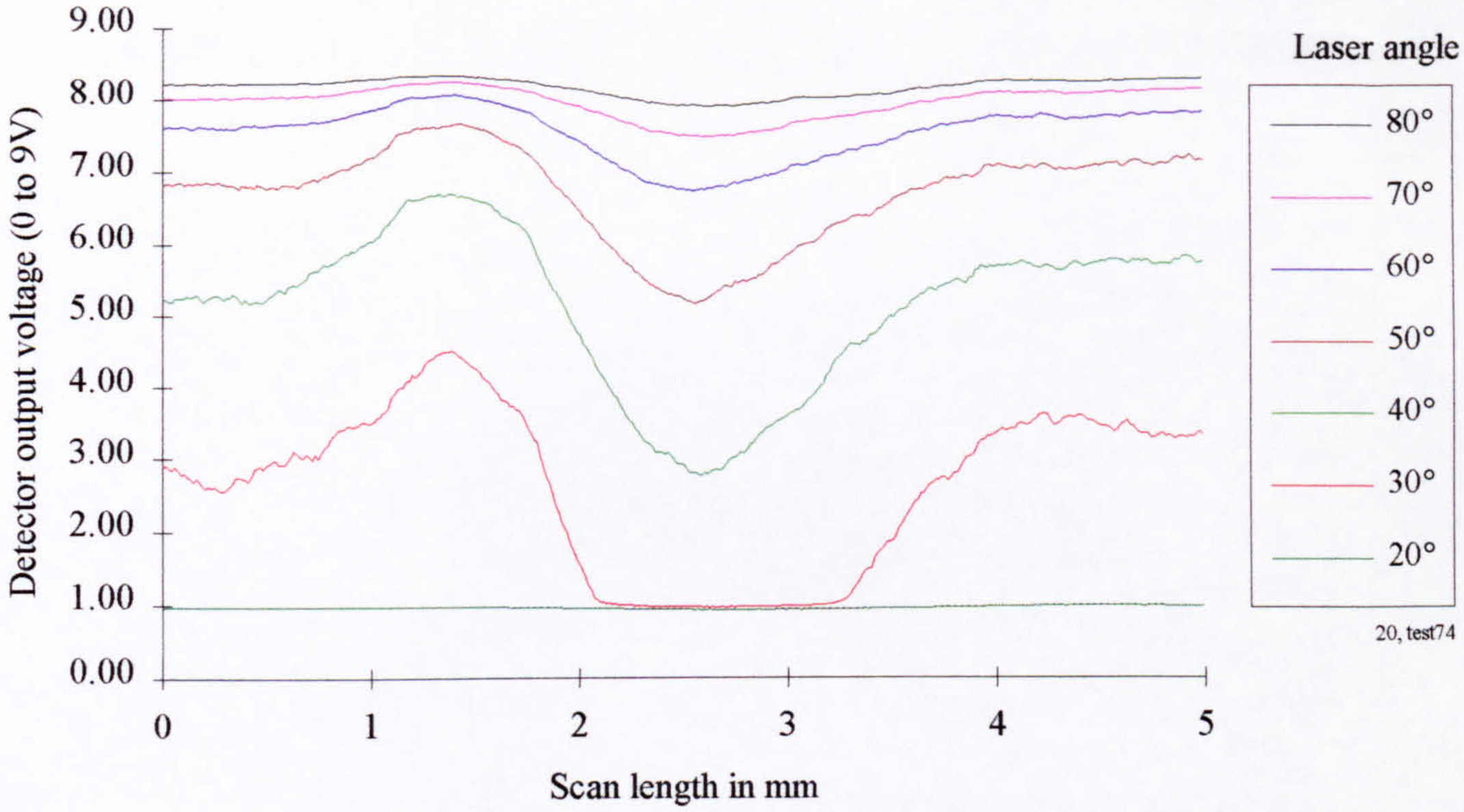

Figure 5-94 3.2 μm Shot blast sample with BUE defect and fixed detector angle of 20°

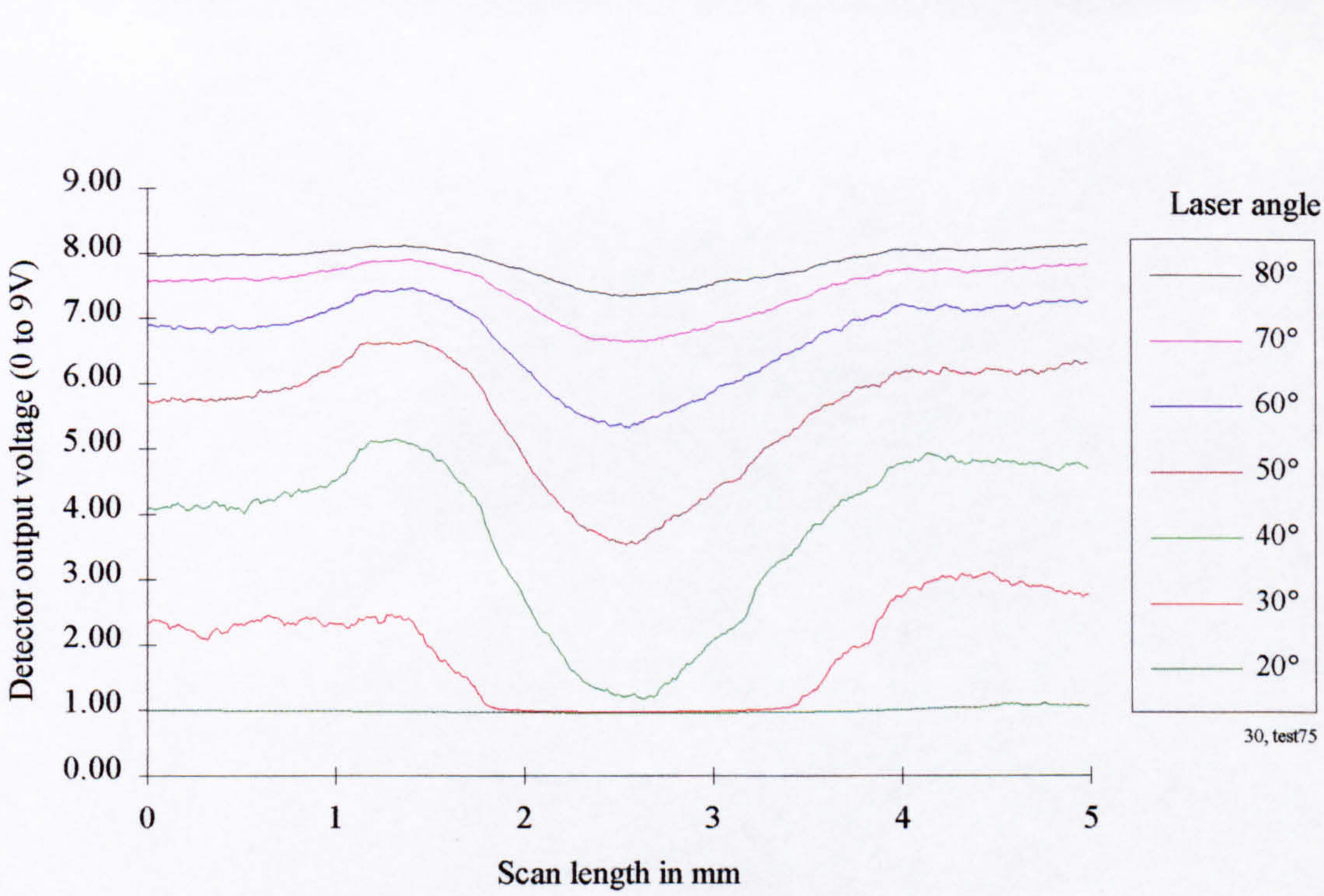

Figure 5-95 3.2 μm Shot blast sample with BUE defect and fixed detector angle of 30°

Graphical results continued (3.2 μm Shot blast sample with BUE defect)

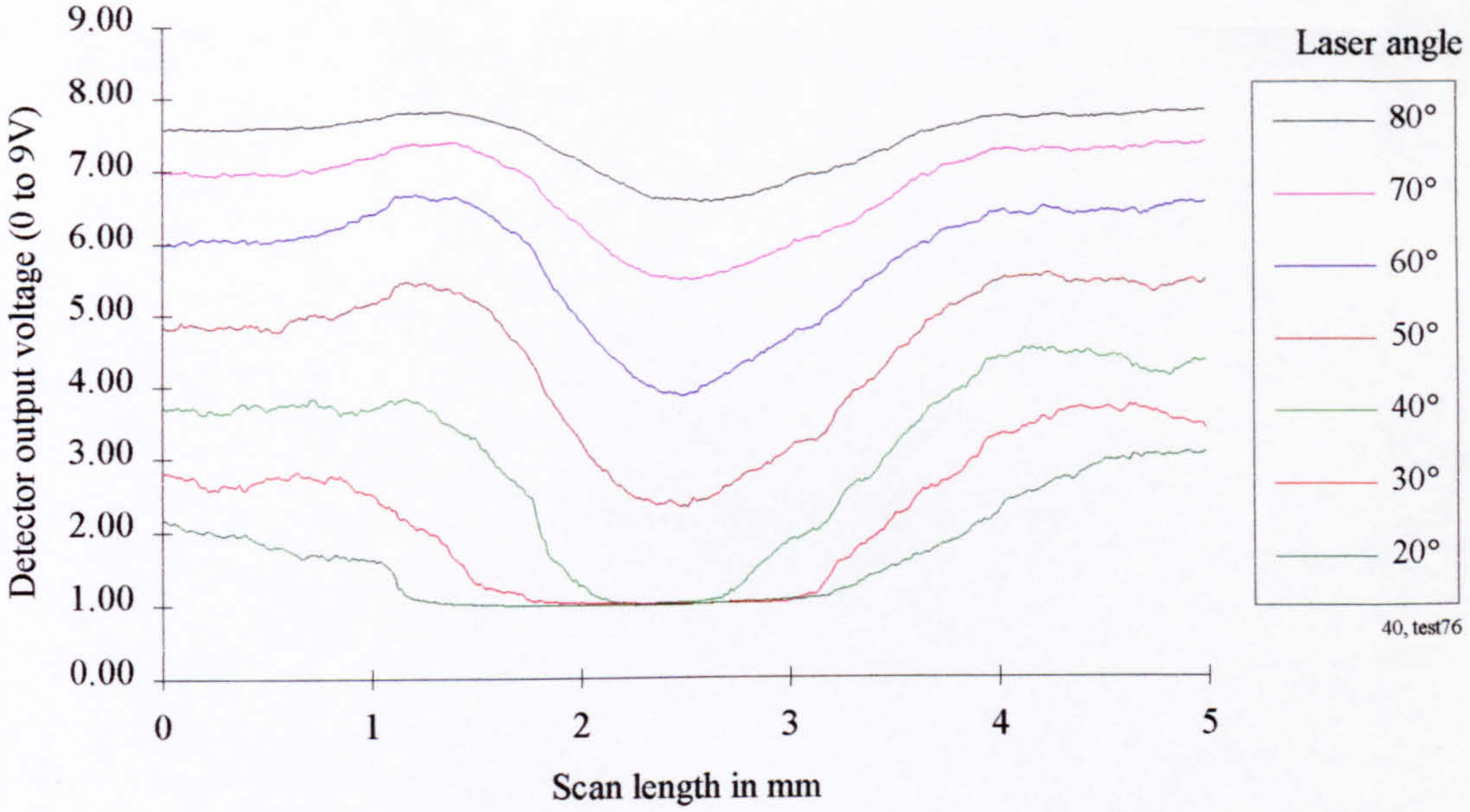

Figure 5-96 3.2 μm Shot blast sample with BUE defect and fixed detector angle of 40°

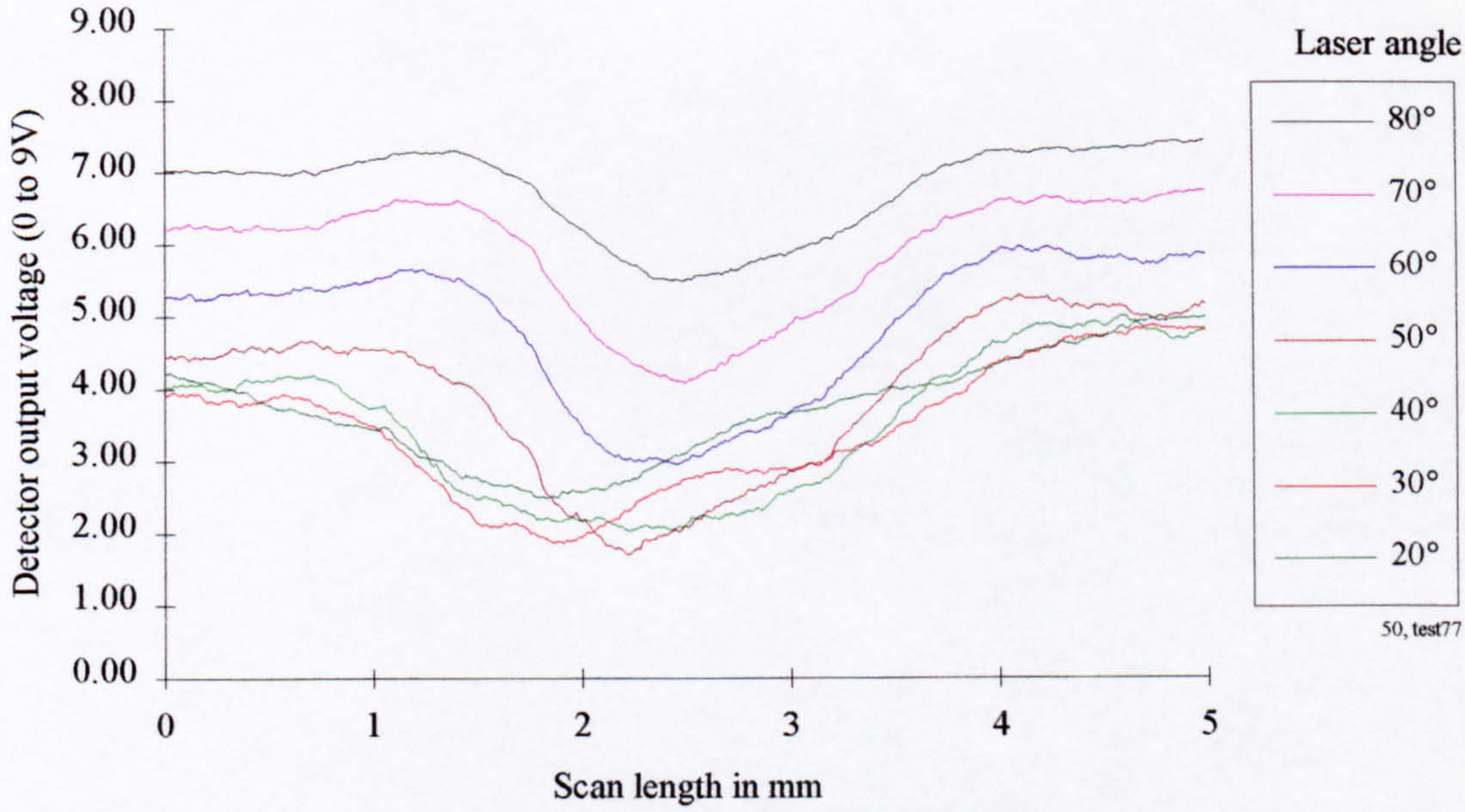

Figure 5-97 3.2 μm Shot blast sample with BUE defect and fixed detector angle of 50°

0.5 μm Plain polished control sample

Photograph of inspected surface (0.5 μm Plain polished sample)

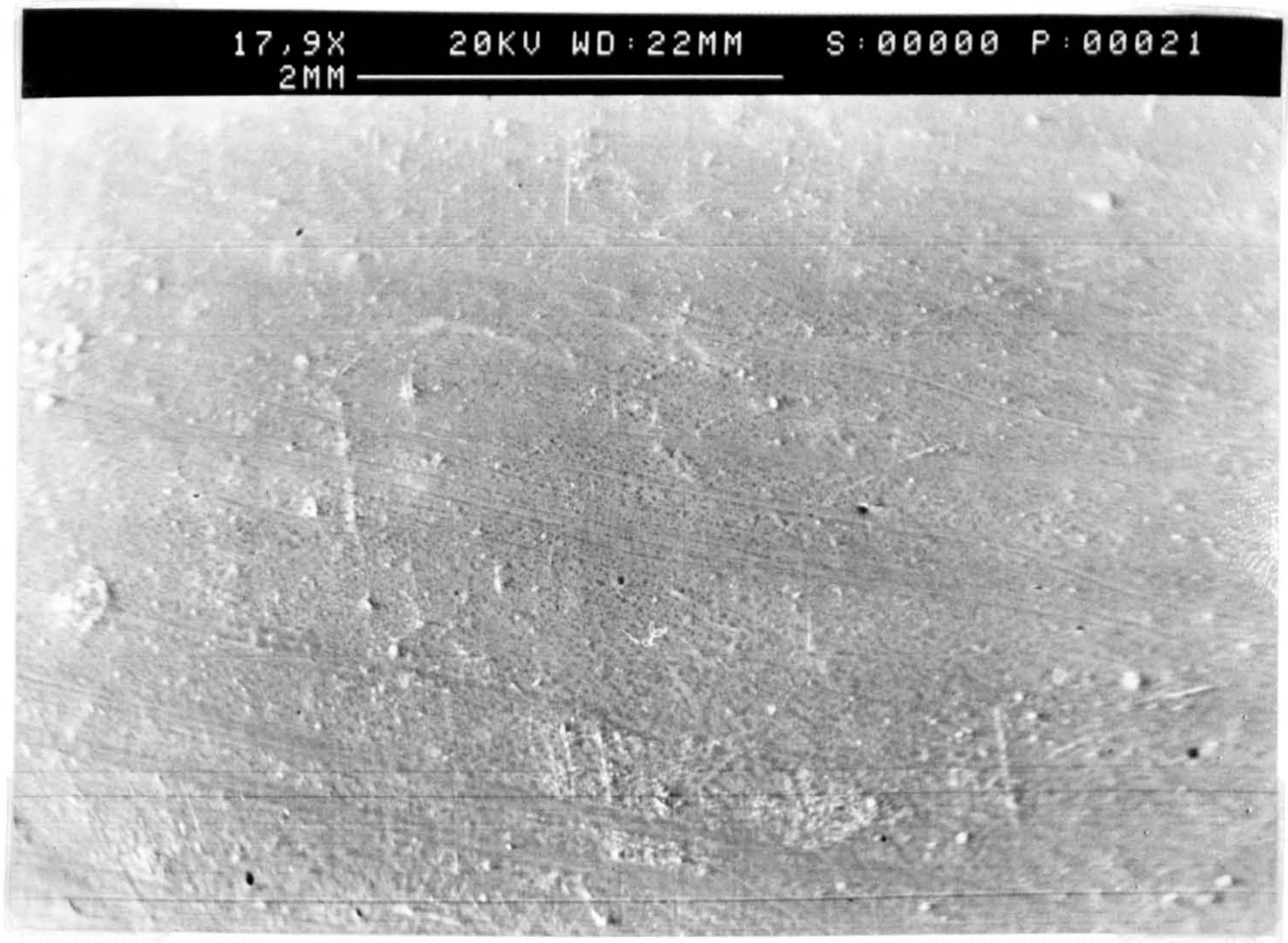

Figure 5-98 0.5 μm Plain polished sample, surface photograph

Surface topography trace (0.5 μm Plain polished sample)

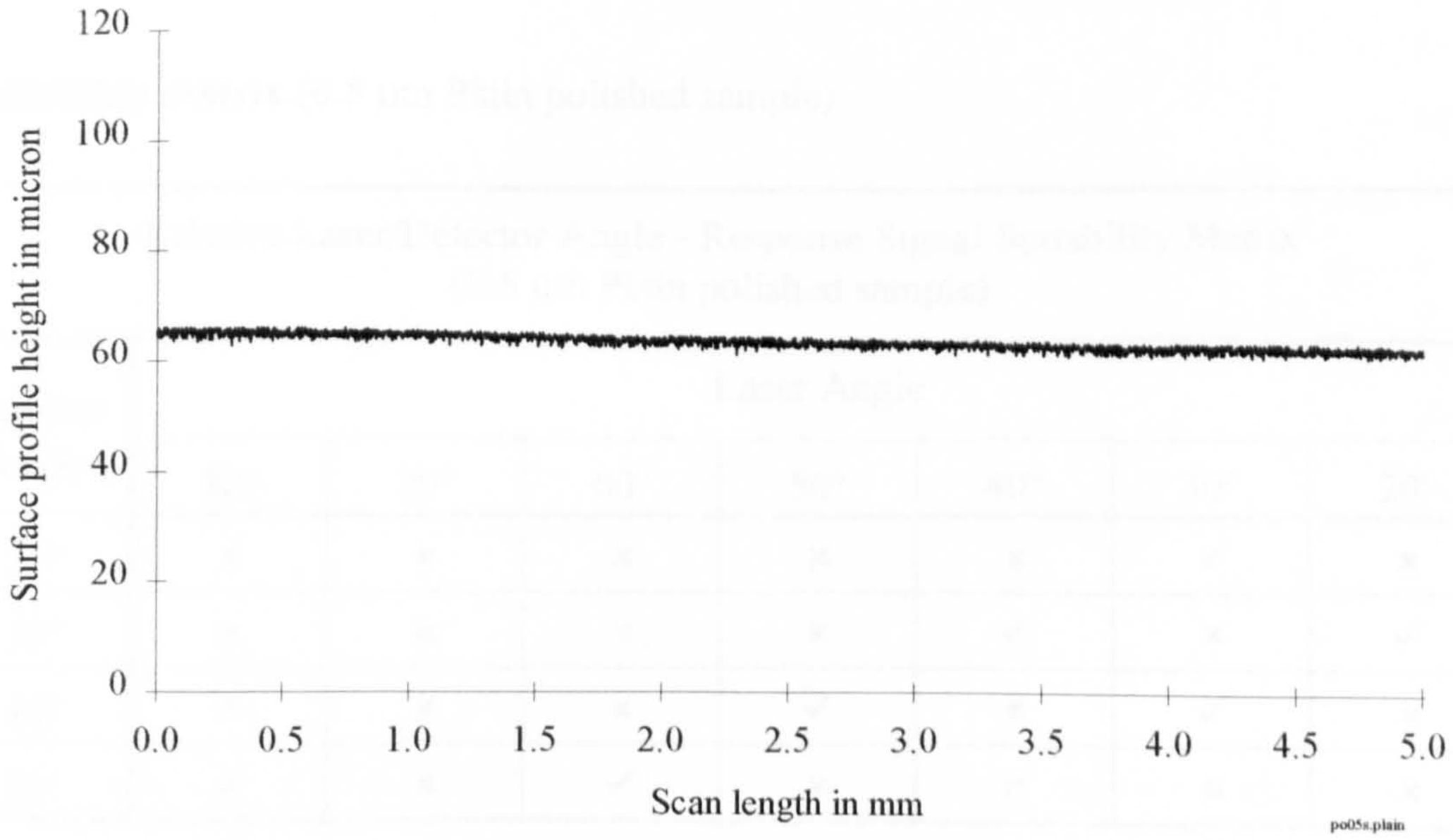

Figure 5-99 0.5 μm Plain polished sample, surface profile

Discussion of results (0.5 μm Plain polished sample)

The specular nature of the reflected light is immediately apparent when the results are analysed in detail. With identical laser and detector angles, response saturation occurs. This condition is bordered by signals containing surface information (non-saturated), for every case under consideration. The suitability matrix portrays this scenario with two parallel and diagonal lines of ticks which contain a single line of crosses (Common laser and detector angles). Other configurations yield signals which tend towards the dark signal confine. The consistent image angle introduced and discussed earlier is seen to apply to this case also. Consistent image angles of 100° and 80° should be adopted to obtain response results that contain surface character information. However a consistent image angle of 90° produces response saturation and furthermore, angles greater than 100° or less than 80° consistently result in a response contained by the dark signal confine. This characteristic scenario is clearly depicted in the illustration of figure 5-4.

The system is also noted to be extremely sensitive, with small changes in the angular setting of the detector/laser (2° approximately) resulting in the response signal swinging from one confine to the other.

Suitability matrix (0.5 μm Plain polished sample)

Relative Laser/Detector Angle - Response Signal Suitability Matrix (0.5 μm Plain polished sample)							
Detector Angle	Laser Angle						
	80°	70°	60°	50°	40°	30°	20°
20°	✗	✗	✗	✗	✗	✓	✗
30°	✗	✗	✗	✗	✓	✗	✓
40°	✗	✗	✗	✓	✗	✓	✗
50°	✗	✗	✓	✗	✓	✗	✗

Table 5-16 0.5 μm Plain polished sample, response signal suitability matrix

Graphical results (0.5 μm Plain polished sample)

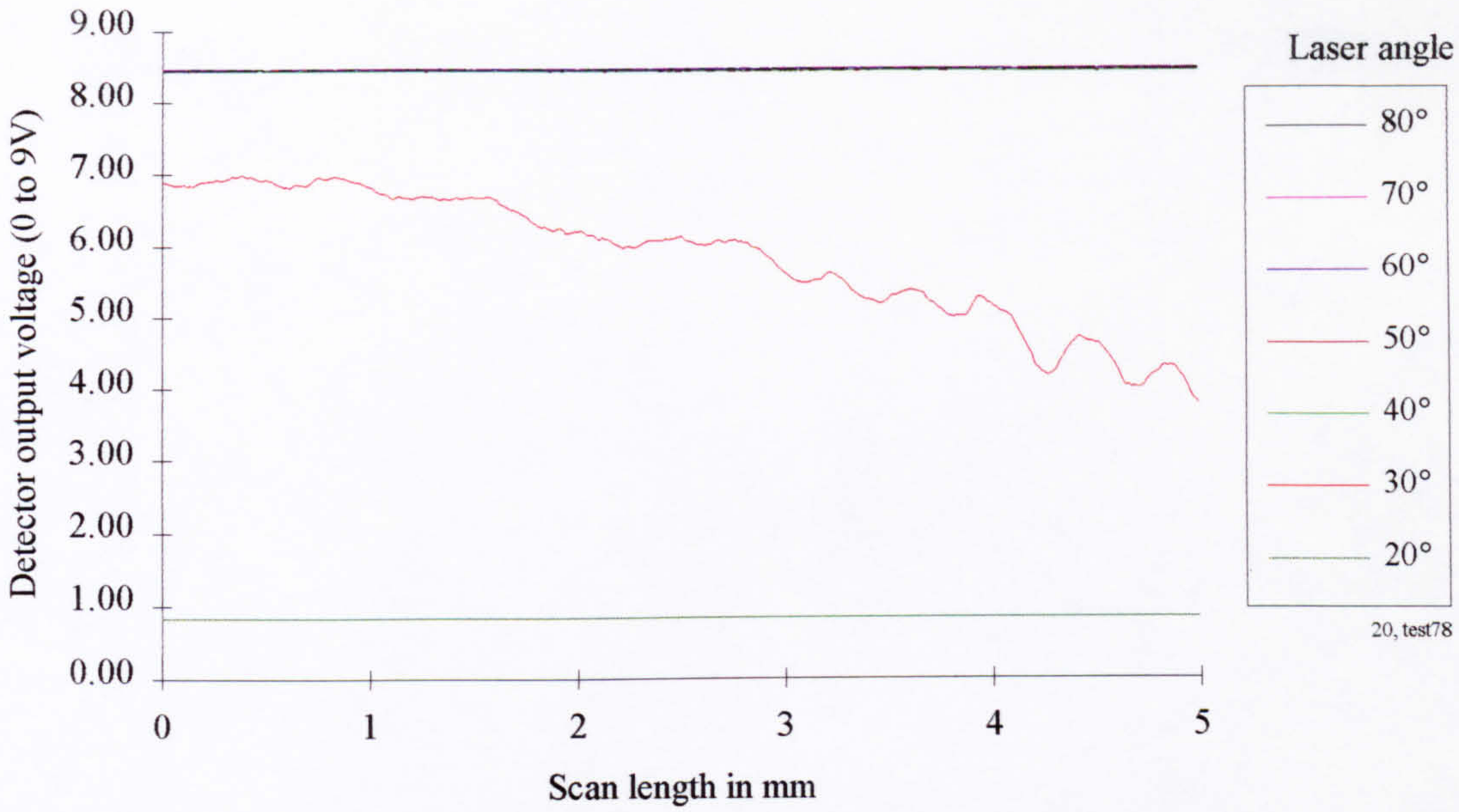

Figure 5-100 0.5 μm Plain polished sample with fixed detector angle of 20°

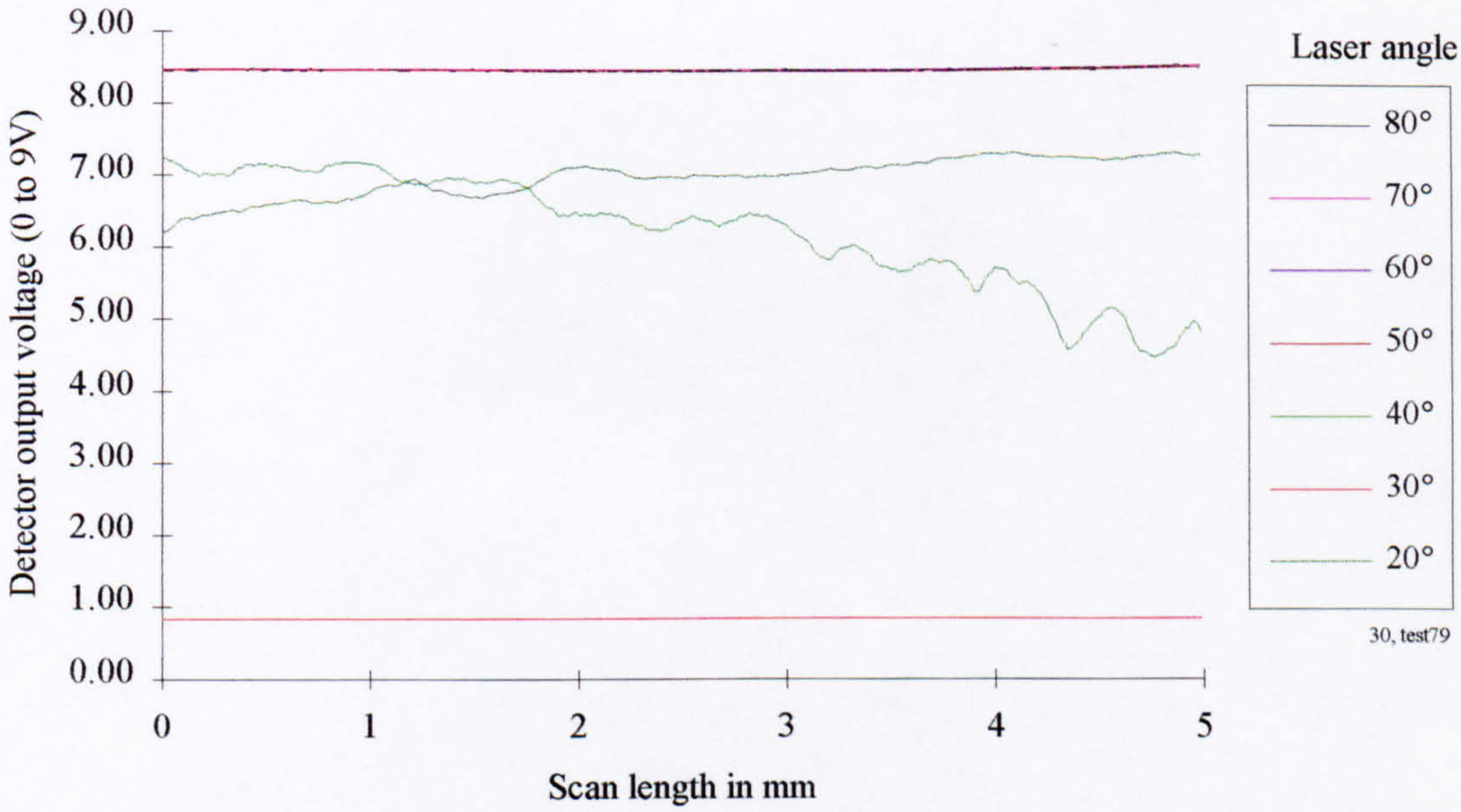

Figure 5-101 0.5 μm Plain polished sample with fixed detector angle of 30°

Graphical results continued (0.5 μm Plain polished sample)

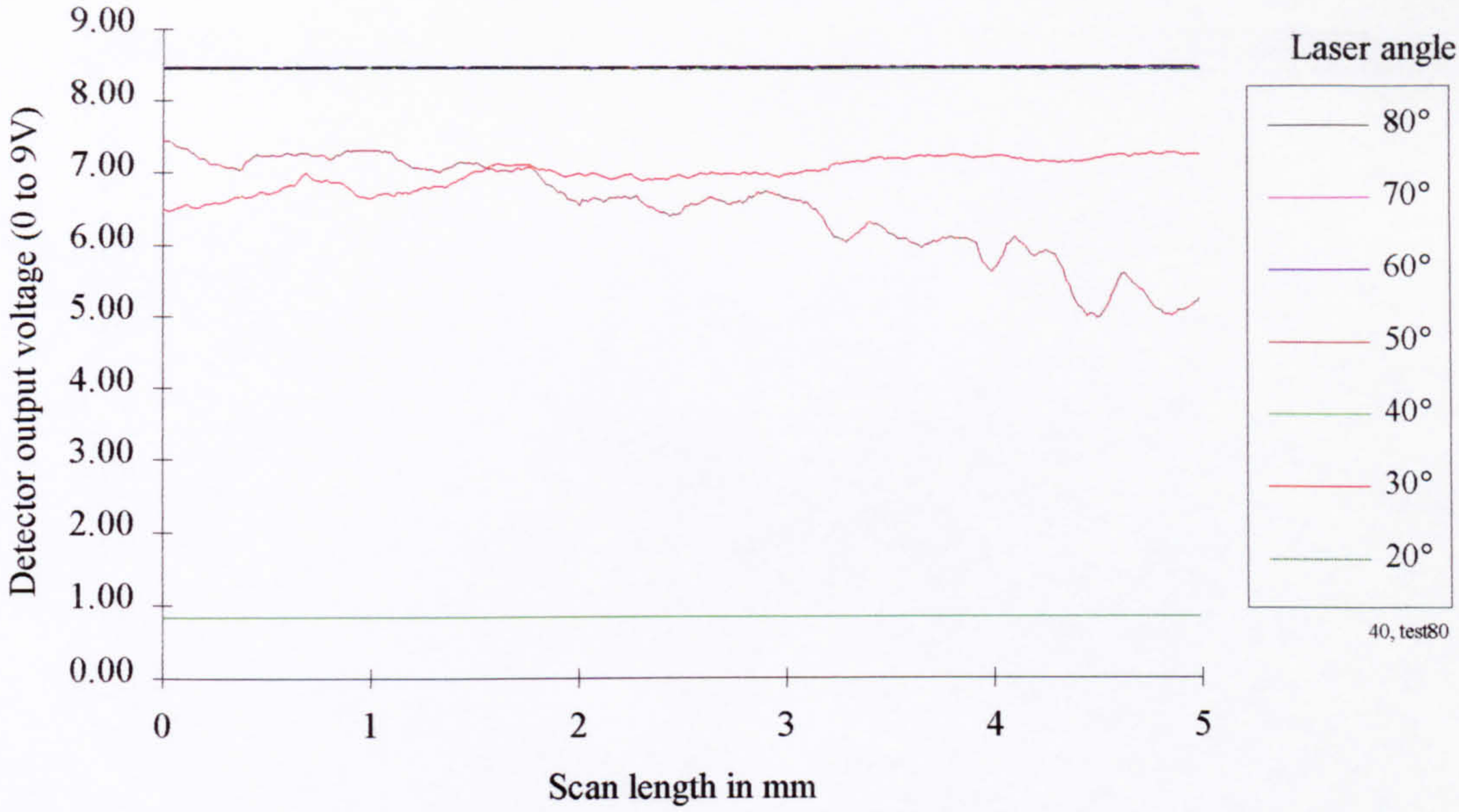

Figure 5-102 0.5 μm Plain polished sample with fixed detector angle of 40°

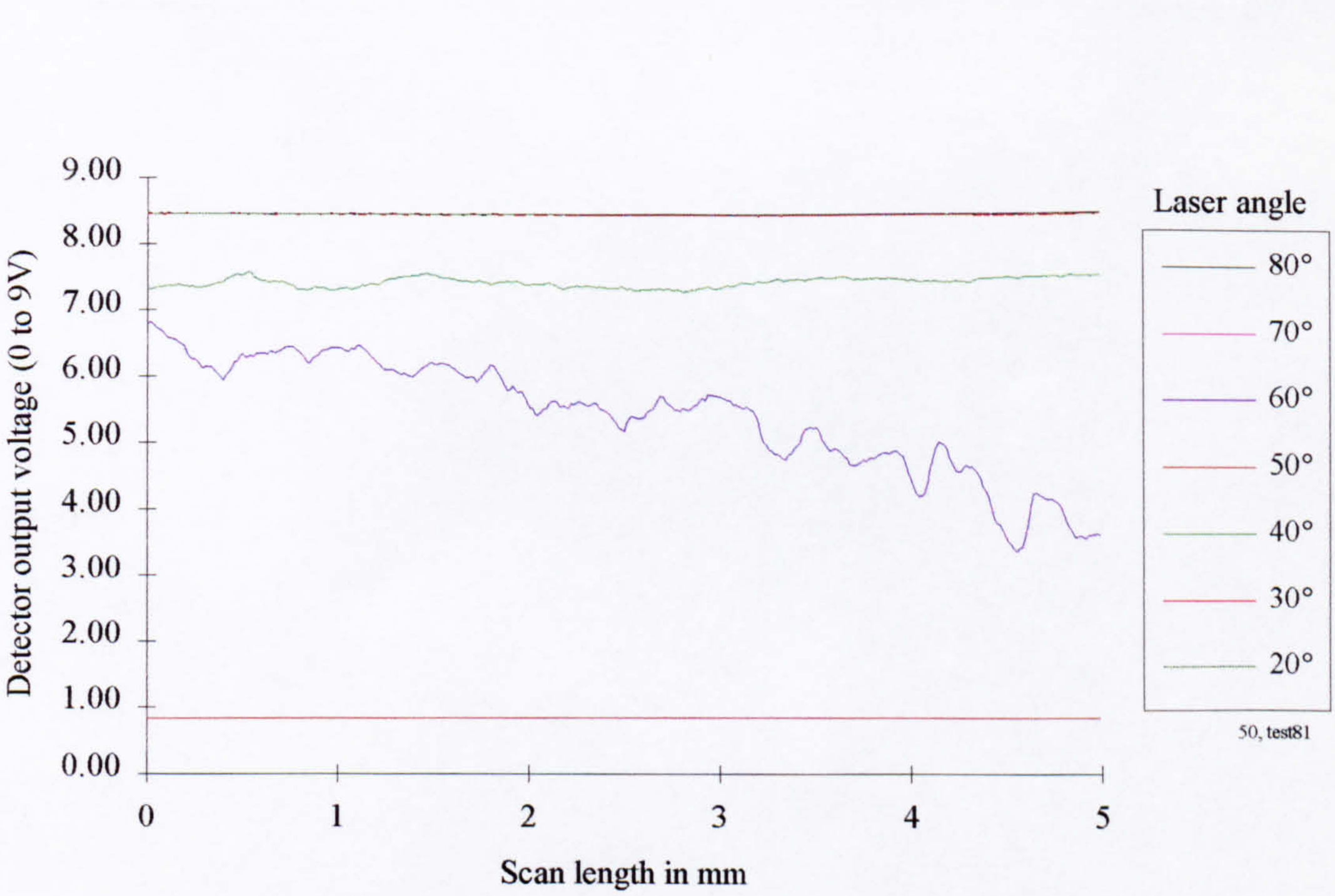

Figure 5-103 0.5 μm Plain polished sample with fixed detector angle of 50°

0.5 μm Polished control sample with scratch defect

Photograph of inspected surface (0.5 μm Polished sample with scratch defect)

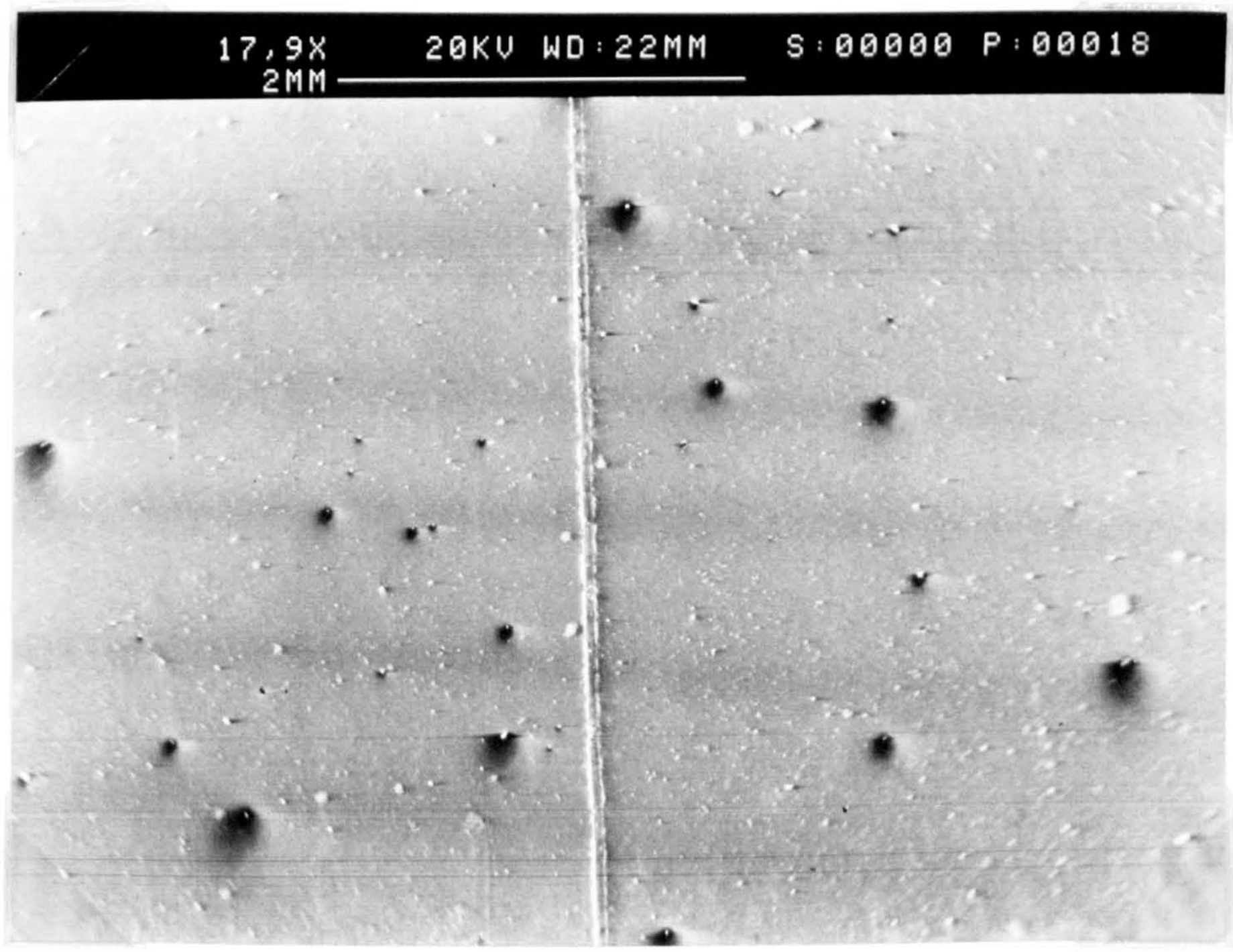

Figure 5-104 0.5 μm Polished sample with scratch defect, surface photograph

Surface topography trace (0.5 μm Polished sample with scratch defect)

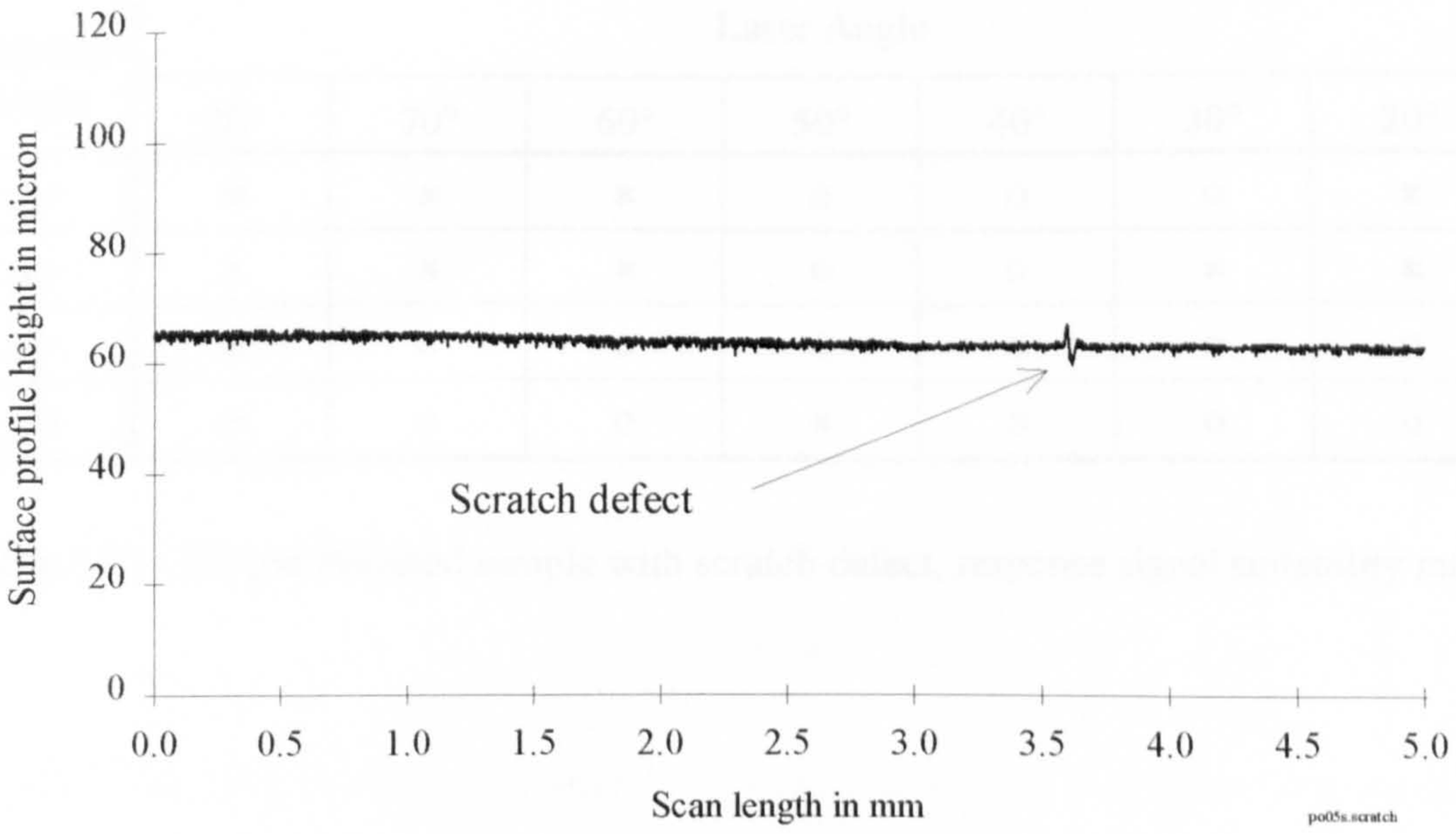

Figure 5-105 0.5 μm Polished sample with scratch defect, surface profile

Discussion of results (0.5 μm Polished sample with scratch defect)

Light reflected from a specular (highly polished) surface tends to contain little information about the surface from which it is reflected. This is apparent from the flat horizontal lines in the graphical results of figures 5-106 to 5-109 which represent the response signals for the polished sample with buit-up-edge defect. The majority of the responses are coincident with the dark signal confine. Additionally, when the laser and detector angles are common the response tends to the saturation confine as expected for the polished sample. Around these limitations signals are apparent which contain infromation/evidence of the presence of a defect on the sample surface (denoted by a naught in the table below). A consistent image angle of 100° is considered most appropriate for defect detection, under the conditions imposed.

Suitability matrix (0.5 μm Polished sample with scratch defect)

Relative Laser/Detector Angle - Response Signal Suitability Matrix (0.5 μm Polished sample with scratch defect)							
Detector Angle	Laser Angle						
	80°	70°	60°	50°	40°	30°	20°
20°	×	×	×	o	o	o	×
30°	×	×	×	o	o	×	×
40°	×	o	o	o	×	×	o
50°	o	o	o	×	×	o	o

Table 5-17 0.5 μm Polished sample with scratch defect, response signal suitability matrix

Graphical results (0.5 μm Polished sample with scratch defect)

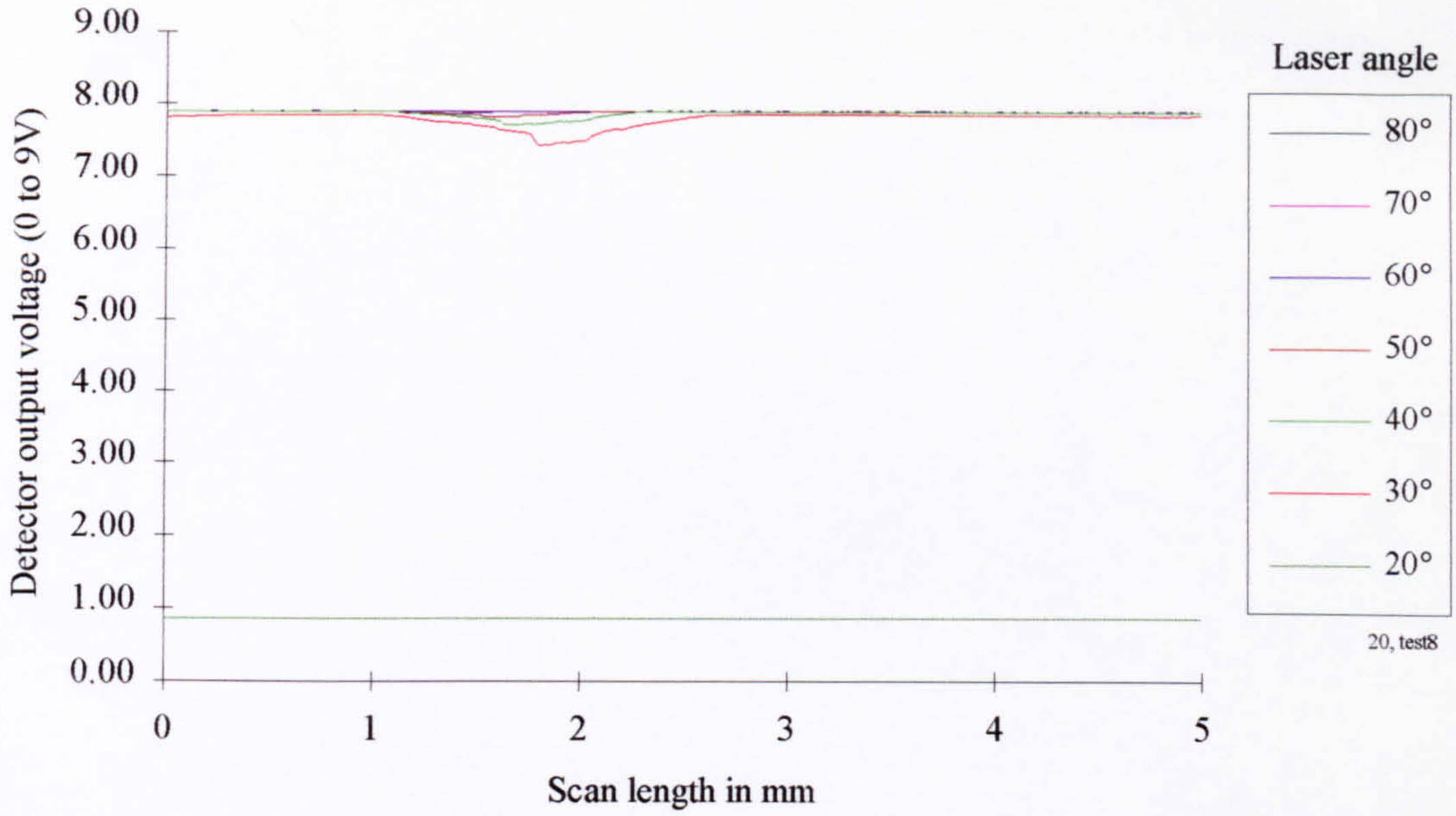

Figure 5-106 0.5 μm Polished sample with scratch defect and fixed detector angle of 20°

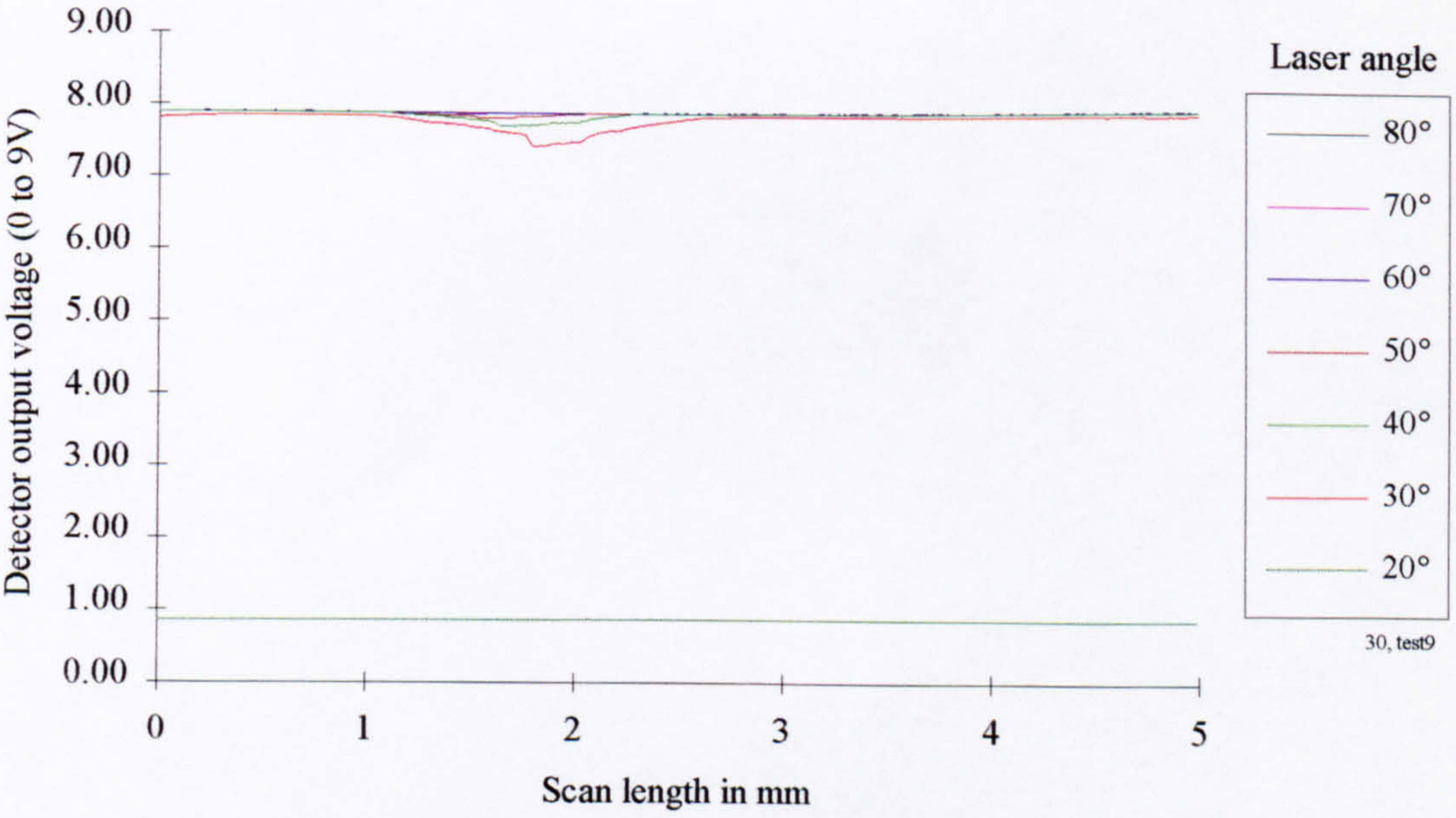

Figure 5-107 0.5 μm Polished sample with scratch defect and fixed detector angle of 30°

Graphical results continued (0.5 μm Polished sample with scratch defect)

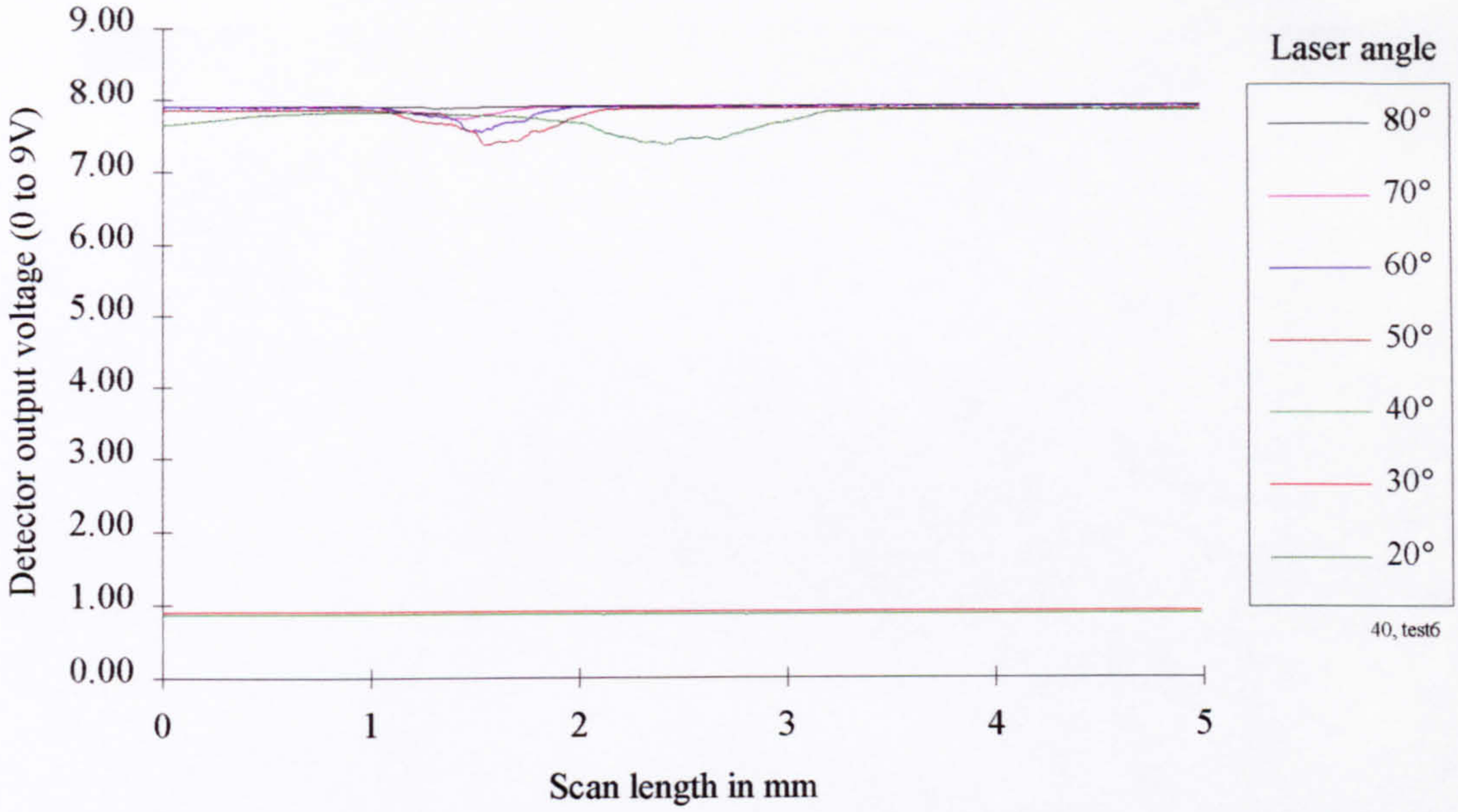

Figure 5-108 0.5 μm Polished sample with scratch defect and fixed detector angle of 40°

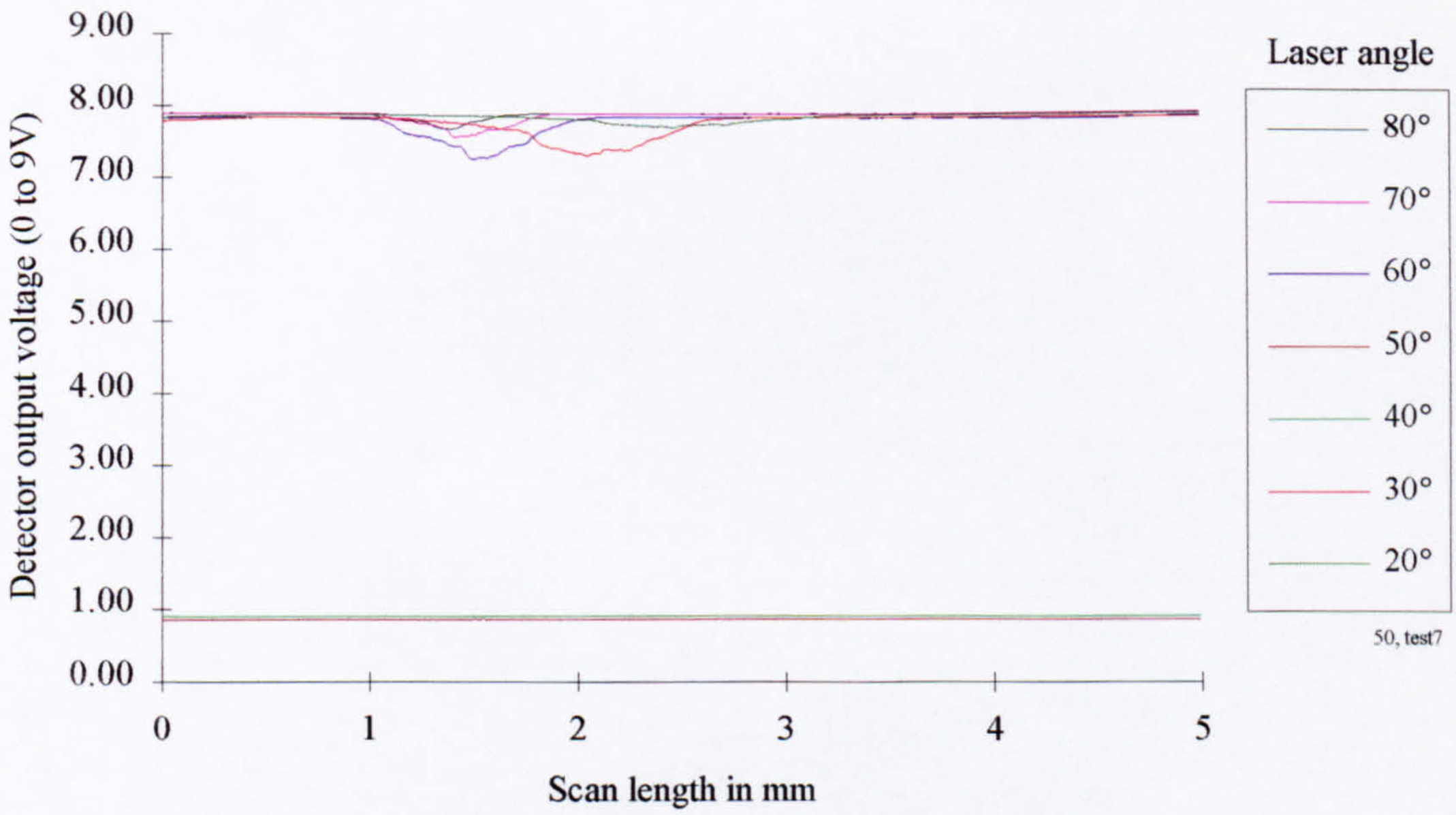

Figure 5-109 0.5 μm Polished sample with scratch defect and fixed detector angle of 50°

0.5 μm Polished control sample with built-up edge (BUE) defect

Photograph of inspected surface (0.5 μm Polished sample with BUE defect)

Figure 5-110 0.5 μm Polished sample with BUE defect,surface photograph

Surface topography trace (0.5 μm Polished sample with BUE defect)

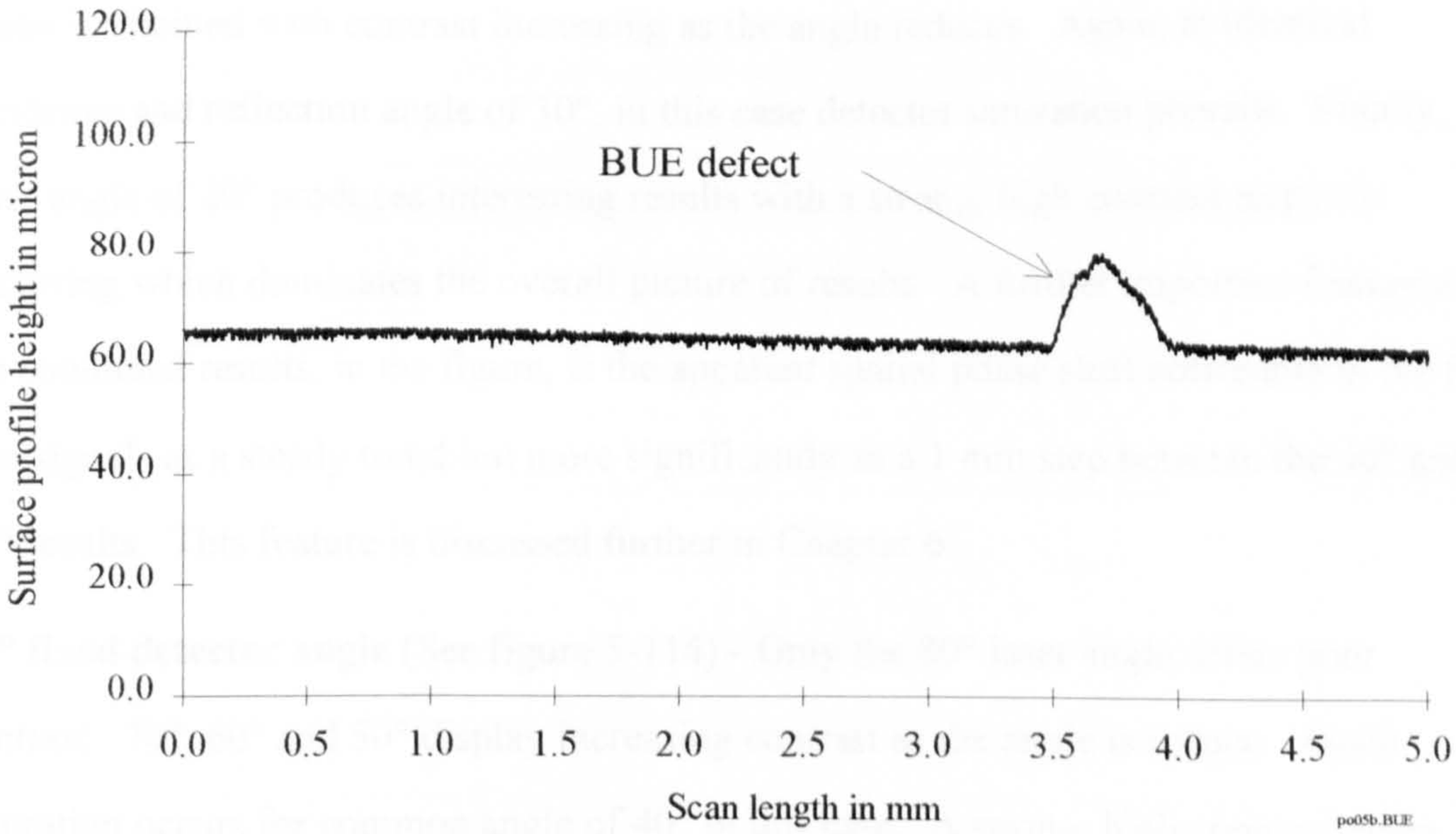

Figure 5-111 0.5 μm Polished sample with BUE defect, surface profile

Discussion of results (0.5 μm Polished sample with BUE defect)

20° fixed detector angle (See figure 5-112) - The built up edge is apparent from the response signals at laser angles of 50°, 40° and most predominantly 30°. For steeper laser angles of 80°, 70° and 60° an extremely weak response is attained. The mirror finish sample caused detector saturation when the laser and detector angles were the same.

30° fixed detector angle (See figure 5-113) - With an increased detector angle (from 20° to 30°) it is apparent that the response signals cascade down one place in the sequence when compared to those illustrated in the above figure. The weakest signal, above, which represented a laser angle of 80° is no longer represented. However, the current 80° laser angle response signal almost replicates that for the 70° laser angle from the previous results, the second curve in the series. This relationship is repeated throughout the sequence. A significant deviation from this general observation is made apparent by the prominent final signal. The high contrast peak of this response clearly indicates the presence of a object/defect on the scanned specimen. The magnitude of the signal in this case is greater than any produced by an increase in laser angle.

By observation, laser incidence angles of 80° and 70° offer poor contrast signals with a response being just visible. For an decrease in angle to 60°, 50° and 40° an improved signal is attained with contrast increasing as the angle reduces. Again, at identical incidence and reflection angle of 30°, in this case detector saturation prevails. Finally, the laser angle of 20° produces interesting results with a strong, high contrast response occurring which dominates the overall picture of results. A further important feature of the combined results, in the figure, is the apparent spatial phase shift noticeable in the first five signals as a steady trend but more significantly as a 1 mm step between the 40° and 20° results. This feature is discussed further in Chapter 6.

40° fixed detector angle (See figure 5-114) - Only the 80° laser angle offers poor contrast. 70°, 60° and 50° display increasing contrast as the angle is reduce. Again saturation occurs for common angle of 40° in this case. A strong, high contrast, steep sided signal evolves when the laser angle is 10° less than that of the detector. A further

laser angle reduction, down to 20°, exhibits a further step change in the format of response signal. The signal moves away from the saturation up to the dark signal confine. Furthermore it takes on a form similar to that produced at lesser angles, portraying some character of the scanned surface. The spatial phase shift is also apparent in this set of results, adopting a similar trend to that discussed for the previous results. One significant difference however is the spatial phase stagnation exhibited by the signals representing laser angles of 30° and 20°.

50° fixed detector angle (See figure 5-115) - This group of data continues the trend already demonstrated by the same family of results discussed previously. Laser angles of 80° through 60° offer responses with a degree of contrast which also contain information relating to the character of the surface defect being scanned. Saturation occurs for a common incidence and reflection angle of 50°, resulting in the signal tracing a horizontal line at the saturation confine. Again, for a laser angle (40°) just 10° below that of the detector, a strong steep sided response, rising from the saturation confine, is attained. Further reductions in the incidence angle (for 30° and 20° specifically) produce signals which flip from the lower to the upper (dark signal) confine and which once again contain information loosely related to the nature of the surface being scanned.

Suitability matrix (0.5 μm Polished sample with BUE defect)

Relative Laser/Detector Angle - Response Signal Suitability Matrix (0.5 μm Polished sample with BUE defect)							
Detector Angle	Laser Angle						
	80°	70°	60°	50°	40°	30°	20°
20°	o	✓	✓	o	o	o	×
30°	✓	✓	o	o	o	×	×
40°	✓	o	o	o	o	×	×
50°	o	o	o	o	o	o	o

Table 5-18 0.5 μm Polished sample with BUE defect, response signal suitability matrix

Graphical results (0.5 μm Polished sample with BUE defect)

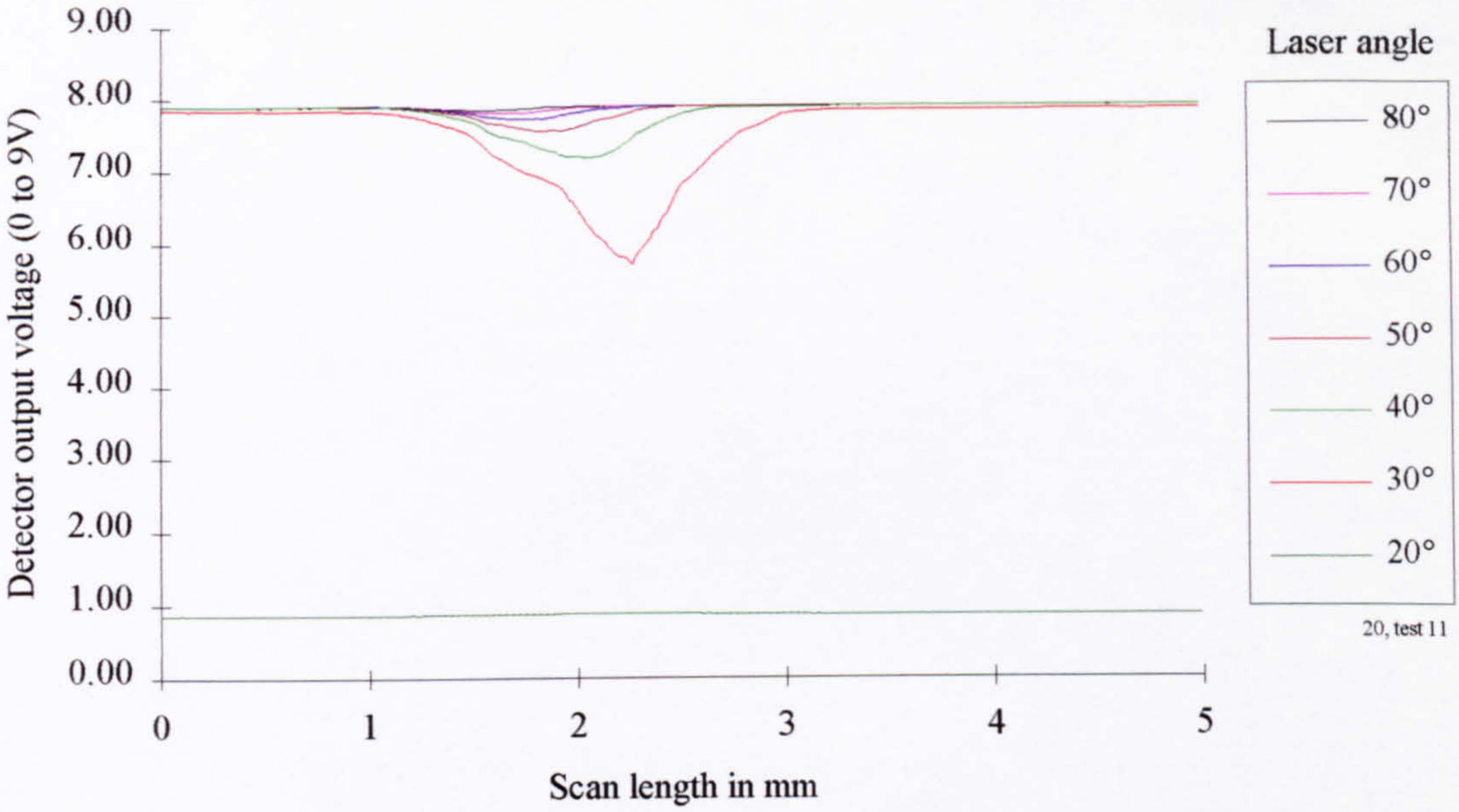

Figure 5-112 0.5 μm Polished sample with BUE defect and fixed detector angle of 20°

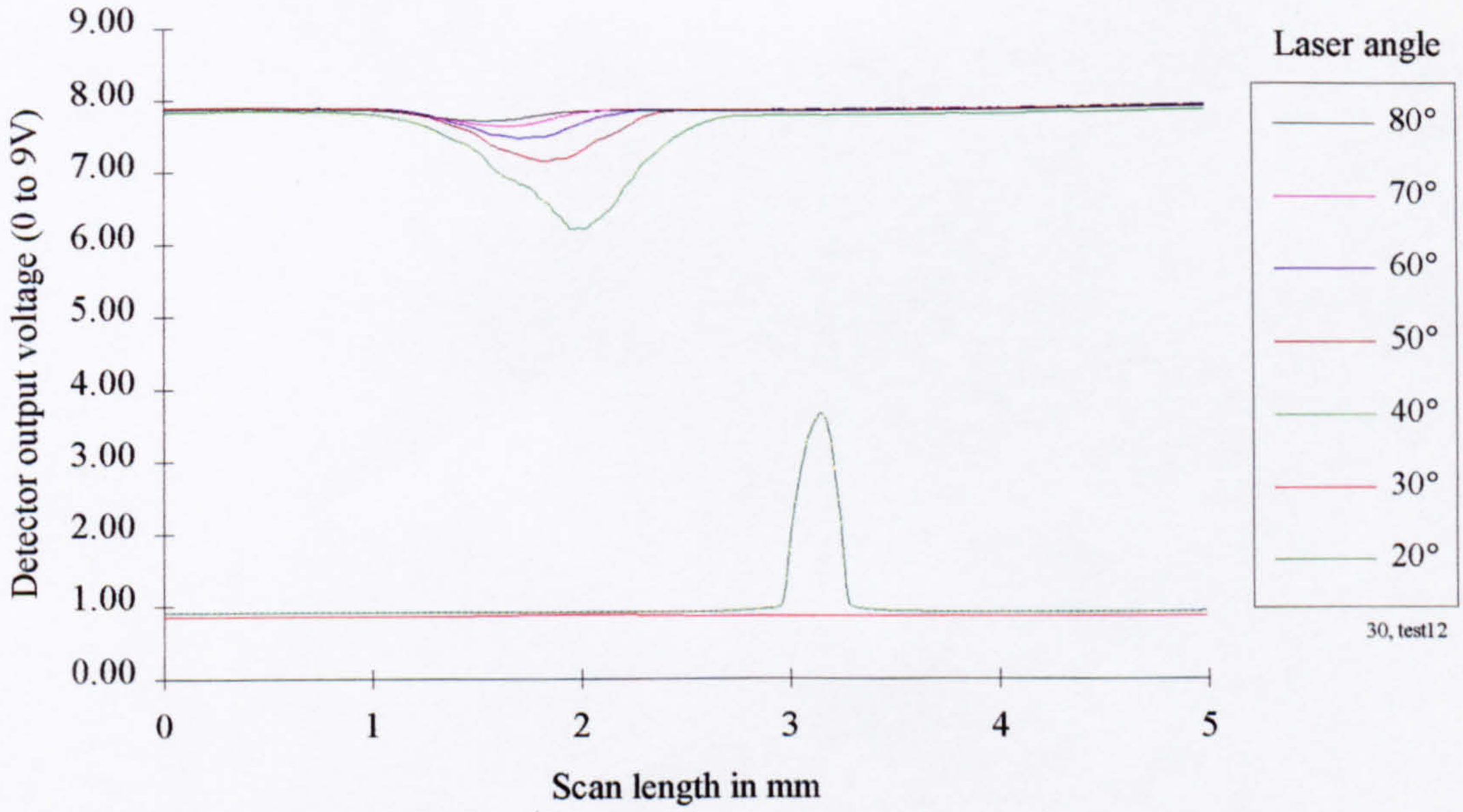

Figure 5-113 0.5 μm Polished sample with BUE defect and fixed detector angle of 30°

Graphical results continued (0.5 μm Polished sample with BUE defect)

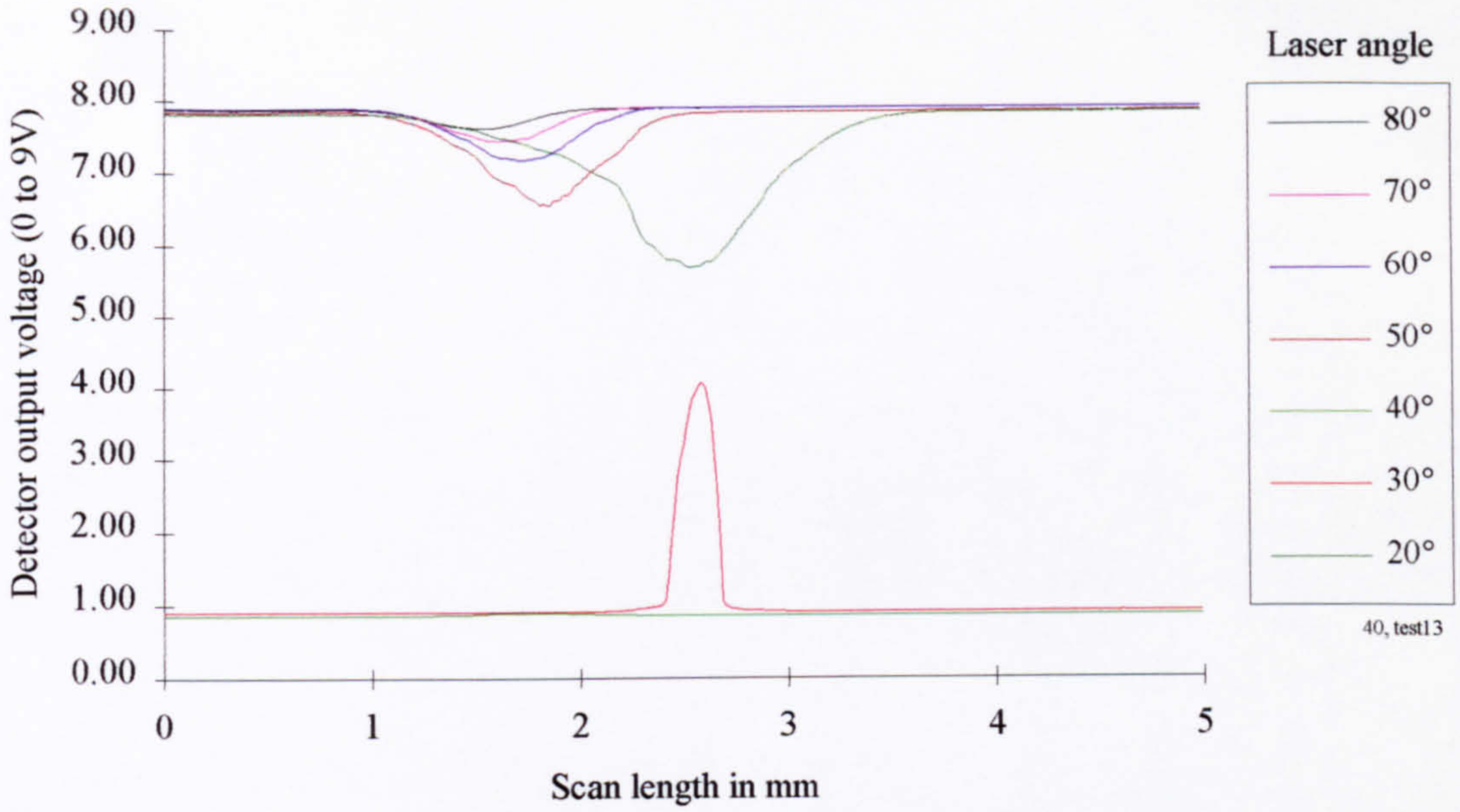

Figure 5-114 0.5 μm Polished sample with BUE defect and fixed detector angle of 40°

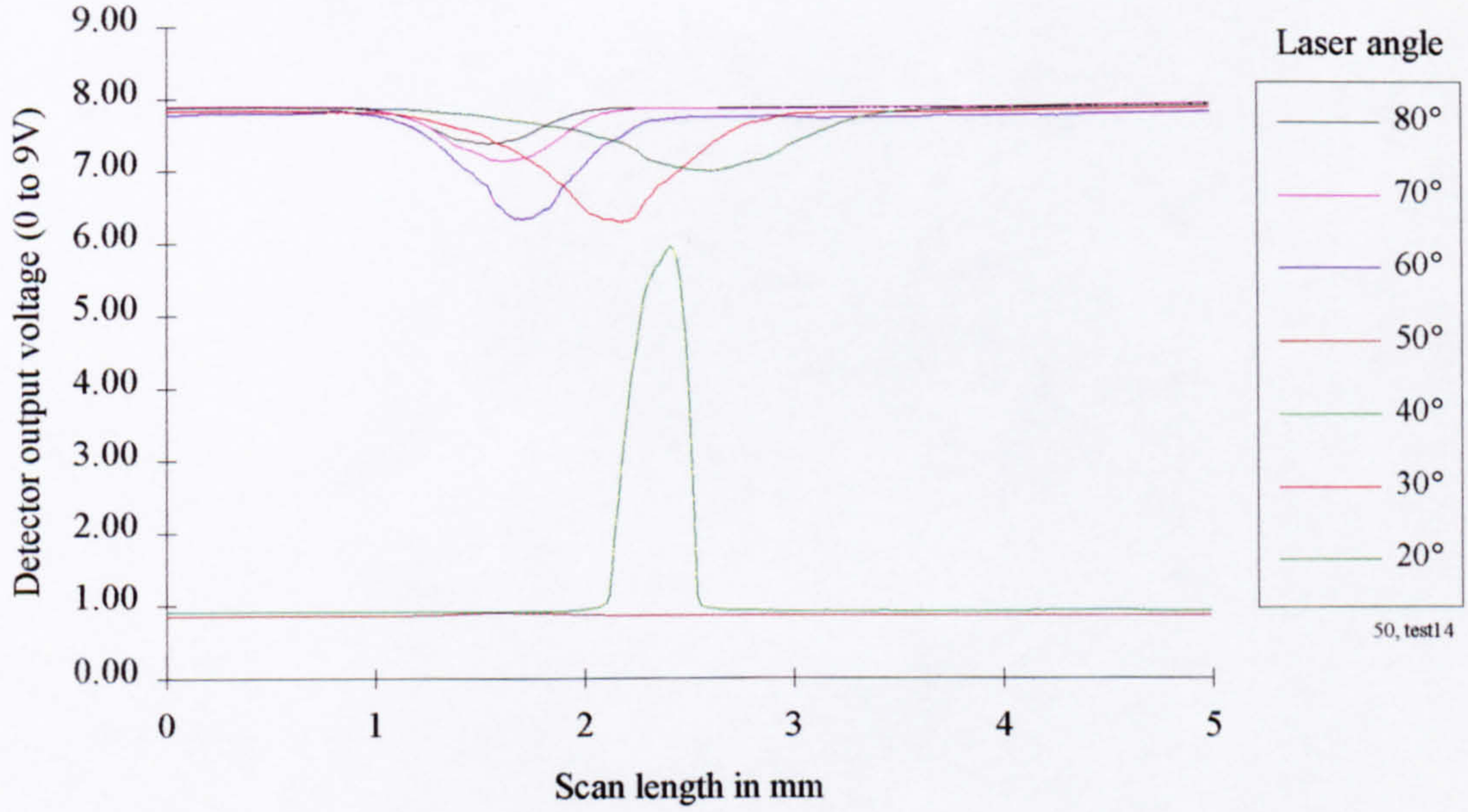

Figure 5-115 0.5 μm Polished sample with BUE defect and fixed detector angle of 50°

5.1.4 Optimisation of the laser spot size (diameter)

Early in the research program it was established that the laser spot size was a critical parameter in the inspection system's ability to detect surface features and defects. In an attempt to optimise the V-scanner laser spot size, when applied to defect detection, a series of tests were undertaken which are presented and discussed below.

With the already established optimum angle for incidence and reflection a control sample was presented to the surface topography inspection device. A sequence of scans was then made with the laser spot size being incrementally increased for each. The spot size ranged from approximately 0.1 mm to 1.0 mm in diameter. The variation was conveniently obtained be sliding the laser towards/away from the control sample surface which was under interrogation. The natural divergence of the laser beam produced an increase in spot size as the offset distance was increased beyond the focal length.

A laser offset of 61 mm coincided with the laser's focal length and thus produced a spot of minimum diameter (0.1 mm approximately). At an offset of 70 mm the laser spot was found to be 1.0 mm in diameter, approximately. By geometry it was determined that for each millimetre of laser offset the spot diameter would increase by 0.1 mm. This reasoning was applied during collection of the following data sets.

Laser spot size optimisation (0.1 μm Ground sample with scratch defect)

Laser and detector angles were set in accordance with those most suited to the specific application (See table 5-5 0.1 μm Ground sample with scratch defect, response signal suitability matrix):

Laser Angle	60°
Detector Angle	30°

A control sample scan length of 2.8 mm was recorded, with successive increases in laser spot diameter. The ten resulting graphs are illustrated in figure 5-116, over leaf.

For this specific application it is evident from the figure that a spot diameter of 0.3 to 0.5 mm is most practical, with a degree of high frequency filtering taking place but no significant degradation of defect signal.

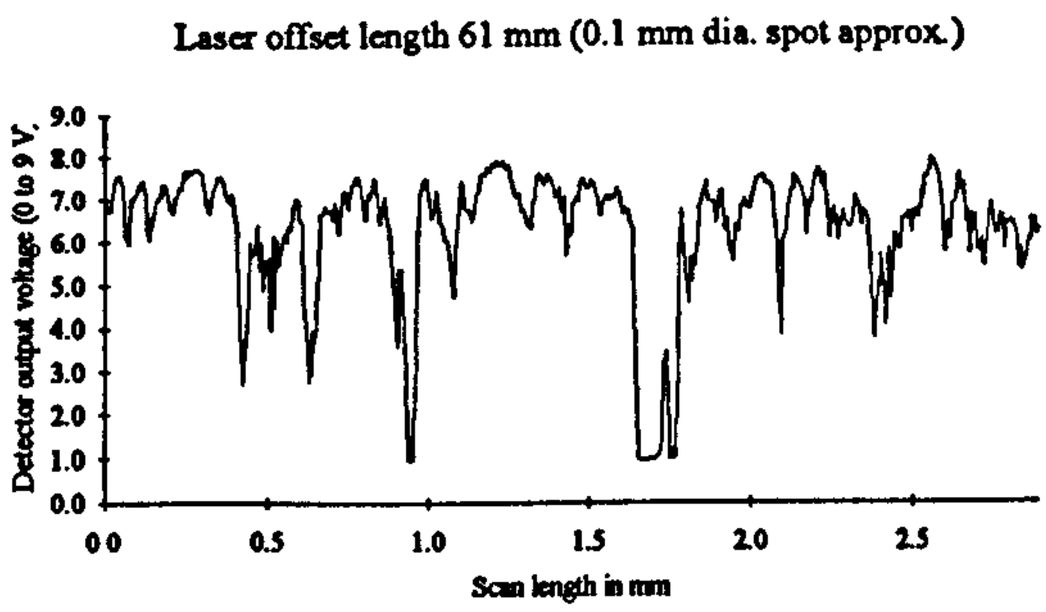

Figure 5-116 The effect of laser spot size on defect detection (0.1 μm Ground sample with scratch defect)

Laser spot size optimisation (12.5 μm End mill sample with scratch defect)

Further spot size optimisation tests were undertaken for completeness. These were performed on an end mill control sample possessing a surface roughness of 12.5 μm (Roughness average, R_a) complete with scratch defect . Laser and detector angles were configured as follows (In accordance with the implied optimum settings of table 5-2, 12.5 μm End mill sample with scratch defect, response signal suitability matrix):

Laser Angle	70°
Detector Angle	30°

A control sample scan length of 4.8 mm was recorded, with successive increases in laser spot diameter. The seven resultant graphs are illustrated in figure 5-117. The regular peaks of the end mill surface form are clearly visible in the majority of the graphs of this figure. However, for a spot diameter in the range of 0.4 to 0.6 mm the defect and general surface form are both apparent and furthermore could be readily separated.

In practise the following configurations were found to provide acceptable signals for a wide range of surfaces;

Laser spot size

A laser spot size in the range of 0.4 to 0.6 mm would best suit the application under consideration for the envisaged level of signal detail required.

Laser/detector angles

From the summary table below (table 5-19) the following recommendations for laser and detector configuration have been drawn.

A suitable response can be gained for all of the plain ground specimen surfaces for a consistent image angle of 130° and 120°. From the range of configurations observed this translates to a laser /detector angle arrangement of 60°/20° through to 80°/40° and 50°/20°

through to 80°/50° in the extremes (See table 5-19). This situation is apparent by the combined presence of the circled numbers 2, 3 and 4 in the appropriate table cells.

Consistent image angle 130° ▒▒▒▒▒▒ Consistent image angle 120° ▒▒▒▒▒▒

(relevant circled numbers are placed in the cells where a tick (✓) or a naught (o) was present in the corresponding tables for the previously discussed laser/detector optimisation tests);

Relative Laser/Detector Angle - Summary Matrix (Plain control samples)							
Detector Angle	Laser Angle						
	80°	70°	60°	50°	40°	30°	20°
20°	③④	③④	①②③④	①②③④	①②③④⑤	③④⑤⑥	③④⑤
30°	③④	①②③④	①②③④	①②③④⑤	③④⑤⑥	③④⑤	③④⑤⑥
40°	①②③④	①②③④	①③④	③④⑤⑥	④⑤	④⑤⑥	④⑤
50°	①②③④	①③④	①③④⑤⑥	④⑤	④⑤⑥	④⑤	②④⑤

Key:

① End mill sample	② Ground sample 0.1 μm	③ Ground sample 1.6 μm
④ Ground sample 3.2 μm	⑤ Shot blast sample	⑥ Polished sample

Table 5-19 Relative laser/detector angle - Summary Matrix

Other values which can also be considered as suitable are;

laser/detector angles of 40°/20° and 50°/30° highlighted in the above table by a heavy boarder. However, these values fall outside of the characteristic trend of results and are part constituted by naughts, thus the class of suitability can not be considered equal to those previously mentioned.

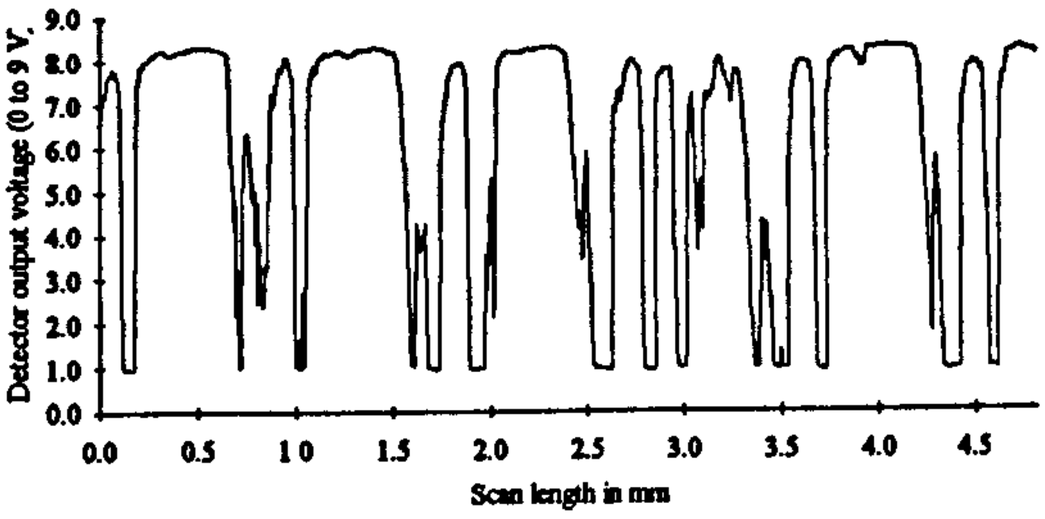

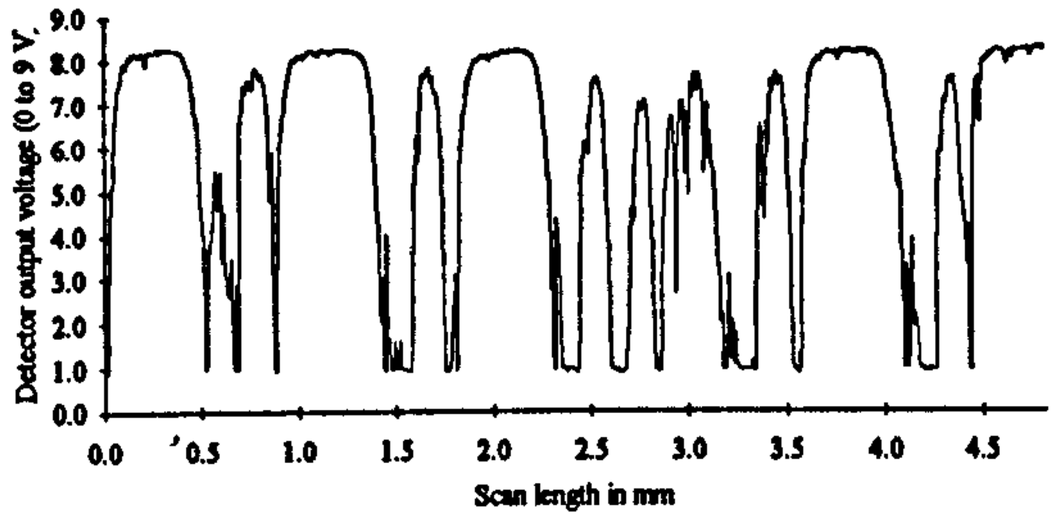

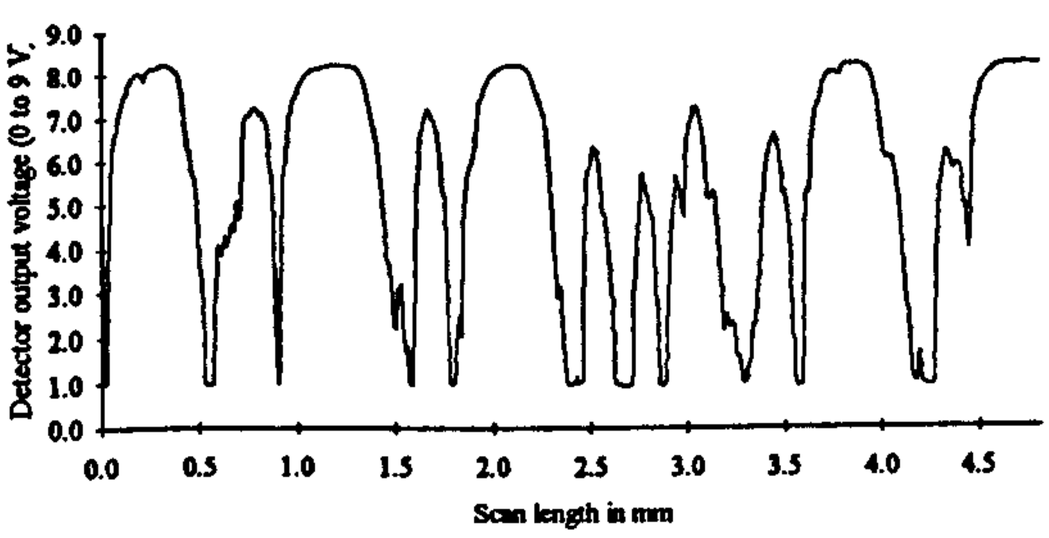

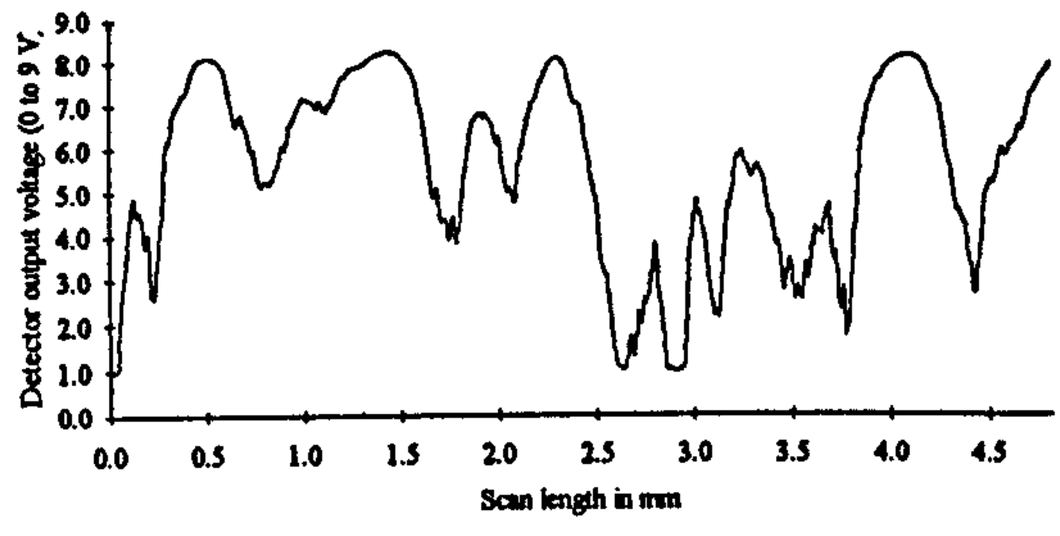

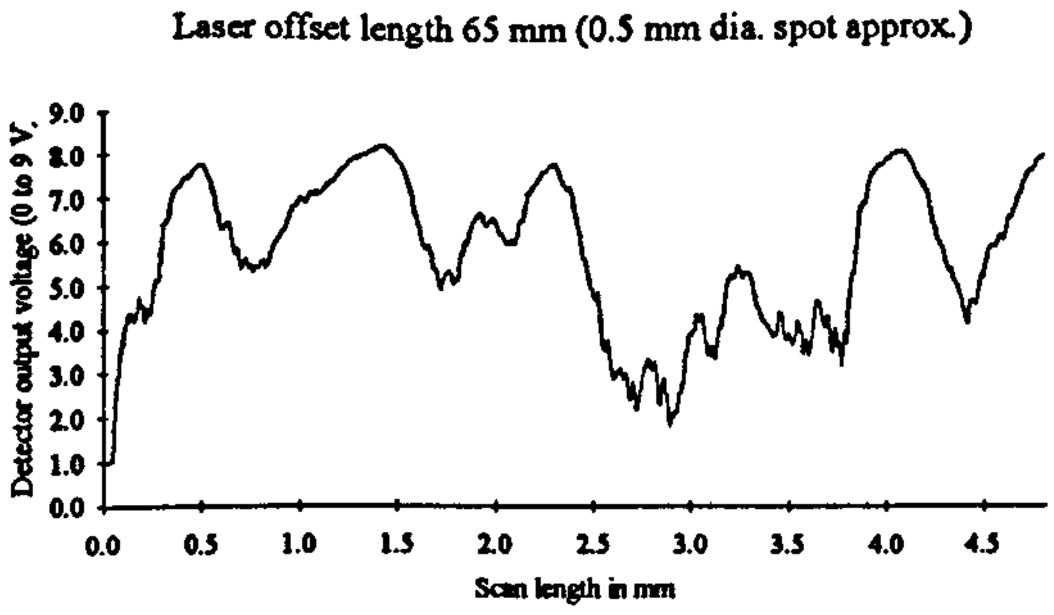

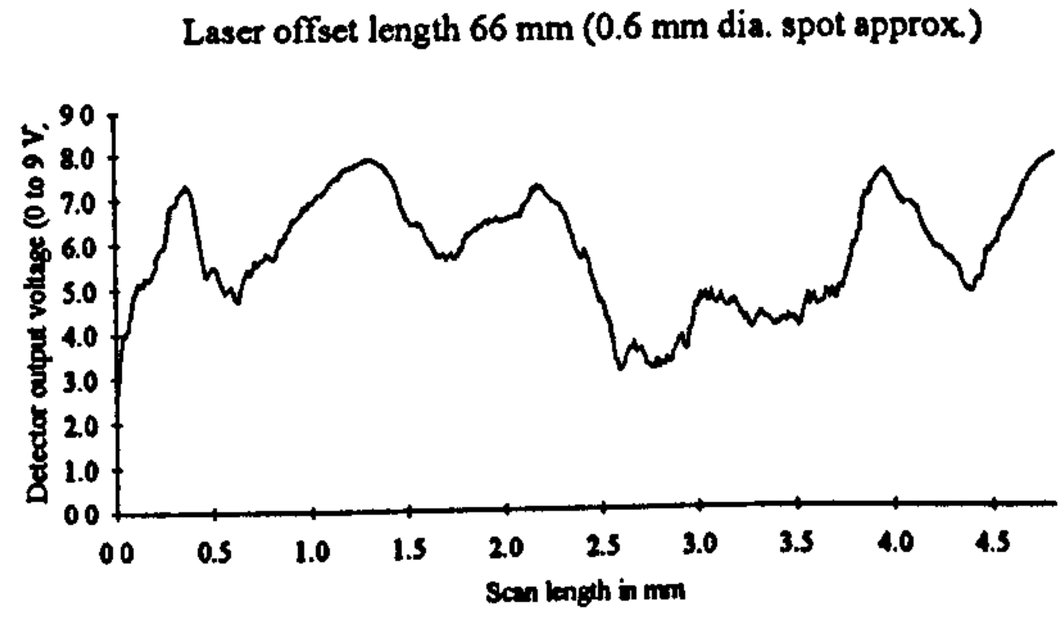

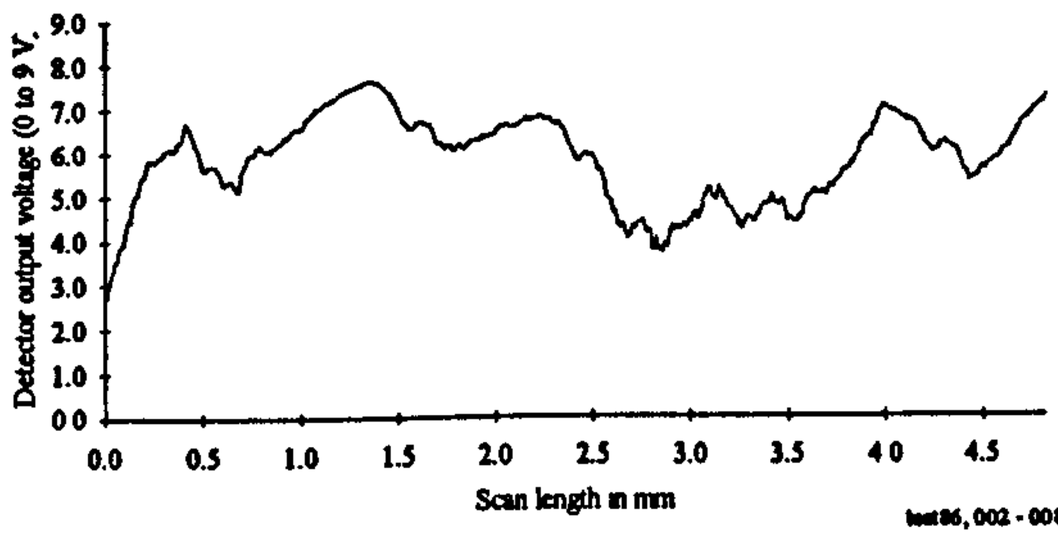

This space is intentionally blank

Sufficient results obtained

Figure 5-117 The effect of laser spot size on defect detection (12.5 μm End mill control sample with scratch defect)

5.2 Laser-based cutting tool condition monitoring

The main thrust of the research activities was to develop a fundamental understanding of the V-scanner laser based inspection technique aimed at a specific application to cutting tool condition monitoring. Some of the central aspects which govern the sensitivity, repeatability and reliability of the laser scatter principle have been investigated in the preceding sub-sections. The series of tests undertaken clearly illustrated that response results could be optimised, provided that critical parameters (such as spot size and viewing angles) were formulated correctly. In an attempt to verify the experimental work undertaken and transform it from a laboratory to a practically applied base, the following work was undertaken.

5.2.1 Optimised system configuration for monolithic cutting tool inspection

During the investigation a range of cutting tools (monolithic and insert) and discrete inserts were inspected using the apparatus described in Chapter 4.0. In the latter stages of the work, however, improved response results and an increased reliability were achieved. This was largely due to the inspection system configuration being latterly based around the knowledge gained from the extensive tests performed on the surface topography inspection device (presented and discussed in the early subsections of Chapter 5.0). Thus the trial and error or best guess approach were no longer a necessary practice.

The modified two-axis inspection device allowed the results of the earlier work to be implemented and proven, at a practical level, on the sample range of tools.

The three monolithic cutting tools which were chosen as a proving ground for the transfer of the test results for laser/detector angle and laser spot size are illustrated in figure 5-118 below; Top - Slot drill # 1, Middle - Slot drill # 3, Bottom - Slot drill #2. The figure clearly illustrates the similarity in form but different diameters and/or flute helix angles for the range.

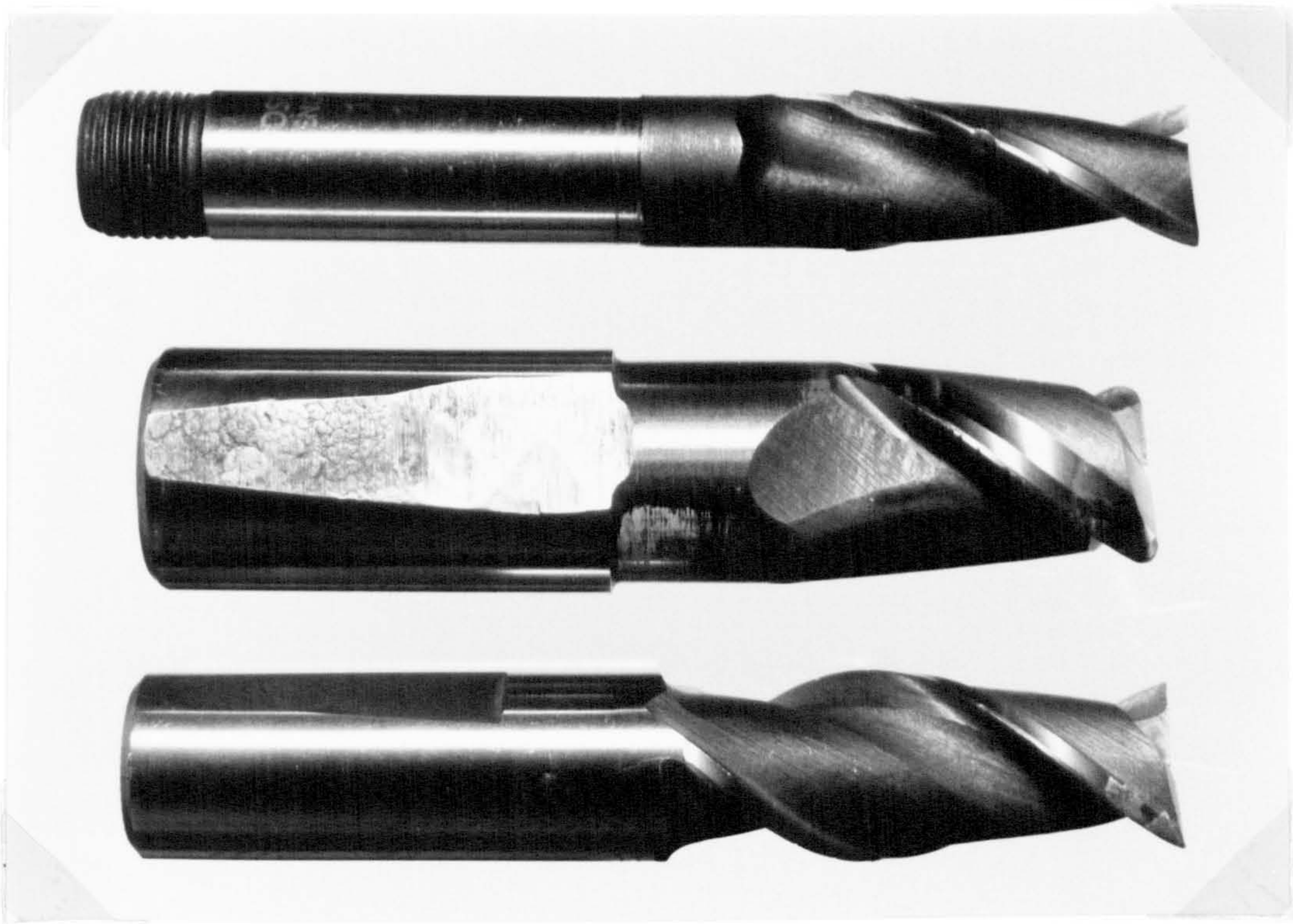

Figure 5-118 The sample range of monolithic cutting tools

The cutting tool geometric variations are tabulated, below;

Tool identification number	Diameter (mm)	Depth of cut (mm)	Flutes	Flute helix angle (°)
1	18	34	2	28
2	18	50	2	38
3	23	30	2	37

Table 5-20 Sample cutting tool geometrical data

Equally important to the work undertaken was the fact that each tool exhibited one or more defects of differing type and severity. The defects are identified and illustrated in the following paragraphs and are associated with specific cutting tools. The inspection results for each of the three tools are also introduced and discussed below.

Monolithic cutting tool #1

The results of the incidence and reflection angle tests were initially consulted so as to determine the optimum angles for this application (1.6 μm ground sample: laser 60°, detector 30°). The look-up tables proved extremely useful and were simple to use with information being extracted easily. Furthermore, the laser spot size was anticipated to offer best scanning results when at 0.5 mm diameter (See concluding comments of sub-section 5.1.4). For this system configuration the laser/detector angles would produce a signal with full form and saturate only at the site of an extremely severe defect. The laser spot size however was chosen to smooth the captured data by reducing the high frequency component. This made the form of the signal more apparent and the important defect elements more pronounced. A further software based high frequency filtering procedure was also applied to the data in order to remove an increased level of the high frequency noise. The figures below illustrate the striking effect this operation had on improving signal quality for defect detection purposes.

The raw signals for the tool are shown in the figure below.

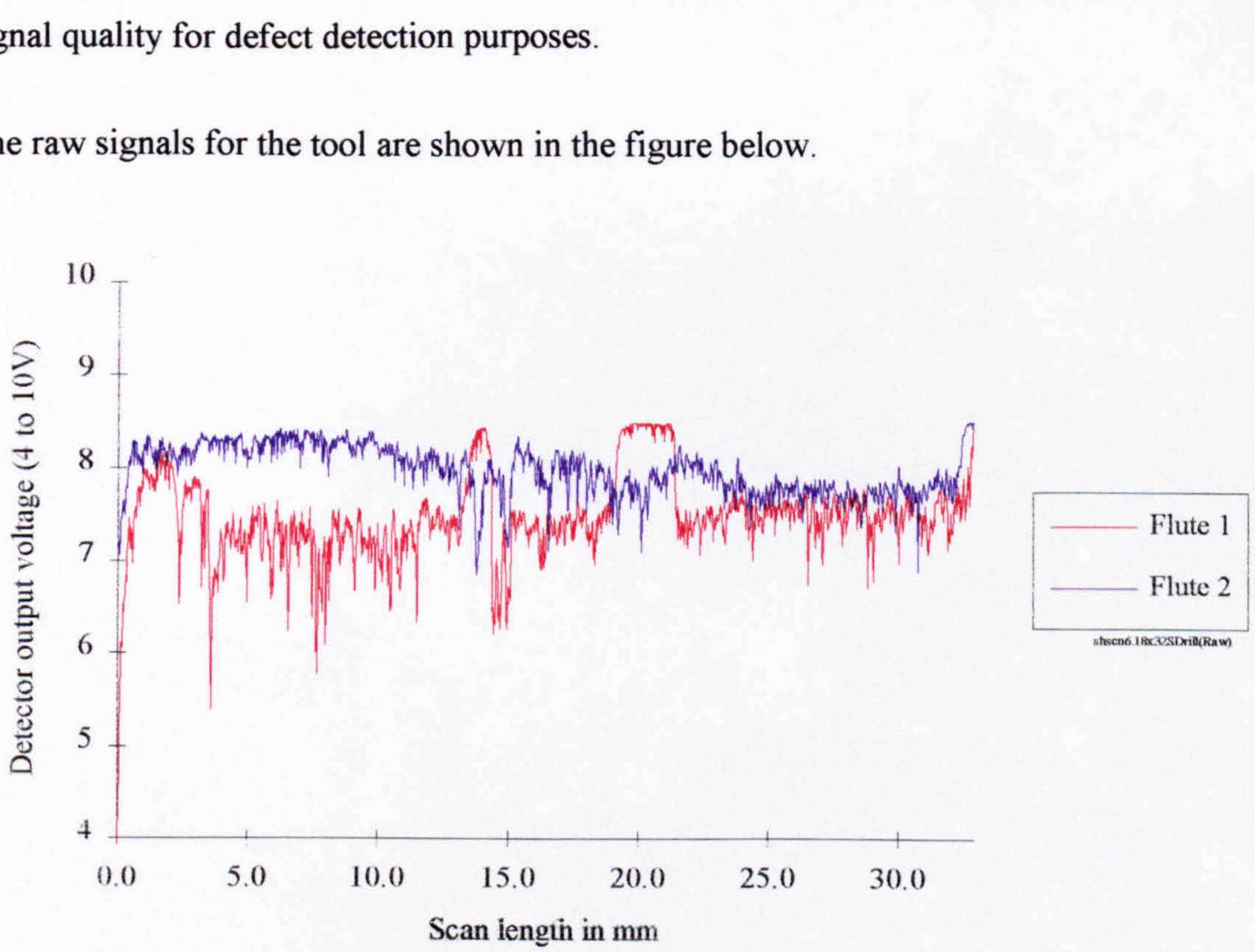

Figure 5-119 Raw signal for monolithic cutting tool 1

To improve the overall signal quality by reducing the spiky nature of the raw signal a moving average function was applied to the captured data sets. The effect of the moving average function (encompassing ten data items) was to smooth the signal and thus act as a software based high frequency blocking filter. As a consequence of this operation the general form of the resultant signal became far more evident, as can be seen in the figure below which is based on the same data as that for the previous figure.

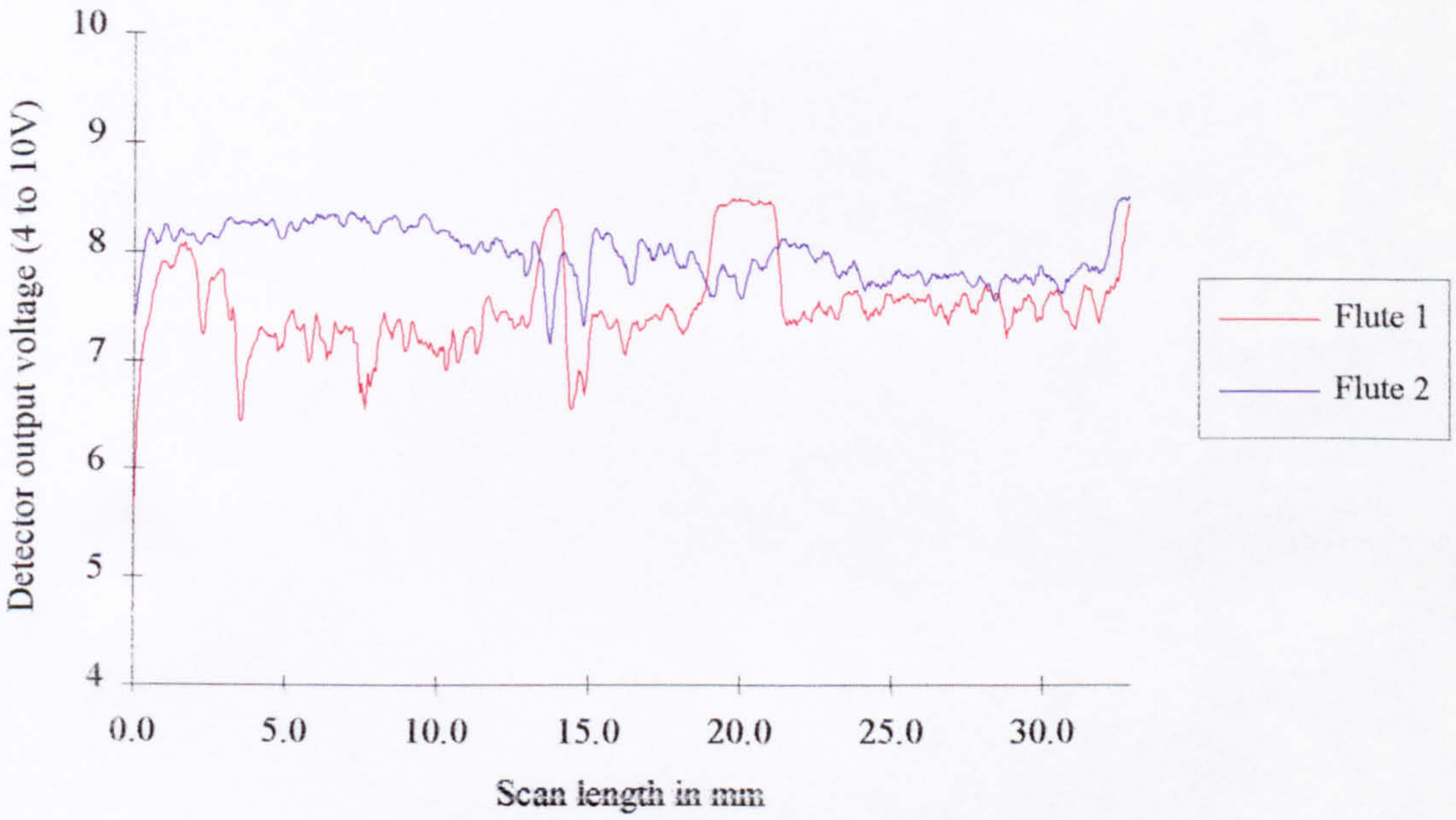

Figure 5-120 Smoothed response signals for cutting tool 1

The jagged high frequency nature displayed by both flute signals, in the figure above, is typical of that for a ground surface. The grinding marks which are still visible on the flank (scanned) edges of the cutting tool are thus easily detected by the inspection system. To dampen the effect of the ground surface signal a broader high frequency blocking filter must be applied. At this stage it is far more desirable to filter the signal by software means as the level of filtering can be varied to suit, whereas a hardware based filtering action, achieved through increased laser spot size, would produce irreversible effects with high frequency signal components being irretrievably lost. Initial detection of surface texture, perhaps through measuring high frequency content in the signal, could be followed by a further smoothing operation prior to defect detection. An approach which could not be

achieved if the signal been initially smoothed further, by an increased laser spot size. In its simplest form a moving average mathematical function offers a simple but effective means of software based signal smoothing/filtering. The degree of smoothing is dependent upon the number of data items which form the moving average data set. A weighting of ten has been applied to all the following examples and is seen to be appropriate.

A pictorial representation of cutting tool one is shown in the figure below. Each of the significant defects associated with this cutter are illustrated by a photograph and referred to on the tool illustration. By this means, the general position of the cutting edge defects are established prior to the scans being presented graphically and discussed.

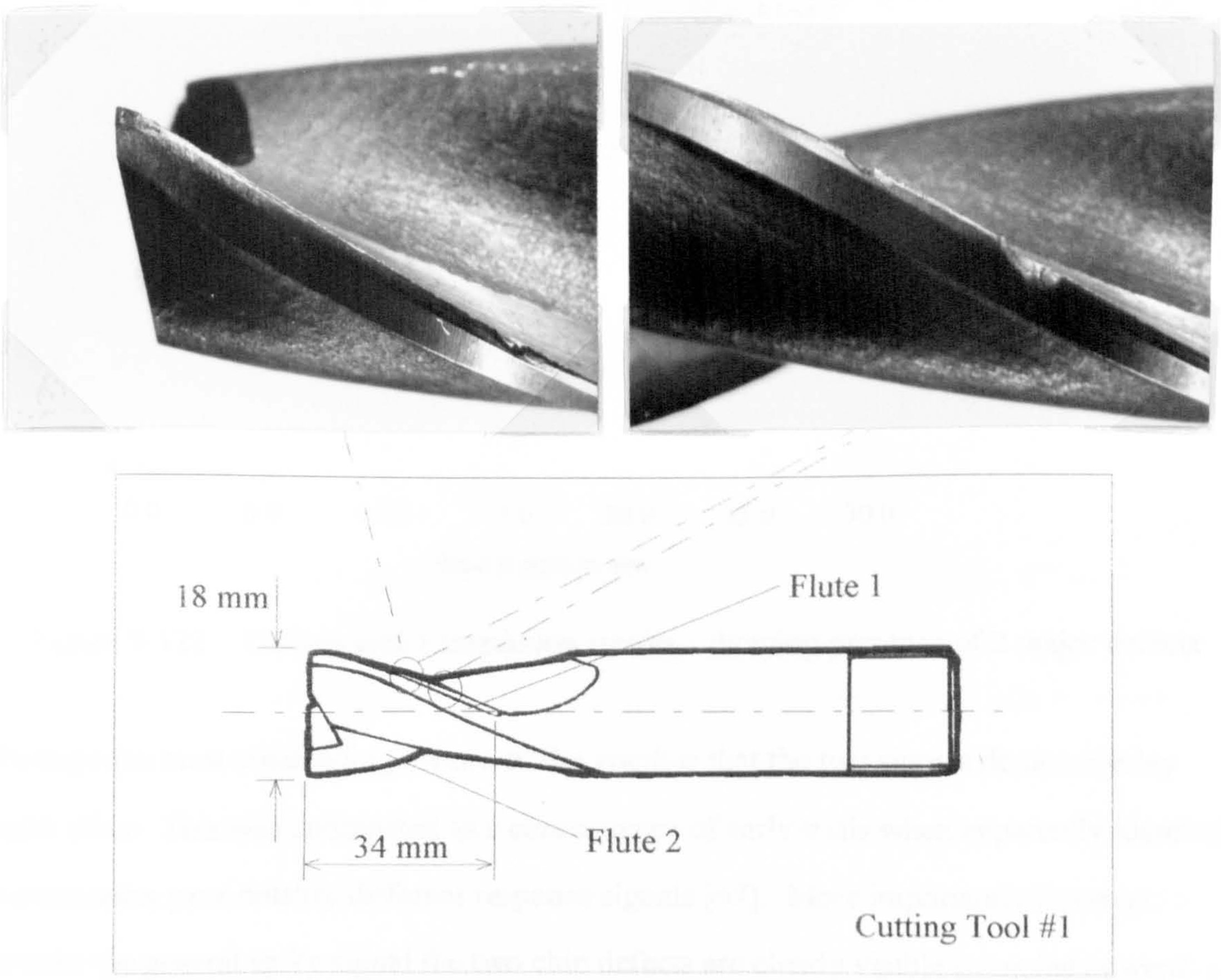

Figure 5-121 Cutting tool 1 showing defects and defect locations

The optical system settings used were:

Laser Angle	60°
Detector Angle	30°
Laser spot size	0.2 mm (Cutting tool datum detection)
Laser spot size	0.5 mm (Cutting tool inspection)

The inspection signals captured for each of the two cutting edges (Flutes) are shown in the figure below. Both are full form signals. The lead-in and lead-out of the cutting edge signals are evident at the extreme ends of each trace.

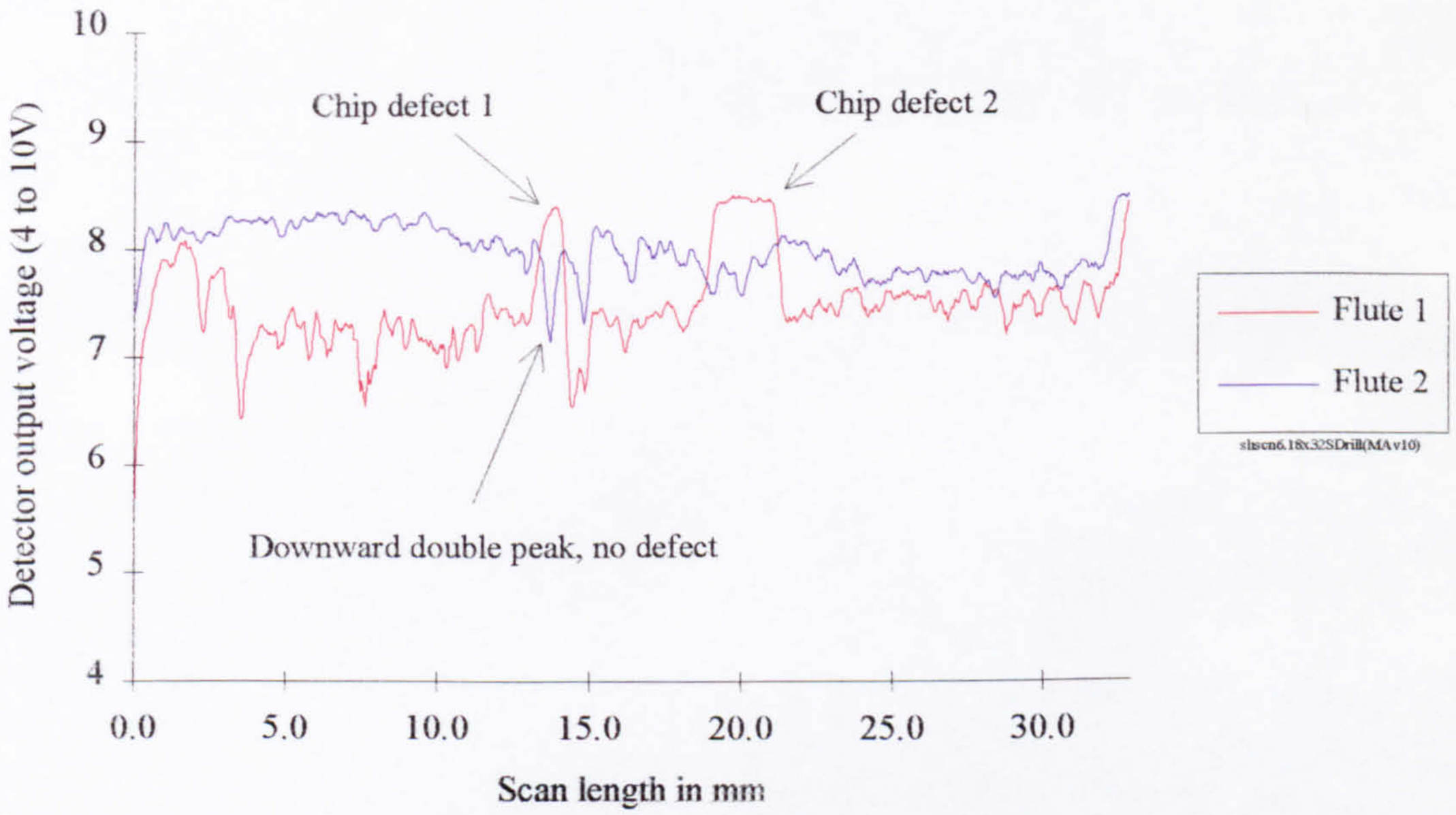

Figure 5-122 Cutting tool 1 inspection results - showing presence of 2 major defects

Perhaps the most outstanding feature of the graph is that the two signals do not overlay each other. This was anticipated as a consequence of early trials when apparently identical components gave notably different response signals [47]. More importantly however, amidst the general spiky signal the two chip defects are clearly visible (rounded upward jutting peaks, centred on 13 mm and 20 mm).

To justify the selected settings for the test presented above, the same test was repeated but for a slightly different laser and detector configuration. Laser and detector angles of 50°

and 30° respectively were applied with the spot size maintained at 0.5 mm. The following graphical results were obtained.

The optical system settings used for this test were:

Laser Angle	50°
Detector Angle	30°
Laser spot size	0.2 mm (Cutting tool datum detection)
Laser spot size	0.5 mm (Cutting tool inspection)

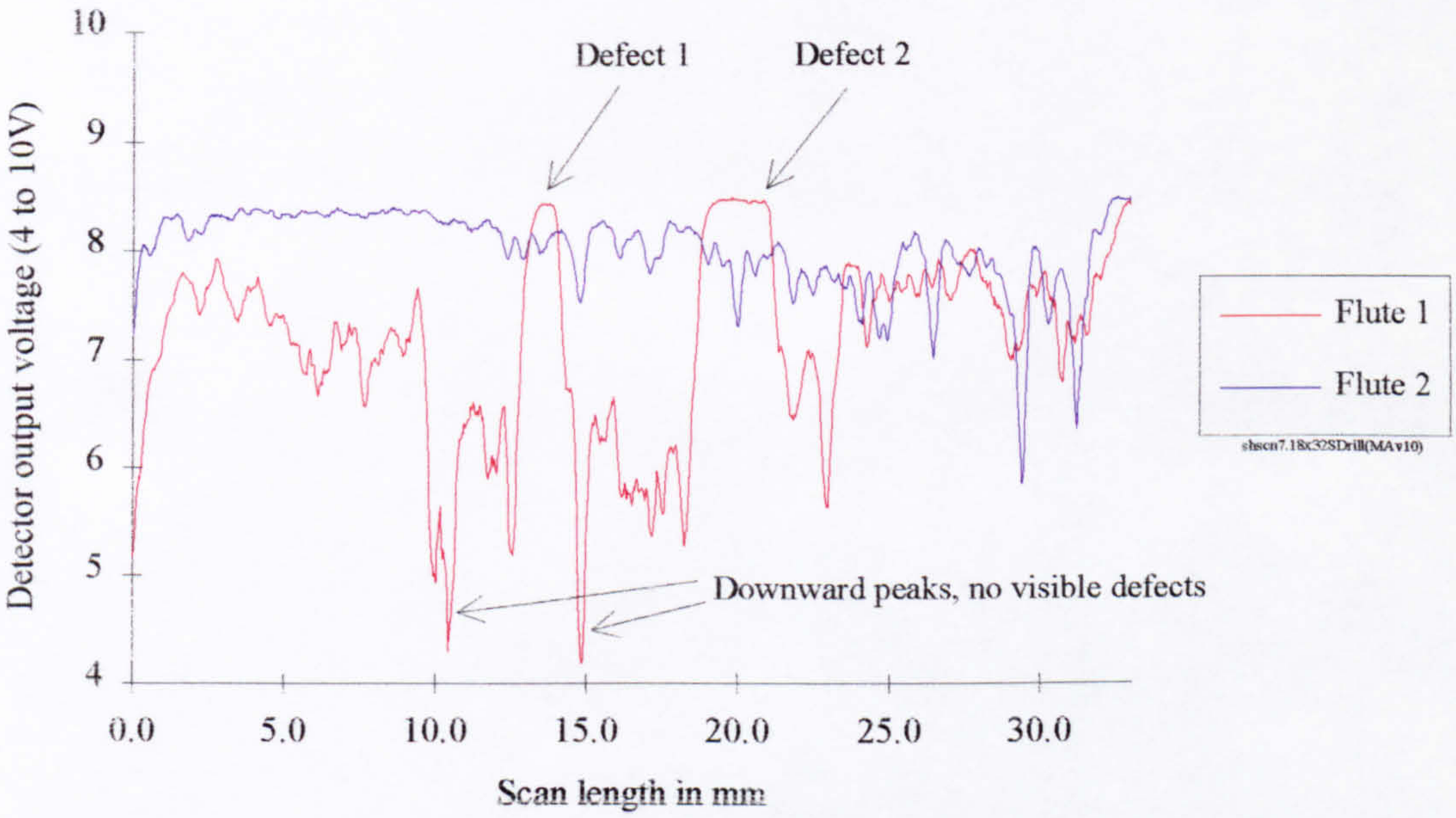

Figure 5-123 Cutting tool 1 inspection results - reduced laser angle 60° to 50°

The most significant difference in the form of the signals are their spiky/jagged nature. The sharp, downward jutting spikes which constitute a major part of both traces would create severe difficulties when subsequent signal processing were applied and attempts made to detect and delineate cutting edge based defects. The typical signal characteristic associated with a narrow scratch/chip defect is not unlike the deep spikes prevailing in the above figure (see the results for cutting tool 2). Due to this observation alone the above inspection system configuration was considered inappropriate.

A further revision was made to the settings of the inspection system in an attempt to further justify those originally prescribed and to underpin comments already made on the response/nature of the laser scanning system. With the laser and detector angles returned and fixed at 60° and 30° respectively the laser spot size was increased to 0.6 mm. It was anticipated that the larger spot size would smooth the signal and reduce the sensitivity towards the information contained within it. The following graphical results were obtained which support the prediction.

The optical system settings used for this application were:

Laser Angle	60°
Detector Angle	30°
Laser spot size	0.2 mm (Cutting tool datum detection)
Laser spot size	0.6 mm (Cutting tool inspection)

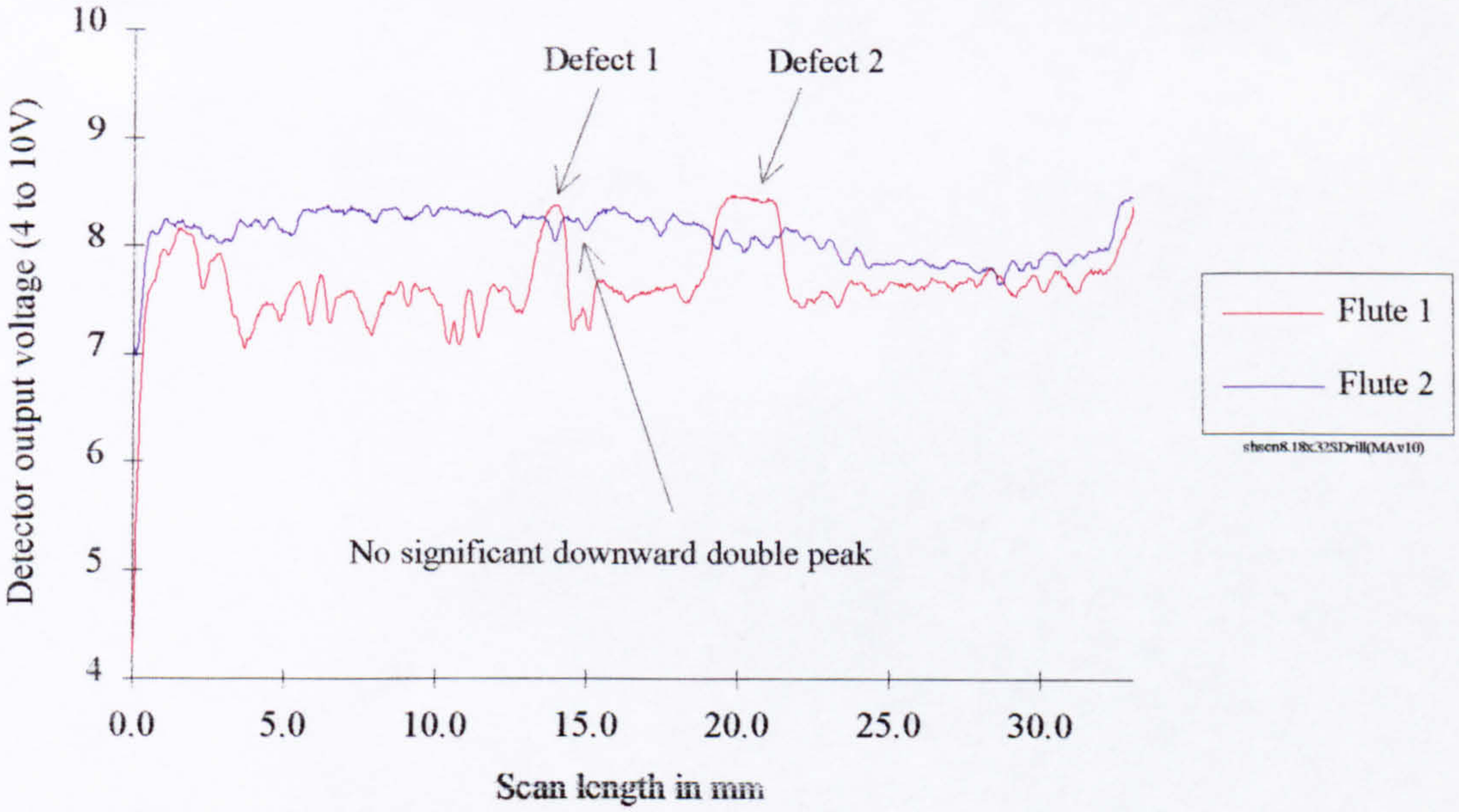

Figure 5-124 Cutting tool 1 inspection results - increased laser spot size

When compared to the first of the three main graphs (figure 5-122) the above figure bears strong similarities. The most notable difference is the lack of the downward jutting double peak centred at 14 mm on flute two, which is most prominent in figure 5-122. Other

downward extending peaks are also seen to be suppressed in the above figure when inspected more closely. As a direct consequence of this, the latter settings would prove to be more suited to the detection of defects of this particular scale/magnitude but at the expense of reduced small-scale surface detail.

The three tests presented above once again illustrate the sensitive nature of the laser scanning system. However, it is now clearly apparent that when crucial settings are optimised response results are obtained which contain significant information pertaining to cutting tool edge quality and integrity. Subsequent processing and analysis through defect detection, delineation and identification can be dramatically aided by the initial system configuration. Furthermore, as a consequence of this work it is immediately apparent that for the majority of trial and error configurations, defect detection would be inefficient and, in the extreme, impossible. This situation would be entirely due to poor response signal quality as a result of inappropriate system configuration.

Defect detection - cutting tool #1

As discussed in Sub-section 4.1.3, one of the most widely used and simple, yet largely reliable, methods of defect detection is thresholding. To illustrate this defect detection process the response results for cutting tool number one were manipulated in the following prescribed manner. Initially the signal was conditioned to remove gradual variations due to local changes in surface reflectivity and flatness. This was achieved through polynomial curve fitting with regression. The effect of this process is shown in the graph below.

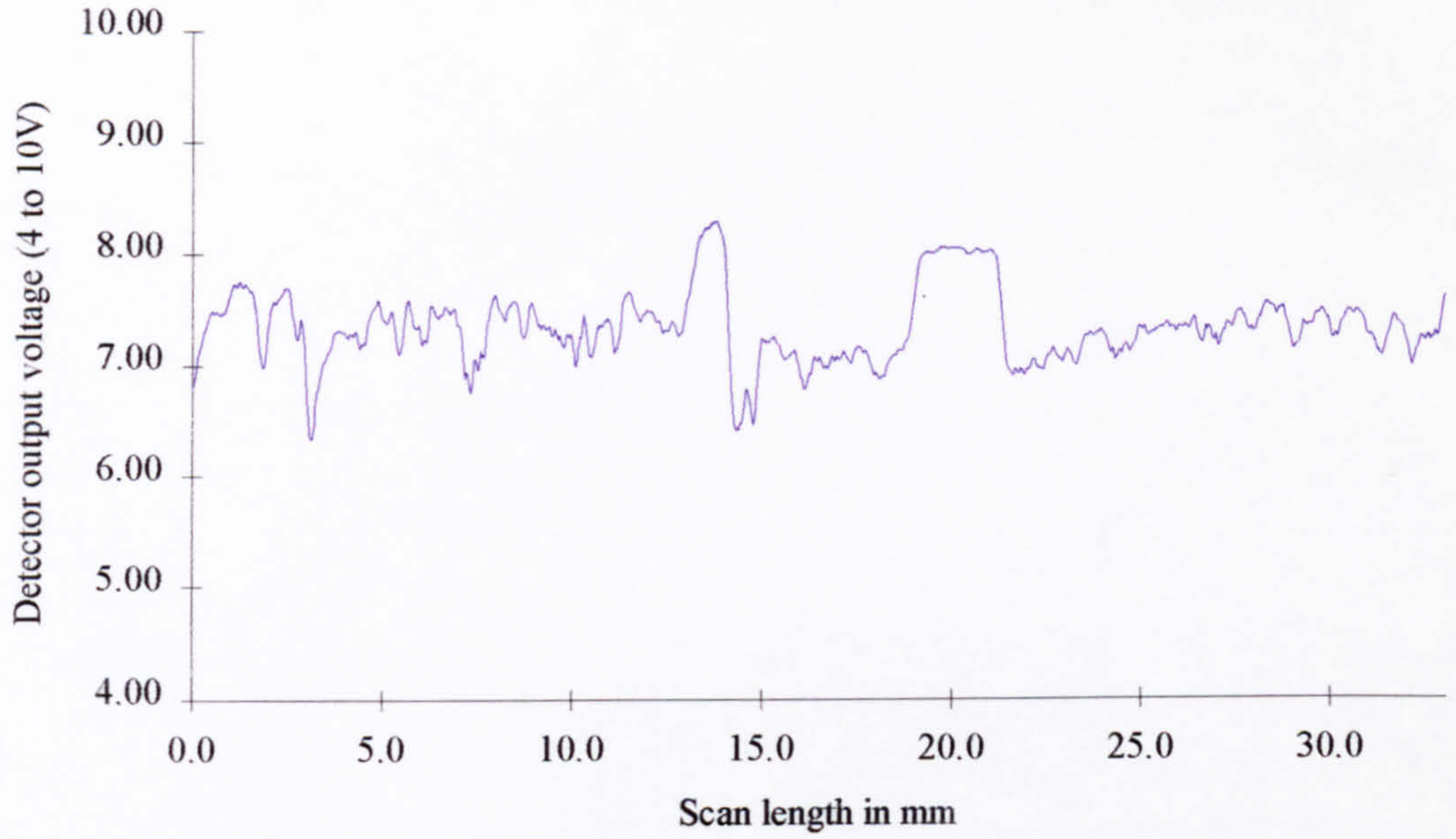

Figure 5-125 Polynomial curve fitting with regression for signal flattening - Flute 1

With the objective of defect detection, the thresholding technique can be subsequently applied to the data resulting from the curve regression signal processing phase. For this example a threshold equivalent to ±0.6 Volts (Y-axis graph scale units) on the overall signal average has been arbitrarily applied.

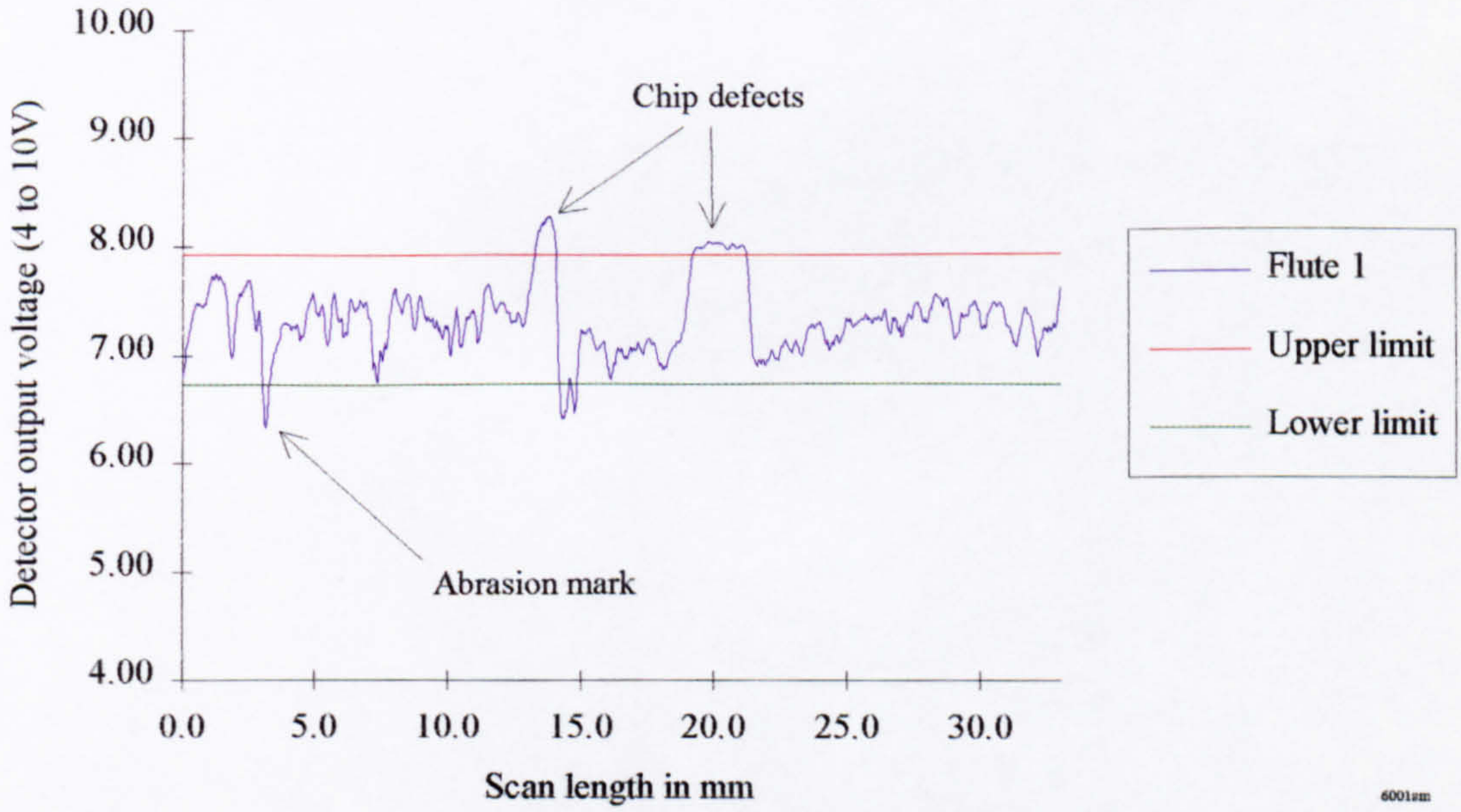

Figure 5-126 Defect detection by way of curve regression and thresholding

(Cutting tool 1, Flute 1)

With reference to the previous graph, the response signal extends outside the limit of the upper threshold at the locations of the two chip defects. By virtue of this, the defects are detected. Additionally, the response breaches the lower threshold at the site of a small cutting edge abrasion. This surface mark was not considered relevant, however, it is natural and acceptable for the system to detect such features as a part of the tool screening process (discussed earlier in Sub-section 3.3.2).

For an automated, commercial application the true magnitude of the threshold would have to be established by thorough investigation.

When applied to the second flute of cutting tool 1, the same process yielded the following results.

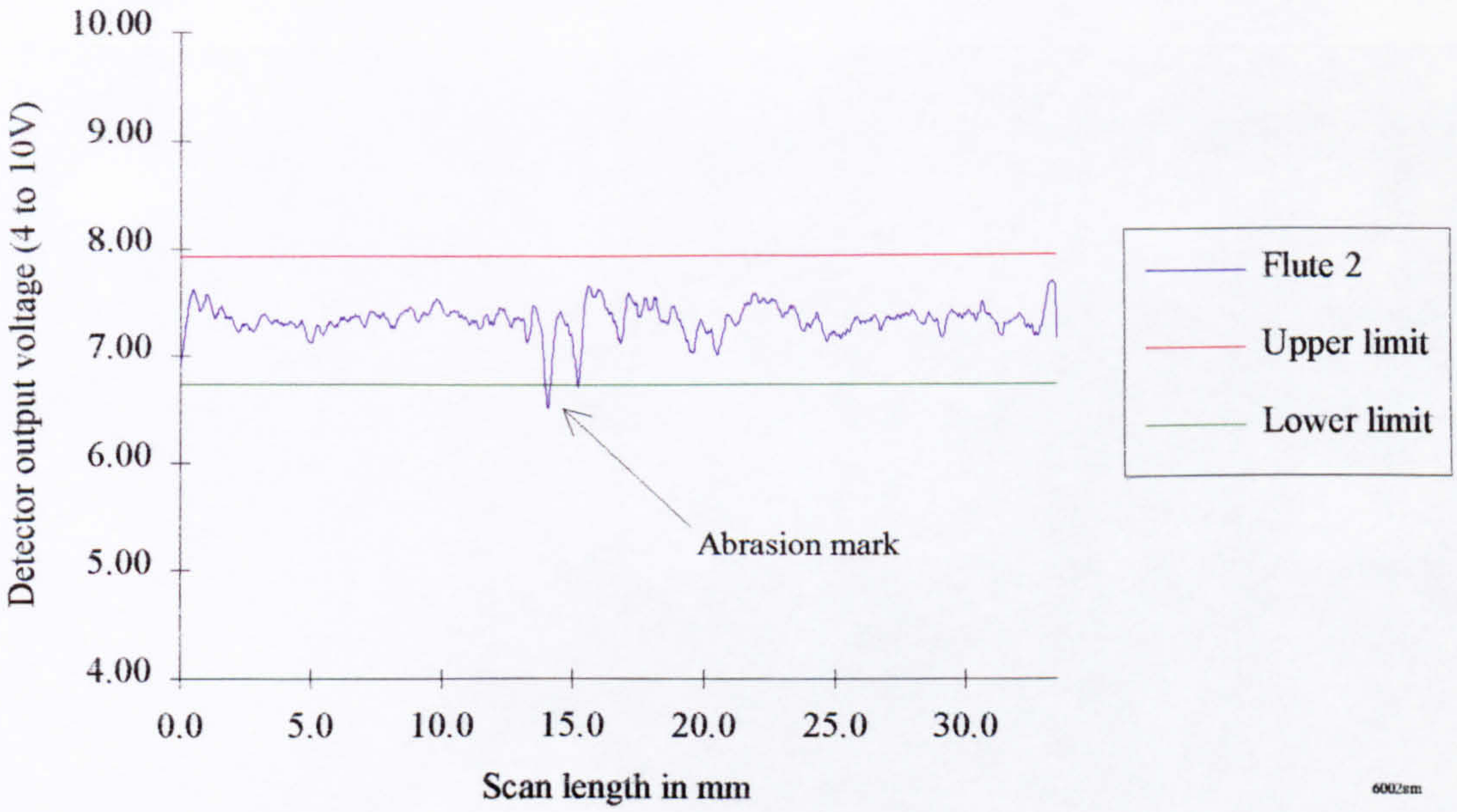

Figure 5-127 Defect detection by way of curve regression and thresholding

(Cutting tool 1, Flute 2)

Again, an insignificant cutting edge abrasion was the only feature to be detected in the above graph. For the same reasons as mentioned previously, this would not cause concern in the overall screening program. Most importantly, no defects went undetected on either of the inspected cutting tool flutes.

Monolithic cutting tool #2

As for cutting tool number one, a range of three different system configurations were applied to the second cutting tool during the work undertaken. Despite being of the same diameter as that already previously tested, cutting tool 2 differed considerably in that it was far longer and possessed an increased helix angle. Furthermore, the defects which it exhibited were significantly different to those already observed on the previous tool. Two built up edges (BUE) were the most pronounced defects, one at the leading edge of each flute tip, and a small chip in the first flute approximately 27 mm into the scan. Other minor defects and surface irregularities existed but were not considered relevant at this level [62]. A pictorial representation of the cutting tool is shown below with the defects highlighted and their location on the tool identified.

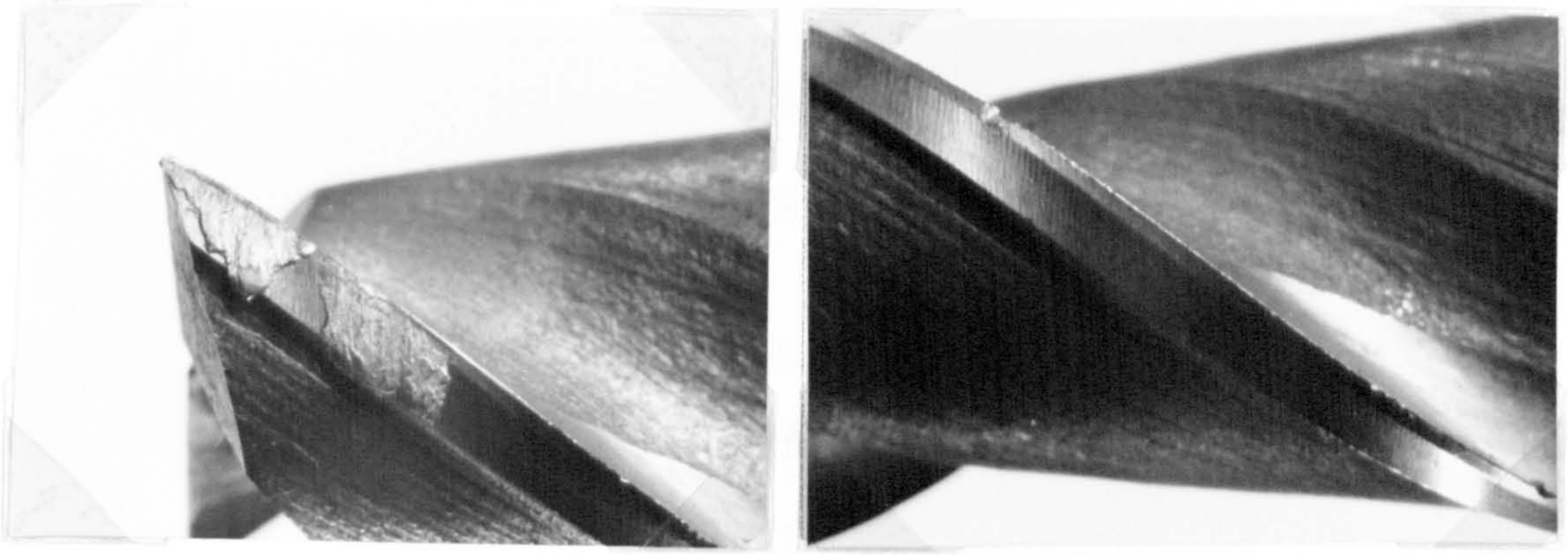

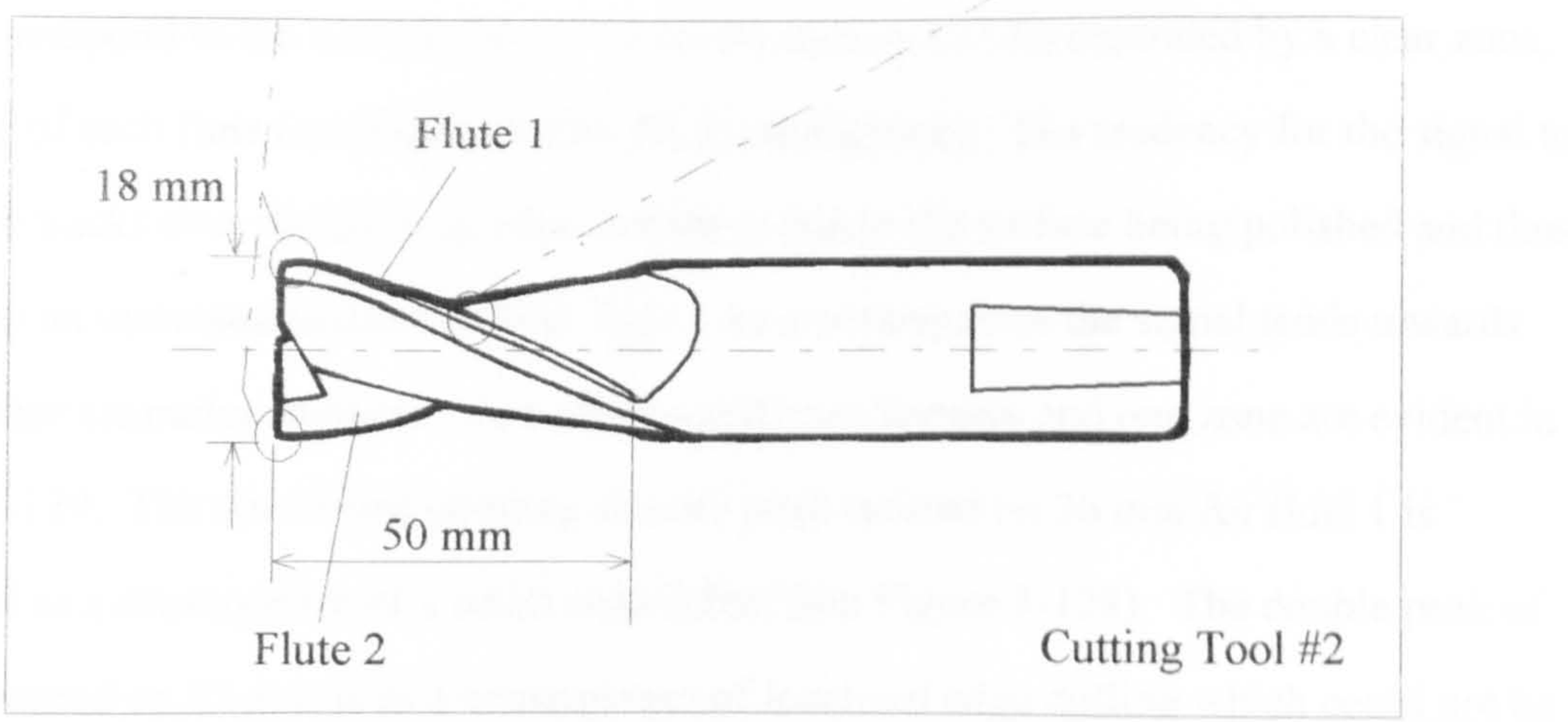

Figure 5-128 Cutting tool 2 showing defects and defect locations

With laser and detector angles configured as per optimum results for the 1.6 μm Plain ground sample and laser spot size 0.5 mm, the two flutes were scanned. The graphical results of the tool inspection are shown in figure 5-129, below.

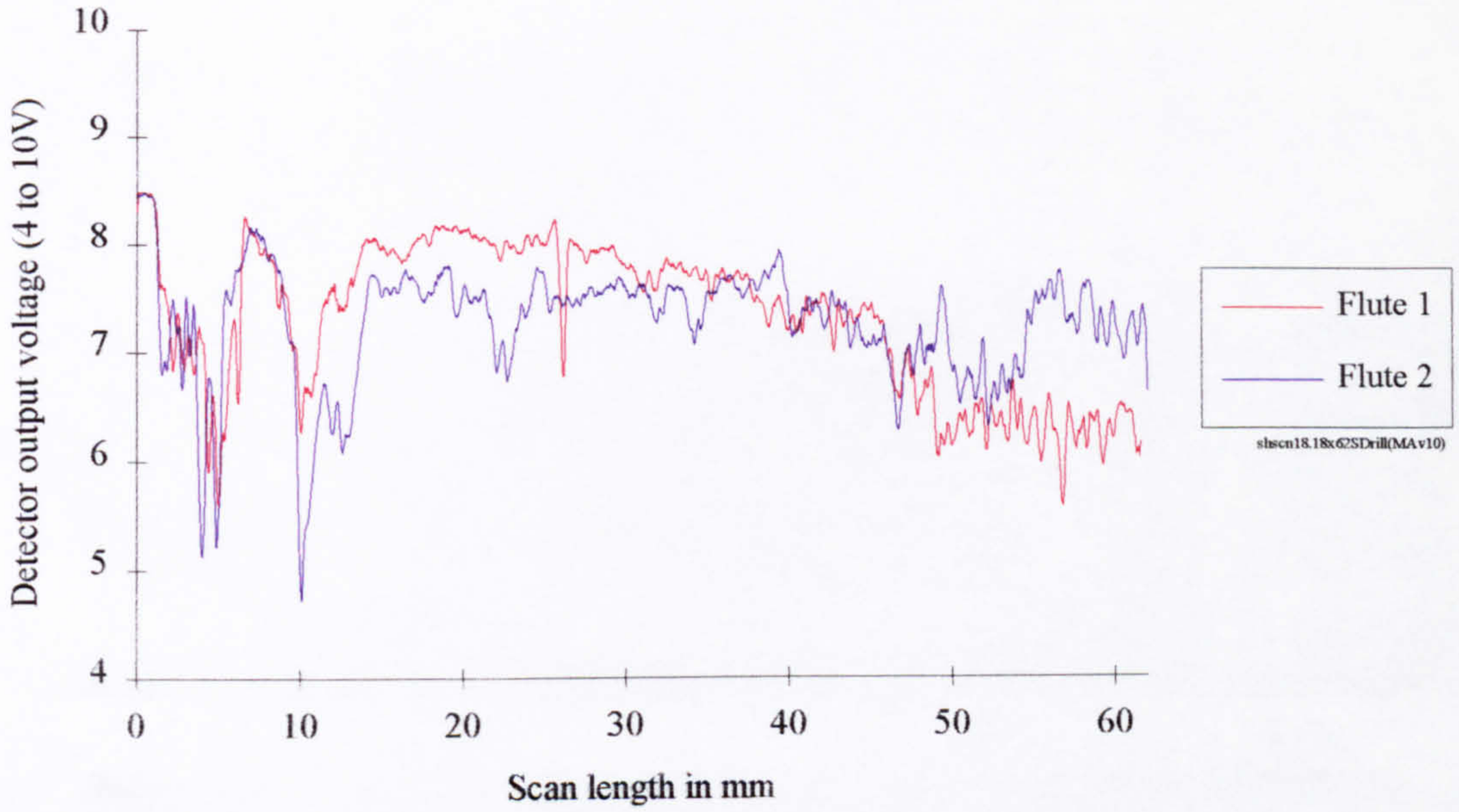

Figure 5-129 Cutting tool 2 inspection results - showing presence of 3 major defects

For both flute response signals the built-up edge is visible and can be easily identified, in this case, by steep sided downward jutting peaks. Two clusters of peaks are evident for both flutes, one centred on 4 mm and the other on 10 mm approximately. The double peaks correspond to the two patches of fused aluminium (BUE) separated by a clear zone, at the tip of each flute (see Figure 5-128, BUE photograph). The tendency for the signal to drop as it tracks over the built-up edge defects is due to the surface being polished and thus reflecting an increased amount of laser light. As a consequence the signal tends towards the detector saturation confine. Two other significant features and one zone are evident in Figure 5-129. The downward pointing slender peak centred on 26 mm for flute 1 is produced as a consequence of a small chip defect (see Figure 5-128). The double peak of flute 2 centred on 23 mm is as a consequence of localised edge dulling which could not be photographed due to its subtle nature. It was anticipated that this surface defect would not significantly degrade cutting-tool performance and so would not require detection. The

zone common to both flute signals extending from 46 mm to 62 mm is characterised by an increase in amplitude of the general signal. It was thought after close scrutiny of the cutting edges, that the tool may have been used in cutting operations up to that particular depth of cut (36 mm or 46 mm measured along the flute). As a consequence, the surface grinding marks on the cutting edge were polished at regions where cutting had taken place, leaving relatively pronounced surface grinding marks at unused regions (scan length 46 to 62 mm).

The following repeat tests were undertaken with associated results shown:

For a laser and detector arrangement of 60° and 40° respectively and a decreased laser spot size 0.4 mm, the results of figure 5-130 were obtained.

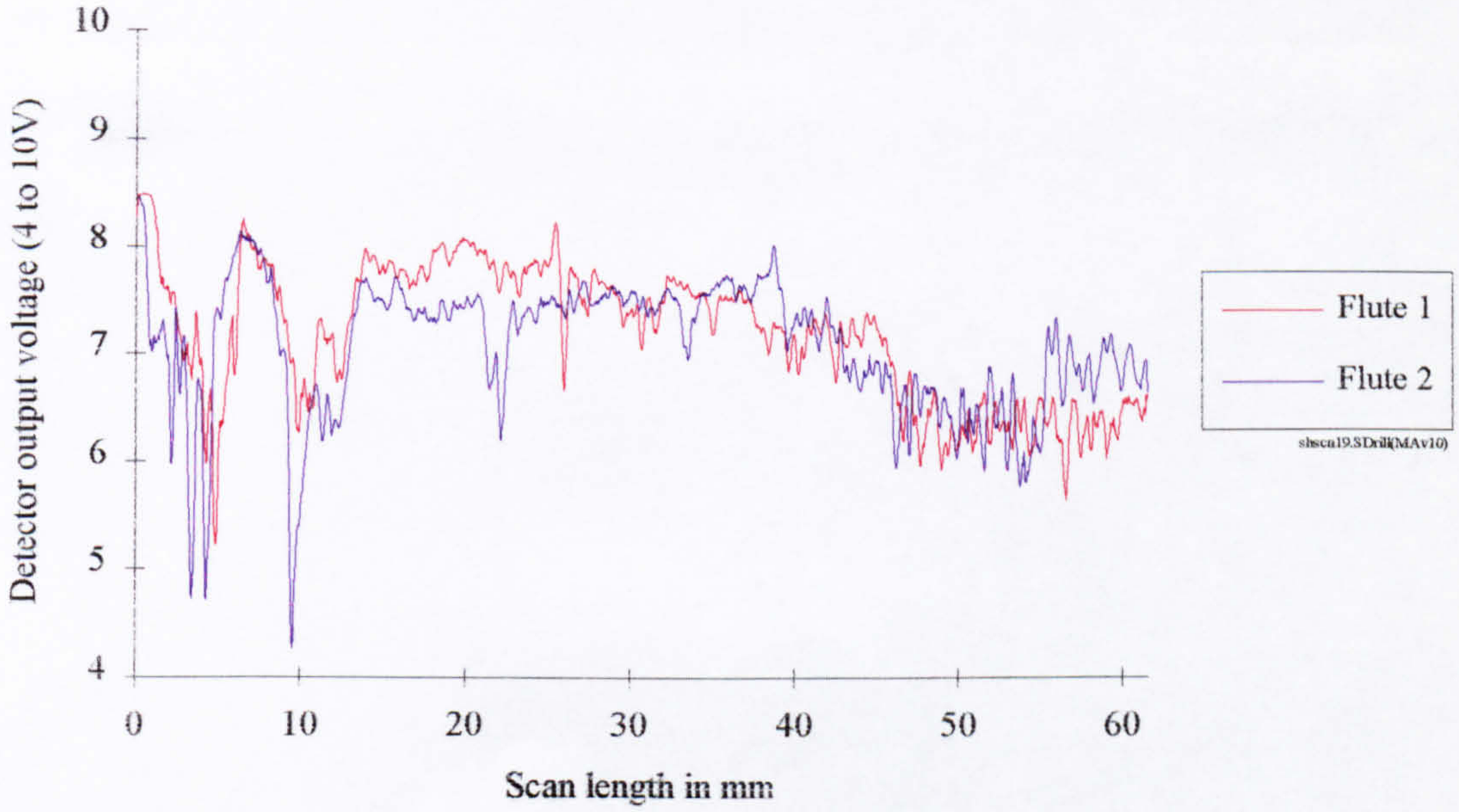

Figure 5-130 Cutting tool 2 inspection results - decreased laser spot size

For a laser and detector arrangement of 60° and 40° respectively and an increased laser spot size 0.6 mm, the results of figure 5-131 were obtained.

Subtle differences exist between the three graphs, however, the results of the first graph are well proportioned and can be readily applied to the screening process.

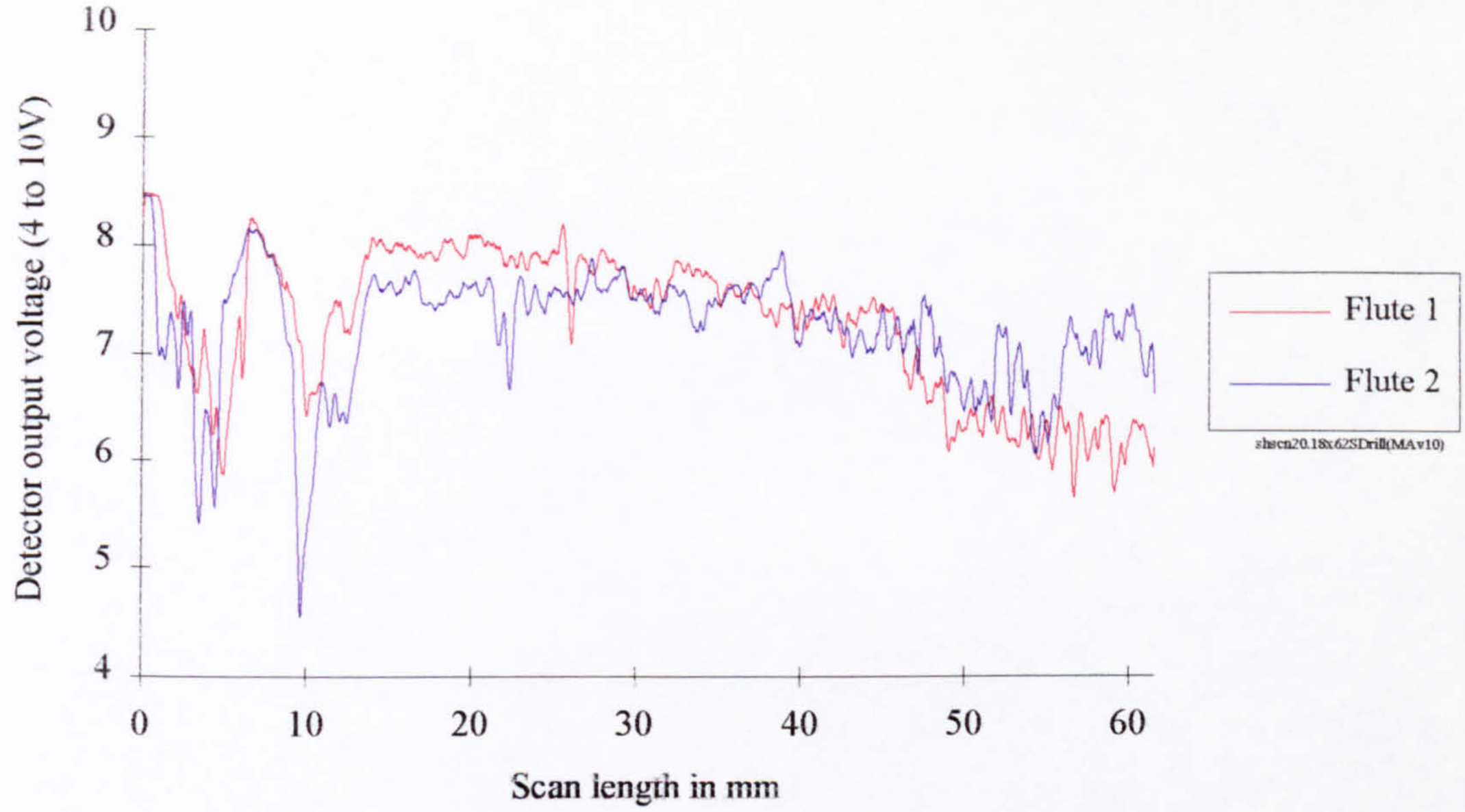

Figure 5-131 Cutting tool 2 inspection results - increased laser spot size

Defect detection - cutting tool #2

The aforementioned process for defect detection was applied to the data presented in figure 5-129 above. The results after curve regression are presented below.

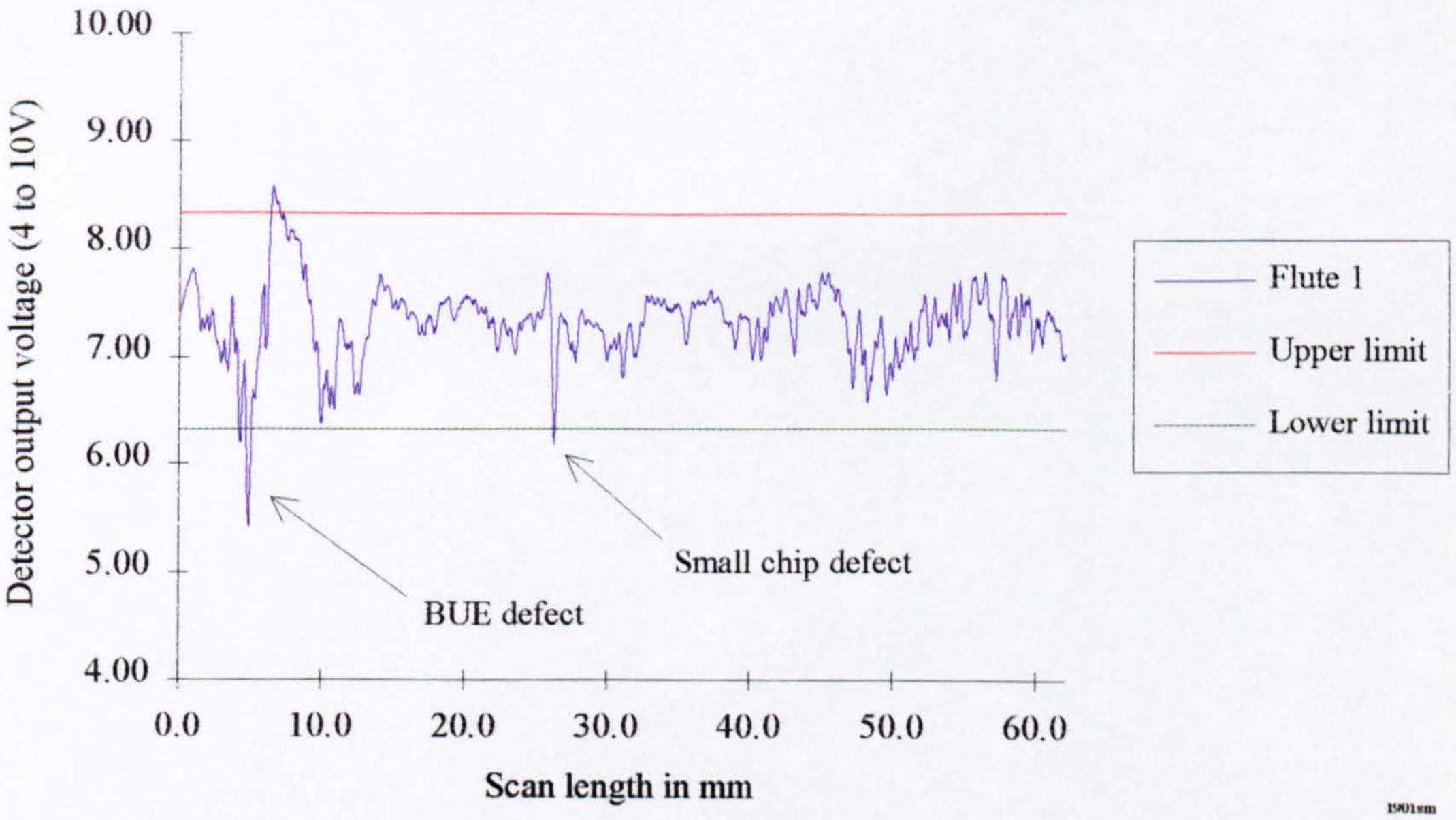

Figure 5-132 Defect detection by way of curve regression and thresholding

(Cutting tool 2, Flute 1)

An arbitrary threshold of ±1 Volt was used in this example. Both of the previously identified defects are located (Built up edge and small chip).

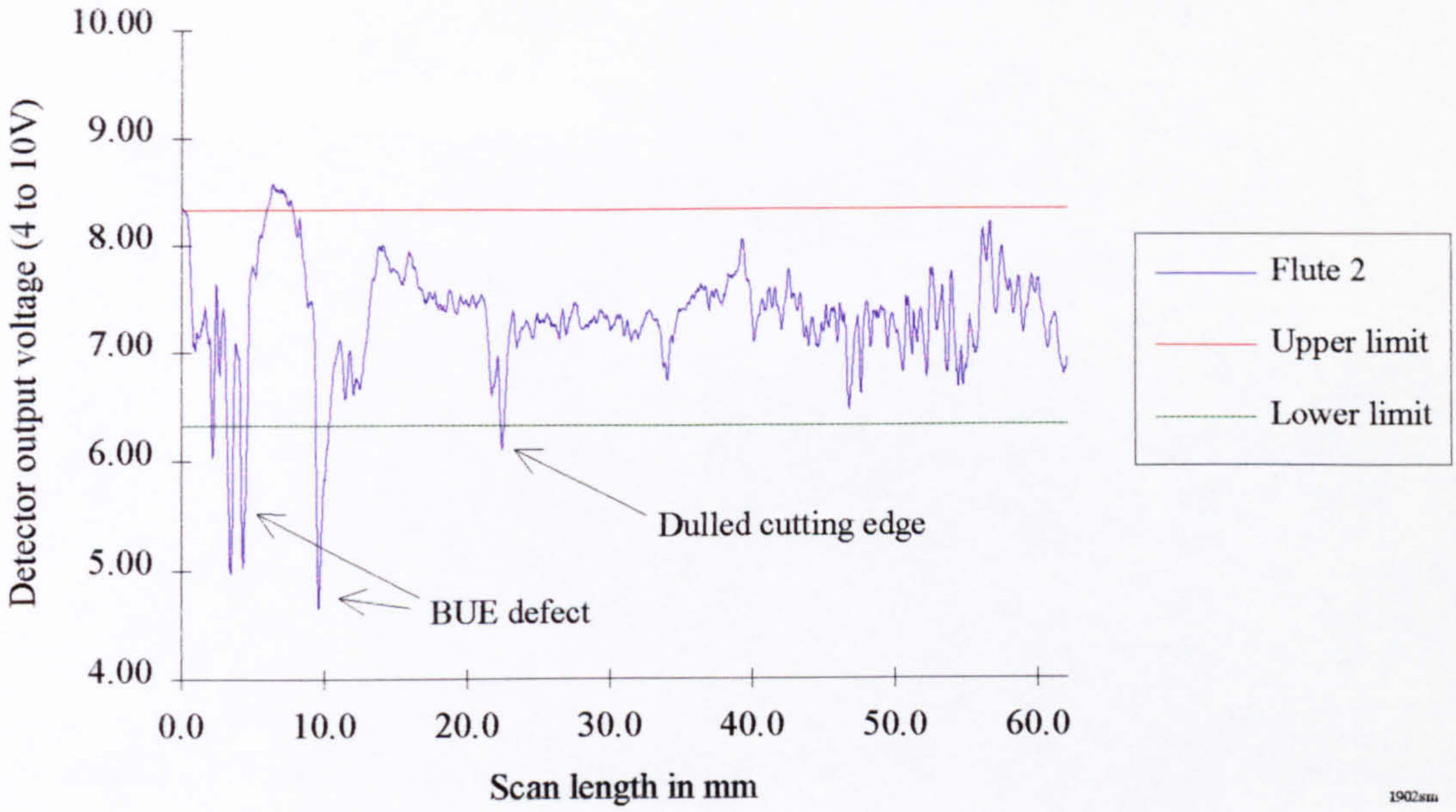

Figure 5-133 Defect detection by way of curve regression and thresholding (Cutting tool 2, Flute 2)

Again with the same threshold applied, to the second flute of the same tool, the BUE defect was detected. In addition to this a further defect, not identified by manual inspection, was also located. Closer observation revealed localised dulling of the cutting edge.

As stressed in earlier discussions of the defect detection process, it was considered vital that the system was able to locate all relevant defects. In order to achieve this goal it was anticipated that a number of defects which may be considered insignificant to the tool condition at this level would also be detected. A subsequent software or hardware based screening process would eliminate rogue signals.

Monolithic cutting tool #3

A pictorial representation of cutting tool 3 is shown below with the relevant defects illustrated and located on the tool body.

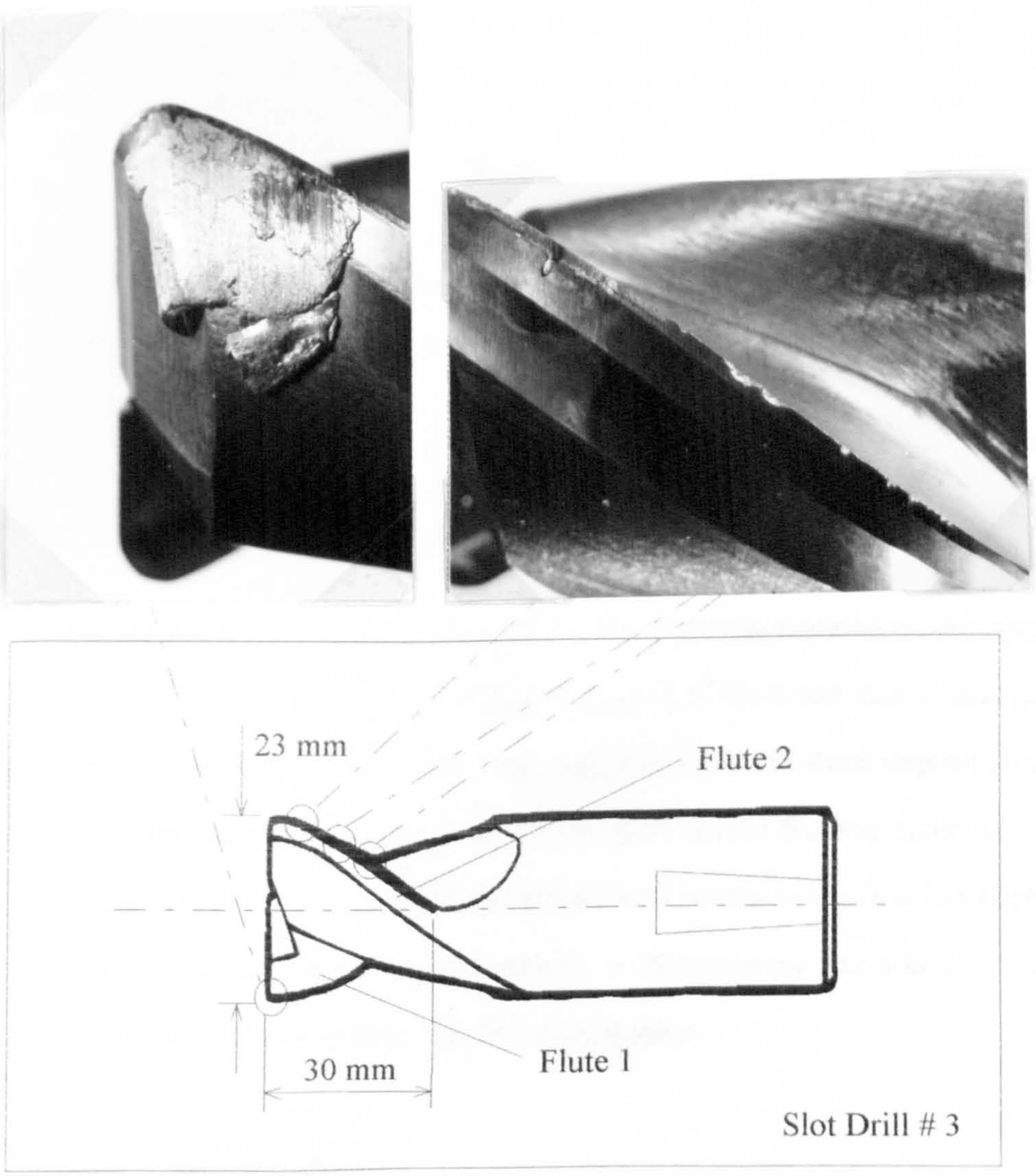

Figure 5-134 Cutting tool 3 showing defects and defect locations

The most imposing defect is the BUE which is displayed in the left hand photograph above. An additional BUE is seen to be forming on the second flute of the tool along side a series of six chips which run almost half the length of the cutting edge. The chips are of varying severity, but those shown in the centre of the right-hand photograph (above) are the most significant.

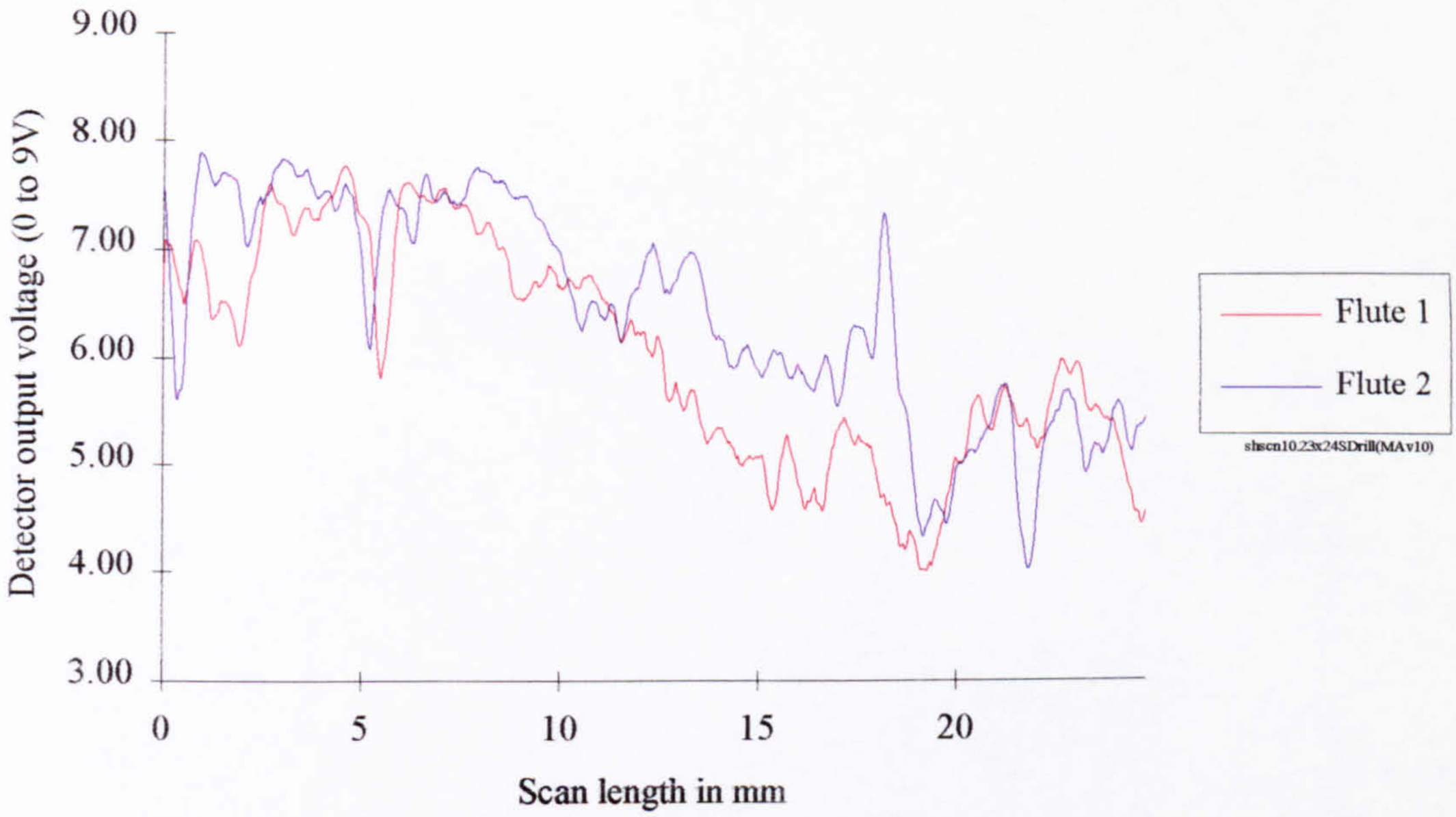

Figure 5-135 Cutting tool 3 inspection results - showing presence of a range of defects

The built-up edge which is a major visible feature on the cutting tool is not apparent on the response signal shown above. This is largely due to the tracking position of the laser along the cutting edge. Close inspection of the defect (Figure 5-134) reveals that a clear passage is possible and the cutter edge is relatively clean and free from the metal deposit (Built-up edge). Three possible solutions are; revise the tracking to ensure that the defect is subsequently detected, perform a repeat scan which runs parallel to the first but slightly in from the edge to provide a broader inspection band, or alternatively, use a larger laser spot size but at the expense of loosing fine, detailed information.

Defect detection - cutting tool #3

With the same threshold limits applied (±1.0 Volt (Y-axis graph scale units) above and below the overall signal average) the following graphical results were obtained for cutting tool #3. A small section of the BUE defect is detected by the inspection process. This is at the site where a narrow band of fused aluminium crosses the rake face. The increased reflectivity of the included aluminium surface causes the response signal to momentarily tend towards the saturation confine. No further defects are present nor detected on flute 1.

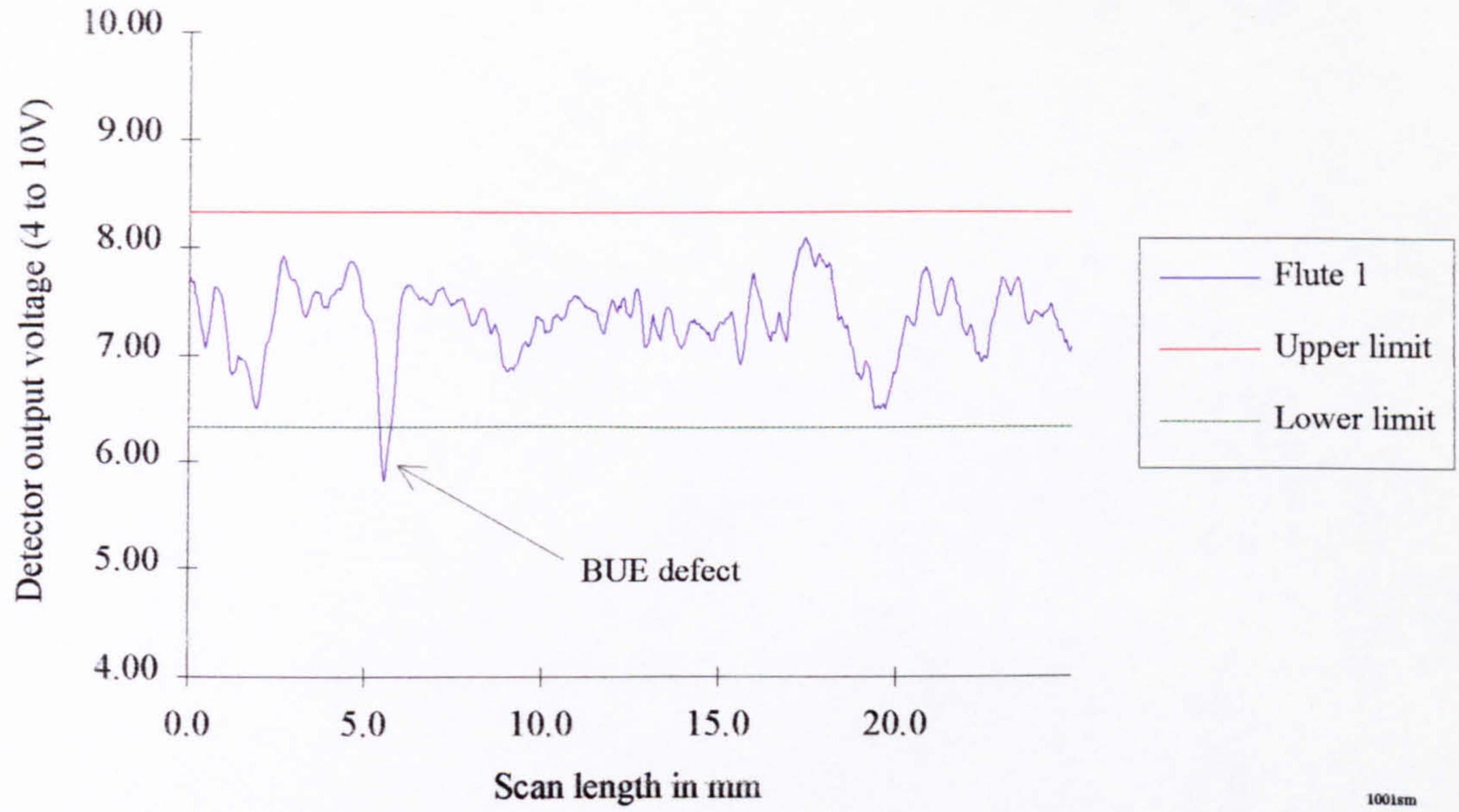

Figure 5-136 Defect detection by way of curve regression and thresholding

(Cutting tool 3, Flute 1)

Several features are detected on the second flute of cutting tool 3. As previously indicated a nucleation site for a BUE is apparent in addition to a series of small chip defects.

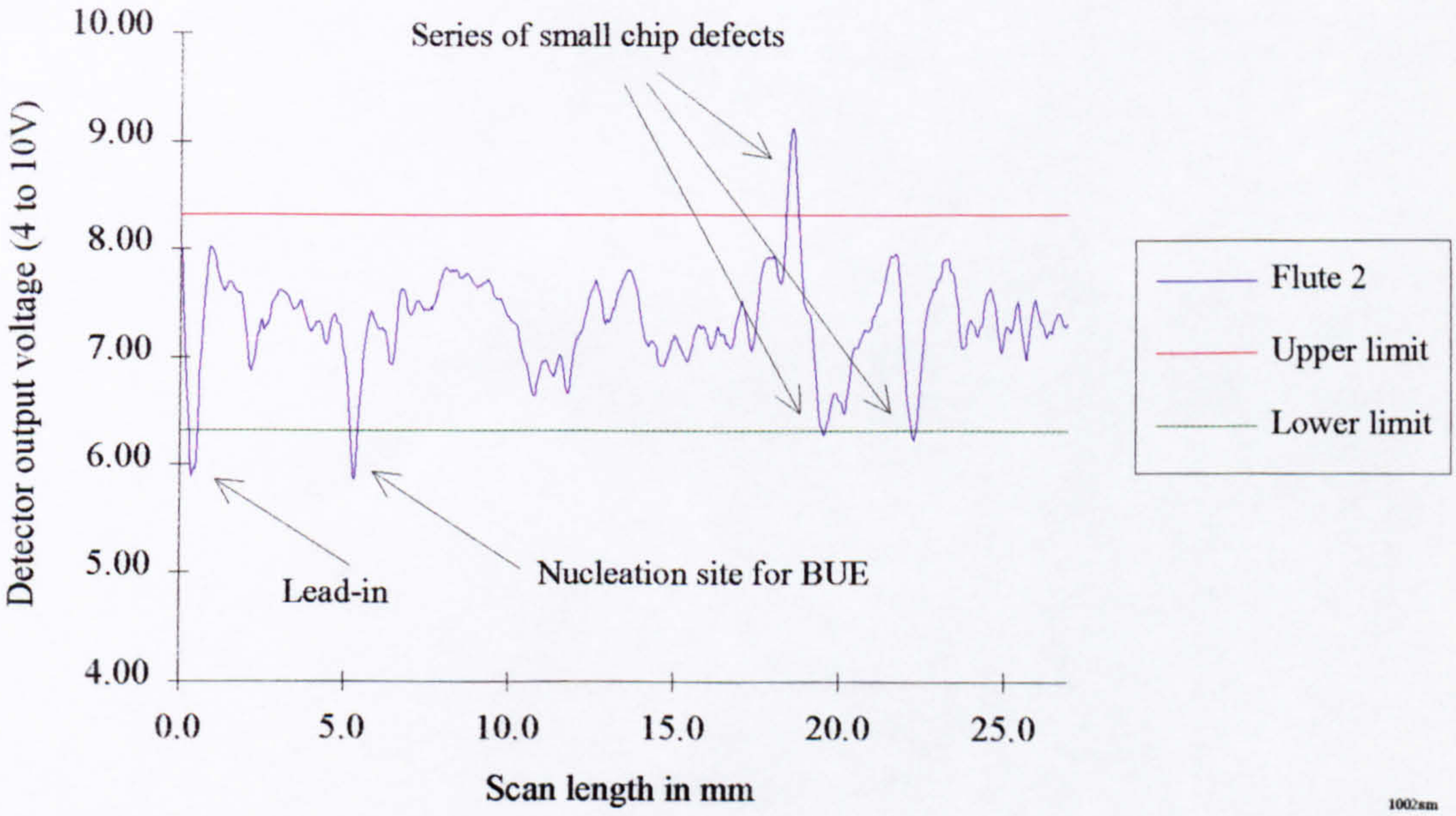

Figure 5-137 Defect detection by way of curve regression and thresholding

(Cutting tool 3, Flute 2)

The lead-in is visible at the left hand end of the response. A clipping algorithm or tighter scanning movements would be essential to eliminate this type of unwanted feature.

Chapter 6.0

Conclusions and Recommendations

6.0 Conclusions and recommendations

From the results obtained it is considered that the research program was successful. Prior to the reported work, laser/detector alignment and setting was largely intuitive with little scientific background. With the basic foundations now in place a more logical and structured approach can be adopted when configuring the optical head for a V-scanner, laser-based inspection device.

When applied to cutting tool condition monitoring the optimised settings for the laser and detector were seen to offer good response results. Defects and surface features located in the response signals by means of the simple but efficient thresholding technique illustrated the effectiveness of the optimised system configuration. Using the reported equipment the optimum settings could be applied swiftly to a range of tools with amendments being equally easy to apply. However, earlier work based around less flexible test equipment required far more time, patience and skill to configure with response results being largely unrepeatable. This was especially the case when arranging the optical head to locate the tool datuming mark (cross). Thus the foundation work was considered a success after being proven on the range of select cutting tools.

It is recognised that a restricted range of the scanning optimisation results were subsequently used in the concluding cutting tool inspection tests. However, the broad range of fundamental test specimens were purposefully chosen so as to represent the range of surface finishes generally found on a typical cutting-tool. It was anticipated, as a consequence, that the results may be called upon by future researchers working in related fields, particularly those based in the laser tooling laboratory at The University of Hull. Thus, the fundamental work was completed so as to produce a data base and support on-going and related inspection research activities.

Similar fundamental work could be undertaken in the domain of component/feature identification. A series of tests to identify the optimum settings of the laser/detector

V-scanner inspection head when applied to grooves, screw threads, steps and holes for example would enable simple, subsequent system configuration. This would be particularly useful to industries where small parts must be identified/screened on automated assembly lines which require flexible tooling. The optimum settings, for a known component form/feature, could be drawn from an established data base and easily applied to the laser-based inspection system by automatic or manual means. This would eliminate the existing trial and error approach which is widely used.

Several pertinent points have arisen from the program of work, which are worthy of mention;

The qualitative decision making employed during screening of the response signals in the angle optimisation tests should be replaced by a more quantitative measure. This arrangement could be simply accommodated in a spread sheet macro (extensively used to manipulate the graphical results). Further automation of the reported and proposed signal processing is highly recommended should this particular line of investigation continue (due to the volumes of data being handled).

When selecting the spot size for a V-scanner using the data provided it is suggested that very small spots should be avoided as the response results they produce tend to be extremely erratic (high amplitude and frequency). It was found that when this type of response is super-imposed on a master signal a direct match is rarely achieved. This situation was usually due to stray outlying points scattered above and below the main trend.

Accurate laser spot size calibration through use of a linear CCD array could offer more consistent results and better control over response signal quality in the fundamental tests. Furthermore, the laser spot measurement system could form an integral part of the inspection system and thus provide the benefit of a self calibration facility. With the laser mounted on a motorised axis the spot size could be automatically modulated in a calibration sequence or when an increased/decreased spot size were demanded by the scanning

application. Figure 6-1 illustrates how the automatic calibration system should be configured.

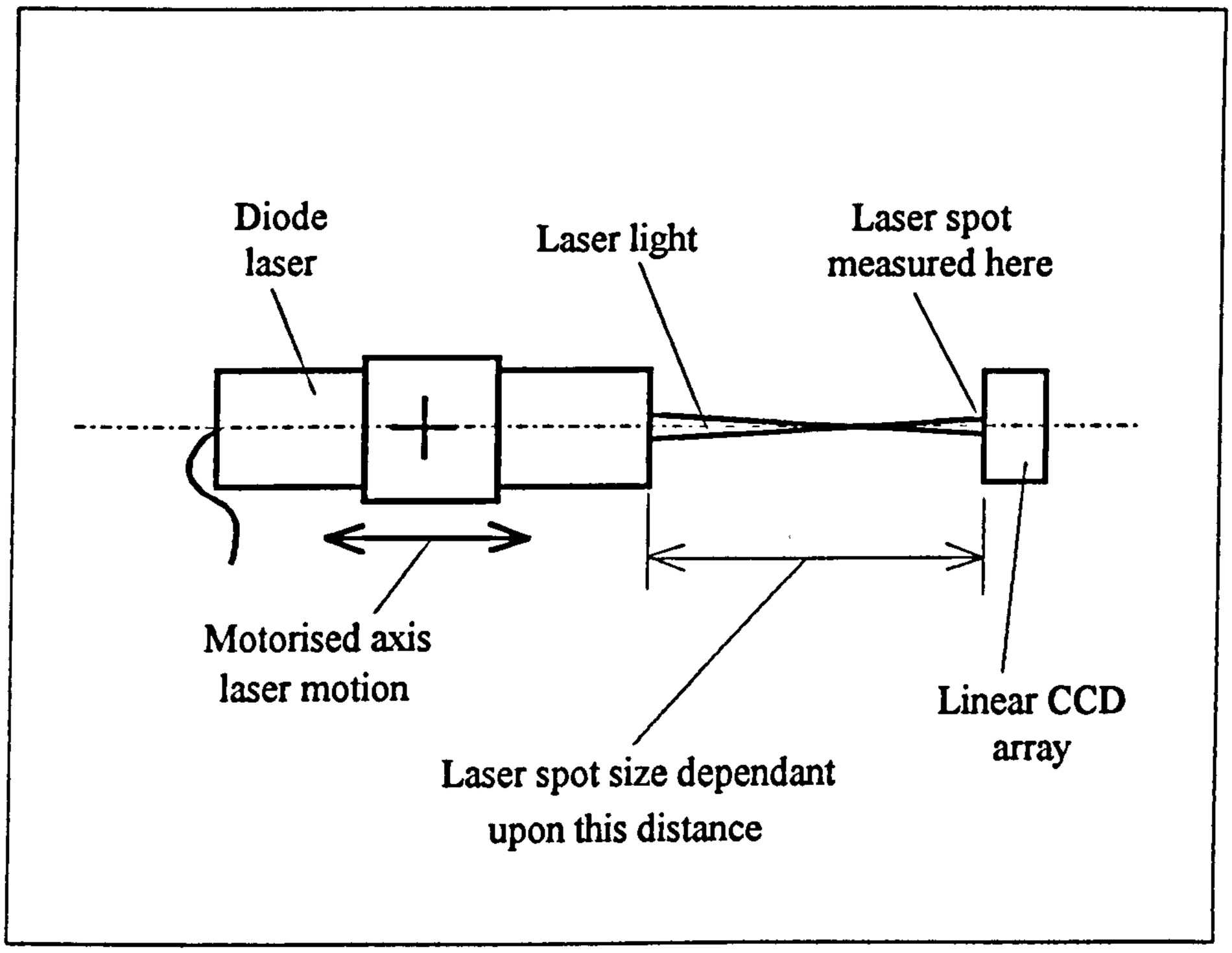

Figure 6-1 Linear CCD array based laser spot calibration system

Inclusion of a polarising filter in the optical system would produce two benefits;

- Produce increased contrast in the response signal,
- Due to the natural efficiency of the filter a reduced level of light would reach the photo detector. Consequently less saturation of the detector would occur.

Problems/observations in identifying surface defects in response signals acquired by a surface scanner are as follows [57];

- The defects tend to be very variable in form and can be characterised only on a statistical basis. A statistically valid description of the various defect types must be obtained by examining as many samples of each defect type, taken at widely separated times from different machines.

- Since it is intended that the identification method will ultimately be used in an industrial environment, hardware implementation must be possible which is fast and inexpensive enough to be commercially acceptable.

- Information useful for identifying defects is present in the scanner response signal in two basic forms; the shape of the signal caused by the presence of a defect and the spatial pattern of the defect signal across two or more cutting edges.

With the inclusion of extra detector units, additional defect/feature information could be gained leading to a more informed and reliable decision being made on the type of feature and/or the extent of damage. Future work should address the possible benefits and consider potential arrangements for a multiple sensor optical head. A stereoscopic vision system is a feasible and practical technique, which has been successfully applied in the steel industry, Baker et al [31]. CCD technology has progressed considerably since the reported work was undertaken and furthermore powerful computer hardware is more readily available. Thus potential benefits of the matrix imagers (CCD arrays) should now be reviewed in light of these developments.

New widely available software technologies such as Fuzzy logic and Neural networks should be investigated and their suitability to this particular application assessed Aitchison and James [65]. It is anticipated that they could contribute significantly to the reliability and flexibility of the inspection system. Work reported by Rangwala et al. [66], *Sensor integration using neural networks for intelligent tool condition monitoring* outlines one approach to this type of application.

Use of the moving average smoothing function was considered more appropriate than use of a larger laser spot size or reduced sampling rate for signal filtering. This decision was based on the fact that signal information could be recovered with the former technique but not the latter two.

A phase shift in response signal peaks was noted as the laser angle was varied. This was thought to be due to inaccuracies in the apparatus and/or the set-up, resulting in the laser spot being displaced slightly as the incidence/reflection angles were varied (i.e. focal point not coincident with surface of control sample). This situation illustrated the importance of maintaining a coincident laser/detector focal point on the inspection sample surface.

The repeatability error investigated early in the research program (Sub-section 5.1.2 Repeatability) was thought to produce conservative results. From experience the 0.05% repeatability error band was considered too narrow and thus requires further investigation. Repeat or alternative tests using a similar experimental arrangement should be undertaken and the results compiled. A maximum error band could then be identified and implemented as a direct consequence.

Enhanced fully automated operation could be achieved through the introduction of the bar-code (for example) for tool datuming and embedded tool information. By this means, manual data transfer errors could be eliminated.

The stability of the laser light source should also be assessed. Despite the supplier's guarantee of many thousand operational hours the light intensity was noted to vary over the period of work. The overall stability of the light source is considered crucial due to the mode of operation of the inspection system and thus it is of paramount importance that a suitable and reliable source is identified. Automatic self calibration of the optical system would potentially eliminate this problem.

Constraints imposed by the physical limits on the surface topography inspection device restricted the range of angular measurements recorded during optimisation tests for the incidence and reflection angles. The limits were; 20° - 80° for the laser angle and 20° - 50° for the detector angle. The inclusion of steeper angles may have produced a fuller understanding of the V-scanning process.

If further similar fundamental tests are to be undertaken then the surface topography inspection system requires further development/modifying. This should include;

- A detachable optical head (laser/detector sub-assembly) so that the unit can be located on other inspection devices with the angles and settings generally preserved.
- A wider range of incidence and reflection angles to enable telecentric operation in the extreme.
- Automated data capture, processing, comparison and presentation (on screen and hard copy) to speed up the relative comparison of different system configurations.

Despite the success of the work to date [67], [68] a great deal more time and effort must be dedicated to the application of laser-based scanners to cutting-tool condition monitoring to make the concept rugged and reliable enough for an industrial environment.

In the short term, particular attention should be focused on;

- The development of a reliable software/hardware based system for defect and feature detection/analysis, using proven Digital Signal Processing (DSP) techniques, Fuzzy logic and Artificial Neural Networks.

- The basic mode of operation of the laser-based inspection device. A V-scanner was used throughout, but other configurations/formats of scanner exist. These should be critically assessed and their suitability noted. Particular reference is drawn to a CCD based system where a complete image of the cutting-tool is captured and the cutting-edge quality information is subsequently extracted from the mass of data. Only recently has the technology been made available at an affordable price for feasibility studies on such a line of research to be pursued.

- Cutting-tool cleaning and preparation. This was not considered in the reported work but it obviously has a critical influence on the defect detection processes.

Long term objectives should also be considered if a competitive, reliable and commercially attractive inspection system is to evolve from the work currently being undertaken. Long term consideration should encompass the following related topics;

- Self calibration of inspection unit
- Fully automated operation
- Application to a wide range of complex form cutting-tools (insert and monolithic type) and compatibility with the associated tool holders.
- Software, hardware and data interface requirements for integration into a manufacturing network
- Human machine interface
- Integration with a machine-tool
- Cost/affordability

It is satisfying to know that related laser-based inspection work is currently ongoing in the Laser Tooling Laboratory at The University of Hull and furthermore that it is funded and supported by industry [65].

References

References

[1] Yoshimi Ito, Malaysian Institute of Economic Research (MIER), *Recent and Near Future Trends of Japanese Machine-Tools and Related Technologies.* Japanese Machine-Tool Builders' Association, Kuala Lumpur, Malaysia, November 1991.

[2] Micheletti G.F., Koenig W., Victor H.R., 1976, *In Process Tool Wear Sensors for Cutting Operations.* Annals of the CIRP Vol. 25 no. 2: pp 483-496.

[3] Iwata K., *Sensing Technologies for Improving the Machine Tool Function.* 3rd IMEC Session II.

[4] Lister P. M., Barrow G., 1991, *Tool Condition Monitoring Systems.* Proc 26th MRDR Conference 1986: pp271-288.

[5] Stauffer R. N., 1978, *A New Concept in Flexible Automation.* Manufacturing Engineering, Vol. 80, Issue 1: pp66-68.

[6] Giusti F., Santochi M., Tantussi G., 1984, *A Flexible Tool Wear Sensor for N.C. Lathes.* Annals CIRP Vol 33/1: pp229-232.

[7] Pedersen K. B., 1989, *Wear Measurement of Cutting Tools by Computer Vision.* Int. J. Machine Tool Manufacture, Vol 30 no 1: pp 131-139.

[8] Litu T. I., 1990, *Computer Vision Approach for Drill Wear Measurement.* Journal of Materials Shaping Technology Vol. 8, no.1: pp11-16.

[9] Cook N. H., 1978, *Micro Isotope Tool Wear Sensor.* Annals of CIRP Vol. 27 No. 1: pp73-78.

[10] Codling B., 1953, *Wear Studies of Irradiated Carbride Cutting Tools.* Nucleonics: pp46-49.

[11] Jetley S., 1984, *Measuring Tool Wear On-Line.* Manufacturing Engineering, Vol. 93, Issue 1: pp55-60.

[12] Wilkinson A.J., McClean W., 1979, *Instrument for the in-process measurement of tool wear.* IEE Conference publication - conference on electronic test and measurement, (June), 174: 27-29.

[13] Suzuki H., Weinmann K. J., *An On-line Tool Wear Sensor for Straight Turning Operations - Design and Evaluation.* Taken from "Sensors and Controls for Automated Manufacturing and Robotics". Presented at, The Winter Annual Meeting of the American Sociated of Mechanical Engineers.

[14] Takeyama H., Doi Y., Mitsuoka T., Sekiguchi H., 1967, *Sensors of Tool Life for Optimisation of Machining.* Advances in Machine Tool Design Res Vol. 1: pp191-208.

[15] Sandvik Coromant Tool Monitoring System.. *Plate Sensor.*

[16] Sandvik Coromant Tool Monitoring System. *Feed Force Sensors.*

[17] Sandvik Coromant Tool Monitoring System. *Multi-channel Tool Monitor Unit.*

[18] Amtri, *Hydrostatic Force-Sensing for Spindles.*

[19] Uehara K., 1979, *Automatic Tool Wear Monitoring.* Annals of CIRP Vol. 28, Issue 1: pp39-42.

[20] Colwell L. B., 1971, *Methods of Sensing Tool Wear.* Annals of CIRP, Vol. 19, Issue 4: pp647-651.

[21] Constantinides N., and Bennett S., 1987, *An Investigation of Methods for the On-line Estimation of Tool Wear.* Int. J. Machine Tools Manufacture Vol 27 no 2: pp225-2377.

[22] Inasaki I., Yonetsu S., *In process detection of cutting tool damage by acoustic emission measurement.* Proc. 22nd MTDR conference, 1981, p261 - 268.

[23] Kaklind Y., 1980, *In-Process Detection of Tool Breakage by Monitoring Acoustic.* Proc of An International Conf Cutting Tool Mat L FT Mitchell Kentucky Sept: pp25-39.

[24] Robbins W. P., Bischoff B., Ramalingen S., 1988, *Insert Mounted Thin Film Sensors for Real-Time Monitoring of Tool Conditions.* Thin Solid Films, 166: pp3887-396.

[25] *EUCHNER-Acoustic pulse detector:* Unit 2, Petre Drive, Sheffield, S4 7PZ.

[26] Luk F., Huynh V.,1987, *A Vision System for In-Process Surface Quality Assessment.* Vision '87 Conference Proceedings.

[27] Pekelharing A. J., Orelio J. M. B., *When does a Cutting Tool Crack.* North American Manufacturing Research Conf Proc 8th, May: pp8-11.

[28] Billett R. A., 1968, *Studies of Cutting Temperature Control Applied.* Advances in MTDR Issue 2: pp1273-1287.

[29] Colwell L. V., 1975, *Cutting Temperature Versus Tool Wear.* Annals of CIRP Vol. 24 Issue 1: pp73-76.

[30] Brook R.A., 1971, *Automatic Inspection of Flat Surfaces.* Steel Times Annual Review: pp91-98.

[31] Baker A. J., Brook R.A., 1978, *A Design Study of an Automatic System for Online Detection and Classification of Surface Defects on Cold-Rolled Steel.* Optica ACTA Vol. 25: pp 1187-1196.

[32] West R.N., 1982, *Laser Scanners for Automatic Inspection of Strip Products.* In. Proc. 6th Int. Conference (April) on Automated Inspection and Product Control IFS Publications Ltd., Beford UK: pp 287-295.

[33] Clarke G.M., 1974, *Application of the Laser Scanning Analyser for High Speed Detection of Visible Defects in Strips.* In Proc. SIMA Conf. SIMAC 74: pp2/1-2/10.

[34] West R.N., Stocker W.J.., 1977, *Automatic Inspection of Cylinder Bores.* Metrology and Inspection (July): pp9-12.

[35] Dewhurst R.J., Swift K.G, 1989, *Recent Advances in Laser Tooling for Flexible Handling Systems.* Optics and Lasers in Engineering, Elsavier Science Publishers Ltd., Vol. 10: pp27-41.

[36] 1974 (September), *Detecting Defects in Glass Sheet.* Glass. Lasers in the Glass Industry. (Steel Times Annual Review 1971): pp309-312 &314.

[37] Giusti F., Santochi M., Tantussi G., 1987, *On-Line Sensing of Flank and Crater Wear of Cutting Tools.* CIRP Vol. 36/1: pp41-4.

[38] DeGarmo E.P, Temple Black J, Kohser R.A, *Materials and processes in manufacturing,* Collier Macmillan Publishers, London, 1988.

[39] Schmalfuß H.J., 1990, *Laser Scanner Versus CCD Camera: A Comparison.* Elsevier Science Publishers B.V., Industrial Metrology Vol 1: pp155-64.

[40] Cieszynski J., 1989, *Servicing Compact Disc Players.* Television March 1989.

[41] Teague E. C., Varburger T. V., 1981, *Light Scattering from Manufactured Surfaces.* Ann CIRP Vol 30: pp 563-9.

[42] Campana S. B., 1977, *Techniques for Evaluation Charged Couple Imagers.* Optical Engineering (May) Vol.16: pp267-274.

[43] Yanagi K., Maeda T., Tsukada T., 1985, *A Practical Method of Optical Measurement for the Minute Surface Roughness of Cylindrical Machined Parts.* From a paper presented at the Third International Conference on Metrology and Properties of Engineering Surfaces, Teesside Polytechnic, Teesside (April)

[44] Purll D. J., 1978, *Automated Surface Inspection with Solid-state Image Sensors.* Prod SPIE: pp18-25.

[45] Batchelor B.G, Hill D.A, Hodgson D.C, *Automated visual inspection,* IFS (Publications) Ltd, UK, 1985.

[46] Meade M.L, Dillon C.R, *Signals and systems, models and behaviour,* Van Nostrand Reinhold (UK) Co. Ltd., 1986.

[47] Aitchison D. R., James R. D., 1990. *Automated Quality Control of Ceramic Roller Bearing Elements.* A report on a preliminary feasibility study, on behalf of SKF Bearings Ltd. Dept., EDM, Hull University 1992.

[48] Hill W.J., 1977, *Defect recognition in automated surface inspection.* PhD thesis, Department of Systems Science, The City University.

[49] Norton W.L., Hill W.J., 1976, *Advanced Signal Processing in Automated Inspection.* Proc. VII IMEKO Congress, London, May 1976.

[50] Chapman S.A., 1993, *Automatic handling of Engineering Components.* Final year student project, Dept. Engineering Design & Manufacture, The University of Hull.

[51] Lord Rayleigh, 1901, Polish. Nature, 64, pp385-388

[52] Spiewak S., Wu S. M., 1988, *Tool Wear Monitoring and Breakage Detection based on "Intelligent Filtering".* Int. J. Machine Tools Manufacture Vol 28 no 4: pp483-494.

[53] Matsushima K., Kawabata T., 1979, *Recognition and Control of the Morphology of Tool Failure.* Annals of CIRP Vol. 28/1: pp43-7.

[54] Clarke G.M., 1977, *Laser Scanning Systems for Image Acquisition.* Proc. SPIE Vol. 130 (September): pp68-74.

[55] Photodiodes - Manufacturers stock catalogue
Hamamatsu, March 1987

[56] Mohri N., Bertok P., Sata T., 1982, *In Process Monitoring of Tool Breakage Based on Autoregressive Model.* Proc. IFAC. Symp. on Information Control; Problems in Manufacturing Technology: pp 41-5.

[57] Norton-Wayne 1977, *Automatic Visual Inspection of Moving Steel Surfaces.* British Journal of Non-Destructive Testing (September): ppp242-248.

[58] Hopper I.S, *Flexible control of a laser tooling system,* Dept. Engineering Design and Manufacture, The University of Hull, 1992.

[59] Torrance K. E., Sparrow E. M., 1967, *Theory of Off-Specular Reflection From Roughened Surfaces.* Journal of the Optical Society of America Vol 57 no. 9: pp1105-1114.

[60] Birkebak R. C., Ecckert E. R. G., 1965, *Effects of Roughness of Metal Surfaces on Angular Distribution of Monochromatic Reflected Radiation.* Journal of Heat Transfer: pp85-93.

[61] Sweeney F., Spedding T. A., 1986, *A Simulation Technique to Investigate Rough Surface Scatter.* Dept. of Production Engineering, Coventry Lanchester Polytechnic Coventry UK.

[62] Detection and Determination of Cutting Edge Damage on Solid Carbide Drills Quality Control Manual (Hertel A.G.), 1992: pp 9-12.

[63] Vainberg V. E., Lekhtyar L. I., 1990, *Use of logic recognition principles for identifying the condition of objects from acoustic emission signals.* Soviet Journal of Nondestructive Testing, Vol 26 no 4, pp 246-250

[64] Vajpayee S., Sampath A., 1990, *Development of a computer-based AE system for tool condition monitoring,* Computers and Industrial Engineering,Vol 18 no 2, pp 211-223

[65] Aitchison D.R., James R.D., *Developments in laser scanners for defect detection in cutting tools.* 11th NCMR, September 1995.

[66] Rangwala S.,Dornfeld D., 1990, *Sensor integration using neural networks for intelligent tool condition monitoring.* Eng. for Ind.Transactions ASME, Vol 112 no 3, pp 219-228

[67] Jame R.D., Aitchison D.R., 1994, *Laser-based inspection of cutting tools for advanced manufacturing systems.* IEE Factory 2000 - Advanced factory automation, 3-5 October, pp 502-508.

[68] James R.D., Aitchison D.R., 1992, *Development of an intelligent tool condition monitoring system for FMS.* IMechE AeroTech., 14 - 17 January.

Appendices

Appendix I - Sensing techniques for tool wear/failure under research or development

(An extract from reference [3])

Appendix I Sensing techniques for tool wear/failure under research or development

(An extract from reference [39] - Data originally supplied by the Japanese Machine Tool Manufacturers Association)

Direct Measurement Methods

Converted Signal	Main sensors studied in the past	Examples of sensors studied since 1984	Feature	Researcher	Year
Light	Photomultiplier, Phototransistor, Photodiode, Fibre optics and photoc	CCD camera and fibre optics	Lathe (flank wear, crater wear), computer vision techniques used VICOM general-purpose image processing system Repeat measuring error: Flank waer 4.2 % or less; crater wear 7.8% or less Agreement with measurement results using tool microscope	Y H Lee et al (GM)	1987
	ITV	ITV fiber optics and laser beam	Turning (flank wear, crater wear); light source sned laser beam to cutting face through two lenses and differaction grating to measure crater wear Resolution: flank wear 0.01mm, crater wear 0.02mm Maximum error: ±0.03mm	F Guisti et al (Italy)	1987
	Silicon photoelectric element, Collimator, Laser	CCD camera and halogen lamp	Turning (wear and chipping); 4 halogen lamp are used as a light source Measuring limits: 0.048mm long; 0.06 mm^2 in area	Yamanishi et al	1987
Voltage	Foil resistor	Metal film circuit resistor	Turning (flank wear); resistance circuit made of Ti	Aoyama et al	1986
X-ray, Electromagnetism Fluid	Scintillator, Eddy current meter, Magnetic head, Air micrometer				

Indirect Measurement Methods

Cutting force (torque)	Strain gauge	Strain gauge	Flanked wear and crater wear are estimated from variations in main/feed components of force at the start of process in which chips are produced. Specifically, flank wear is estimated from maximum feed component/main component of force.	Ishibashi et al	1986
		Strain gauge	Cutting force calculated from cutting model is compared with feed copnent of force measured, and the state of cutting is estimated in process. Wear or damage to ceramic tools is estimated from feed component of force at start of cutting.	G Warnecke & A Jenewein (West Germany)	1988
	Force converter Cutting dynamometer	Cutting dynamometer	Using cutting force, flank wear, crater wear, cutting conditions as models, process parameters are calculated in sequence. Model base approach estimating amount of wear by measuring main cutting component of force.	Y Koren et al (USA)	1986
		Cutting dynamometer	On-line tool wear monitoring during milling Third level model is used Vibration sensor is also used.	C Johnson et al (USA)	1988
	Torque sensor	Torque, thurst, temperature sensor	Tool holder type FM Small-diameter (0 to 4mm) drill breakage prediction	Hatamura et al	1985
Cutting power consumption	Ammeter Wattmeter				
Vibration	Piezoelectric acceleration pickup	Piezoelectric acceleration pickup	Sensor frequency response 0.01 to 3kHz Chipping of turning tool or drill is predicted from increased ratio of vibration. Practical detector fabricated.	Noh	1987

		Piezoelectric accelerometer	Chipping in mill are predicted from changes in peak position and shape of primary torsional frequency spectrum Little affected by disturbances.	D Greshaher et al (USA)	1987
		Piezoelectric accelerometer	Turning tool wear Frequenc-hand energy method used.	C Y Jiang et al (China)	1987
Sound (AE)	Microphone, AE sensor	AE sensor	Detection of tool wear and chipping. Average value, standard deviation, coefficient of variation, skewness, light intensity, and other statistical quantities are used for evaluating amptitude distribution.	Sakata et al.	1986
		AE sensor	Turning tool monitoring system developed (normalised AE mode used as standard)	O Blum et al Aida et al	1987
		AE sensor	Tool wear and breakage pattern detection Linear discrimination function based on pattern classification method, or minimum least square method, used.	E Emel et al (USA)	1986
		AE sensor	Tool wear detection in turning, drilling, and milling.	P Souquet et al (France)	1987
		AE sensor	Auto adaptive system developed	Iwata et al	1988
		AE sensor	Adaptive time series modeling and meuro network used	D Dornfeld et al (USA)	1987
		AE sensor	Crater wear and flnak wear are discriminated from each other using AE energy value (RMS) Tool wear detection and identification while cutting oil is running.	Y Naerheim & M Lan (USA)	1988
		AE sensor	Thin transducer glued to one side of cutting tool tip. Milling tool damage detectable in real time.	S Ramalingham et al (USA)	1988

Appendix II - Tool stock study

Leading U.K. Aerospace Industry

Tool Stock Study

Introduction

After two weeks of study in the current tool room environment it was found that there was obvious scope for improvement. The tool room is the backbone to manufacturing and the tool management system relies heavily on the knowledge of only a few personnel. This was demonstrated when information was required from the 'IBM Toolstock' database. A computer operator in a remote building was required to extract the information which should be generally available within the relevant departments.

Figure 1 shows a schematic diagram of the flow of cutting tools through the company, from purchasing to scrap. The tool management system does however have problems in that once the cutter assemblies have left the tool room and have been used on the machines, there are no accounts of their whereabouts. Therefore, the tools which arrive back for re-grinds are treated as new stock and after re-grinding they are re-coded.

The central handling areas of the cutting tools revolve around the grinding area and assembly/inspection. In the grinding area, either blanks or used cutting tools are ground, logged and then entered into the storage carousels for use in desired cutting operation. The tools are then request for use, assembled, visually inspected, offset measurements taken and/or tool balancing* if required, and the complete assembly is then sent to the desired CNC machine. Once the tool is in operation it will be classed as defective if:

- the operator notices any obvious defects on the tool or workpiece,
- if the machine spindle feedback senses an undesirably high torque,
- or the tool has been used over it's set period, or the machining operation has finished it's cycle.

In each of these cases, tools returned from the machine shop are inspected and if defects or blunting of the cutting edges are found, it is dismantled into its component parts. The tools are then placed into a box ready for re-grinding (if eligible).

Problems with severe chipping were found on returned tools after dismantling which occurred when the tools were placed in their storage boxes. The hard carbides can be easily chipped, creating large chips which cannot be ground out, resulting in the tool becoming scrap. These are then wasted resources, as the tools can be re-ground many times using the in-house grinding facilities. Problems such as these can be easily resolved by having dedicated boxes for the tooling, preventing damage by collision.

Other problems occurred with the tools requested by the NC programmers. For specific cutting operations, a series of codes comprising of the cutting tools, taper sizes and collets are sent to the tool room for the fitters to assemble. It is here that, because of the lack of current up to date information, repetition of the tools can be built, or very similar assemblies

to the one wanted are dismantled to create the new one (this only happens when their is a shortage of fittings, which the NC programmers assume never happens).

The Current Tool Management System

There were three methods of collecting tool data. The current database system, 'IBM Tool store', which has weekly updated information on the numbers and types of tooling within the Linvar carousels. The Linvar carousels themselves have information of every tool type within their stores and their storage positions on the shelving systems, but a more accurate assessment of the throughput of tools can be obtained from the stock ordering requests. The tools for either re-ordering, or re-grinding, are recorded and can be seen in Table 1 and Chart 1. From the chart, one can see the main group types and the orders of magnitude of the tools used. This however, does not take into account the more expensive solid carbide tools which can be seen on Table 2 and Chart 2. The re-ground tools are both the tools which require sharpening after their machining operation and the tools which are re-manufactured from blanks. There is a colour coding system for all of these tools to identify undersized tools. This is for the benefit of the fitters because the CNC machines will measure and compensate for these smaller cutting tools.

The tools are booked out of stores by the fitters etc., by signing them out. This works to an extent, but relies on the honesty of the fitters and notification of when the tooling has reached a minimum stock level. When this level is reached, a card system is completed and at the end of the week all the cards are collected and orders for the tool requirements are made. Table 3 and Chart 3 show the magnitude of ordering compared to the tools booked out of the stores. The discrepancy is due to:

- tools not being booked out,
- tools not returning from the machine shop,
- replenishing fallen stock levels,
- and inadequate information for minimum stock ordering.

If an enclosed store was in operation there would be accurate data on the tool usage rates because all tools would be booked out for specific jobs only.

From the 'IBM Toolstock' database system, the full selection of available tooling was collected for comparison with the actual tools available in the Linvar carousels and it was found that redundant tooling from past aircraft are still being stored in these stores.

The following numerical data was collected:

Total number of tool types in Linvar 1	-	1226 Tool types
Total number of tool types in Linvar 2	-	716 Tool types
Total	-	**1942** Tool types.

From the above data:

- in Linvar 1 there were 49 types of tooling not accounted for in 'IBM Toolstock', and
- in Linvar 2 there were 29 types of tooling not accounted for.

From the listing of 'IBM Toolstock', it was found that there were 80 types of tooling not stored in the Linvar carousels.

A previous report was on a similar exercise was carried out in April 1987 by Mr S Walker (Asst FMMS Development Eng), but undertook a more comprehensive stock take of all the tools in storage and on the shop floor. A summary of the results can be seen below:

Quantities:

ME... Imperial		7000	
ME... Metric	5000		
CST...		1500	
0811		6000	
TOTAL		19500	
Tools on the shop floor		8500	
Re-grinds		4000	
TOTAL		**42000**	Error 15%

The above information excludes reamers, drills, carbides and insert tooling.

The flow of the tools through the tool stores was also calculated and the following was found:

Cutters bought	120/week
Cutters re-manufactured	200/week
Cutters re-ground	530/week
TOTAL	850/week

The above report gave some estimates on the tooling costs of between £30 and £40, but the above information excludes the more expensive carbides. using the above as a basis, estimates on the current tooling within the Linvar tool stores, i.e. excluding the tools on the workshop floor and assembled in the tooling area, one can estimate the following:

Total number of cutting tool types	-	£1942	Calculated from Linvar printouts.
Cost per cutting tool	-	£50	Estimated from above and the inclusion of carbide tooling
Numbers of each tool types	-	£30	Estimated from the minimum order levels.
TOTAL	-	**£2913000**	

For an inspection station to be implemented into the tool room at the manufacturing site, or as a machine fixture, it is logical to assume that it would inspect the most common tooling

types. These are the ME3200 series of slot drills (i.e two flutes) and over the past five months the data on Table 4 and Chart 4 shows the usage rate. The most common ME2300 tool types were:

ME3200-20	Dia 12mm x 38mm Long, Square end.
ME3200-35	Dia 19mm x 45mm Long, Square end.
ME3200-42	Dia 25mm x 32mm Long, 3.15 End radius.
ME3200-45	Dia 25mm x 57mm Long, Square end.
ME3200-70	Dia 19mm x 65mm Long, Square end.

The dash number represents the characteristics of the tool type, i.e. the tool length, diameter, radius and minimum stock number. In the above cases, where the tool has a square end, the tools can be ground to any desired radius on the in-house grinding machines. This ensures stock can be replenished at short notice.

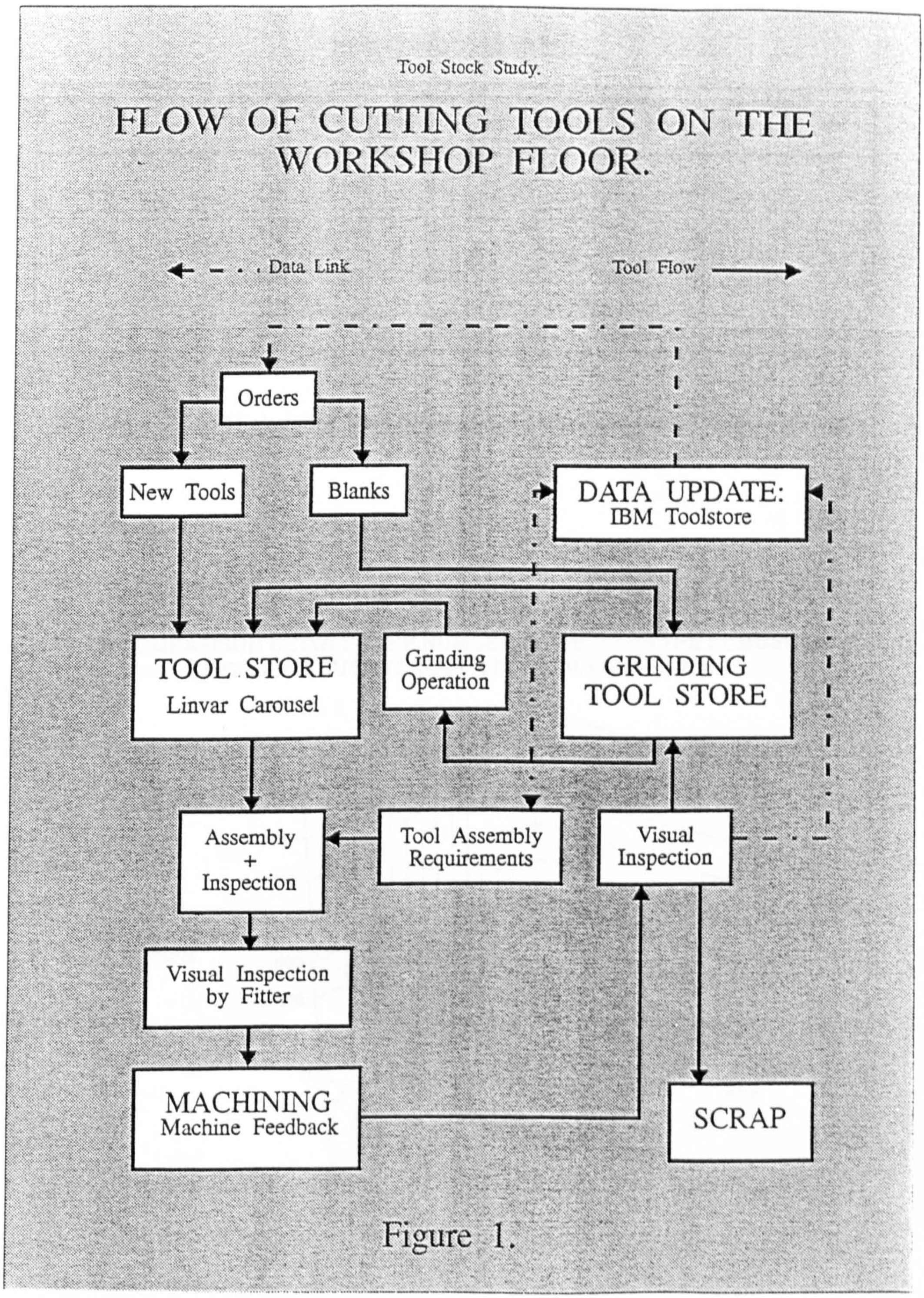

Figure 1.

Figure 1 Schematic of the flow of cutting tools throught the company

HIGH SPEED STEELS.

DATES	SLOT DRILLS		END MILLS		ROUTERS		SPECIALS	
	Grinding	New	Grinding	New	Grinding	New	Grinding	New
May	715	158	151	28	0	0	0	74
June	1265	640	80	0	0	0	10	42
July	1164	577	190	117	116	10	56	112
August	1020	790	245	0	122	0	8	21

Table 1 High speed steel tools re-ordered or re-ground May - August

A COMPARISON BETWEEN THE NUMBER OF NEW AND THE NUMBER OF RE-GROUND CUTTING TOOLS PER CALENDAR MONTH.

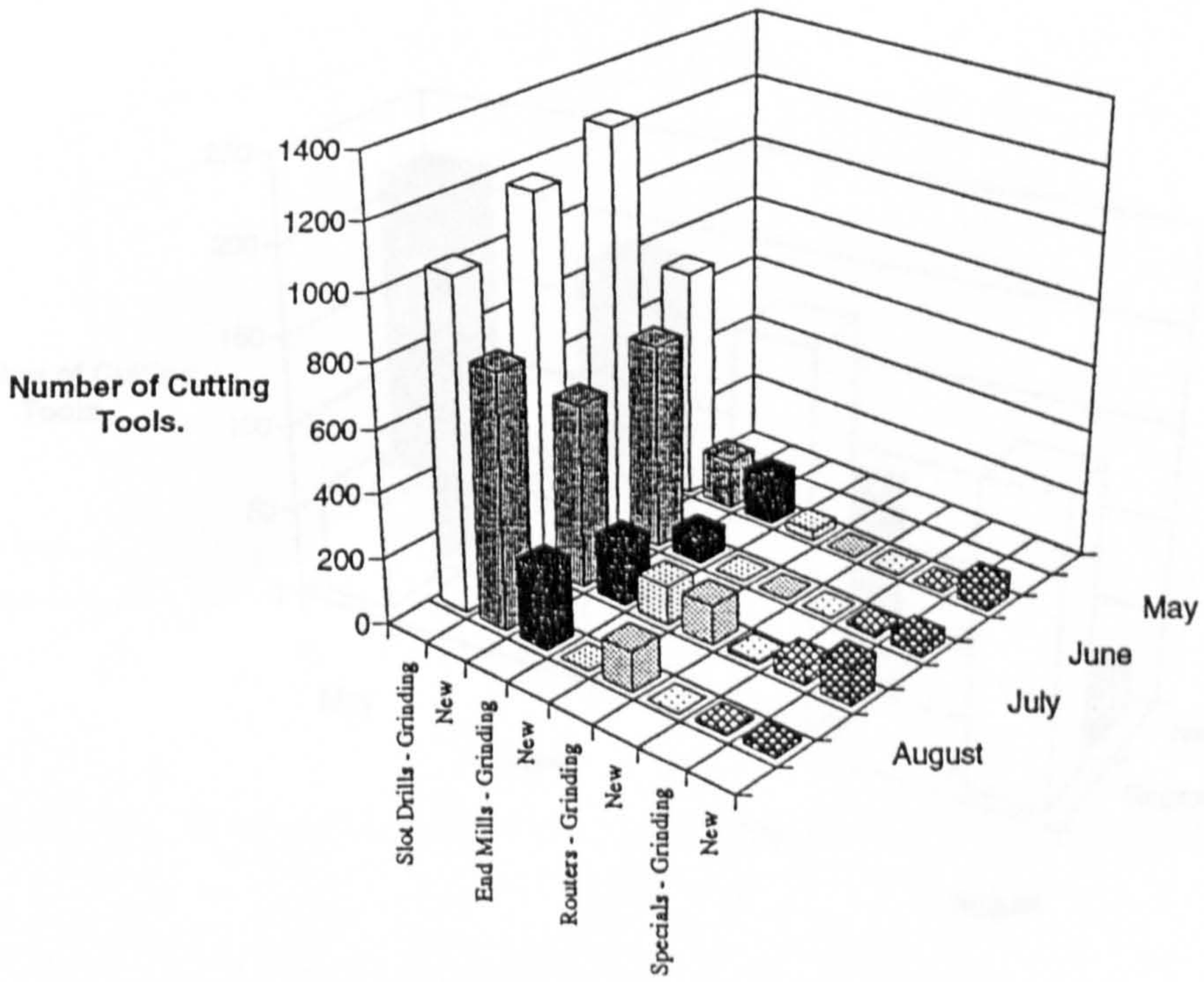

Chart 1 High speed steel tools re-ordered or re-ground May - August

CARBIDES.

DATES	SLOT DRIILS	
	Grinding	New
May	61	218
June	91	189
July	203	95
August	161	27

Table 2 Solid carbide tools re-ordered or re-ground May - August

A COMPARISON OF CARBIDE AND HIGH SPEED STEEL TOOLS ORDERED TO REPLENISH STOCKS OVER THE STUDIED PERIOD.

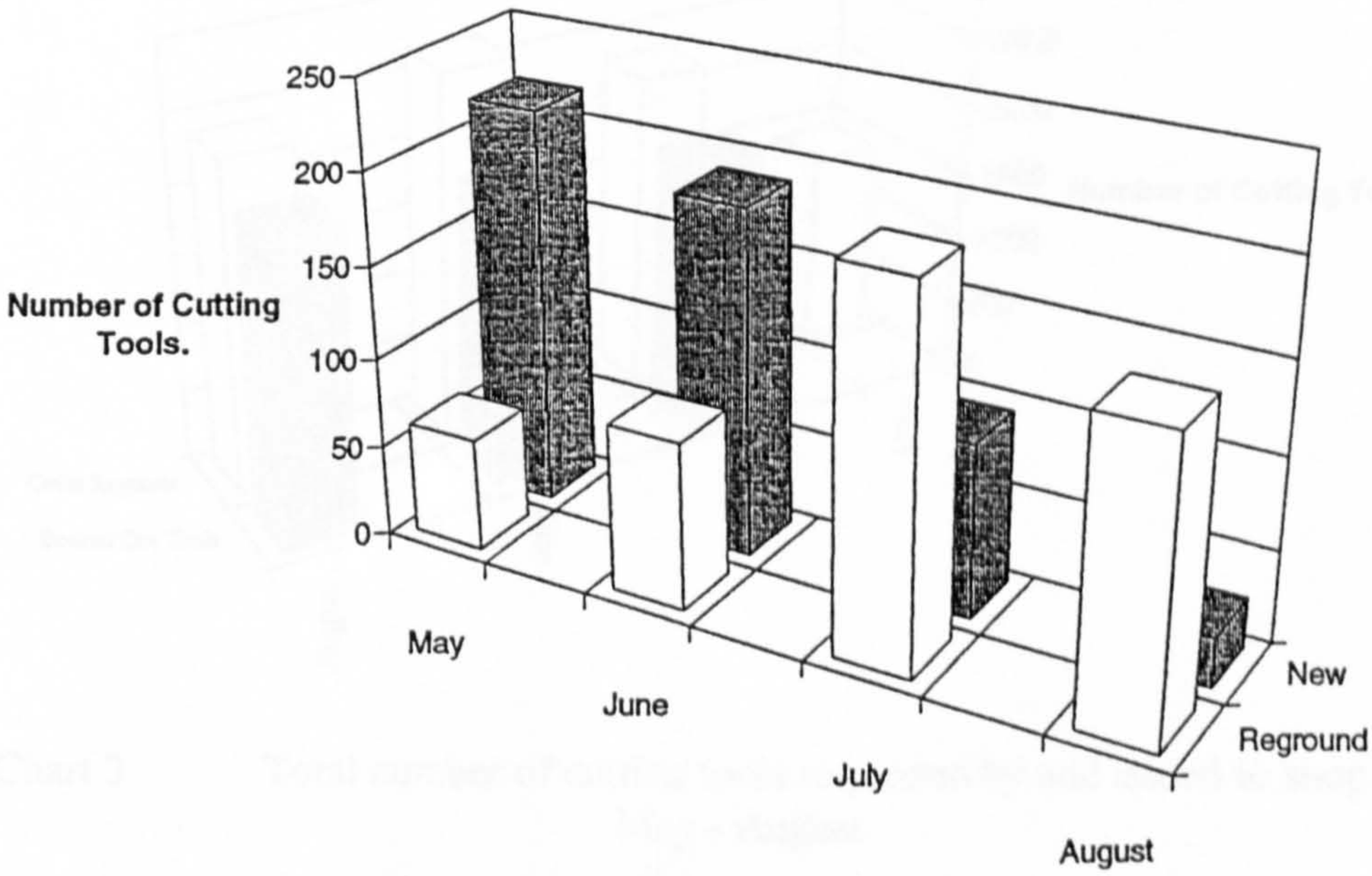

Chart 2 Solid carbide tools re-ordered or re-ground May - August

TOTALS.

DATES	ORDER REQUESTS	BOOKED OUT CUTTING TOOLS
May	1405	
June	2317	1936
July	2666	2048
August	2390	2145

Table 3 Total number of cutting tools requested by and issued to shop floor May - August

A COMPARISON BETWEEN THE NUMBER OF BOOKED OUT CUTTING TOOLS AND ORDERED STOCK IN THE STUDY PERIOD.

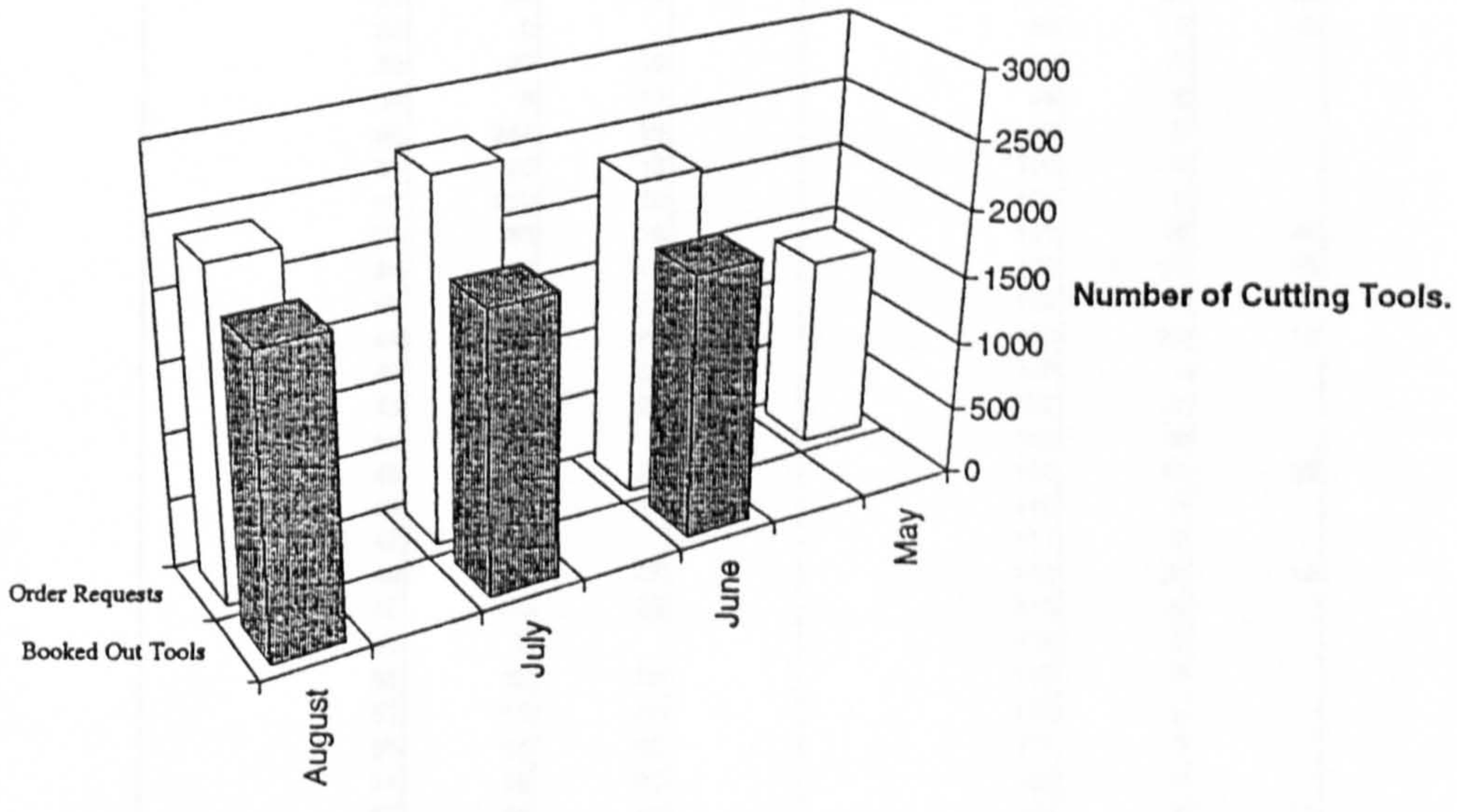

Chart 3 Total number of cutting tools requested by and issued to shop floor May - August

NUMBERS OF ME3200 TOOLS ORDERED OVER A THREE MONTH PERIOD.
- From June to August 1992.

ME Dash Number		No. Off	Tool Dia
ME3200 -	1	36	6
	2	0	
	3	0	
	4	0	
	5	0	
	6	0	
	7	0	
	8	20	6
	9	0	
	10	0	
	11	0	
	12	0	
	13	0	
	14	24	9
	15	12	9
	16	0	
	17	0	
	18	24	12
	19	46	12
	20	300	12
	21	123	12
	22	142	12
	23	42	12
	24	12	12
	25	0	
	26	14	12
	27	40	12
	28	40	19
	29	0	
	30	158	19
	31	62	19
	32	0	
	33	40	19
	34	8	19
	35	344	19
	36	20	19
	37	120	19
	38	80	19
	39	80	19
	40	50	25
	41	20	25
	42	220	25
	43	44	25
	44	0	
	45	181	25
	46	100	25
	47	0	
	48	57	25
	49	40	25
	50	0	
	51	12	25
	52	12	25
	53	14	25
	54	18	25
	55	80	40
	56	110	40
	57	30	40
	58	40	40
	59	0	
	60	15	40
	61	0	
	62	0	
	63	8	40
	64	0	

ME Dash Number		No. Off	Tool Dia
ME3200 -	65	6	40
	66	10	40
	67	16	40
	68	12	25
	69	30	19
	70	269	19
	71	42	19
	72	30	25
	73	10	19
	74	8	19
	75	0	
	76	0	
	77	0	
	78	0	
	79	63	12
	80	12	19
	81	18	25
	82	14	25
	83	0	
	84	8	9
	85	0	
	86	0	
	87	10	38
	88	48	19
	89	10	25
	90	8	25
	91	42	19
	92	0	
	93	24	25
	94	12	19
	95	20	25
	96	5	40
	97	0	
	98	0	
	99	0	
	100	0	
	101	0	
	102	16	40
	103	12	40
	104	0	
	105	29	14
	106	0	
	107	0	
	108	0	
	109	12	25
	110	0	
	111	0	
	112	22	12
	113	0	
	114	0	
	115	0	
	116	0	
	117	0	
	118	0	
	119	5	14
	120	6	14
	121	41	14
	122	0	
	123	0	
	124	0	
	125	6	25
	126	6	19
	127		
	128		

Table 4 The frequency of use of common cutting tools May - August

DISTRIBUTION OF ME3200 TOOLING ORDERED OVER A THREE MONTH PERIOD.

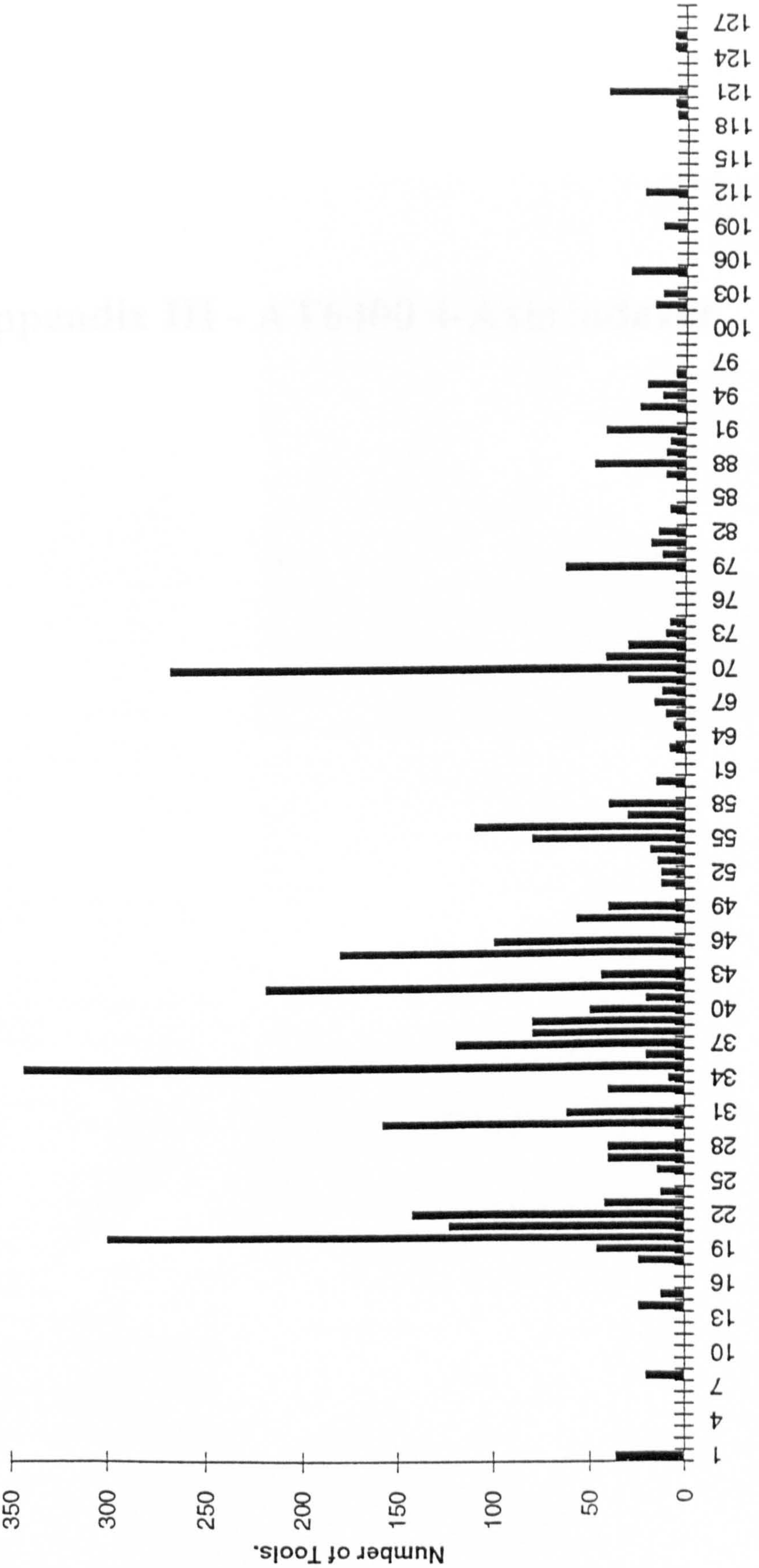

Chart 4 The frequency of use of common cutting tools May - August

Appendix III - AT6400 4-Axis indexer

Compumotor

AT6400

4-Axis Indexer

Introduced October 1991

Compumotor's new AT6400 motion controller is a PC-AT* bus based indexer for industry standard step and direction motor drives. The AT6400 can synchronize 2, 3, or 4 axes of motion. Incremental encoder feedback on all four axes provides the ability to detect stalls, verify position, and correct for positioning errors generated by inaccurate mechanical transmissions. The 1.6 MHz maximum step output frequency allows precise control of microstepping motor drives, and high speed control of servo drives which accept step and direction input. The AT6400 also boasts a very powerful command language that is flexible enough to implement complex motion control applications, and simple enough to not overwhelm the novice programmer. Many useful features are incorporated into the command language, including feed-rate override, two-axis contouring, subroutine definition, conditional programming, unit scaling, programmable I/O, registration, and mathematical functions.

Software support includes an advanced program developer and terminal emulator for use with Microsoft Windows. The program developer allows the user to create and edit programs for use with the AT6400. The terminal emulator allows the user to execute the programs created by the program developer. In addition to the program developer and terminal emulator, other terminal emulator software examples, which illustrate controlling and communicating with the AT6400 under the DOS environment, are also included.

The AT6400 comes standard with an auxiliary connector board. The connector board provides phoenix screw terminal connectors for all I/O except the motor drive (15 pin 'D' shell), joystick (25 pin 'D' shell), and the 24 inputs and 24 outputs (50 pin headers). The connector board also contains an on-board power supply capable of supplying 1.5 amps to use with encoders and I/O. A five foot cable connects the AT6400 to the auxiliary board.

Features

- 1 to 4 axes of step and direction control with encoder feedback
- Microsoft Windows™ and DOS™ support standard
- Separate adaptor board to simplify connections and optically isolate I/O
- Home limit, CW and CCW end of travel limits provided for all axes
- 24 programmable inputs
- 24 programmable outputs
- 4 analog inputs that can be used for joystick or feed-rate override control
- 4 interrupt-driven inputs for use with registration or encoder capture
- Two 10-ft drive cables included
- Support software written in ASSEMBLY, BASIC, C and PASCAL
- Direct access to motor and encoder position information, I/O and system status
- Programmable PC-AT* interrupt conditions
- 25000 bytes of RAM for program storage
- Encoder channels can be configured as hardware up/down counters
- Capability to interrupt program on error conditions
- 2-axis circular, and 4-axis linear interpolation
- Variable storage, conditional branching, and math capability
- Binary input mode for faster processing of command input
- Program debug tools—trace mode, break points, and simulation of I/O
- Scaling of distance, velocity and acceleration parameters
- Programmable timer

Parker

Model AT6400

4-Axis Indexer

Command Language*

The AT6400 is easily programmed with the new 6000 Series language. Each command is an ASCII character mnemonic with numeric parameters for each of the 4 axes following the command. The commands can be transferred to the AT6400 in either ASCII format, or in a 2 byte hexadecimal format. Command transfers are done one character at a time, or as part of a block transfer where up to 256 characters are transferred.

The following command example sets the acceleration on all four axes: A10,15,20,30

Conditionals

IF( )	If Statement
REPEAT	Repeat Statement
WAIT( )	Wait for a Specific Condition
WHILE( )	While a Condition is True

Encoder

ENC	Encoder / Motor Step Mode
EPM	Position Maintenance Mode Enable
EPMDB	Position Maintenance Deadband
ERES	Encoder Resolution
ESDB	Encoder Stall Deadband
ESTALL	Stall Detect Enable

Homing

HOM	Go Home
HOMA	Home Acceleration
HOMAD	Home Deceleration
HOMBAC	Home Backup Enable
HOMEDG	Home Reference Edge
HOMFD	Home Final Direction
HOMFV	Home Final Velocity
HOMLVL	Home Active Level
HOMV	Home Velocity
HOMZ	Home to Z-channel Enable

I/O

INFEN	Enable Input Functions
INFNC	Input Function
OUTFNC	Output Function
OUT	Turn On/Off Outputs

Interrupts

INTHW	Hardware Interrupt
INTSW	Software Interrupt

Joystick

JOY	Joystick Mode Enable
JOYA	Joystick Acceleration
JOYAD	Joystick Deceleration
JOYCDB	Joystick Center Deadband
JOYVH	Joystick Velocity High
JOYVL	Joystick Velocity Low

Limits

LH	Hard Limit Enable
LHAD	Hard Limit Deceleration
LHLVL	Hard Limit Active Level
LS	Soft Limit Enable
LSAD	Soft Limit Decelration
LSCCW	Soft Limit CCW Range
LSCW	Soft Limit CW Range

Mathematical

+	Addition
-	Subtration
*	Multiplication
/	Division
&	Boolean And
I	Boolean Or
SIN	Sine
COS	Cosine
TAN	Tangent
ATAN	Arc Tangent
SQRT	Square Root

Miscellaneous

;	Comment
BINARY	Binary Mode
DRIVE	Drive Enable
ERRORP	Error Program
L	Loop
MA	Absolute / Incremental Mode Enable
MC	Preset / Continuous Mode Enable
PSET	Define Position Counter
CNTINT	Counter Value to Interrupt PC-AT®
READ	Read a Value from PC-AT®
RESET	Reset AT6400
TIMST	Reset and Start Timer
STEP	Single Step Mode Enable
WRITE" "	Transmit a String to the PC-AT®

Motion

A	Acceleration
AD	Deceleration
D	Distance
GO	Initiate Motion
GOL	Initiate Linear Interpolated Motion
REG	Registration
S	Stop
SSV	Start / Stop Velocity
V	Velocity

Path Contouring

PARCP	Radius Specified CW Arc
PARCOP	Origin Specified CW Arc
PLIN	Move in a line
PRUN	Execute Path

Scaling

SCALE	Enable Scaling
SCLA	Accel / Decel Scale Factor
SCLD	Distance Scale Factor
SCLV	Velocity Scale Factor

Subroutines

DEF	Define a Subroutine
GOSUB	Execute a Subroutine with Return
GOTO	Execute a Subroutine without Return

Transfer Information

TAS	Transfer Axis Status
TANV	Transfer Analog Input Value
TCNT	Transfer Counter
TIN	Transfer Input Status
TINT	Transfer Interrupt Status
TLIM	Transfer Limit Status
TMEM	Transfer Memory Usage
TOUT	Transfer Output State
TPE	Transfer Position of Encoder
TPM	Transfer Position of Motor
TTIM	Transfer Timer

* Partial Command List

Parker

Model AT6400

4-Axis Indexer

Specifications

Parameter		Value
Power		
	AT6400	+5VDC, 1.8 Amps maximum (supplied by PC-AT backplane)
	-AUX1 (auxiliary board)	90-130VAC 55-400 Hz or 115-165VDC
Performance		
	Position Range	±2,147,483,648 steps
	Velocity Range	1 to 1,600,000 steps/sec
	Acceleration Range	1 to 24,999,975 steps/sec^2
Inputs		
	Encoder	Differential comparator accepts two phase quadrature incremental encoders with differential (recommended) or single ended outputs (+5 VDC TTL compatible). Maximum frequency = 1.6 MHz, post-quadrature. Minimum time between transitions = 625 ns.
	24 Programmable	Plug compatible with OPTO-22™ signal conditioning equipment (50 pin header). Internal pull-up, TTL compatible, voltage range 0-24 VDC. Optically isolated.
	4 Specific Interrupt	Internal pull-up, TTL compatible, voltage range 0-24 VDC. Optically isolated.
	Analog (joystick)	Voltage range 0-2.5 VDC, 8-bit A/D converter. Optically isolated.
	Home Enable, CW and CCW Limits, Pulse Cutoff, Joystick Trigger, Joystick Release, Joystick Select, Joystick Velocity, Drive Fault, In Position	Internal pull-up, TTL compatible, voltage range 0-24 VDC. Optically isolated
Outputs		
	24 Programmable	Plug compatible with OPTO-22™ signal conditioning equipment (50 pin header). Open collector output will sink up to 30 mA, and allow up to 24 VDC. Optically isolated.
	Step, Direction, Shutdown	Differential Drive. Signal high > 3.5 VDC @ 60 mA, signal low < 0.75 VDC @ -60 mA. Optically isolated.
Environmental		
	Operating	32 to 122 °F (0 to 50°C)
	Storage	-22 to 185 °F (-30 to 85°C)
	Humidity	0 to 95% non-condensing

* Contact Factory for Availability

Parker

Model AT6400

4-Axis Indexer

AT6400-AUX1 Connections

Drive 1-4
15 Pin "D"

Pin No.	Signal
1	Step +
2	Direction +
3	Reserved
4	In Position
5	Drive Fault
6	Reserved
7	+5 VDC (out)
8	Shield
9	Step -
10	Direction -
11	Shutdown +
12	Shutdown -
13-14	Ground
15	Reserved

Encoder 1-4
9 Pin Screw Terminal

Pin No.	Signal
1	Shield
2	Ground
3	Z-
4	Z+
5	B-
6	B+
7	A-
8	A+
9	+5 VDC (out)

Joystick
25 Pin "D"

Pin	No.Signal
1	Analog Ch. 1
2	Analog Ch. 2
3	Analog Ch. 3
4	Analog Ch. 4
8	Shield
14	Ground
15	Axes Select
16	Velocity Select
17	Joystick Release
18	Joystick Trigger
19	Joystick Auxiliary
23	+5 VDC (out)

Limits 1 & 2, 3 & 4
9 Pin Screw Terminal

Pin	No.Signal
1	Shield
2	Ground
3	Home
4	CCW
5	CW
6	Ground
7	Home
8	CCW
9	CW

Auxiliary
9 Pin Screw Terminal

Pin No.	Signal
1	Ground
2	Pulse Cutoff
3	Test
4	Ground
5	Input Pull-up
6	Output Pull-Up
7	+5 VDC
8	Ground
9	+5 VDC

Trigs
9 Pin Screw Terminal

Pin No.	Signal
1	Shield
2	Ground
3	Input 4
4	Ground
5	Input 3
6	Ground
7	Input 2
8	Ground
9	Input 1

-AUX1 Dimensions

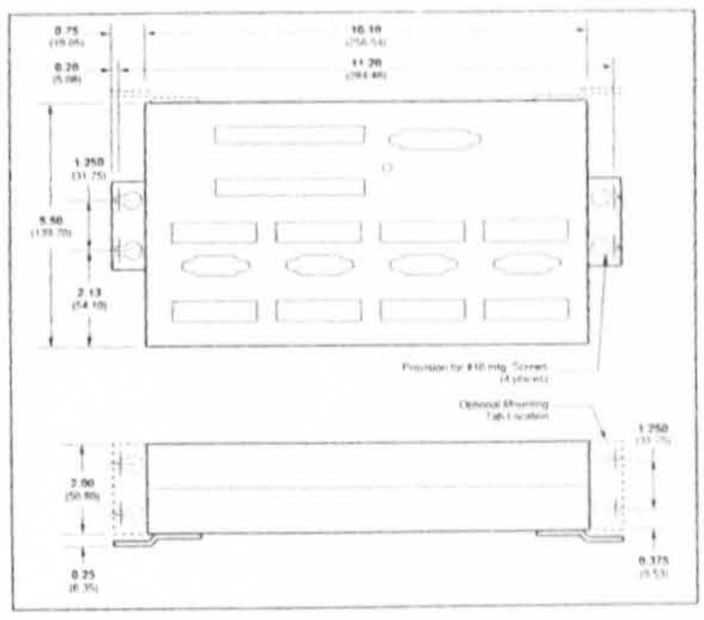

Configurations

AT6400-AUX1	AT6400 with auxiliary connector board described in this flyer.
AT6400-AUX2	AT6400 with reduced auxiliary connector board. Contact factory for details.
AT6400-AUX3	AT6400 with reduced auxiliary connector board. Contact factory for details.

Accessories

VM50	50 pin header to screw terminal breakout board.
71-010432-10	15 Pin "D" to 25 Pin "D" Indexer to drive cable.

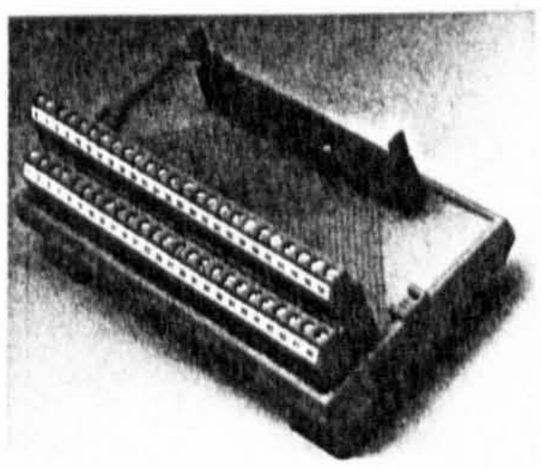

Compumotor
Parker Hannifin Corporation
Compumotor Division
5500 Business Park Drive
Rohnert Park, CA 94928
707/584-7558
FAX 707/584-8015

Digiplan
Parker Hannifin Corporation
Digiplan Division
Balena Close, Poole
Dorset, England BH177DX
(0202) 69 9000
FAX (0202) 69 5750

Bulletin #8335A 9/91 5M Printed in USA